Assessment of outer membrane permeability in *Pseudomonas aeruginosa* to β-Lactams: some aspects of the role of OpdP in carbapenem resistance

Francesco AMISANO

A thesis submitted in fulfillment of the requirements for the degree of Doctor of Philosophy in Science

Doctoral college in Biochemistry, Molecular and Cellular Biology

Promoter: Prof. Moreno Galleni

Academic year 2024-2025

To my parents and grandparents,
who instilled in me the curiosity to study.

To bacteria and ancestors,
their exponential growth continues
to nurture my passion for studying them.

Acknowledgement

As you will see, the list of people to thank is pretty long, but it is only right to acknowledge here all those who have contributed to helping me reach this milestone.

First of all, I would like to thank Professor Moreno Galleni for the trust he placed in me by giving me the opportunity to work on this thesis project funded by the WBI. He always believed in me and constantly encouraged me. Thanks are also due to Paola, for all those long conversations we had about the thesis and about everyday life—they were indeed invaluable for reaching the final goal!

A special thanks goes to Jean-Marie Frère for suggesting to me to work on this fascinating and intriguing thesis project. His support never faltered, and his constant passion for research was an immense source of inspiration during moments when I thought I would never see the light at the end of the tunnel.

I also want to thank all my colleagues at CIP for all those moments of scientific and human sharing over the years in Liège. I did learn a lot scientifically from those conversations, and the family atmosphere I found there is what I will miss the most about Belgium—along with the pleasant Trappist Fridays. Among my colleagues, I think it is only right, however, to give a special mention to Simona, Alessia, Stefano, Gilles, Fred, Mathieu, Marylène, Cristina, Elodie, and Romain. A thought also goes to Fabienne, Anne Marie, Iris, Caroline, and Raphael, who over the years have always contributed in a valuable way to the smooth running of the laboratory (and also to keeping us well-fed with delicious gaufres!). A special thanks also goes to a former CIPiste, Bernard Lakaye, for his willingness to search for the old plasmids described in his work

I want to thank Prof. Luca Bini, who, by granting me the opportunity to participate in the Erasmus program, enabled me to join the laboratory in Liège, and whose collaboration, along with the precious help of Dr. Assunta Gagliardi, led to achieving the proteomics results.

I also want to thank Dr. Steven Fanara for his valuable help with RT-PCR; his assistance allowed us to obtain interesting results on porin expression and taught me a technique that, only a few months later, would unfortunately become widely known for SARS-CoV-2 diagnostics and my “daily bread” in the diagnostic lab.

Last but not least, I want to thank Olivier Verlaine; his contribution for the genome analysis and limitless PC assistance was fundamental.

I cannot fail to acknowledge the precious help from people who have (almost) never set foot in Belgium. To Alberto, a true friend, always ready to listen to my frustrations and to give me the right advice on the latest developments in diagnostics. To Angelo, Marina, Mauro, Valentina, Tiziana, and all the technical colleagues at the Tortona hospital, for restoring my confidence. Overcoming that dark period of the pandemic made me realize that finishing the thesis would not be impossible. To my uncle Gianni, who caringly revised this manuscript for language and has always supported me in reaching this goal. To Alessandro for his graphic, aesthetic, and IT help. A constant motivator during long discussions steeped in scientific research, but especially in studies on the history of the 1400s in the history of Monferrato. I would never have thought that such different worlds could work together.

Scientific contributions aside, friendships and family relationships were of the utmost importance. Contrada is the essence of life: it allowed me to maintain that carefree spirit that life's circumstances had done everything to take away. Thanks to Beatrice, who always helped me so that I would not be far from what has always been home for me; to Renato for his support in a foreign land; to Guccio, Giulia, Francesco, Donatella, Sylvie, and Emy, who were particularly close to me, but more generally to everyone—because the Civetta is home and family. Thanks to Tommaso, whose presence in Brussels was often a lifesaver; although not physically present in Belgium, I would also like to thank Alessandro, Marco, Maria, and Fabio, because friendships overcome distances.

To my "Cuginette" Ornella and Clelia—the long chats about "little skeletons", ceramics, and dives into the sea contributed in their own way to the scientific results.

Finally, and certainly not least, I want to thank my friends from Valenza, especially Manuel, Valeria, Martina, and Niccolò, and my cousin Serena; these were complicated years, and they were there when a bit of comfort was needed.

Thesis Structure

This thesis is written in cumulative form. It includes a general introduction where I focus on the goals of the thesis, and where I made an in-depth investigation on the state of the art concerning porins and efflux pump system.

A paper on my project describes the main experiences performed, while additional collateral experiments are reported successively. All results are further discussed and brought into perspectives at the end of the thesis.

Summary

Pseudomonas aeruginosa is a Gram-negative opportunistic pathogen responsible for severe infections in immunocompromised and vulnerable patients. This microorganism is characterized by a marked intrinsic resistance to antibiotics, mediated by the constitutive expression of β-lactamases and efflux pumps, combined with the lack of large, non-specific porins, that renders its outer membrane poorly permeable to antibiotics.

In addition to this intrinsic resistance, *P. aeruginosa* can further acquire resistance to the limited therapeutic options available, either through the acquisition of exogenous resistance determinants, such as plasmid-encoded β-lactamases, or through the overexpression of endogenous systems, including efflux pumps and the chromosomally encoded β-lactamase AmpC. Furthermore, resistance to imipenem (and a general decrease in susceptibility to carbapenems) is a well-established fact in the literature and results from the loss of OprD porin expression. This association is explained by the structural similarity between arginine, the natural substrate of OprD, and the side chain of imipenem. To date, available studies investigating the role of other porins in the permeation of β-lactams have been scarce and fragmented.

In this study, we refined a previously described methodology designed to measure the periplasmic entry of β-lactam antibiotics by expressing BlaR-CTD, a high-affinity sensor for these antibiotics, in the periplasmic space. The results are summarized as follows.

First of all, this approach allowed us to evaluate the outer membrane permeability of the wild-type *P. aeruginosa* PAO1 strain and of several mutant strains lacking one or more porins. The comparison between PAO1 and an isogenic *oprD*-deficient mutant demonstrated that phenotypic variations in carbapenem susceptibility, with the exception of imipenem, were not correlated with a decreased rate of periplasmic entry. A reduction in the entry rate of other carbapenems was only observed in a strain simultaneously deleted for both *oprD* and *opdP*, thus defining the synergistic contribution of these two porins in the uptake of meropenem and biapenem.

Secondly, to further confirm the involvement of OpdP in antibiotic resistance, we assessed its increased expression in response to OprD loss. Additionally, we showed that the single deletion of *opdP*, which does not affect MIC values or permeability coefficients compared to wild-type PAO1, can nonetheless favor the selection of carbapenem-resistant strains in the presence of sub-inhibitory concentrations of meropenem. While the so derived resistance is typically mediated by mutations in *oprD*, we also identified a previously unreported mechanism of negative regulation of OprD expression.

Finally, as previously documented, multiple lineages of PAO1 exist. Unexpectedly, in our case, some of these lineages, although never directly utilized in our experiments, carried a mutation leading to the overexpression of OpdP.

All these results significantly advanced our understanding of the function of OpdP, a key porin for carbapenems uptake whose role had so far remained unclear.

Résumé

Pseudomonas aeruginosa est une bactérie à Gram-négatif pouvant provoquer de graves complications chez les patients fragiles. Elle se caractérise par une résistance intrinsèque marquée aux antibiotiques, médiée par l'expression constitutive de β-lactamases et de pompes d'efflux, ainsi que par l'absence d'expression de larges porines non spécifiques, ce qui rend sa membrane externe faiblement perméable aux antibiotiques.

En outre, cette bactérie peut développer des résistances aux rares options thérapeutiques disponibles, soit par l'acquisition de déterminants de résistance exogènes, tels que des β-lactamases plasmidiques, soit par la surexpression de systèmes constitutifs comme les pompes d'efflux ou la β-lactamase AmpC. De plus, la résistance à l'imipénème (et la diminution générale de la sensibilité aux carbapénèmes) est bien documentée et résulte de l'absence d'expression de la porine OprD. Cette association est due à la similarité structurale entre l'arginine, substrat naturel de cette porine, et la chaîne latérale de l'imipénème. Les études disponibles dans la littérature concernant le rôle d'autres porines dans la perméation des β-lactamines étaient jusqu'à présent rares et fragmentaires. Dans ce travail, nous avons affiné une méthodologie précédemment décrite permettant de mesurer l'entrée d'un β-lactamine dans le périplasme par la production dans ce compartiment cellulaire du BlaR-CTD, un senseur à haute affinité pour ces antibiotiques.

En premier lieu, nous avons ainsi déterminé la perméabilité de la membrane externe de la souche sauvage *P. aeruginosa* PAO1 et de différents mutants délétés pour une ou plusieurs porines.

La comparaison entre PAO1 et un mutant isogénique délété de la porine *oprD* a montré que les variations phénotypiques de sensibilité aux carbapénèmes, à l'exception de l'imipénème, n'étaient pas corrélées à un ralentissement de la vitesse d'entrée dans le périplasme. Pour observer un ralentissement dans l'entrée d'autres carbapénèmes, il était nécessaire de considérer une souche délétée simultanément des gènes *oprD* et *opdP*, définissant ainsi le rôle synergique de ces deux porines dans la pénétration du méropénème et du biapénème.

En second lieu, pour corroborer l'implication d'OpdP dans la résistance aux antibiotiques, nous avons vérifié l'augmentation de son expression en réponse à l'absence d'OprD. Par ailleurs, nous avons montré que la délétion unique d'*opdP*, qui n'entraîne aucune variation ni de la CMI ni du coefficient de perméabilité en comparaison de la souche sauvage PAO1, peut néanmoins favoriser la sélection de souches résistantes aux carbapénèmes en présence de concentrations sous-inhibitrices de méropénème. La résistance qui en résulte est généralement médiée par des mutations dans le gène

oprD, mais nous avons également mis en évidence un mécanisme inédit de régulation négative de la porine OprD.

En dernier lieu, nous avons aussi constaté l'existence de plusieurs lignées de PAO1 (un fait bien connu). De façon inattendue certaines d'entre elles (qui n'ont jamais été utilisées directement dans nos expériences) présentaient une mutation provoquant une surexpression d'OpdP.

Dans l'ensemble, ce travail a permis de faire progresser de manière significative la compréhension de la fonction d'OpdP, une porine clé dans l'absorption des carbapénèmes, dont le rôle restait jusqu'ici mal défini.

List of abbreviations

2-DE: two-dimensional gel electrophoresis

ABC: ATP-binding cassette superfamily

BAM: β-Barrel Assembly Machine

BCA: bicinchoninic acid assay

BCCM: Belgian co-ordinated collections of micro-organisms

BlaR-CTD: C terminal domain of the *Bacillus licheniformis* β-lactams receptor BlaR

C55-P: undecaprenyl phosphate molecule

CF: cystic fibrosis

CFU: colony-forming unit

CLSI: Clinical and Laboratory Standard Institute

CM: cell membrane

CV: column volume

D-Ala: D-alanine

D-Glu: D-glutamic acid

DBO: diazabicyclooctane

DOPE: 1,2-dioleoyl-sn-glycero-3-phosphoethanolamine

DOPG: 1,2-dioleoyl-sn-glycero-3-phosphoglycerol

DPA: dipicolinic acid

DPH I: dehydropeptidase I

DPPE: 1,2-dipalmitoyl-sn-glycero-3-phosphoethanolamine

DPPG: 1,2-dipalmitoyl-sn-glycero-3-phosphoglycerol

DTT: dithiothreitol

EARS-Net: European Antimicrobial Resistance Surveillance Network

EDTA: ethylenediaminetetraacetic acid

ESBL: extended-spectrum β-lactamase

EUCAST: European Committee on Antimicrobial Susceptibility Testing

FDA: Food and Drug Administration

Glc*N*Ac: *N*-acetylglucosamine

Gly-Glu: glycine-glutamate dipeptide

HAE1: hydrophobe/amphiphile efflux 1

HAI: Healthcare-Associated Infections

HME: heavy metal efflux

HMM-PBP: high molecular mass PBP

HRP: horseradish peroxidase

IATS: International Antigenic Typing Scheme

IEF: isoelectric focusing

IM: inner membrane

IMAC: immobilized metal affinity chromatography

IMP: inner membrane protein

IPG: immobilized pH gradient

IPTG: isopropil-β-D-1-thiogalactopyranoside

L-Ala: L-alanine

L-Lys: L-lysine

LB: Luria-Bertani

LBA: Luria-Bertani agar

LC-MS: liquid chromatography-mass spectrometry

LMM-PBP: low molecular mass PBP

LPS: lipopolysaccharide

MALDI-TOF: matrix-assisted laser desorption/ionization time-of-flight

MATE: multidrug and toxic compound extrusion family

MBL: metallo-β-lactamases

MD: molecular dynamic

***m*DAP**: meso-diaminopimelic acid

MDR: multidrug resistant

MFP: membrane fusion protein

MFS: major facilitator superfamily

MHB II: Mueller Hinton II broth

MIC: minimal inhibitory concentration

MRSA: methicillin resistant *Staphylococcus aureus*

MS: mass spectrometry

Mur*N*Ac: *N*-acetylmuramic acid

Occ: outer membrane carboxylate channel

OD: optical density

OM: outer membrane

OMF: outer membrane factor

OMV: outer membrane vesicle

OS: core oligosaccharide

PACE: proteobacterial antimicrobial compound efflux family

PAβN: phenylalanine-arginine β-naphthylamide

PBP: penicillin binding protein

PBS: phosphate-buffered saline

PCR: polymerase chain reaction

PDC: *Pseudomonas*-derived cephalosporinase

PDR: pan-drug resistance

PG: peptidoglycan

PVDF: Polyvinylidene fluoride membrane

RND: resistance/nodulation/cell division family

RT-qPCR: Reverse transcription quantitative (real time) polymerase chain reaction

SBL: serine β-lactamase

SDS-PAGE: sodium dodecyl sulphate-polyacrylamide gel electrophoresis

SMR: small multidrug resistance family

SOB: super-optimal broth

SOC: super-optimal broth with catabolite repression

TAE: Tris-acetate, EDTA buffer

TBDT: TonB-dependent transporter

TBS: Tris-buffered saline

TES: Tris-HCl, EDTA, sucrose buffer

TTBS: Tris-buffered saline added with Tween-20

UDP-Glc*N*Ac: UDP-N-acetylglucosamine

UDP-Mur*N*Ac-pentapeptide: uridine diphosphate-N-acetylmuramyl-pentapeptide

WHO: World Health Organization

XDR: extensively drug resistance

List of figures

List of tables

Table S3: Molar extinction coefficients for antibiotics tested for permeability coefficient determination.

Table of contents

1 INTRODUCTION

1.1 Pseudomonas aeruginosa

Pseudomonas aeruginosa is a Gram-negative rod-shaped bacterium (1–5 μm long and 0.5–1.0 μm wide), belonging to the class Gammaproteobacteria, to the order Pseudomonadales and is the main pathogen in the family *Pseudomonadaceae*.

The German botanist Joseph Schroeter suggested the name *Bacterium aeruginosum* based on experiments with pigmented microbes conducted around 1870 (Schroeter, 1872). The first pure culture was however isolated almost ten years later by Carle Gessard in Paris and was described in his dissertation "*De la pyocyanine et de son Microbe*" (Gessard, 1882). Gessard also linked the bacterium to clinical infections and named it *Bacillus pyocyaneus*. In the same period at the University of Karlsruhe, Walter Migula continued to study the bacterial species, changing its name first to *Pseudomonas pyocyanea* and later to *Pseudomonas aeruginosa* (Migula, 1894). The term used to define the genus derives from the Greek *pseudo*, which means false, and *monas*, which means unity and refers to the tendency of this bacterium to associate in pairs. The name of the species instead derives from the Latin *aerugo*, or rust/verdigris (as the result of copper ‘s corrosion) and refers to the resemblance of the typical blue-green of bacterial chromopeptides to oxidized copper (Garrity *et al*., 2005).

Its genome contains about 6.3 million base pairs, coding for more than 5000 genes. Historically, the *P. aeruginosa* strain PAO1, isolated in 1954 from a wound in Melbourne, Australia, is regarded as the reference strain for this species, and was the first to be sequenced in 2000 (Stover *et al*., 2000). The worldwide propagation of *P. aeruginosa* PAO1 among laboratories and strain collections has produced several mutations, generating a great diversity in the PAO1 sublines. This microevolution has brought scientists to work on different PAO1 strains with marked differences in relevant characteristics, like antibiotic resistance, virulence, or bacterial fitness, jeopardising the research reproducibility (Klockgether *et al*., 2010).

P. aeruginosa is known to be extremely versatile in its ability to catabolize various species of naturally occurring organic compounds, allowing it to colonize a wide range of ecological niches; it has in fact been isolated in water (fresh or salty), air, soil, animals and plants and is therefore considered ubiquitous (Alonso *et al*., 1999; Zarei *et al*., 2018; Crone *et al*., 2020); moreover, it can metabolize a variety of simple and complex organic substrates as a sole carbon and energy source, thus being able to growth on minimal medium (Ambreetha *et al*., 2024). This versatility is thought

to result from the presence of numerous cellular regulatory systems, including 90 two-component regulatory systems present in the bacterial genome, which, in the simultaneous presence of multiple substrates, are activated in an orderly manner based on survival needs (Sivaneson *et al*., 2011; Ambreetha *et al*., 2024).

1.1.1 Microbiological characteristics

P. aeruginosa is a non-lactose-fermenting facultative aerobic/anaerobic bacterium and derives energy from carbohydrates by oxidation. During aerobic incubation it grows on most media, liquid or solid, without needing special supplementary nutrients, although it prefers to grow in the oxygen-rich air-media interphase.

It grows in a temperature range between 4 ºC and 42 °C with an optimal temperature of 37 °C. It is a fast-growing bacterium with an average duplication time in Luria-Bertani (LB) medium at 37 °C of 25-35 minutes (LaBauve *et al*., 2012).

It is able to use a wide variety of carbon sources for the production of energy, favoring tricarboxylic acid cycle intermediates, amino acids or sugars, like glycerol even if glucose does not appear to be a substrate of choice (Dolan *et al*., 2020; Rojo, 2010). This feature, useful for bacterial growth in soil and other environments, however, raises great concern with regard to infection control, especially in hospital settings.

P. aeruginosa can also grow anaerobically, using nitrates (NO_3^-) or nitrites (NO_2^-) as terminal electron acceptors, compounds found readily in infection sites such as the airway mucus of patients with cystic fibrosis (CF) (Wu *et al*., 2005).

P. aeruginosa does not ferment lactose. This characteristic is used in MacConkey medium, a selective medium for Gram-negative bacteria. Only the strains capable of fermenting this sugar will in fact exhibit a color with various shades of red while the non-fermenters, such as *P. aeruginosa*, will remain colourless.

The presence of cytochrome C oxidase determines the positivity to the oxidase test, useful for distinguishing *Pseudomonadaceae* from Enterobacterales (a family that includes other common non-lactose fermenters). It also turns out to be positive for the catalase test due to the production of catalases such as KatA, KatB and KatE (Heo *et al*., 2010).

Depending on the specific pH, the *P. aeruginosa* colonies, and sometimes the surrounding media, can assume a different blue/green pigmentation due to the production of pyocyanin, a soluble chromopeptide belonging to the group of tricyclic phenazines. Other chromopeptides produced by these bacteria include pyorubin (red) pyomelanin (brown-black) and/or pyoverdine (yellow-green

or yellow-brown). These substances are important virulence factors, responsible for oxidative stress induction. They can also act as siderophores for iron uptake and take part in the regulation of quorum sensing (Kothari *et al*., 2022).
The growth of *P. aeruginosa* also develops a characteristic grape or apple odor, due to the secretion of 2'-aminoacetophenone, a volatile compound derived from the tryptophan catabolic pathway, which may represent a further help in an early identification (Cox *et al*., 1979).

1.1.2 *P. aeruginosa* pathogenicity

P. aeruginosa has a large arsenal of virulence factors that allow it to disrupt the human innate immune system and modulate human adaptive immune mechanisms, thus allowing the bacterium to establish systemic or chronic infections, particularly in immunocompromised patients. First, *P. aeruginosa* virulence factors include a variety of extracellular toxins (exotoxin A, phospholipase C, elastase) that can cause extensive damage to host tissues through their enzymatic activities and these factors play an important role in acute infections. Another group of virulence factors are adhesion and motility organelles, including flagella and pili (Jurado-Martín *et al*., 2021).
In the case of chronic infections, *P. aeruginosa* is known for its conversion from a non-mucoid (environmental) phenotype to a mucoid (clinical) phenotype. It is able to synthesize a mucilaginous film mainly made of alginate, which confers the ability to aggregate in biofilms to the colonies. The production of alginate increases the virulence and survival of *P. aeruginosa* in several ways since this compound acts as a barrier for bacterial cells against phagocytes and antibodies. It interferes with both opsonophagocytic killing and with non-opsonic phagocytosis (Pier *et al*., 2001; Mishra *et al*., 2012). It allows the bacteria to be less exposed to the host immune system and to antibiotics (Mann *et al*., 2012; Jurado-Martín *et al*., 2021); finally, it is believed that alginate is able to minimize the toxic effect mediated by oxidative radicals released by phagocytic cells (Simpson *et al*., 1993).
The biofilm has a rather complex organization, with bacterial populations exhibiting a differentiated metabolism related to their localization within this structure. This type of growth is particularly prevalent in the lungs of patients with CF, making it almost impossible to eradicate the bacterium (Mathee *et al*., 1999; Moradali *et al*., 2019).
P. aeruginosa appears to be an opportunistic human pathogen, with a remarkable ability to cause hospital acquired infections, being able to virtually infect all body parts, but with a marked tropism for respiratory, urinary, and skin infections. It is a common infectious agent in patients with immunodeficient conditions and is the most common pathogen colonizing patients with CF (Weber *et al*., 2007; Lamas Ferreiro *et al*., 2017; Jurado-Martín *et al*., 2021; Staudinger *et al*., 2014).

The most recent data available for *P. aeruginosa* incidence in Healthcare-Associated Infections (HAI) range between 7.1 % and 8.0 %, confirming the importance of this pathogen in public health management (ECDC 2023; Weiner-Lastinger *et al*., 2020).

P. aeruginosa appears to be of great concern in critical wards, such as intensive care units, where its incidence doubles compared to the generality of hospital infections, also due to numerous outbreaks noticed worldwide, causing a marked worsening of the clinical outcome (Ribeiro *et al*., 2019; Khedr *et al*., 2022).

1.1.3 Therapeutic options, resistance, and epidemiology

P. aeruginosa is intrinsically resistant to different classes of antibiotics and the few available therapeutic options include some β-lactams, aminoglycosides, quinolones, polymyxins and fosfomycin. To increase the chances of therapeutic success, especially during empirical therapy, a combination therapy consisting of a β-lactam plus a second drug belonging to a different class is recommended (Bassetti *et al*., 2018).

The β-lactams active against *P. aeruginosa* are aztreonam, cefepime and carbapenems (imipenem and meropenem). However, the combination of β-lactams and β-lactamase inhibitors, such as piperacillin/tazobactam, ceftazidime/avibactam, ceftolozane/ tazobactam and imipenem/relebactam are being increasingly preferred lately (Angrill *et al*., 2020; Curran *et al*., 2018; Zhanel *et al*., 2018; Sader *et al*., 2021). More recently, the introduction of cefiderocol, a siderophore cephalosporin capable of overcoming the intrinsic impermeability of *P. aeruginosa* and exhibiting good stability against β-lactamases, including carbapenemases, is emerging as an alternative that is included into therapeutic options (Sato *et al*., 2019; Rayner *et al*., 2023).

Regarding the other classes of antibiotics, the aminoglycosides that exhibit activity against *P. aeruginosa* include gentamicin, tobramycin, amikacin, netilmicin while colistin and polymyxin B are the two polymyxins that can be successfully administered (Bassetti *et al*., 2018). Finally, the quinolones that are effective for therapy are ciprofloxacin, levofloxacin and ofloxacin (Sihotang *et al*., 2022).

Unfortunately, *P. aeruginosa* acquires various resistance mechanisms which can compromise the success of chemotherapy. The resistant bacteria can be classified as multidrug resistant (MDR) if it is resistant to at least one compound belonging to 3 different classes of antibiotics, or as eXtensively Drug Resistant (XDR) where the strain remains susceptible to only one or two antimicrobial categories. Finally, there can be strains resistant to all available antibiotics that are defined as Pan-Drug Resistant (PDR) (Magiorakos *et al*., 2012).

The widespread diffusion of antibiotic resistance in *P. aeruginosa* is a serious problem, which compromises the appropriate treatments and is therefore associated with significant morbidity and mortality. For example, in 2023 in Europe the European Antimicrobial Resistance Surveillance Network (EARS-Net) highlighted how 32 % of *P. aeruginosa* isolates involved in invasive infections presented at least one resistance to at least one of the antibiotic groups and of these at least 67 % carried of at least one mechanism of resistance to β-lactams. Among the most interesting data, it was reported that 14.5 % of the isolates were resistant to carbapenems and 15 % to piperacillin/tazobactam, in line with the World Health Organization (WHO) indications that inserted carbapenem-resistant *P. aeruginosa* among the high priority pathogens for which the development of new molecules is required (WHO, 2024).

The disease severity and the inauspicious clinical outcome, mostly associated to antibiotic resistance has resulted in the inclusion of *P. aeruginosa* in a group of particularly relevant pathogens. This group includes ***E****nterococcus faecium*, ***S****taphylococcus aureus*, ***K****lebsiella pneumoniae*, ***A****cinetobacter baumannii*, ***P****seudomonas aeruginosa*, and ***E****nterobacter spp.*, whose initials gave birth to the acronym ESKAPE. They are associated to MDR and XDR profiles, achieved in different ways. β-lactams, including carbapenems, resistance represents a worrisome problem for *A. baumannii*, *P. aeruginosa*, *K. pneumoniae* and *Enterobacter spp*., while *S. aureus* can be resistant to methicillin and vancomycin and *E. faecium* displays resistance to vancomycin. Infections by these pathogens are associated to a high mortality risk, and increased health care costs. WHO has highlighted the need for new therapeutic molecules that might act against different targets. However, an approach that aims to improve the use of the already existing antibiotics might be successful. In Gram-negative bacteria, a better understanding of the outer membrane (OM) permeability is undoubtedly closely related to this purpose (Mulani *et al*., 2019).

1.2 Bacterial cell walls

The great ability of bacteria to adapt to different environments and to escape toxic compounds, including antibiotics and detergents, is mostly mediated by their capacity to isolate themselves from the environment.

To reach this goal, bacteria have been exploiting the properties of peptidoglycan (PG) to secure protection and rigidity outside the phospholipid cell membrane (CM).

PG is an heteropolymer constituted by long, acylated saccharide chains of variable length. These consist of monomeric subunits of *N*-acetylglucosamine (Glc*N*Ac) and *N*-acetylmuramic acid (Mur*N*Ac), cross-linked through β-(1,4) glycosidic bonds. Each disaccharide monomer carries a

short peptide chain (from three to five amino acids) linked to the Mur*N*Ac carboxylic group and presenting a precise sequence.

The PG synthesis is quite conserved among different bacteria, but its architecture has evolved in two completely different cell wall organizations, both efficiently performing their protective functions.

The bacterial cell wall is involved in many different functions, such as allowing bacterial shape maintenance but also associated to specific inserted structures. Bacterial cell wall also performs important tasks in bacterial pathogenesis, being responsible for their adherence to host cells and involved in the host immunological response.

1.2.1 Gram-positive bacteria

We know from the first experiments made in 1884 by the Danish scientist Hans Christian Gram that bacteria have different response to crystal violet staining, reflecting the properties of their envelopes. Gram-positives possess a thick layer (20-80 nm) of bacterial wall, mostly composed of PG and teichoic acids (Figure 1); this structure, as a consequence, retains the crystal violet staining fixed with Lugol's iodine, resulting in a purple colour.

In general, in Gram-positive bacteria, the sequence of the Mur*N*Ac linked pentapeptide stem is L-alanine (L-Ala), D-glutamic acid (D-Glu), L-lysine (L-Lys), D-alanine (D-Ala) and D-Ala, although some substituents of these peptides have been identified (Vollmer *et al*., 2008).

Teichoic acids can be bound to the diacylglycerol inserted in the CM, giving rise to lipoteichoic acids, thus creating a thin chamber identified as periplasm, whose existence has long been debated (Erickson *et al*., 2021).

This organization confers stress resistance but allows the diffusion of molecules up to a mass of 57 kDa, allowing different antibiotics to cross this barrier (Lambert, 2002).

Some Gram-positive bacteria like *Streptococcus pneumoniae* and *Streptococcus agalactiae* possess a further shell formed by polysaccharides, that is called capsule. This structure might be extremely variable, and differences found in capsular structures have been used to antigenically differentiate capsular serotypes. For instance, 98 different *S. pneumoniae* serotypes have been identified up to now (Geno *et al*., 2017).

The capsule facilitates the escape of the microorganism from the opsonophagocytic killing mediated by the host immune response, but it is also effective in reducing interactions with external hydrophobic toxic compounds.

1.2.2 Gram-negative bacteria

Gram-negative bacteria have a double envelope structure, that is an OM over a PG layer, and the CM, also defined as inner membrane (IM) (Figure 1). The OM and the CM create a space exhibiting a thickness between 10-50 nm called periplasm.

The OM, the CM and the periplasm, including the PG within it, constitute the cell envelope which differs from that of Gram-positive bacteria by their particular OM organization and by the limited (5 %) PG contribution to the structure.

This arrangement in Gram staining determines the iodine-fixed crystal violet decolorization after an ethanol wash, leading to the typical pink/red coloration of the safranine counterstaining.

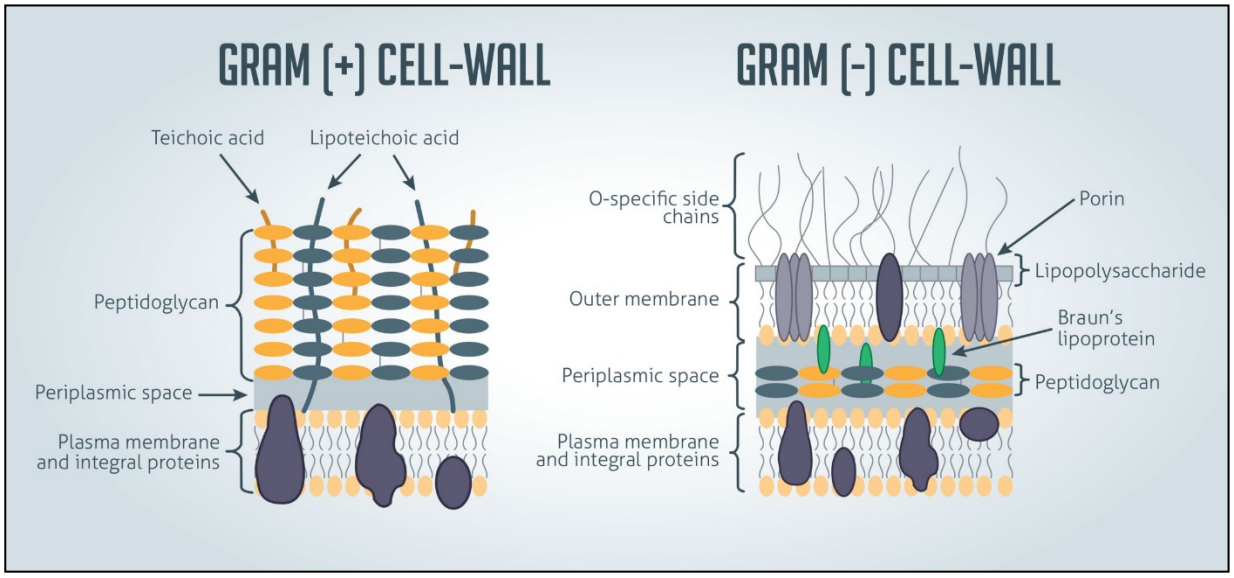

Figure 1: Comparison between Gram-positive (left) and Gram-negative (right) wall structures (https://www.technologynetworks.com/immunology/articles/gram-positive-vs-gram-negative-323007).

1.2.2.1 Outer membrane (OM)

The OM is an asymmetric lipid bilayer. Its internal layer is formed by phospholipids similar to those in the CM, whereas its external layer consists of glycolipids, in particular lipopolysaccharides (LPS). The OM inner leaflet composition includes phospholipids highly conserved in living cells, such as 1,2-dipalmitoyl-sn-glycero-3-phosphoethanolamine (DPPE), 1,2-dioleoyl-sn-glycero-3-phospho-ethanolamine (DOPE), 1,2-dipalmitoyl-sn-glycero-3-phosphoglycerol (DPPG) and 1,2-dioleoyl-sn-glycero-3-phosphoglycerol (DOPG) (Li *et al*., 2018).

The LPS is a negatively charged, heat-stable, semi-rigid amphiphilic macromolecule, with distinct lipidic and polysaccharidic portions; it plays a crucial role in the defence against environmental stress and in bacterium-host interactions.

Its rigid structure and strong electrostatic interactions make LPS a semi-impermeable barrier that allows the passage of small hydrophilic compounds such as sugars and amino acids, but drastically slows down the permeation of hydrophobic molecules and negatively charged antibiotics (Ruiz *et al*., 2009). This feature, present in all Gram-negative bacteria, is particularly important in *P. aeruginosa,* given the absence of large non-specific porins.

LPS is also known for its toxicity properties mediated by a host hyper-inflammatory response and, for this reason, it is also referred to as endotoxin.

LPS, as shown in Figure 2, is composed of the following three elements that are independently synthesized before being assembled:

- **Lipid A** is a conserved structure that enables the anchorage of the LPS into the inner leaflet of the OM mediated by electrostatic and hydrophobic interactions. It contains glucosamine disaccharides, bonded to phosphate groups (amide-linked fatty acids and ester-linked fatty acids).

  P. aeruginosa lipid A is characterized by shorter fatty acids when compared to that of Enterobacterales. In particular, it contains a hexa-acylated structure due to the addition of secondary fatty acids that can be further modified to facilitate the escape from the host immune response (Ernst *et al*., 2006).

- **Core oligosaccharide (OS)** can be further divided into an inner and an outer core. The inner core is a tetrasaccharide that acts as the anchor site through a covalent bond with the lipid A; it consists of two residues of 3-deoxy-D-*manno*-oct-2-ulosonic acid and two residues of L-*glycero*-D-*manno*-heptose highly phosphorylated (Knirel *et al*., 2006).

  The outer core is connected to the O-antigen, and is constituted of one D-galactosamine, substituted on N2 by an alanyl group, one L-rhamnose and three D-glucose residues. It may be acylated, a feature particularly frequent in bacteria involved in chronic infections, probably due to a role in the escape from host opsonization. Moreover, several modifications have been reported, thus creating heterogenicity and participating in evading the host immune response (Knirel *et al*., 2006).

- **O-polysaccharide (O-Antigen)**, also known as somatic antigen, is the outermost part of LPS and is the result of the assembling of a high number (up to 50) of saccharide units composed of 1 to 8 residues, including 6-deoxyhexosamines, 2-amino-2-deoxyhex-uronic, 2,3-diamino-2,3-dideoxyhexuronic or 5,7-diamino-3,5,7,9-tetradeoxynon-2-ulosonic acids (Knirel *et al*., 2006).

  The O-antigen exhibits an extreme variability across different strains belonging to the same species, and is considered as the antigenic determinant of the LPS, responsible for its immunogenic properties.

  In *P. aeruginosa*, the various O-Antigen compositions and organization results in the definition of 20 different serotypes, according to the International Antigenic Typing Scheme (IATS) (Kocíncová and Lam, 2011).

  The LPS molecules containing the O antigen are termed "capped", while the possible absence of the O-Antigen produces colonies with a rough appearance and a pronounced sensitivity to the human immune response. However, it has been shown that LPS remodelling with the lack of O-Antigen can be used to modulate the biofilm growth and the detachment from the polysaccharide matrix of the biofilm (Augustin *et al*., 2007).

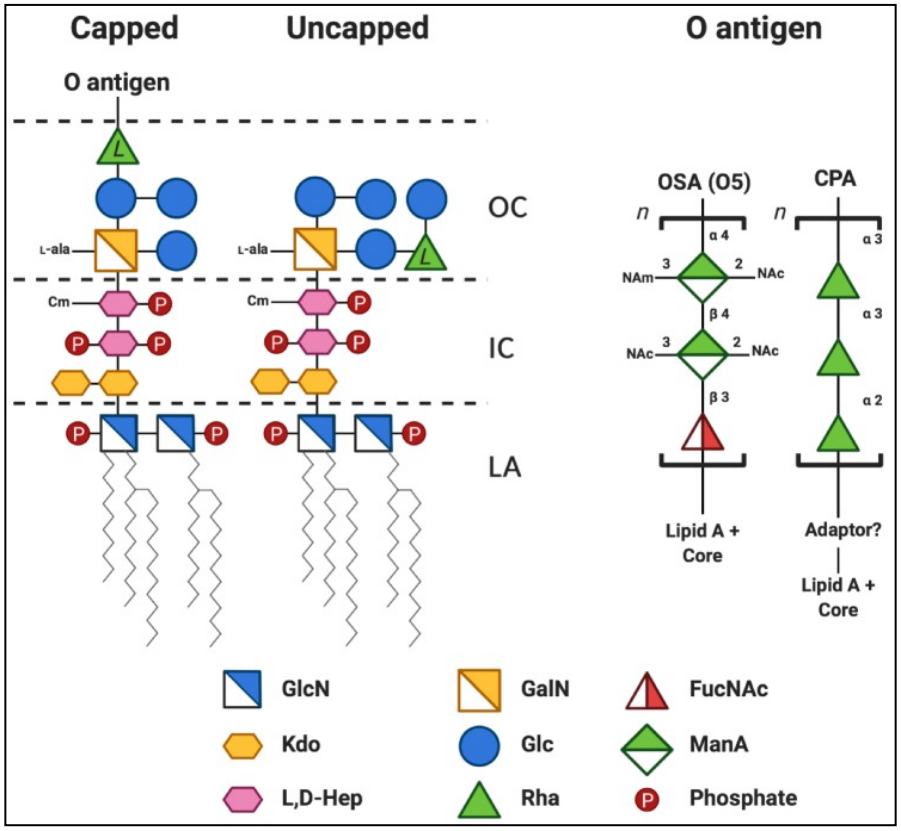

Figure 2: Simplified chemical structure of *P. aeruginosa* PAO1 LPS; the different aspect of the colonies, smooth or rough, depend to the presence or absence of the O-Antigen. The proposed O-antigen structure refers to the serotype O5. The predominant penta-acylated lipid A structure is

shown. The l-configuration of the rhamnose in the core is denoted by l to distinguish it from d-rhamnose found in the CPA repeat unit.
OC, outer core; IC, inner core; LA, lipid A; GlcN, glucosamine; GalN, galactosamine; FucNAc, N-acetyl-d-fucosamine Kdo, 3-deoxy-d-manno-oct-2-ulosonic acid; Glc, glucose; ManA, manuronic acid; l,d-Hep, l-glycero-d-manno-heptose; Rha, rhamnose; Cm, 7-O-carbamoylation; l-Ala, 2-l-alanylation; n, variable number of repeats; NAm, N-amidino; NAc, N-acetyl (Huszczynski *et al*., 2019).

Up to 163 proteins are inserted into the OM that are involved in various mechanisms essential for the survival of the bacterium (Hancock and Brinkman, 2002).
Notably, the OM contains the β-Barrel Assembly Machine (BAM), a system composed of a β-barrel membrane protein, BamA, and four lipoproteins, BamB, BamC, BamD, and BamE. Its role is to direct the proper insertion of β-barrel proteins, including porins, into the OM. Its activity is therefore essential and any alterations in the BAM system can affect the functionality of the porins themselves (Jansen *et al*., 2012; Hoang *et al*., 2011).
One can find proteins involved in LPS and PG synthesis such as PagL and LptD, the flagellum anchoring proteins FlgH and FliF and proteins involved in fimbrial biosynthesis like PilQ.
Other proteins that are located in the OM mediate specific functions, such as alginate production, essential for biofilm production (AlgE), or the type III secretion system, taking part in virulence and host cells colonization (PopN and PscC).
However, the most represented group (approximatively 64) belongs to the porin family, involved in the uptake of nutrients or, when associated with efflux pump systems, in the extrusion of waste compounds. We will deal with these specific proteins in the next chapters.

1.2.2.2 Periplasm and peptidoglycan synthesis

The periplasmic space is a compartment filled by a concentrated gel-like matrix, called periplasm. Within this compartment, we can find the PG that is thinner (2-3 nm) than in Gram-positive bacteria. Its small dimensions notwithstanding, even in Gram-negative bacteria PG plays a fundamental role in the stability to the structure.
In Gram-negative bacteria, the Mur*N*Ac linked pentapeptide stem is composed of L-Ala, D-Glu, meso-diaminopimelic acid (*m*DAP), D-Ala and D-Ala (Vollmer *et al*., 2008).
The PG synthesis implies three stages (Figure 3):

- The first one, the cytoplasmic phase, results in the synthesis of uridine diphosphate-N-acetylmuramyl-pentapeptide (UDP-Mur*N*Ac-pentapeptide) starting from UDP-N-acetylglucosamine (UDP-Glc*N*Ac) by means of MurA and MurB, a transferase and a

reductase, respectively. Notably, the structural similarity between a MurA substrate (the phosphoenolpyruvate) and the antibiotic fosfomycin allows the inactivation of Mur A (Kahan *et al*., 1974).

The subsequent peptide addition is catalysed by four ATP-dependent ligases namely MurC, MurD, MurE and MurF.

The UDP-Mur*N*Ac-pentapeptide is then ligated to the cytosolic membrane through the addition of an undecaprenyl phosphate molecule (C55-P), mediated by the MraY transferase, leading to the synthesis of the intermediate named lipid I.

Interestingly, this stage is the target of peptidyl nucleosides, a class of natural antibiotics that is widely produced by bacteria, generated by the assembly of nucleotides into peptide scaffolds. Different peptidyl molecules are able to inhibit MraY and they might represent promising candidates for the development of new compounds that might become useful in clinical settings (Walsh *et al*., 2011).

The MurG glycosyltransferase is then responsible for the Glc*N*Ac addition to lipid I, leading to the formation of another intermediate named lipid II.

- The second phase leads to the transport across the cytoplasmic membrane of lipid II by the MurJ flippase.
- The third phase takes place in the periplasm and leads to PG polymerization. It involves a first transglycosylation step, *i.e*., the formation of glycan chains derived from the polymerization of the lipid II saccharide units, and the consequent detachment of a pyrophosphate derivative of C55-P.

  Subsequently, the cross-linking between glycan chains catalysed by DD-transpeptidases takes place. This involves the binding of the *m*DAP of one chain to D-Ala in the fourth position of the adjacent chain, using the stem terminal D-Ala-D-Ala as an acyl donor and, thus improving the elasticity and strength to the PG. Interestingly, those enzymes are also defined as Penicillin Binding Proteins (PBPs). The β-lactam antibiotics act as suicide inhibitors (Tipper and Strominger, 1965) due to their structural analogy with the D-Ala-D-Ala natural substrates.

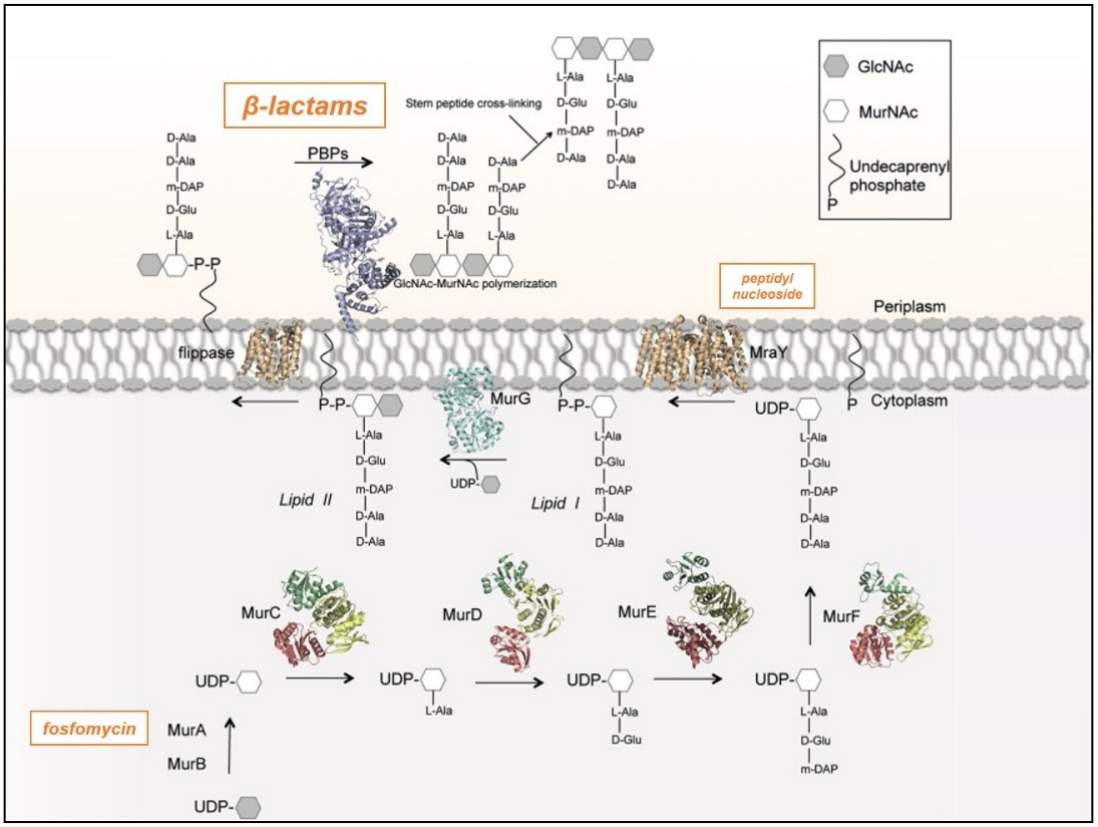

Figure 3: Schematic representation of cytoplasmic and membrane-related steps of PG biosynthesis; the antibiotics that could interrupt the PG formation are reported. It is important to note that the DD-transpeptidase activity of PBPs is the target of the large family of β-lactam antibiotics (Laddomada *et al*., 2019).

Depending on their size, PBPs can be divided into **h**igh (> 45 kDa) and **l**ow (< 45 kDa) **m**olecular **m**ass (HMM and LMM, respectively). HMM-PBPs can be further distinguished for their dual transpeptidase and glycosyltransferase activity (Class A HMM-PBPs) or sole transpeptidase activity (Class B HMM-PBPs); both appear to be essential for bacterial survival. LMM-PBPs, defined as Class C PBPs exhibit carboxypeptidase or endopeptidase activity and take part in cell separation, maturation, and PG recycling. However, LMM-PBPs are not essential, and their deletion do not result in a significant effect on bacterial viability or growth (Chen W. *et al*., 2016).

P. aeruginosa manufactures 8 PBPs, of which 5 HMM-PBPs (1a, 1b, 2, 3 and 3a/3x) and 3 LMM-PBPs (4, 5/6 and 7) (Chen W. *et al*., 2016).

In addition to PG, the periplasm of *P. aeruginosa* is characterized by an oxidizing state with salt and pH levels similar to those of the extracellular medium, but lacking ATP as energy source (Allen *et al*., 2009).

The periplasm also contains specific enzymes involved in the synthesis and in the assembly of different components of the OM, and proteins involved in the extrusion of compounds out of the periplasm, such as efflux pumps and secretion systems. Among the different reactions that take place

in the periplasm, we can mention protein folding, cell division regulation, and different signaling functions (Imperi *et al*., 2009). In particular, periplasmic chaperones have evolved the ability to store energy from the substances they bind to, ensuring the correct folding of various proteins.

P. aeruginosa chaperones contribute significantly to bacterial virulence. We can for instance mention Skp, responsible for the folding of Lipase A that is involved in the response against the host's immune response, and PaFkbA that operates via the negative alginate regulator MucD involved in biofilm formation (Allen *et al*., 2009; Huang *et al*., 2021; Papadopoulos *et al*., 2022).

Among the periplasmic processes, we have to mention that the synthesis of pyoverdine, a fluorescent chromopeptide that plays a primary role under iron-limiting conditions, is finalized within this cellular compartment (Ringel and Brüsel, 2018).

Moreover, there is a periplasmic phase in the assembly of the flagellum and the type III secretion system, and these structures contain a periplasmic domain (Galle *et al*., 2012; Bouteiller *et al*., 2021).

Last but not least, we must remember how the periplasm, together with the external membrane, constitutes an additional filter that slows down or prevents the entry into the cytoplasm of toxic molecules, including antibiotics. Moreover, enzymes capable of hydrolyzing β-lactams (β-lactamases) that managed to cross the external membrane can be present in this compartment. The combined effect of poor penetration and drug inactivation makes many Gram-negative bacteria inherently resistant to different β-lactam antibiotics (Montaner *et al*., 2023).

1.2.2.3 Inner membrane (IM)

In *P. aeruginosa* the internal limit of the periplasm is defined by the CM formed by four lipid chemical classes: phosphatidylethanolamines, phosphatidylcholines, phosphatidylglycerols and cardiolipins (Kondakova *et al*., 2015).

Phospholipids are composed of an acyl chain whose length varies from C14 to C18 and can further be saturated, unsaturated or cyclopropylated. These different organizations represent responses to the environmental conditions to which the bacterium is exposed, in order to modulate the stability and fluidity of the membrane (Benamara *et al.,* 2014).

Furthermore, it has recently been highlighted that amphiphilic aminoglycoside derivatives are able to interact with cardiolipins, thus inducing an IM permeabilization with dysregulation of the respiratory chain. This antimicrobial activity might be associated with other antibiotic compounds to improve their response and allow therapeutic success (El Khoury *et al*., 2017; Swain *et al*., 2018).

Numerous proteins are also inserted into the internal membrane, and they are involved in various essential processes for the bacterium; examples of these are translocons, regulatory proteins and

export systems, involved in bacterial adaptation and virulence (Bleves *et al*., 2010; Casabona *et al*., 2013).

1.2.2.4 Capsule and extracellular polysaccharide matrix

Different Gram-negative bacteria produce an outer polysaccharidic protective layer, the capsule, that surrounds the OM and is attached to lipid A. The capsule protects the bacterium from phagocytosis by polymorphonuclear granulocytes and prevents bacterial death caused by bactericidal serum factors (Williams and Tomas, 1990). In addition, it can provide resistance to desiccation, confer adherence to host cells and is responsible for the glistening property of colonies grown in rich media plates (Roberts, 1996; Brisse *et al*., 2006). The main pathogen characterized by capsule production is *K. pneumoniae* for which more than 80 capsular types have been described, with various involvements in determining virulence (Ørskov and Ørskov, 1984; D'Andrea *et al*., 2014).

Conversely, *P. aeruginosa* has the ability to produce an exopolysaccharide matrix, that can be constituted of alginate (D-mannuronic and L-guluronic acids), Psl (D-mannose, L-rhamnose, and D-glucose) or Pel (glucose-rich) polymers (Ryder *et al*., 2007; Franklin *et al*., 2011; Whitney *et al*., 2012). The exopolysaccharide differs from a capsule because it is not attached to the OM (Costerton *et al*., 1981; Cescutti, 2010).

Exopolysaccharides and capsule equally contribute to protect bacteria and to increase the impermeability of the envelope to different compounds, including antibiotics. In particular, alginate is implicated in biofilm formation, enhancing the bacterial isolation from the hostile environment (Hentzer *et al*., 2001; Yin *et al*., 2013; Li *et al*., 2019). This mucoid phenotype is often found in strains involved in CF respiratory infections but, notably, it has not been found in reference *P. aeruginosa* PAO1 and PA14 strains (Wozniak *et al*., 2003; Yin *et al*., 2013).

1.3 Porins

The Gram-negative diderm envelope confers an effective protection against toxic compounds. This feature also allows the bacteria to reduce their exposure to antibiotics that generally target periplasmic or cytoplasmic pathways and thus must diffuse through one or two membranes, of which the outermost is extremely impermeable to hydrophilic compounds. However, the bacterial physiological needs imply that nutrients and other substrates must cross the OM barrier. This function relies on specific OM porins that represent entrance doors, with different levels of selectivity.

In this chapter we focus on the *P. aeruginosa* porin repertoire, highlighting also differences and similarities with the systems expressed by *Escherichia coli*. We focus on three of the four porin families produced by *P. aeruginosa*, with a particular description of their role in antibiotic penetration. Due to a different involvement in antibiotic resistance, the same attention has not accorded to all members of the *P. aeruginosa* porin arsenal. For this reason, the information related to some channels remains elementary, while for other porins numerous studies have focused on various aspects, supplying a more elaborate knowledge.

We therefore provide an exhaustive overview of the general and substrate specific porins while the TonB-dependent transporters (TBDTs) will be treated in a more general way due to their abundance and their lower involvement in classical antibiotic permeation. Concerning substrate specific porins, the main focus will be on OprD, whose expression represents a well-recognized model for modifying the OM permeability thus conferring antibiotic resistance. The other substrate specific porins belonging to the OprD family are reviewed in order to assess their possible implications in antibiotic permeation. A summary of the various characteristics of the substrate specific porins is reported in Table 1. Details on the different pathways that lead to a reduced or absence of OprD expression are given in the chapter dealing with β-lactam resistance mechanisms.

Porin	Alternative name	Preferential substrate	Antibiotic	Mass (kDa)	Preferential conductance (pS)
OprF	PA1777	*Structural*		37.6	-
OprD	OccD1 (PA0958)	Arg, Lys, His	Imipenem, Meropenem.	45.9	21
OpdP	OccD3 (PA4501)	Gly-Glu, Arg	Meropenem	53.0	670
OpdC	OccD2 (PA0162)	His, Arg		48.9	20
OpdB	OccD7 (PA2700)	Pro			-
OpdT	OccD4 (PA2505)	Tyr		49.8	158
OpdI	OccD5 (PA0189)	Tricarboxylates, citrate, aconitate.		48.9	20
OprQ	OccD6 (PA2760)	Arg	Meropenem	46.9	420
OpdJ	OccD8 (PA2420)	Arg	Aztreonam	51.3	
OpdK	OccK1 (PA4898)	Vanillate, benzoate	Carbenicillin, temocillin, cefoxitin, tetracycline.	45.8	240
OpdF	OccK2 (PA0240)	Glucoronate	Carbenicillin, temocillin, cefoxitin, gentamicin.	46.1	242
OpdO	OccK3 (PA2113)	Pyroglutamate	Cefotaxime	44.3	144
OpdL	OccK4	Phenylacetate, pyruvate		46.0	50
OpdH	OccK5	Cis-aconitate, citrate, succinate, glutamate.	Ceftazidime	47.0	353
OpdQ	OccK6	Nitrobenzoate	Pipera/tazo, meropenem.	46.7	71
OpdD	OccK7	Short-chain fatty acids, dicarboxylates	Meropenem	46.5	379
OprE	OccK8	Arg, Pro, glutamic acid, succinate	Ceftazidime, cefepime	49.7	216
OpdG	OccK9	Phtalate		45.4	-
OpdN	OccK10	5-aminolevulinate, glutamate		47.8	-
OpdR	OccK11	Phenylacetate		45.7	-
OprB	PA3186	Glucose, glycerol, fructose, mannitol.	Tobraycin, amikacin.	38.0	-
OprB2	PA2291	Glucose		37.0	-
OprB3	PA4099	Glucose		47.3	
OprP	PA3279	Monophosphate	Fosfomycin, fosmidomycin.	48.2	-
OprO	PA3280	Di-, poly-phosphate.	Fosfomycin, fosmidomycin.	47.8	-
FadL	PA1288	Fatty acid		45.6	-
FadL2	PA1764	Fatty acid		59.0	-
FadL3	P4589	Fatty acid		49.7	-
OprG	PA4067	Hydrophobic molecules, Fe^{2+}	Ceftazidime, tetracycline, kanamycin.	25.2	-
OprH	PA1178	Membrane stabilization	Polymyxins	21.6	-
Tsx	PA0165	Nucleosides, deoxynucleosides.		31.4	-
Tsx	PA0234	Nucleosides, deoxynucleosides.		31.1	-
SphA	PA5325	Sphingosine		35.5	-
QbdB	PA3772	Sphingosine		32.7	-

Table 1: List of substrate specific porins described throughout this chapter; the alternative names, according to the Occ nomenclature, and the PAO1 gene annotation is reported together with the molecular mass. Preferential substrates, antibiotics for which some involvement has been reported, even if not directly correlated to the transport and the conductance measurements described in the text are also reported (in the case of more sub-states, the value ascribable to the most prevalent is reported).

1.3.1 *P. aeruginosa* and *E. coli,* similarities and differences

The OM of Gram-negative bacteria is rich in transmembrane β-barrel proteins that consist of antiparallel β-strands, connected by extra membrane loops governing the uptake of nutrients and other hydrophilic compounds that otherwise would not permeate through the OM. These proteins are water-filled diffusion channels known as porins and first described in *E. coli* in 1976 (Nakae, 1976).

Gram-negative bacteria generally possess non-specific general porins (like OmpF, OmpC and PhoE in *E. coli*) consisting in a trimeric structure, where each monomer is composed by 16 intramembrane β-strands and, as a consequence, the channel is formed inside these three monomers (Cowan *et al*., 1992). They enable passive diffusion depending on the size, shape, charge, and polarity of the substrates and on their concentration gradients. The passage takes place without binding the substrates with a measurable affinity and the general porins are highly efficient in allowing the diffusion of molecules up to a defined size exclusion limit. Their function is commonly exploited by antibiotics to cross the OM.

Gram-negative bacteria, owing to the presence of the additional OM barrier, possess additional specific porins responsible for the internalization of essential compounds that might be in low concentration in the environment. We can mention for instance the *E. coli* porins LamB and Tsx, which constitute a path for sugars and nucleosides respectively (Klebba *et al*., 1994; Ye and van den Berg, 2004).

However, *P. aeruginosa* produces only the latter type of proteins and, despite the differentiation between general porins and specific channels, the literature generally refers to *P. aeruginosa* channels as “porins” (Henderson *et al.,* 2016).

In *P. aeruginosa* the absence of large nonspecific pores is one of the causes of its high intrinsic impermeability. It has long been known, in fact, that its OM permeability is up to 100-fold lower than that of *E. coli* (Nikaido and Hancock, 1986).

In the *P. aeruginosa* PAO1 genome at least 70 porins have been identified and these can be subdivided into four different types: 1) general/non-specific, 2) substrate specific, 3) TonB family of gated porins and 4) OprM family, involved in efflux pump systems (Stover *et al*., 2000; Hancock and Brinkman, 2002). We now focus on the first three types, while we will discuss the OprM family porins as a part of efflux pump systems.

1.3.2 General porins

In this subclass of porins in *P. aeruginosa* we find only one member, but for its features is important for bacterial survival and essential for its virulence (Jurado-Martín *et al*., 2021).

The monomeric 37.6 kDa OprF is the most expressed porin in *P. aeruginosa*. Firstly identified in 1979 as protein F, it can be considered as homologous of *E. coli* OmpA, due to a 76 % similarity in the C-terminal region (Hancock *et al.,* 1979; Duchêne *et al*., 1989).

Usually, there are approximately 10^5 to $3 \cdot 10^5$ OprF copies in each cell (Nicas and Hancock, 1983). Nevertheless, *P. aeruginosa* is defined by a low effective permeability for small sugars, as a result of the OprF 40-fold lower permeability when compared to *E. coli* OmpF for this type of substrates (Yoshimura *et al*., 1983).

However, OprF allows the passage of larger molecules than its *E. coli* orthologues, enabling the uptake of solutes up to 3 kDa, while for instance OmpF is able to translocate solutes only up to 500/600 Da (Bellido *et al*., 1992; Hancock and Brinkman, 2002; Eren *et al*., 2012).

The porin exhibits two conformers, a closed state representing approximatively 95 % of the expressed porins, and 5 % as an open conformer. The current model supposes that the porin can alternate between both structures, depending also on environmental factors (Sugawara *et al*., 2006; Nestorovich *et al*., 2006).

It has been argued that the closed conformer is required for the structural integrity of the cell envelope and its stability, probably due to interactions with other proteins such as OprI, an OM lipoprotein, or the PG-associated OM protein OprL (Navare *et al*., 2015).

The open state resides in the first 162 amino acids that fold as a single β-barrel domain, forming a 2 nm pore that determines the exclusion size limit. In this conformation, the porin is not associated with structural proteins, but different OprF molecules can oligomerize and form multiprotein complexes (Brinkman *et al*., 2000; Sugawara *et al*., 2006).

This dual nature has generated many controversies regarding its role in permeation. Despite the large number of studies concerning this porin and its involvement in various biological processes, its role in the penetration of substrates still remains unclear and seems anyway very marginal.

OprF plays instead a very important role in other processes. For example, it is required for cell-shape maintenance, bacterial adhesion to different substrates, like the glial or the pulmonary epithelial cells and it is essential in quorum sensing, enhancing bacterial virulence (Fito-Boncompte *et al*., 2011). Moreover, OprF has also been associated with biofilm formation, for example interacting with the fucose binding protein LecB, and acting in cooperation for the adhesion that is required for biofilm growth (Funken *et al*., 2012). OprF is also found in the Outer Membrane Vesicles (OMVs), the

micelles commonly produced by Gram-negative bacteria. The OMVs are generated by budding from the OM, thus inheriting its structural components, and are filled with periplasmic content. They represent a response to stress and transport communication or virulence factors and are also involved in the escape from host immune system (Kulp and Kuehn, 2010).

Interestingly, a strain with an *oprF* deletion has shown anyway an OMV overproduction (Wessel *et al*., 2013). This seems to indicate that OprF is not an essential element for OMV functionality, but can be present in these structures due to its abundant presence in the OM.

Due to its elevated expression in *P. aeruginosa* cells, OprF has promisingly been investigated for designing an antipseudomonal vaccine (Gomi *et al*., 2017; Hassan R. *et al*., 2018), but further studies are necessary before this porin becomes a practical target for therapeutic purpose.

1.3.3 Specific porins

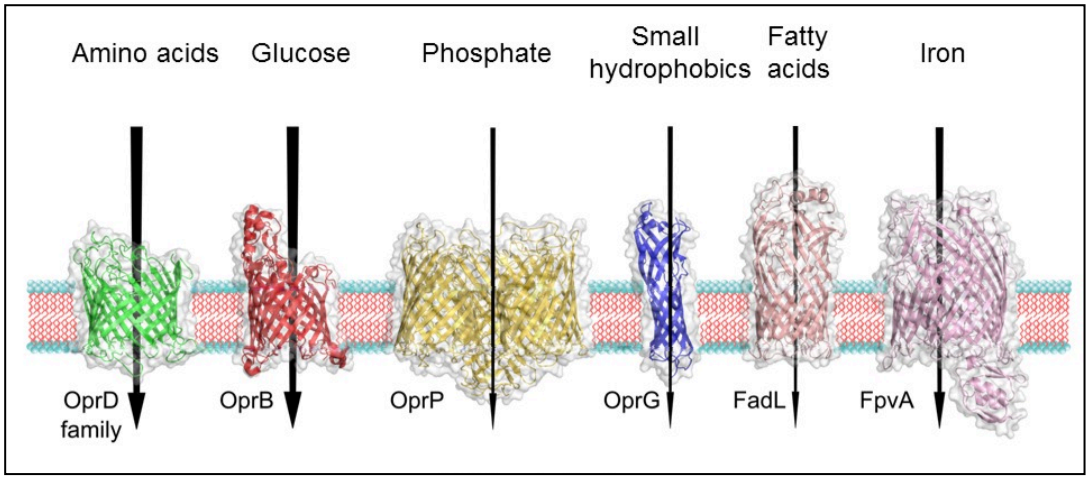

Figure 4: Graphic representation of different substrate specific and TBDT porins expressed by *P. aeruginosa* (www.translocation.eu).

This group of *P. aeruginosa* porins includes more than 30 members, all characterized by the presence of specific sites that allow single molecules to bind (Figure 4). These specific sites enable the uptake of substrates present in the external medium in low concentrations, a function that would not be possible with the non-specific porin OprF. The abundance of such channels in *P. aeruginosa,* probably derived from duplication events occurred during its evolution, is one of the reasons for the extreme versatility of this bacterium (Stover *et al*., 2000). These porin genes are often found in the genome adjacent to genes encoding for specific proteins, whose substrates can be internalized by the same specific porin. This genetic organization often allows a positive induction of the porin when its preferred substrate is present in the external medium (Tamber *et al*., 2006). Nevertheless, the

possibility that some compounds can diffuse through these porins, albeit less efficiently, in a concentration gradient-dependent manner cannot be completely ruled out (Tamber *et al*., 2006). Traditionally, these porins have been named with the prefix Opr (**o**uter membrane **pr**otein), followed by a letter that identifies the specific porin. For example, OprP and OprO are specific porins for phosphate and polyphosphate respectively, OprC is involved in copper homeostasis, and OprD is responsible for the uptake of basic amino acids. The mapping of the first *P. aeruginosa* genome led to the identification of a total of a further 18 OprD paralogs, sharing 46 to 57 % sequence similarity and to the definition of the new discovered porins with the prefix Opd (**o**uter membrane **p**rotein **D**) (Figure 5) (Tamber *et al*., 2006). Interestingly, the same type of channels is detectable in other species, like *A. baumannii* that possesses at least five orthologues (Eren *et al*., 2012). Within these 19 porins, a further subdivision was made between 7 porins than share a greater amino acid sequence similarity with OprD and have a marked propension for cations uptake, while 10 porins are more related to OpdK and involved in anions translocation (Liu *et al*., 2012a; Liu *et al*., 2012b). This feature resulted in a second nomenclature, based on the prefix Occ (**o**uter membrane **c**arboxylate **c**hannel) that refers to the common characteristic, followed by a letter (D or K depending on the higher affinity with OprD or OpdK) and a progressive number (Eren *et al*., 2012). Despite their homology, the 19 Occ family porins are well distinguished on the basis of the specific substrate transported and, ultimately, for the peculiar ability to enable antibiotic permeation. It must be noted, however, that the role of substrate spectrum differences between the two porin groups has recently been considered to be less important, since it has been shown that both porin groups play a role in facilitating the permeation of different molecules (Ude *et al*., 2021). Finally, the same authors have reconsidered the porin functions in *P. aeruginosa*, emphasizing the possibility that many antibiotics and nutrients might be able to permeate via a porin-independent pathway (Ude *et al*., 2021).

1.3.3.1 OpdD subfamily

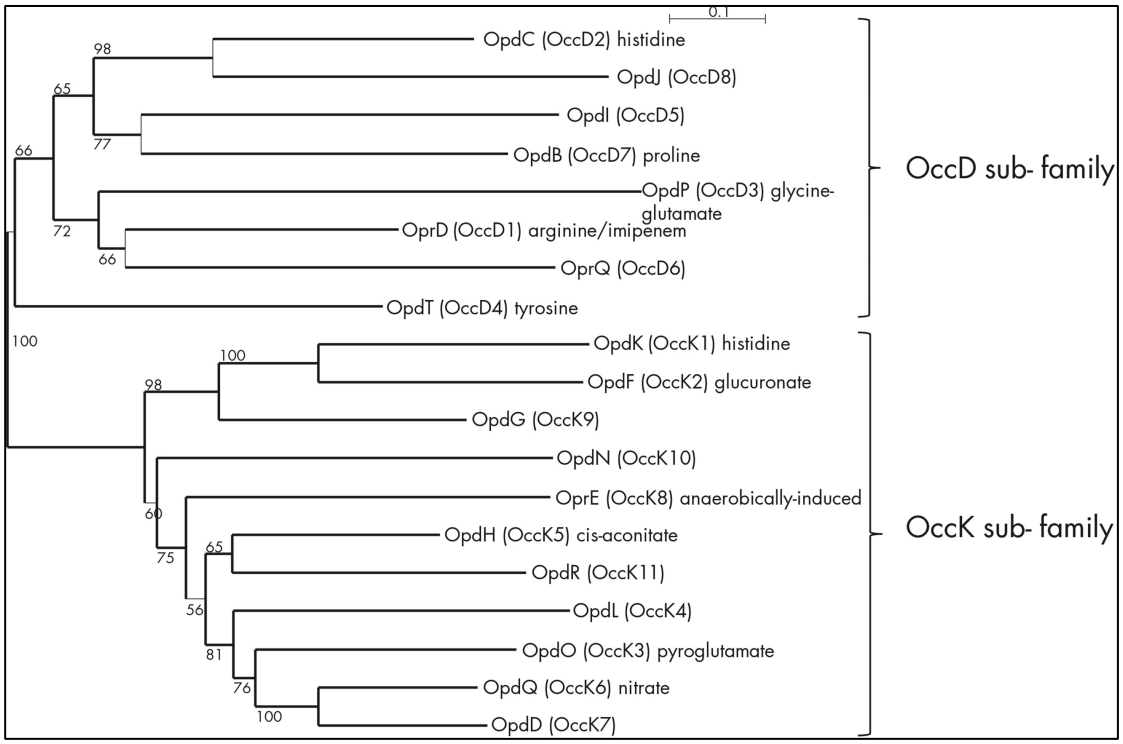

Figure 5: Phylogenetic relationships among OprD and its 18 paralogs sequences from *P. aeruginosa* PAO1. Both nomenclatures (Opr and Occ) are reported, and the principal substrates related to each porin are shown. The unrooted dendrogram was generated using neighbor-joining algorithm from evolutionary distances; bootstrap values correspond to 1000 pseudo-replicates (Chevalier *et al*., 2017).

1.3.3.1.1 OprD

OprD is the most studied substrate specific porin, because of its role in carbapenems uptake and antibiotic resistance that was firstly highlighted in 1990, only five years after the beginning of imipenem clinical use (Trias and Nikaido 1990b). Initially known as outer membrane protein D2 or OprD2, and currently also named OccD1, it is a 45.9 kDa monomeric protein consisting of 443 amino acids, structured into 18 β-sheets, connected by 8 loops on the periplasmic side and 9 on the external side (Eren *et al*., 2012). The solved crystal structure revealed a negative charged, narrow pore (~ 2,15 Å), whose width is delimited by loops 3 and 7 and characterized by two positively charged arginine residues (Figure 6).

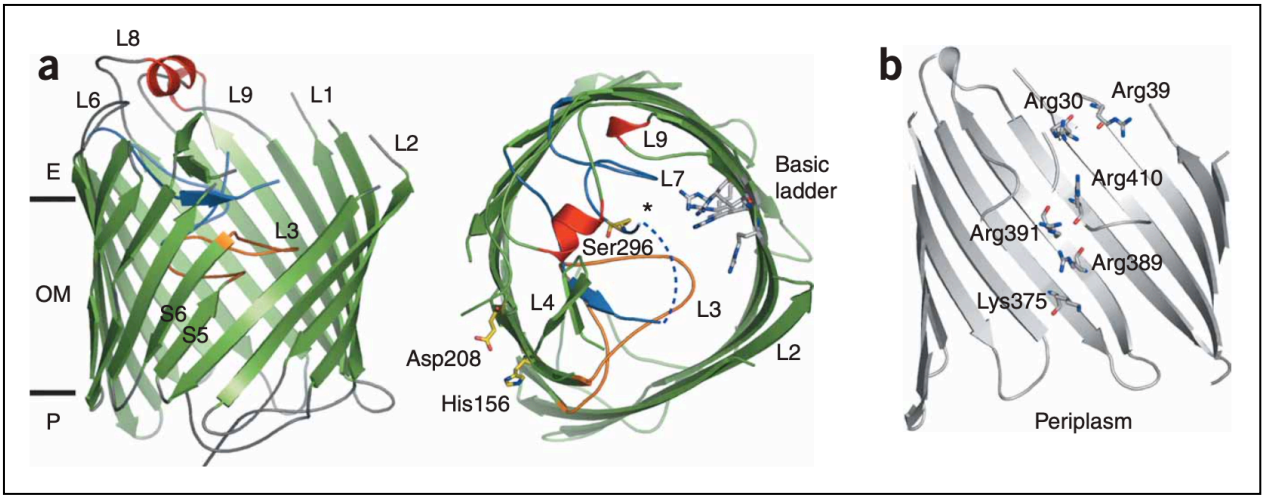

Figure 6: Structure of *P. aeruginosa* OprD. **a)**: OprD from the side (left) and from the extracellular environment (right). β-strands are represented in green; loops and turns in gray; α-helices in red; constrictions loops L3 and L7 in orange and blue, respectively **b**): representation of OprD basic ladder (Biswas *et al*., 2007).

The presence of a basic ladder is a conserved feature among OccD porin family members. This basic ladder is responsible for an asymmetric charge distribution that may drive the flux of substrates, particularly those with an acidic group (Figure 7) (Biswas *et al*., 2007; Eren *et al*., 2012).

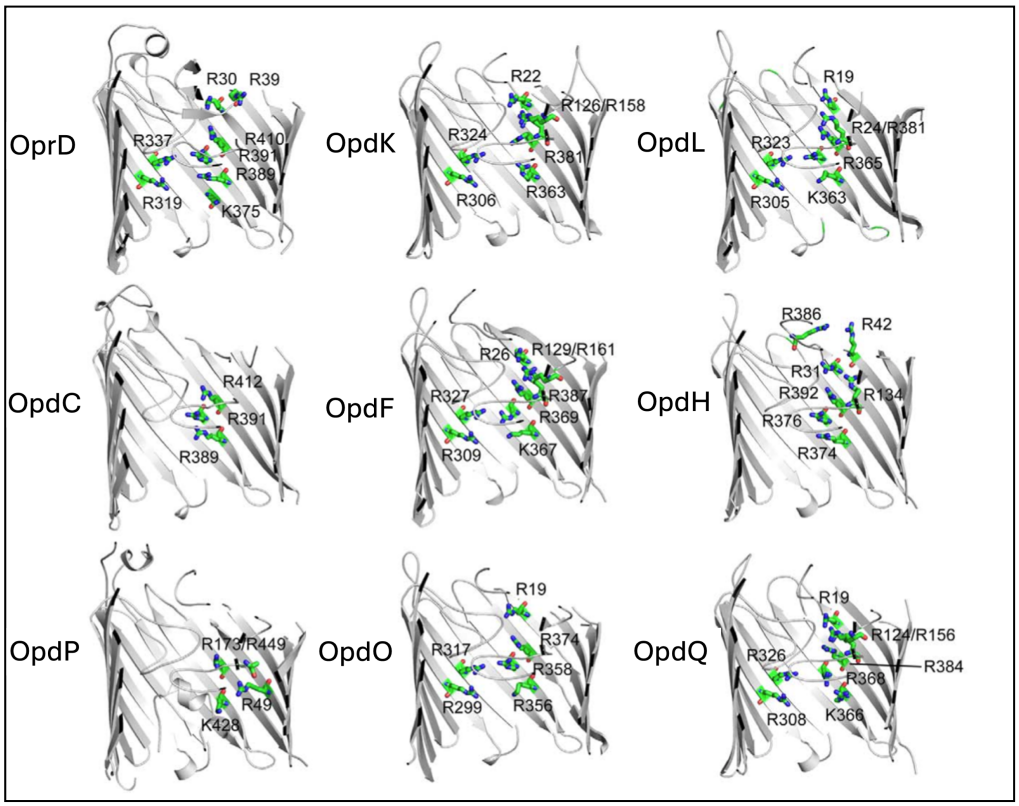

Figure 7: Representation of the conserved basic ladder among OprD and other eight porins belonging to the OprD subfamily. Porins are shown in identical orientations and the specific basic residues are numbered (Eren *et al*., 2012).

The OprD association to form a labile trimeric structure conformation was also suggested, but it appears to be unstable (Biswas *et al*., 2007). OprD exhibited a preferential and stable open state defined by low conductance (21 ± 3 pS) and the occurrence of rare and shorts spikes that can reach up to 900 pS (Liu *et al*., 2012a). One of the reasons of the low conductance stems from the constriction region formed by loop 3. In fact, an OprD with a mutated loop 3 was shown to possess a higher than usual conductance (~ 90 pS) (Biswas *et al*., 2007). Despite its usually low conductance, due to its abundant expression, OprD is a porin of great interest for *P. aeruginosa* viability.

OprD is synthetized in the cytoplasm as a pre-protein, with a 23-amino acid signal peptide and addressed to the IM via the Sec translocon. In the periplasm, it loses the signal peptide and is subsequently inserted in the OM via the BAM complex (Solov'eva *et al*., 2012; Klein *et al*., 2019). OprD possess a narrow constriction pore predominantly negatively charged, where two positively charged arginine residues on one face of the pore give rise to an asymmetric charge distribution. Four others positively charged residues (arginine and lysine), located on the pore constriction and on the extracellular funnel, constitute an electrophoretic path that promote the uptake of molecules containing an acidic group (Figure 6) (Biswas *et al*., 2007). Given these features, even a limited number of amino acid substitutions can alter the OprD ability to be correctly inserted into the OM or can modify the translocation specificities of the pore (Huang *et al*., 1995; Li *et al*., 2012).

OprD is the major pathway for the translocation of basic amino acids, like arginine, lysine, and histidine. Its involvement in small peptide (Ala-Lys, Lys-Ala, Thr-Ser-Lys, and Pro-Phe-Gly-Lys) and gluconic acid uptake have also been established (Trias and Nikaido, 1990a; Huang and Hancock, 1993).

On minimal medium, this expression of the porin has been shown to be positively induced by arginine, glutamate, or histidine when these amino acids are added as sole carbon or nitrogen sources. This regulation appears to be mediated by ArgR, an arginine regulator, in the case of arginine mediated induction (Ochs *et al*., 1999b). However, a glutamate OprD induction is also possible in an *argR* deficient mutant, indicating the presence of other regulators that contribute to a more complex modulation (Ochs *et al*., 1999a). A negative regulation has also been shown after exposure to the preferred carbon sources, but this effect appeared to be due to the presence of metals such as zinc, copper, and the aromatic weak acid salicylate (Ochs *et al*., 1999a). The key factor behind zinc mediated OprD repression is the regulator CzcR (Caille *et al.*, 2007), while CopR is involved in porin downregulation in presence of copper (Perron *et al*., 2004). Moreover, OprD expression is inversely proportional to that of the MexEF-OprN efflux pump, that is regulated by a different mechanism and could also be influenced by several mutations (Ochs *et al*., 1999a). All these mechanisms contribute

to shed light on OprD expression that is carefully regulated in order to protect the bacterium when it is exposed to toxic compounds, by reducing its uptake capacity, and increasing its extrusion ability. OprD is one of the preferred porins used by carbapenems to diffuse across the *P. aeruginosa* OM and, as a consequence, any variation in OprD expression results in changes in its susceptibility to carbapenems (Hancock and Speert, 2000; Gutiérrez *et al*., 2007). The OprD involvement in imipenem uptake is due to the structural similarity between the natural substrate arginine and the antibiotic, and more specifically to the carboxyl group and the substituent on C2 of the imipenem molecule (Figure 8) (Trias and Nikaido, 1990a). A confirmation of this involvement arises also from the evidence that the addition of L-Lysine to the medium during antibiotic susceptibility determination contributes to an increase in the imipenem minimal inhibitory concentration (MIC) value, ranging up to 8-fold (Fukuoka *et al.,* 1993).

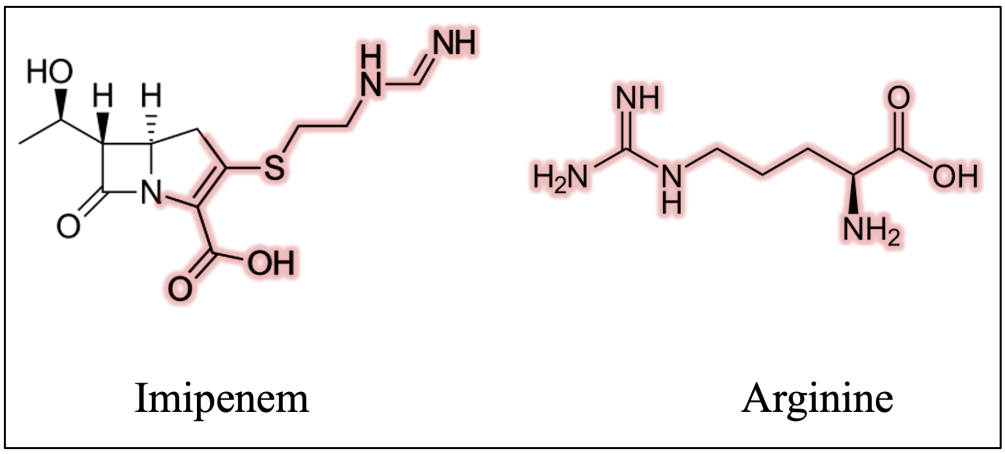

Figure 8: Comparison between the structures of the amino acid arginine and the carbapenem imipenem.

In the literature, unfortunately, there is a great confusion about the OprD role in the uptake of other carbapenems. Pérez and coworkers assumed that meropenem resistance was not influenced by OprD downregulation, due to the tendency of meropenem and others carbapenems, with the exclusion of imipenem, to use different channels for their translocation (Pérez *et al*., 1996). However, this assumption was soon refuted by Köhler's group that observed a 4 to 8-fold reduction of meropenem susceptibility in a strain deleted of OprD porin, although a clear resistance phenotype was solely associated with the overexpression of the MexAB-OprM efflux system (Köhler T. *et al*., 1999a). A similar conclusion was also reached by Sakyo and coworkers in 2006, who verified the increased resistance to different carbapenems (meropenem and doripenem) in *P. aeruginosa* isogenic mutants lacking the OprD porin (Sakyo *et al*., 2006). The disagreement about the real involvement of OprD in resistance to meropenem and other carbapenems can be due to the fact that the porin deletion causes an increased MIC endpoint for all carbapenems but not a clear resistance profile, according to the

clinical breakpoints for carbapenems published by the Clinical and Laboratory Standards Institute (CLSI) and the European Committee on Antimicrobial Susceptibility Testing (EUCAST), with the exception of imipenem (Hombach *et al*., 2012).

1.3.3.1.2 OpdP

OpdP or OccD3 is the largest substrate porin expressed by *P. aeruginosa,* with a molecular mass of approximatively 53 kDa with 51 % homology to OprD. It is a monomeric 18-stranded β-barrel porin, synthetized in the cytoplasm and addressed outwards after the cleavage of a predicted 25 amino acids signal peptide. Similarly to OprD, the pore contains a basic ladder and is delimited by loops 3 and 7, but differs by a larger diameter (~ 3 Å). In the N-terminus 30 residues contribute to shrink the hole that otherwise would be larger (Liu *et al*., 2012a; Soundararajan *et al*., 2017). The porin is also known as PA4501, from the first PAO1 genome annotation (Stover *et al*., 2000). It is important to note that sometimes OpdP is erroneously referred to as OpdD, most likely due to an imprecise initial genome annotation. Unfortunately, this attribution is still reported in a number of articles, generating a lot of confusion among researchers who try to shed further light on this porin's properties (*e.g.,* Sonnleitner *et al*., 2012; van Delden *et al*., 2013; Bitar *et al*., 2022; Salvà-Serra *et al*., 2023). To the best of our knowledge, OpdD refers to OccK7, another substrate specific porin with no marked homology with OpdP, albeit in the annotated *P. aeruginosa* PAO1 (www.pseudomonas.com) the porin was named OpdD until July 2023. Our group has recently flagged this incongruence to the administrators of the *Pseudomonas* database, and the reference to OpdD has since been eliminated to avoid further confusion.

The OpdP porin is strictly correlated to the ATP-binding cassette superfamily (ABC) dipeptides transporter system, consisting of different proteins responsible for the amino acid uptake, in particular dipeptides in stationary phase, thus enlarging the bacterial metabolic versatility (Kiely *et al*., 2008; Pletzer *et al*., 2014; Chevalier *et al*., 2017). The network includes an ABC transporter (DppBCDF), four dipeptide-binding proteins (DppA1-4), a Metallo dipeptidase (MdpA) and the repressor PsdR. A further component (DppA5), located downstream (~ 940000 base pairs away) in the genome, has been identified for its homology to the other dipeptide binding proteins, and appears to be related to the other four dipeptide-binding proteins (Kiely *et al*., 2008; Pletzer *et al*., 2014).

In general terms, after a protein's extracellular degradation mediated by different proteases, the mechanism should perform the dipeptide transfer from the outside into the periplasm through the OpdP porin. The subsequent translocation into the cytoplasm is mediated by the ABC transporter and the cytoplasmic cleavage is performed by various peptidases. Among these, the MdpA

dipeptidase enables the dipeptide metabolism as carbon sources and, by consequence, this pathway is associated with a faster bacterial growth in the absence of other nutrients (Kiely *et al*., 2008; Pletzer *et al*., 2014).

However, two different gene organizations have been proposed for this machinery. The first one assumes that *opdP* belongs to the *dppA4BCDF* operon, that also encodes the proteins mentioned before, all regulated by PsdR (Kiely *et al*., 2008). On the other hand, the same region has been described to be organized as a shorter operon, only including the *dppBCDF* ABC transporter, regulated by PsdR. In addition, a second operon is constituted by the dipeptide binding proteins *dppA4* and *opdP* (Pletzer *et al*., 2014). Also in this description, the regulation and transcription of the dipeptidase and the dipeptide binding proteins are reported as correlated for a successfully internalization of metabolites, especially in nutrient deprivation conditions (Pletzer *et al*., 2014; Willsey and Wargo, 2015). Furthermore, recent studies have shown that *psdR* is prone to acquire mutations but their impact on the OpdP expression have not been described yet (Asfahl *et al*., 2015; Liu *et al*., 2012a; Smalley *et al*., 2022).

In any case, irrespective of how the expression of these genes is described, there is no doubt that this ABC transport system is participating in recruiting nutrients, involved in alternative metabolic systems, modulated for instance by the catabolite repressor control or by the alginate regulator (Browne *et al*., 2010; Sonnleitner *et al*., 2012; Hua *et al*., 2022). In addition, we should not forget its role in strengthening biofilm formation and regulation, thus acting as an important virulence factor (Pletzer *et al*., 2014; Lee Y. *et al*., 2018).

The *dpp* operon is quite conserved in Gram-negative and Gram-positive bacteria, including *E. coli* and *Bacillus subtilis* (Abouhamad and Manson, 1994; Slack *et al*., 1995). By way of illustration, in *E. coli* it has been established that its expression is correlated with chemotaxis regulation and is more expressed during the stationary phase of bacterial growth (Abouhamad *et al*., 1991; Abouhamad and Manson, 1994). Although no evidence of a growth dependent regulation of this operon in *P. aeruginosa* has been mentioned in the literature, the possibility that, in the stationary phase, the bacteria can induce a different metabolism when the primary carbon sources are being consumed, as observed for *E. coli,* might apply also to *P. aeruginosa*.

The pioneering work of Hancock and coworkers has demonstrated that OpdP is induced by the glycine-glutamate dipeptide, that appears to be its natural substrate (Tamber *et al*., 2006). Furthermore, its involvement in arginine uptake has been proposed, especially in an OprD-deficient isogenic mutant. An arginine-mediated induction was also verified, highlighting a redundancy of OprD and OpdP porins for the translocation of the basic amino acid arginine. However, its role in the

uptake of the basic amino acid analogous antibiotics imipenem and meropenem was only supposed without a clear demonstration (Tamber and Hancock, 2006).

It was only in 2015 that Miller and coworkers discovered the OpdP role in antibiotic uptake. In a nutshell, they constructed a transposon insertion mutant in a *P. aeruginosa* PAO1 *ΔoprD* strain and they subjected it to meropenem stress (0.5 μg/mL, that corresponds to 1 x MIC), identifying strains with an *opdP* disrupted gene as the only porin mutants with a selective advantage in response to this antibiotic (Isabella *et al*., 2015). Another proof of the OpdP involvement in meropenem uptake was provided by Van Bambeke's group. They simply showed that the MIC value for meropenem in a PAO1 *ΔoprD* strain increases 2-fold (from 2 to 4) when 10 mM glycine-glutamate (Gly-Glu) dipeptide, the natural OpdP substrate, was added to the medium (Chalhoub *et al*., 2016). In view of these considerations, we can speculate that the hypothetical porin reported in 1999 by Köhler's group might be OpdP. They studied a *P. aeruginosa* PAO1 Δ*oprD* and found, after exposure to meropenem, a spontaneous mutant with a decreased expression of an unknown 55-kDa porin. Interestingly, this mutant revealed a slightly increased MIC for meropenem, compared to its parental strain (Köhler T. *et al*., 1999a).

Conductivity studies, performed by Winterhalter and colleagues on planar lipid bilayers, revealed that OpdP, when in its unique open conformation, is characterized by a higher conductance compared to the ortholog OprD (1 nS vs 20 pS, respectively) and to the other OccD subfamily members. Similar results were obtained by Liu and coworkers that determined OpdP conductance as approximatively 670 pS (Liu *et al*., 2012a). These results report conductivity values that are more similar to the non-specific *E. coli* porins that, by way of comparison, are OmpF ~700 pS per monomer and OmpC ~900 per monomer (Saint *et al*., 1996; Biró *et al*., 2010). In addition, it has been shown that the presence of negatively charged residues in the constriction zone of loop 7 and in the basic ladder of the OpdP porin is important. Indeed, the residues in both locations play a crucial role in the translocation of compounds with an amino group such as imipenem and meropenem, demonstrating an active role of OpdP for carbapenem uptake (Soundararajan *et al*., 2017). The expression levels of OprD and OpdP are nevertheless unbalanced, with that of the former higher than that of the latter, in this way showing that OpdP contributes minimally to the wild type strain carbapenem uptake.

Despite the fact that some evidence on the possible role of OpdP in antibiotic resistance has emerged, no strain with the only mutation in this porin defined by a carbapenem resistance phenotype has been isolated yet. Nevertheless, a recent study has started taking into consideration the carbapenem translocation through OpdP in clinical strains characterized by OprD deletion/mutation, that did not however exhibit the characteristic phenotype of the specific imipenem resistance.

This study has indeed shifted the attention on OpdP as a target for research, in particular with the aim of quantifying its expression, in order to better understand its contribution to the final resistance phenotype in clinical strains (Atrissi *et al*., 2021).

All the results and evidence reported so far are particularly interesting because OpdP expression appears to be regulated within an operon by different external stimuli. In a naturally low OM permeability situation, during the stationary growth phase and/or in biofilm growth, a more pronounced expression of a porin with some carbapenems selectivity might emerge. This is an interesting possibility that should be kept in mind.

1.3.3.1.3 OpdC, OpdT and OpdB

OpdC, also known as OccD2 shares a 58 % homology with OprD. It is induced by histidine and for this reason it has been correlated to the uptake of this amino acid, but it appears to be involved in low levels of non-specific uptake of basic amino acids and dipeptides (Tamber and Hancock, 2006; Tamber *et al*., 2006). It is conserved among different *P. aeruginosa* strains, possessing a narrow pore (< 3 Å) and having a conductance of approximatively 20 pS (Chevalier *et al*., 2017; Liu *et al*., 2012b). Interestingly, OpdC expression appears to be regulated by SigX as a stress response (Schulz *et al*., 2015; Fléchard *et al*., 2018).

OpdB, also known as OccD7, as the other members of the OccD subfamily, shares a 57 % homology with OprD and its sequence appears to be conserved among different *P. aeruginosa* strains. It is constitutively expressed and involved in proline permeation (Tamber *et al*., 2006). It is included in an operon, together with the hypothetical proteins PA2699 and PA2701 that seems to be involved in histidine metabolism and/or in the twin-arginine translocation (Ulrey *et al*., 2014; Ball *et al*., 2016). Up to now however, the available data related to the proteins included in this operon are still too scant to allow a determination of their specific function.

OpdT or OccD4 was described for tyrosine uptake (Tamber *et al*., 2006), and unlike other members of the OccD subfamily, it is not responsible for arginine influx (Eren *et al*., 2012). In its open state a conductance of about 158 pS was determined (Liu *et al*., 2012a). OpdT seems to be induced by copper stress, that causes the simultaneous OprD downregulation via the Czc regulation system. As already mentioned, this event was postulated to be a compensatory mechanism to modulate the OM permeability as a response to copper exposure (Perron *et al*., 2004; Teitzel *et al*., 2006; Wright *et al*., 2019).

The expression of these three porins is relatively low and none of them has been shown to be correlated with the uptake of a specific antibiotic in contrast to OprD. However, in an experiment of

RNA seq, OpdC, OpdB and OpdT were included in the first five porins (after OprD and OpdP), expressed by a *P. aeruginosa* PAO1 strain grown in minimal medium. During this study, an isogenic mutant with the deletion of the five porins was obtained, but the phenotypic resistance profile was similar to that of the single *oprD* knock-out strain (Isabella *et al*., 2015).

1.3.3.1.4 Other OpdD-subfamily porins

Other OprD analogues, OpdI (OccD5), OprQ (OccD6) and OpdJ (OccD8) are expressed in a low copy number and appear to be used for the translocation of arginine, but no clear involvement in antibiotic uptake or resistance has been determined (Chevalier *et al*., 2017).

OpdI is poorly expressed and together with OprQ is apparently the only entry pathway for tricarboxylates, citrate and aconitate (Ude *et al*., 2021). In addition, OpdI has a low conductance signature (~20pS) (Liu *et al*., 2012a), so that its role in OM permeability is marginal.

OprQ, once known as OprE3, was defined for its ability to bind to human fibronectin, emerging as a virulence factor. In addition, its deletion resulted in strains with an increased growth rate under metal deprivation stress, underlying a potential role of the porin in the decrease of the *P. aeruginosa* multiplication rate under unfavorable conditions (Arhin and Boucher, 2010). The same authors speculate that an OprQ overexpression could lead to a more sensitive profile to some antibiotics, including meropenem, probably due to a different regulation of other proteins that interact with the antibiotic (Arhin and Boucher, 2010). Interestingly, OprQ exhibited two open sub-states, both characterized by a high conductance (~420 and ~1900 pS, respectively), although the same authors consider as implausible that the higher conductance prevails in physiological condition (Liu *et al*., 2012a).

OpdJ deletion was recently conjectured to increase the aztreonam MIC (McLean *et al*., 2019). It is important to consider however that the authors have reported analogous values of increased aztreonam MIC for both OpdJ and OprD deleted mutants, thus resulting in the first report of association between OprD and the aztreonam MIC, after years of experiments conducted with OprD mutants (McLean *et al*., 2019). We therefore believe that this result should be carefully examined and that it would be interesting to clarify the possible presence of other mutations that involve this particular resistance phenotype.

1.3.3.2 OpdK subfamily

This porins group is characterized by a marked homology with the vanillate specific porin OpdK (OccK1). Porins in this group share a characteristic constriction region with positively charged residues that confer a conserved selectivity for anionic substrates containing carboxylate groups. However, this selectivity is different for distinct OccK porins. Moreover, in planar lipid bilayer experiments OccK porins showed a conductance alternance between two or three possible open states, defined by variable openings (Liu *et al*., 2012b).

OpdK possess 18 β-strands and in early studies it has been described to have a kidney-shaped large pore (∼8 Å), characterized by the presence of both positively and negatively charged residues (Biswas *et al*., 2008). The pore size diameter was subsequently reassessed to ∼5 Å, revealing a more complex determination of porin's features on the basis of the solved crystal structures (Liu *et al*., 2012b). The porin is generally expressed as a monomer but, when overexpressed, it reveals a labile trimeric structure in the OM. The same authors determined that the channel's most probable conductance was between 345 ± 65 pS (Biswas *et al*., 2008). In a later study, Liu's group determined a lower conductance (~ 240 pS) but, in any case, they confirmed the higher conductance of OpdK compared to OprD (Liu *et al*., 2012a). OpdK appeared to have three different open-state conformations, depending on the conformational changes in the constriction loop L7, with the propensity for the high conducting O_2 sub-state (Cheneke *et al*., 2011; Pothula *et al*., 2015). The specificity for vanillate and aromatic acids was determined on the genetic context and after substrate exposure, but the real OpdK involvement in vanillate permeation, also due to the vanillate low solubility in water, still remains a subject of debate (Tamber *et al*., 2006; Biswas *et al*., 2008; Wang *et al*., 2012). The search for specific substrates led to benzoate, that was verified to be preferentially internalized through OpdK (Eren *et al*., 2012). However, due to its anion-specificity, OpdK has been proposed to facilitate the diffusion of carboxypenicillins such as carbenicillin and temocillin and the anionic cephalosporin cefoxitin (Eren *et al*., 2012; Chalhoub *et al*., 2017). In addition, disturbances in the normal anionic molecules flux were observed in the presence of tetracycline, a compound that lacks a carboxyl group, also highlighting a possible role in the diffusion of this antibiotic (Eren *et al*., 2012).

OpdF (OccK2) was first described as a glucuronate-specific porin but has also been associated to biofilm formation (Tamber *et al*., 2006; Eren *et al*., 2012; O'Toole, 2003). It has been described to fluctuate between three different open states, with the prevalence for O_2 with an estimated conductance of 242 ± 40 pS that was the highest among the three states (Liu *et al*., 2012b). The crystal structure of OpdF was solved with glucuronate, verifying the importance of the L3 and L7 loops in determining the substrate specificity (Eren *et al*., 2013). It was shown that OpdF shares its β-lactams

uptake specificity with OpdK, but differs by facilitating gentamicin, rather than tetracycline, translocation (Eren *et al*., 2012; Chalhoub *et al*., 2017).

OpdO (OccK3) was thought to mediate pyroglutamate uptake. It has a unique possible open state and a conductance of 144 ± 36 pS was determined (Tamber *et al*., 2006; Liu *et al*., 2012b). OpdO does not seem to have anion-selectivity, in contrast to the other sub-group members (Liu *et al*., 2012b). Interestingly, during a liposome swelling assay testing the pyroglutamate flux through OpdO, a strong disturbance has been observed in the presence of cefotaxime, suggesting the participation of OpdO in cefotaxime uptake (Eren *et al*., 2012). Like OpdP, OpdO is included in an operon, but in this case the genes encode a major facilitator superfamily transporter, involved in pyroglutamate/lactam uptake (Tognon *et al*., 2019). OpdO was found to be overexpressed in an artificial urine medium, probably in order to adapt the metabolism to the limited iron availability, by enhancing different amino acid degradation pathways (Tielen *et al*., 2013). Its upregulation has also been determined, as a consequence of AmiE aliphatic amidase overproduction, thus resulting in a decreased virulence due to a decrease in pyocyanin production (Clamens *et al*., 2017). In contrast to that of other homologues, OpdO expression is decreased upon biofilm growth (Tan *et al*., 2021). A recent study has shown a slight downregulation when *P. aeruginosa* is exposed to meropenem (Salvà-Serra *et al*., 2023).

OpdL (OccK4) was predicted to play a role in phenylacetate permeation and recently a preference for pyruvate has been reported (Ude *et al*., 2021). However, the capacity of OpdL-mediated phenylacetate uptake was determined as moderate but, remarkably exhibited the highest efficacity for this process among *P. aeruginosa* porins (Tamber *et al*., 2006; Eren *et al*., 2012). OpdL is characterized, in its most probable open sub-state, by a conductance of ∼50 pS, although a second conformation with a higher conductance is possible (Liu *et al*., 2012b). The study performed by Bumann and coworkers has emphasized the OpdL capacity to allow a pyruvate metabolism when the porin is singly expressed, revealing a novel function and a possible induction in presence of this substrate (Ude *et al*., 2021).

OpdH (OccK5) was defined as a tricarboxylate (*i.e*., cis-aconitate and citrate) but also succinate and glutamate specific porin (Tamber *et al*., 2006; Tamber *et al*., 2007; Ude *et al*., 2021) but their transport within the porin has not been fully explained (Eren *et al*., 2012; Underhill *et al*., 2022). However, the capacity to facilitate the influx of compounds containing anionic groups in the presence of various cation concentrations was assessed through an all-atom molecular dynamic (MD) simulation (Lee J. *et al*., 2018). OpdH has two possible distinct open state configurations with the most probable one exhibiting a high conductivity of 353 ± 22 pS (Liu *et al*., 2012b).

Similarly to OpdP and OpdO, OpdH is included in an operon (*opdH-tctCBA*) that, as in *Salmonella enterica* serovar Typhimurium, appears to be involved in an ABC tricarboxylate transport system (Tamber *et al*., 2007; Underhill *et al*., 2022). In the presence of a tricarboxylic acid the operon is activated via the two-component system TctD and TctE (Taylor *et al*., 2019). Interestingly, the TctDE regulator is involved in biofilm formation and is also able to maintain a certain level of aminoglycoside (tobramycin and gentamicin) resistance. This evidence was interpreted as implying a mediation by the regulation of OpdH expression (Zhang *et al*., 2013). However, a Δ*tctDE* mutant was found to be unable to growth on citric acid as a sole carbon source, even though the repressor deletion would have increased the OpdH expression, which questions its real contribution (Taylor *et al*., 2019; Underhill *et al*., 2022). The most recent hypothesis is that the tricarboxylates uptake is mainly driven by the tripartite TctCBA system, rather than OpdH, given the growth defects observed with citrate or cis-aconitate as sole carbon sources in a Δ*tctA* mutant and not in a Δ*opdH* strain (Underhill *et al*., 2022).

OpdH expression also seems to be directed by the catabolite repressor control, that manages the metabolism modulation as a response to bacterial stress (Fléchard *et al*., 2018). Moreover, the translocation of ceftazidime through OpdH was demonstrated by an increased MIC in an OpdH knock-out mutant, although this resistance phenotype has not been described yet in clinical strains (Tamber *et al*., 2007). The evidence provided by the literature cited here is not yet sufficient to fully explain the physiological role of OpdH, but these results emphasize the general complexity of porin specificity. Moreover, the availability of many research contributions on OpdH clearly underlines the requirement of a multi-sided approach to allow a better understanding of the properties of porins.

No substrate profile has been defined for **OpdQ** (OccK6) but the genetic context suggests a role associated to nitrobenzoate (Tamber *et al*., 2006) A weak anion selectivity and the ability to mildly allow the uptake of glucose, glutamate and the aromatic amino acid tyrosine have been reported (Liu *et al*., 2012b; Eren *et al*., 2012; Ude *et al*., 2021). Two possible open states have been identified, with a preeminence of the low conductance state, quantified at 71 ± 34 pS (Liu *et al*., 2012b). Little is known about this porin but notably its expression can be modulated by transcriptional and posttranscriptional regulations (Fowler *et al*., 2015). OpdQ expression can be downregulated under hypoxic growth conditions or enhanced as a response to nitrate or oxidative stress, also involving the carbon catabolite control system (Chang *et al*., 2005; Fowler *et al*., 2015; Fléchard *et al*., 2018; Martins *et al*., 2020). In addition, an upregulation in small colony variants has been demonstrated (Wei *et al*., 2011). Recently, two *P. aeruginosa* strains with discrepancies in antibiotic susceptibility were isolated from the same patient. Among the genes with a divergent expression, the increased OpdQ expression has been shown to be correlated with the phenotypic switch from resistant to

sensitive towards piperacillin/tazobactam (Huang *et al*., 2020). Moreover, the exposure to meropenem induced an OpdQ downregulation (Salvà-Serra *et al*., 2023). It is not easy to correlate the OpdQ expression with antibiotic resistance, but this kind of evidence provides a suggestion about the relevance that a porin may have with specific antibiotics.

OpdD (OccK7) may be involved in short-chain fatty acids or dicarboxylates permeation (Tamber *et al*., 2006). In support of this hypothesis, *opdD* belongs to an operon involved in fatty acids metabolism, although further studies are required to fully describe the functions of all the co-transcribed proteins (Ball *et al*., 2019). OpdD can assume three different open states, all of these enabling a good conductance with a preponderance for O_2, whose conductivity was determined at 379 ± 45 pS (Eren *et al*., 2012; Liu *et al*., 2012b). The simultaneous presence of meropenem and of the putative natural substrate benzoate showed a drastic decrease in benzoate uptake, leading to the assumption that meropenem can flow through OpdD (Eren *et al*., 2012). Furthermore, a genome computer-based analysis of clinical *P. aeruginosa* strains revealed the presence of *opdD* mutations in carbapenem resistant strains. However, the concomitant appearance of *oprD* mutations, the presence of Class D β-lactamases, and the lack of information about the efflux pumps expression are all factors that do not allow to conclude in a clear interdependence between OpdD and meropenem resistance (Savinova *et al*., 2021).

OprE (OccK8) has a small pore size with low conductance and a substrate specificity for arginine and proline was originally proposed (Tamber *et al*., 2006). However, its involvement in glutamic acid and succinate translocation was recently reported (Dogan Guzel *et al*., 2021; Ude *et al*., 2021). It was one of the first *P. aeruginosa* porins detected in the late 1980's, due to its relative abundance and its anaerobic induction mediated by the sigma factor RpoN as a stress response (Yamano *et al*., 1993; Yoshihara and Nakae, 1989; Yamano *et al*., 1998). Peculiarly, OprE can assume three different open conformations, distinguished by contrasting uptake properties, with the most likely state characterized by a conductance of 216 ± 20 pS (Dogan Guzel *et al*., 2021). The OprE involvement in ceftazidime and cefepime uptake was demonstrated. This was the consequence of the presence in the scaffolds of these two antibiotics of a negative group that helps the molecules to slide along the basic ladder and, at the same time, a positive group that enables the interaction with a specific residue in the recognition pocket of the porin (Samanta *et al*., 2018).

OpdG (OccK9) was associated to phthalate transport (Tamber *et al*., 2006). We can suppose that it is not an essential porin, on the basis of the detection of *P. aeruginosa* strains lacking this porin or producing a truncated version (Chevalier *et al*., 2017; Nascimento *et al*., 2016). Curiously, bacterial biofilm growth in the presence of *Candida albicans* showed an increased expression of OpdG (Alam *et al*., 2023) but the real role of this variation is still largely unexplained.

OpdN (OccK10) was predicted to be involved in 5-aminolevulinate or glutamate translocation (Tamber *et al*., 2006).

It has been hypothesized that **OpdR** (OccK11) participates in phenylacetate permeation (Tamber *et al*., 2006). Although this porin can acquire mutations, it appears to be conserved in more than 60 *P. aeruginosa* available genomes (Chevalier *et al*., 2017). This result might result from the inclusion of *opdR* into an operon involved in Acyl-CoA dehydrogenase production.

In spite of all the research conducted in recent years and leading to important inroads, little is known about these three porins and more studies are needed to characterize their specificities.

1.3.3.3 Other substrate specific porins

In addition to those belonging to the OprD family, *P. aeruginosa* has other porins that are involved in the internalization of important nutrients. We now provide a succinct description of the main characteristics of the channels that facilitate the uptake of elements essential to the survival of the bacterium.

For example, glucose, an essential sugar for *P. aeruginosa*, is absorbed by OprB and OprB2, two homologous porins that are characterized by a high degree of similarity. A third porin is OprB3 (PA4099), but it has not been widely studied so far. It is present in the *P. aeruginosa* PAO1 genome and shows a marked similarity with the two most studied glucose porins.

OprB was first considered as an 18-strand β-barrel, orthologous to the *E. coli* maltodextrins-specific LamB porin and initially believed to associate in trimeric structures (Hancock and Carey, 1980). However, it was later demonstrated that it is a monomeric 16-strand β-barrel with a specific transport profile for glucose and other monosaccharides such as glycerol, fructose, and mannitol but not for disaccharides (Wyle and Worobec, 1995; van den Berg, 2012). The OprB involvement in antibiotic uptake was excluded, at least for gentamycin, whose structure includes some sugar residues (van den Berg, 2012). However, a transposon mutant lacking OprB and OprB2 was shown to exhibit an increased MIC to tobramycin, another aminoglycoside antibiotic (MacLeod *et al*., 2012). Interestingly, another study showed that the deletion of both porins resulted in a strain with an unchanged growth capacity but with an altered transcription profile, affecting the virulence in animal infection models (Raneri *et al*., 2018). Another important result is that the decreased glucose intracellular availability derived from uptake deficiencies results in the inactivation of glycolysis, that is able to influence the activity of amikacin, and in general of aminoglycoside antibiotics (Tang *et al*., 2022). In this context, the possible reported changes in antibiotic susceptibility are the result of a metabolic response rather than of OM impermeability. OprB belongs to the *gltBFGKoprB* operon,

including *gltB*, that encodes a periplasmic binding protein and the other genes that constitute the specific ABC transporter. Notably, its induction on glucose-enriched media was observed (Hancock and Carey, 1980). Also the related **OprB2** porin is predicted to be included in an operon that contains a TBDT (PA2289) and a glucose dehydrogenase (PA2290), suggesting a precise regulation of nutrients uptake (Chevalier *et al*., 2017).

The phosphate translocation, induced under phosphate starvation conditions, is mediated by two specific porins **OprP** and **OprO**, respectively. They both are homotrimers of 16 strand β-barrels, that form narrow pores and share a 76 % homology (Siehnel *et al*., 1992). They both present an arginine ladder on the extracellular side and a lysine cluster on the periplasmic side, thus facilitating the flow of anionic compounds. However, they show different substrate specificities, due to their properties in the constriction region. OprP prefers the Pi monophosphate, while OprO is more oriented to di- and poly- phosphates (Hancock *et al*., 1992; Golla *et al*., 2022). During infections, they can be upregulated by the action of specific regulators, such as PhoB, while their repression is mediated by the transcriptional regulator TctD (Siehnel *et al*., 1992; Bielecki *et al*., 2015).

Research had documented an involvement of both porins in the uptake of fosfomycin and fosmidomycin, two phosphonic acid antibiotics. Fosfomycin is increasingly found to be a valid option in the case of infections due to MDR strains (Díez-Aguilar and Cantón, 2019). Fosmidomycin, that was in the beginning exploited as an antimalarial drug, has recently been repurposed as a valid therapeutic option against both Gram-positive and Gram-negative MDR strains, including *P. aeruginosa* (Knak *et al*., 2022). In particular, both antibiotics showed a preference for OprP (Piselli and Benz, 2021; Golla *et al*., 2022), although a previous study had emphasized a higher affinity of fosfomycin for OprO (Citak *et al*., 2018). Besides this controversy, the permeation of phosphonic acid antibiotics mediated by the phosphate channel is also extremely interesting for the study of new antibacterial compounds.

Large hydrophobic molecules, such as long-chain fatty acids, cross the OM through the bidirectional 14 strand β-barrel porin **FadL** (PA1288). In addition, also the two cryptic porins **FadL2** (PA1764) and **FadL3** (PA4589) can be involved in this process (Nouwens *et al*., 2002; Martínez *et al*., 2013). The fatty acid translocation proceeds according to a special mechanism conserved in Gram-negative bacteria. This mechanism implies the opening of a lateral opening (~ 8 × 10 Å) inside the transmembrane barrel, that allows the direct integration of hydrophobic molecules into the OM, avoiding the interactions with the external LPS (Hearn *et al*., 2009; van den Berg, 2010). So far, these channels have not been considered yet as involved in antibiotic uptake. However, this peculiar lateral diffusion mechanism could be exploited to develop hydrophobic molecules with an antibacterial activity that could avoid the OM barrier (van den Berg, 2010; Touw *et al*., 2010).

OprG is a small channel, constituted of eight β-strands with a narrow hydrophobic channel, responsible for hydrophobic molecules uptake and relatively highly expressed in *P. aeruginosa* (McPhee *et al*., 2009). It was shown that OprG is overexpressed under anaerobic conditions such as biofilm growth and as a response to high iron ion concentration. The latter piece of evidence leads us to suggest its involvement in iron uptake, similarly to the function of the orthologous OmpW in *A. baumannii* (McPhee *et al*., 2009; Catel-Ferreira *et al*., 2016). Moreover, the similarity with *E. coli* OmpW suggests an involvement in the lateral transport of small hydrophobic molecules similar to that of the FadL porin family (van den Berg, 2010). The tightness of its pore suggests an inability to accommodate small amino acids, like glycine, serine, alanine, or valine. However, the passage of these amino acids through OprG has been confirmed via a liposome swelling assay. A possible lateral gating mechanism, with an involvement of a proline residue was first proposed (Kucharska *et al*., 2015), but an alternative explanation arises from results showing that the porin can aggregate, forming dimers or oligomers (Sanganna Gari *et al*., 2018). In addition, the lack of OprG has been associated with a decreased infectivity and also to a reduced growth rate. An *oprG*-deleted mutant has in fact turned out to be less cytotoxic to human bronchial epithelial cells compared to its parental wilt type strain (McPhee *et al*., 2009). This evidence can be associated to the role of OprG as a laminin-binding protein, thus involved in adherence to the respiratory epithelium (Paulsson *et al*., 2019). OprG was also believed to be involved in the permeation of some antibiotics such as tetracycline and kanamycin, since its downregulation confers resistance to such compounds (Peng *et al*., 2005). Moreover, an *oprG* isogenic mutant exhibited an increased MIC value for ceftazidime (Hwang *et al*., 2016), but this study remains an isolated report. The real involvement of OprG in antibiotic internalization still remains unclear.

OprH is the smallest porin (21.6 kDa), composed of eight β-strands and has an important role of OM stabilization through cross-linking with the LPS (Rehm and Hancock, 1996). Its role in the internalization of nutrients and other substances is still largely unknown. It is included in the *phoP-phoQ* operon and, similarly to the PmrA-PmrB system, it is induced upon magnesium starvation (Macfarlane *et al*., 1999). In addition to this effect, it should be noted that *phoP/phoQ* alterations are associated with modifications in LPS structure and, as a consequence, with resistance to polymyxins (Barrow and Kwon, 2009). This class of antibiotics includes polymyxins B and E (or colistin) and is used, due to its intrinsic toxicity, as the last resource antibiotic to treat infections caused by XDR strains, in some cases also in combination therapy. Polymyxins disrupt the outer and inner membranes by binding to the LPS in a specific cationic binding site. The inactivation of *phoQ* induces the addition of a 4-amino-l-arabinose to lipid A, causing modifications in the LPS electric charge, and consequently polymyxins resistance (Miller *et al*., 2011). Similarly, OprH overexpression interferes

with the correct binding of polymyxins and is involved in the stabilization of the OM under magnesium starvation. This phenomenon contributes in part to polymyxin resistance (Young *et al*., 1992).

Hypothetical proteins, orthologous of *E. coli* Tsx nucleoside specific porin, are found in the *P. aeruginosa* PAO1 genome and are identified as **PA0165** and **PA0234** (Ye and van den Berg, 2004). This subclass of porins is widely distributed in Gram-negative bacteria. They share a 12 β-strand structure with a long and narrow pore. They are primary responsible for the selective uptake of nucleosides and deoxynucleosides, that are found in the external medium in low concentrations (Ye and van den Berg, 2004; Gao *et al*., 2022).

Another group of porins appears to be regulated by sphingosine, a sphingolipid that is generally acquired from bacterial hosts. Sphingosine can enhance bacterial virulence, but it is also described as exhibiting an antimicrobial activity (Heung *et al*., 2006; van den Berg *et al*., 2015). *P. aeruginosa* PAO1 can produce two 12-strand β-barrel porins that are sphingosine induced and involved in its uptake, formerly known as **SphA** (PA5325) and **QbdB** (PA3772) (van den Berg *et al*., 2015).

On the basis of the studies published so far, an involvement of the Tsx or SphA types of porins in antibiotic permeation can be excluded. In support of this conclusion, a mutant where these types of porins have been deleted together with other porins does not exhibit any alteration in the MIC that could be ascribed to their absence (Ude *et al*., 2021).

1.3.3.4 TonB family of gated porins (TBDTs)

The *P. aeruginosa* genome was described to encode 35 porins belonging to the TBDT family, a wide group of transporters involved in the uptake of fundamental nutrients such as metal ions and vitamin B_{12} (Noinaj *et al*., 2010). TBDT systems are commonly found in Gram-negative bacteria, and they consist of a 22-strand β-barrel OM porin that interacts with a TonB-ExbB-ExbD IM complex, the latter extending towards the periplasm. The role of this system is to feed the active transport through the OM porin, using the proton motive force across the IM (Andrews *et al*., 2003; Noinaj *et al*., 2010).

Iron regulation is essential for bacterial survival because of its involvement in various metabolic pathways, where this metal acts as a redox factor. Iron regulation is crucial for *P. aeruginosa* survival, and it has therefore evolved in meticulous mechanisms. Indeed, bacteria must somehow secure an appropriate supply of these ions and, at least in theory, this class of transporters has to be considered as essential.

Metal ions internalization is mediated by specific chelating molecules, defined as metallophores or siderophores. They are produced by bacteria and then extruded through specific efflux pumps in the

external medium to scavenge the free ions in the external medium. Among these molecules, *P. aeruginosa* primarily produce pyoverdines, a group consisting of at least three chromopeptides, that differ in their peptide chain residues. Different strains can produce different chromopeptides (PVDI, PVDII and PVDIII) and, for instance, *P. aeruginosa* PAO1 is a PVDI producer. Pyoverdines are responsible for iron uptake and their production is revealed by the peculiar yellow-green coloring of *P. aeruginosa* cultures (Schalk and Guillon, 2013). Pyoverdine is mainly internalized by FpvA, the most expressed TBDT (8000 to 33000 copies per cell) (Bhamidimarri *et al*., 2021) and FpvB. In addition to the siderophore internalization, the bond between FpvA and pyoverdine also triggers a series of signals that causes a cytoplasmic transcription of several products, including pyoverdine itself (Lamont *et al*., 2002). FpvB has also recently been shown to be able to transport other siderophores with greater efficiency than pyoverdine, in this way behaving as more different from FpvA than previously assumed (Chan and Burrows, 2023).

Moreover, *P. aeruginosa* produces smaller quantities of pyochelin, a second iron siderophore and pseudopaline, that is the principal agent in zinc and cobalt ions uptake (Ghssein and Ezzeddine, 2022). FptA is the porin that enables pyochelin to be internalized (Manzoor *et al*., 2021). Other substrates have additional preferential porins, like zinc or nicotianamine that are internalized via ZnuD and OptC, respectively. In addition, the PhuR and HasR porins are known to be heme transporters.

For over 20 years, TBDTs have attracted increasing attention following the synthesis of β-lactam conjugates to siderophores, although it was only in 2019 that a compound with these features was approved for human use (Braun and Braun, 2002; Wang *et al*., 2024). These antibiotics exploit the above-mentioned capacity to facilitate the metal ion diffusion via TBDT to help them reach their periplasmic target(s).

In *P. aeruginosa* the TBDTs PiuA, PiuB, PiuD and PirA have attracted considerable attention. In fact, they have been associated with the internalization of cefiderocol and other β-lactam-siderophore analogues that are still under study (Luscher *et al*., 2018).

Moreover, mutations in the *pirA*, *piuA*, *piuB*, *fvpB*, *fecA* and *fiuA* genes have been found in clinical strains that present an increased MIC for cefiderocol and might contribute to the appearance of a cefiderocol resistant profile (Sadek *et al*., 2023).

Hence, the *P. aeruginosa* TBDTs reservoir is particularly interesting in order to better assess the interactions that cefiderocol, or other siderophores-conjugated β-lactams, might have with these porins. Another purpose would be to ascertain the possibility of resistance mediated by the deletion of one of these porins, as in the case of imipenem resistance induced by an altered synthesis of the OprD porin.

Finally, another peculiar TBDT is OprC, one of the first porins to be identified in *P. aeruginosa* OM due to its abundance (1000 to 10000 copies per cell). It regulates the copper ion uptake, without the need of siderophores. It presents in fact a methionine track that leads copper towards a site that can irreversibly bind the metal (Bhamidimarri *et al*., 2021). The importance of copper regulation is due to its toxicity, but also to the capacity that copper gives to bacteria to allow the anaerobic respiration, thus increasing the persistence during infections and in biofilm growth. Furthermore, OprC seems to act as a copper accumulator, by ligating it on the extracellular side and proceeding to the TonB mediated internalization only as a response to internal stimuli (Bhamidimarri *et al*., 2021). Due to its unique features, OprC does not seem to be involved in antibiotic uptake. An OprC isogenic mutant was indeed shown to not influence antibiotic MICs (Yoneyama *et al*., 1995).

1.4 Efflux pumps

In *P. aeruginosa* an array of mechanisms performs the extrusion of molecules, including antibiotics, that could be toxic for bacterial survival from the cytoplasm and the periplasm. These include the **A**TP-**b**inding **c**assette (ABC) superfamily, the **s**mall **m**ultidrug **r**esistance (SMR) family, the **m**ajor **f**acilitator **s**uperfamily (MFS), the **m**ultidrug **a**nd **t**oxic compound **e**xtrusion (MATE) family, the **p**roteobacterial **a**ntimicrobial **c**ompound **e**fflux (PACE) family and the **r**esistance/**n**odulation/cell **d**ivision (RND) family (Figure 9) (Lorusso *et al*., 2022).

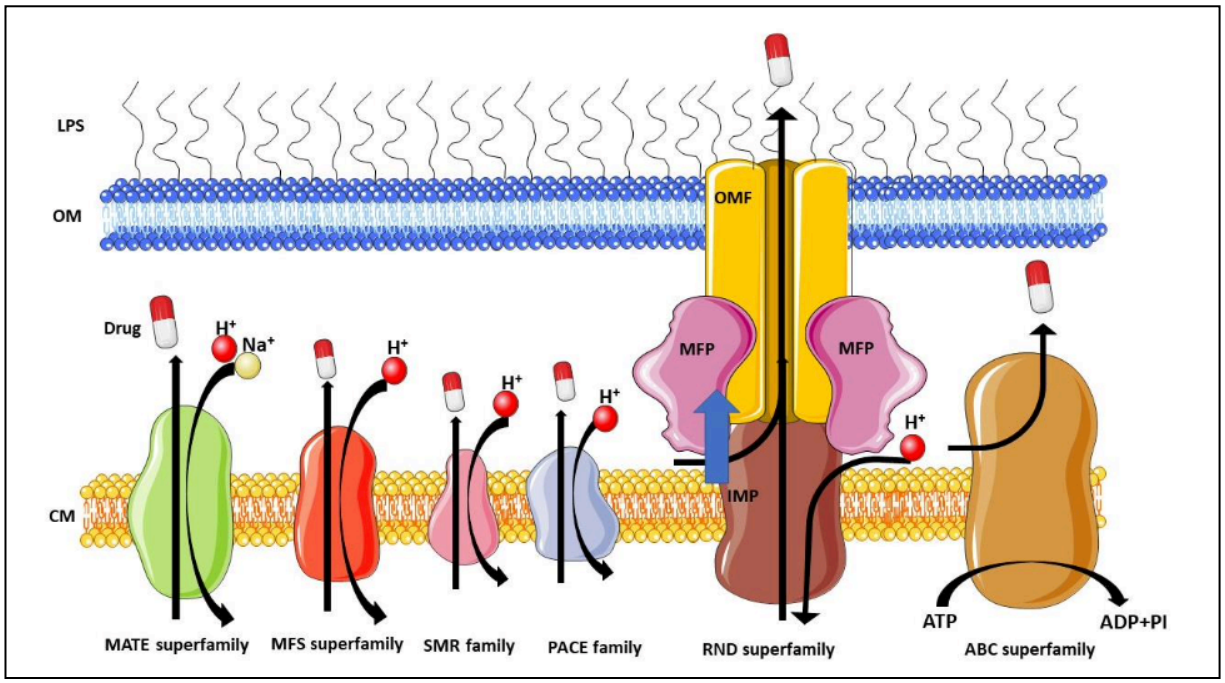

Figure 9: Schematic representation of the six transporter families that contain MDR efflux pumps (Avakh *et al*., 2023).

A complete survey of all the strategies devised by *P. aeruginosa* to eliminate compounds that otherwise would be toxic would be arduous, and beyond the scope of this thesis. For this reason, we will limit our scope to an overview of the six families of transporters, highlighting their involvement in antibiotic and/or relevant toxic compound extrusion. We will start with the efflux pumps associated with important biological processes that are likely to be involved in OM permeability. Subsequently, we will focus on the OM porins belonging to the OprM family. Finally, we will discuss the RND efflux pumps, their role in intrinsic antibiotic resistance and the consequences that their mutations might have in increased antibiotic resistance. Moreover, their relevance for a wider global modulation that includes the porin expression, in particular OprD, will be described.

1.4.1 ABC transporters

The ABC transporters are ATPases widely distributed in living organisms, including humans. They evolved to play different biological roles (Wilkens, 2015). Concerning permeability, they mediate a bidirectional, energy-dependent transport across membranes (Locher, 2009). They are divided into two separate subgroups, one with an import capacity (found only in prokaryotes), and the other with export (prokaryotes and eukaryotes) properties. ABC transporters combine a pair of extremely conserved cytoplasmic components involved in ATP hydrolysis with a pair of transmembrane domains that facilitate passage of the molecules. Single members of this family may have notably different organizations (Locher, 2009).

P. aeruginosa possesses several ABC transporters that are involved in the secretion of important substrates, such as the PvdE and PvdRT-OmpQ systems for pyoverdine extrusion (Yeterian *et al*., 2010; Filloux, 2011; Hannauer *et al*., 2012; Oura *et al*., 2015). The PvdE ABC transporter actively exports into the periplasm a non-fluorescent pyoverdine precursor, that will complete its synthesis in this compartment (Yeterian *et al*., 2010). The PvdRT-OmpQ tripartite ABC transporter features an IM component providing the required energy (PvdT), a periplasmic adaptor (PvdR), and a member of the OprM porins family (OmpQ), all working together to eject periplasmic pyoverdine in multiple ways. PvdRT-OmpQ throws out the newly synthetized pyoverdine and the one that has already released its iron cargo into the periplasm but can also eject the periplasmic pyoverdine that has been chelated with non-iron metal ions (Hannauer *et al*., 2012). Therefore, PvdE and PvdRT-OmpQ, together with the FpvA TBDT that allows the entry of the chelated pyoverdine, act in synergy to assure the iron homeostasis (Yeterian *et al*., 2010; Schalk and Guillon, 2013; Hannauer *et al*., 2012). Within the subgroup of ABC multipartite efflux systems, the Ttg2ABCDE system, together with VacJ OM protein, has been defined for its homology with the *Pseudomonas putida* toluene tolerance genes. In *P. aeruginosa*, this system has been noted to be active for the extrusion of tetracycline, ciprofloxacin, trimethoprim, chloramphenicol, and to confer a basal resistance to various other antibiotics (Chen and Duan, 2016; Yero *et al*., 2021). Due to its similarity to the *E. coli* MacAB-TolC efflux pump, the extrusion function has been thought to be mediated by interactions between VacJ and a porin homologous to the *E. coli* TolC. However, the presence of such a component in *P. aeruginosa* has not been confirmed yet (Yero *et al*., 2021).

The second ABC transporter subgroup mediates molecules uptake by means of specific substrate-binding proteins, released in the periplasm to scavenge their substrates. Once coupled, they head towards two hydrophobic transmembrane permeases that mediate internalization using the energy provided by the cytosolic ATP-binding domains (Higgins, 2001). This mechanism enables bacteria

to enhance their virulence, allowing the internalization of a wide range of amino acids or oligopeptides. A notable member of this subgroup is NppA1A2BCD, that is involved in the uptake of peptidyl nucleoside antibiotics, a class of molecules that target MraY translocase I. This leads to the inhibition of PG synthesis (Pletzer *et al*., 2015). To the best of our knowledge, NppA1A2BCD is not involved in oligopeptides permeation, and its physiological role has not been fully elucidated yet. A second ABC transporter is SppABCD, co-transcribed with the SppR TBDT. It may be involved in siderophores uptake, due to the simultaneous upregulation of the pyoverdine biosynthesis as a response of the *spp* operon overexpression (Pletzer *et al*., 2016). The third component of this subgroup of transporters is the already mentioned DppBCDF transporter, that allows the cytoplasmic internalization of di- and tri- peptides that have crossed the OM via the OpdP porin, thus enlarging the metabolic capacities of *P. aeruginosa* (Pletzer *et al*., 2014). Interestingly, the features of the ABC importers make them interesting candidates for the design of specific antibacterial molecules that could enter via their systems.

1.4.2 Major facilitator superfamily (MFS)

MFS is a large group of proteins, widely distributed in all domains of life, including bacteria, that, acting as uniporters, symporters, and antiporters, enable nutrients uptake and the discharge of a broad spectrum of toxic compounds. Their pivotal structure consists of 12 or 14 transmembrane segments. In Gram-negative bacteria they might be found also as tripartite complexes that reach the OM and excrete toxic compounds in the medium (Quistgaard *et al*., 2016). A noteworthy MFS subgroup is the Tet efflux pumps group, a broad set of MFSs responsible for tetracycline resistance. They enable the extrusion of a magnesium-tetracycline complex using the proton gradient across the IM (Chopra and Roberts, 2001). The Tet group includes TetA, first discovered on a plasmid carried by an *E. coli* strain, that confers resistance to tetracycline and is commonly found in Enterobacterales (Levy and McMurry, 1978). To overcome the resistance mediated by these pumps, tigecycline, a tetracycline derivative that is not recognized by Tet efflux pumps, has been developed (Chopra, 2002). However, this class of tetracycline-specific efflux pumps is not present in the *P. aeruginosa* PAO1 wild type genome; for this reason, it has been widely used as a selectable antibiotic marker for cloning vectors (Kovach *et al*., 1995). The *P. aeruginosa* PAO1 genome encodes at least two MFSs, formerly known as Mfs1 (PA1262) and Mfs2 (PA1282) that have been correlated with toxic compound extrusion, but their activity against antibiotics appears limited. MFSs are induced as a response to oxidative stress, their deletion does not alter antibiotic susceptibility, although their overexpression causes an increased resistance to aminoglycosides and fluoroquinolones. It must be noted that this phenomenon

is best interpreted within the context of a RND efflux pumps overexpression mediated by MFSs induction, that clearly correlates with the above-mentioned antibiotic resistance profiles (Dulyayangkul *et al*., 2021). Interestingly, an acquired MFS encoding gene included in a transposon was found to mediate chloramphenicol resistance in a *P. aeruginosa* strain (Bissonnette *et al*., 1991).

1.4.3 Multidrug and toxic compound extrusion (MATE)

MATE efflux pumps exploit a cations electrochemical gradient for the extrusion of various unrelated compounds, including antibiotics. They were first described in *Vibrio parahaemolyticus* and *E. coli,* and recently they have been widely found in both prokaryotes and eukaryotes (Brown *et al*., 1999). They share a 12-transmembrane helix structure and act as antiporters. The general model implies that ions (in this case Na^+ or H^+) bind to the protein when an open site is exposed to the external side of the membrane. This interaction causes a temporary rearrangement of the protein structure, that directs the protein open site to the interior, allowing binding of the toxic substrates and, subsequently, the outflow of these toxic molecules (Mitchell, 1957). *P. aeruginosa* expresses the MATE PmpM efflux pump that can mediate the extrusion into the periplasm of different toxic compounds, including fluoroquinolones, using H^+ ions as antiporters (He *et al*., 2004).

1.4.4 Small multidrug resistance family (SMR)

The SMR is a wide family that includes small transporters, constituted of four transmembrane α-helices that use the proton motive force to extrude various lipophilic compounds, including β-lactams and aminoglycosides. They are found in both Gram-positive and Gram-negative bacteria, but they are also frequently isolated on mobile genetic elements which increases their dissemination (Bay *et al*., 2008). In the *P. aeruginosa* PAO1 genome, two SMRs are encoded. The first one is EmrE (PA4990), that corresponds to the *E. coli* ethidium multidrug resistance protein E EmrE. The homologous *P. aeruginosa* EmrE associates in dimers or oligomers. It uses H^+ ions to extrude antibiotics such as gentamicin, kanamycin, and neomycin (Gottschalk *et al*., 2004; Wargo, 2013; Cherak *et al*., 2021). The second member is SugE (PA1882), a protein on which few studies are available, that seems to be involved in cationic drug export, as the orthologous SugE in *E. coli* (Duan *et al*., 2003).

1.4.5 Proteobacterial antimicrobial compound efflux (PACEs)

PACEs, the last transport family to be described, are constituted of four transmembrane α-helices that, similarly to SMRs, tend to oligomerize and exploit the proton-motive force as energy source (Hassan *et al*., 2019). They were first identified in *A. baumannii* and have been found in numerous proteobacteria. The family prototype is *A. baumannii* AceI, a conserved efflux protein involved in the extrusion of chlorhexidine, a common antiseptic used in clinics (Hassan *et al*., 2013; Hassan K.A. *et al*., 2018). Their physiological substrates were recently identified as diamines (*i.e.,* cadaverine, putrescine) a group of compounds that share structural similarities with chlorhexidine. Interestingly, PACEs are involved in different biological functions, including the host immune responses and bacterial virulence (Hassan *et al*., 2019). The *P. aeruginosa* PAO1 genome contains PA2880, a recently identified AceI ortholog that, in spite of some sequence divergences, shares with PACE efflux pumps the affinity for chlorhexidine but not with cadaverine (Zhao *et al*., 2022).

1.4.6 Resistance/nodulation/cell division family (RND)

In Gram-negative bacteria, the most important role in the extrusion of toxic compounds is performed by RNDs. These systems are extremely efficient ways of mediating the efflux through the diderm protection. They belong to a permease family widely distributed in living organism. In Gram-negative bacteria, this family has specifically evolved to expel an extremely broad spectrum of antibiotics and toxic compounds, like detergents, disinfectants, or organic solvents. This feature enables bacteria producing RND efflux pumps to increase their virulence, facilitating the host colonization (Fernando and Kumar, 2013).

RND efflux pumps are tripartite protein complexes spanning the IM and OM. They are composed of an **i**nner **m**embrane **p**rotein (IMP), a **m**embrane **f**usion **p**rotein (MFP) and an **o**uter **m**embrane **f**actor (OMF), generally co-transcribed as an operon. They capture their substrates either from the cytoplasm or from the periplasmic space, using a proton gradient to canalize them into the OM porin, allowing their release into the external medium (Piddock, 2006). This feature enables them to also confer resistance to β-lactams, that accumulate in the periplasm. Their expression has been related to a diminished capacity to form biofilms, although the presence of antibiotics in biofilms leads to an increased expression of RND efflux pumps (Fernando and Kumar, 2013; Gillis *et al*., 2005). Based on their substrate specificity, Gram-negative RND efflux pumps involved in toxic compounds extrusion can be classified into two subgroups: the **h**eavy **m**etal **e**fflux (HME) and the multidrug **h**ydrophobe/**a**mphiphile **e**fflux 1 (HAE1) (Nikaido, 2018). Interestingly, their activity is inhibited by

specific compounds that can restore antibiotic efficacy (Compagne *et al*., 2023). The first of such molecules to be discovered was the **p**henylalanine-**a**rginine **β**-**n**aphthylamide (PAβN) (Lomovskaya *et al*., 2001). PAβN acts by binding to the RND efflux pumps in a competitive manner, thus inhibiting their action against certain substrates. Successive studies revealed that PAβN can interfere with the OM stability, thus enhancing antibiotic potency in a double way (Lamers *et al*., 2013). Despite initial great expectations, none of the different molecules identified as inhibitors of the efflux pumps have entered clinical trials, due to their toxicity or limited *in vivo* activity (Compagne *et al*., 2023).
The prototype of this family is the *E. coli* AcrA-AcrB-TolC system, homologous to *P. aeruginosa* MexA-MexB-OprM one; both efflux pumps have been the objects of numerous studies. Given their prominence in the literature, we will now proceed to describe their general structures that can be roughly extended to all RND efflux pump family members.

1.4.6.1 Inner membrane proteins (IMPs)

The IMPs (*i.e.,* MexB) belong to the proper RND superfamily, that includes the entire class of efflux transporters. Starting from the AcrB solved X-ray structure, we know that they consist of symmetrical homotrimers, forming a complex transmembrane structure where each monomer contains three domains (Murakami *et al*., 2002; Murakami *et al*., 2006; Sennhauser *et al*., 2009):

a) A 12 α-helix transmembrane domain presenting a cytoplasmic drug-binding pocket, called the vestibule, situated above the inner membrane, and used by the most hydrophobic substrates. It also contains the machinery that confers energy from the proton-motive force.
b) A pore domain, consisting of a funnel-like structure of each monomer, that has been assumed to perform the capture of less hydrophobic substrates from a periplasmic cleft.
c) A large docking domain that enables the connection to the OMF, that might also act as an entry point for the substrates.

The three different substrate pockets enable the capture of molecules with different physio-chemical properties, and subsequently the RNDs undergo conformational changes that allow the outward addressing of the compounds.

1.4.6.2 Membrane fusion proteins (MFPs)

The MFPs, such as the *E. coli* AcrA or the *P. aeruginosa* MexA, are anchored in the IM, and extend into the periplasm, laterally binding the IM and the OMF (Akama *et al*., 2004b). They have an active role in the assembly of the system, and they are an essential element in the functioning of RNDs (Kim

et al., 2015). The role of MFPs in periplasmic β-lactams capture and transfer into the OMF lumen still remains to be fully elucidated (Catte *et al*., 2022).

1.4.6.3 Outer membrane factors (OMFs)

The OMFs are porins that belong to a specific class, the OprM family, and associate into homotrimers. Their structures comprise two domains (Akama *et al*., 2004a):

a) A conserved OM region, composed of a 12-stranded β-barrel anchored in the OM, with a pore size of approximatively 6-8 Å.
b) A periplasmic extension consisting of a conserved 12 α-helix domain and other structures that interact with the other RND components.

Interestingly, OprM is able to adopt a closed state before the complete assembly of the tripartite efflux pump. That avoids the formation of a hole allowing the entry of external molecules (Phan *et al*., 2010). The *P. aeruginosa* OprM family includes 18 members, but only eight of them are components of RND efflux pumps (Stover *et al*., 2000; Hancock and Brinkman, 2002; Yonehara *et al*., 2016). The active components are: OprM (PA0427), OprJ (PA4597), OprN (PA2495), OpmB (PA2525), OpmD (PA4208), OpmE (PA3521), OpmH (PA4974) and OpmN (PA2522), also known as CzcC.

In addition, we should mention OpmQ (PA2391), OpmL (PA1875), OpmM (PA3404 also known as HasF), AprF (PA1248), OpmK (PA4144) and OpmF (PA4592). These appear to be the OM elements of various ABC transport systems, since they are included in operons encoding the other efflux pump components (Filloux, 2011; Hannauer *et al*., 2012; Oura *et al*., 2015; Poudyal *et al*., 2018; Al-Thabhawee and Al-Dahmoshi, 2022). On the contrary, *opmI* (PA3894) does not seem to be included in any operon encoding an ABC transporter, but the gene is adjacent to the *opuCABCD* operon, that encodes the ABC-type proline/glycine betaine transport system. This evidence leads us to assume that OpmI might be the associated OM porin. However, Hancock and collaborators have shown that *opmI* disruption is associated with an aminoglycoside decreased MIC, without reference to any connection to an ABC transporter (Jo *et al*., 2003). Except for OpmQ, the other porins are components of hypothetical or poorly characterized ABC transporters, on which scant information is available in the literature.

Finally, OpmG (PA5158) OpmJ (PA1238) and OpmA (PA2837) belong to operons encoding tripartite MFS efflux systems, whose functions and structures have not been clearly explained up to now (Heacock-Kang *et al*., 2018). Further studies are required to shed light on these porins that are produced by *P. aeruginosa* and that might have a more important role in antibiotic transport than assumed in past studies.

1.4.6.4 *P. aeruginosa* RNDs

To date, twelve different RND systems have been annotated in the *P. aeruginosa* PAO1 genome, eleven ones belonging to the HAE1 subgroup and one (CzcABC) to the HME subgroup (Stover *et al*., 2000). Beside CzcABC, the other systems have been described to play some role in antibiotic resistance or toxic compound extrusion, thus contributing to the intrinsic resistance of the bacterium (Lorusso *et al*., 2022). As further evidence of this, a knockout strain lacking the six most highly expressed efflux pumps showed a marked decrease in the MICs for various classes of antibiotics, including β-lactams (Cooper *et al*., 2018). In *P. aeruginosa* all the HAE1 efflux pump components IMPs, MFPs and their regulators were named with the acronym Mex, standing for **m**ultiple **e**fflu**x**, followed by a letter. They are defined by the precise association between an RND, an MFP and an OMF, giving rise for example to MexA-MexB-OprM or MexC-MexD-OprJ (Figure 10). However, in the case of an OMF deletion, an interchangeability feature allows, for example, MexAB to associate also with OprJ or MexCD to yield a functional complex with OprM (Yoneyama *et al*., 1998). Different RND efflux pumps are resumed in Table 2.

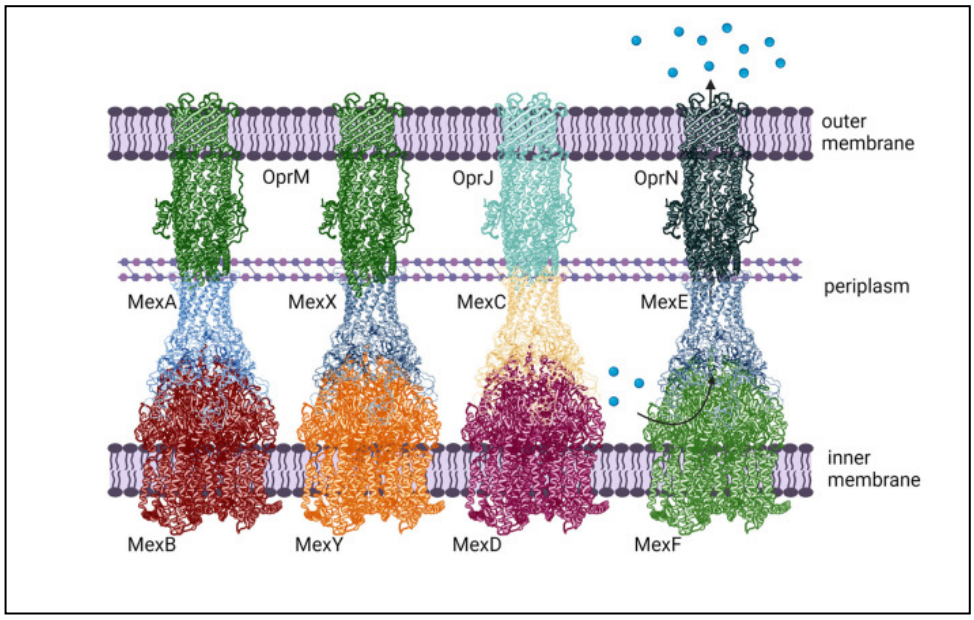

Figure 10: Schematic structures of the four main RND efflux pumps involved in *P. aeruginosa* antibiotic resistance (Lorusso *et al*., 2022).

Name	Main substrates	Regulators
MexAB-OprM	Aminoglycosides, fluoroquinolones, macrolides, tetracyclines, tigecycline, β-lactams (with the exception of imipenem), detergents, biocides.	MexR, NalD, BrlR, CpxR, RocS1/2-A2, AmpR, PA3225, MexT.
MexCD-OprJ	Fluoroquinolones, tetracyclines, tigecycline, some cephalosporins (*i.e.* cefepime, ceftriaxone but not ceftazidime), toxic compounds.	NfxB, EsrC.
MexXY-OprM (or **-OprA)**	Aminoglycosides, fluoroquinolones, macrolides, tetracyclines and some cephalosporins.	MexZ, No, ParRS.
MexEF-OprN	Fluoroquinolones, chloramphenicol, and trimethoprim (no β-lactams), toxic compounds.	MexT, MexS, AmpR, ParRS.
MexJK-OprM (or **-OpmH)**	Erythromycin. Biocide (triclosan).	MexL.
MexGHI-OpmD	Phenazine, Fluoroquinolone (norfloxacin).	-
MexMN-OprM	Chloramphenicol, some β-lactams (*i.e.,* carbenicillin, ticarcillin, aztreonam).	MmnRS.
MexPQ-OpmE	Fluoroquinolones, macrolides, and tetracycline.	CueR.
MexVW-OprM	fluoroquinolones, tetracycline, erythromycin, and chloramphenicol.	-
MuxABC-OpmB	Novobiocin, macrolides, tetracycline, aztreonam.	-
TriABC-OpmH	Biocide (triclosan).	-
CzcCBA	Heavy metal efflux.	CzcRS, CopRS.

Table 2: List of RND efflux pumps described throughout this chapter; main substrates extruded and the main regulators systems are reported. Noteworthy only CzCCBA is an HME, while other efflux pumps belong to the HAE1 subgroup. The different substrate specificity of MexJK due to the association with OprM or OpmH is reported.

1.4.6.4.1 MexA-MexB-OprM

MexA-MexB-OprM, an *E. coli* AcrA-AcrB-TolC orthologous, was the first efflux pump of this group to be described in *P. aeruginosa*. It has a physiological role for pyoverdine release into the external medium, but its antibiotic removal capacity has also been rapidly noted (Li *et al*., 1995). It is the major efflux pump expressed by *P. aeruginosa,* and it enables the extrusion of non-antibiotic substrates such as detergents or biocides such as triclosan. Concerning the extrusion of antibiotics, aminoglycosides, fluoroquinolones, macrolides, tetracyclines, tigecycline and all the β-lactams subfamilies including β-lactamase inhibitors, are substrates of the MexAB-OprM extrusion system. This feature confers to *P. aeruginosa* an intrinsic profile of low susceptibility or resistance to many of these drugs (Lorusso *et al*., 2022; Köhler T. *et al*., 1999a; Dreier and Ruggerone, 2015). Notably, a strain deprived of the four major efflux pumps (MexAB-OprM, MexCD-OprJ, MexEF-OprN, and MexXY-OprM) exhibits a phenotype with a restored susceptibility to different antibiotic classes. In the same study, it was observed that a mutant expressing only MexAB-OprM among the major RNDs, showed an antibiotic resistance profile quite similar to that of the wild-type strain (Morita *et al*., 2001). However, the only exception to the broad-spectrum antibiotic resistance is imipenem, that is poorly captured by MexAB-OprM. A computer simulation study highlighted that this was due to the hydrophilic imipenem side chain that prevents a good affinity to the MexB binding pockets. On the contrary, meropenem, that is efficiently expelled contains hydrophobic groups that ensure better interactions with MexB (Collu *et al*., 2012). MexAB-OprM is constitutively synthetized, although differences have been observed according to the growth-phase. In particular, its expression is increased in the late exponential/early stationary phases of bacterial growth, suggesting a participation in the quorum-sensing regulation (Evans and Poole, 1999). The modulation is mediated by a wide number of regulators. One of these is the repressor MexR, that acts by binding to a specific site in the *mexA-mexR* intergenic region as a response to external stress factors such as reactive oxygen species. The transcriptional start site of another operon is regulated by the NalD repressor that, together with MexR, is responsible for MexAB-OprM inactivation (Sobel *et al*., 2005b; Morita *et al*., 2006). Moreover, the activation of MexAB-OprM can be induced by different activators, including the biofilm-correlated BrlR transcriptional regulator and the multifaceted regulator CpxR (Liao *et al*., 2013; Tian *et al*., 2016). Other regulators that contribute to the expression have been identified in the two-component system RocS1/2-A2 (Sivaneson *et al*., 2011), AmpR (Balasubramanian *et al*., 2012), PA3225 (Hall *et al*., 2017) and in the global regulator MexT (Maseda *et al*., 2004).

1.4.6.4.2 MexC-MexD-OprJ

MexC-MexD-OprJ efflux pump can be induced as a consequence of the lack of MexAB-OprM, and it does not appear to directly respond to the presence of antibiotics (Li *et al*., 2000; Morita *et al*., 2001). Concerning antibiotic resistance, it enables the extrusion of fluoroquinolones, tetracyclines, tigecycline and zwitterionic cephalosporins as does MexAB-OprM. However, MexCD-OprJ, in contrast to MexAB-OprM, is unable to extrude carbenicillin, ceftazidime, and moxalactam (Masuda *et al*., 2000; Morita *et al*., 2012). In contrast, MexCD-OprJ appears to export fourth-generation cephalosporins (*i.e.,* cefepime) with a better affinity than MexAB-OprM (Masuda *et al*., 2000). Moreover, MexCD-OprJ exhibits a selectivity for toxic compounds, such as triclosan. MexCD-OprJ negative regulation is caused by the NfxB repressor, that constantly binds the promoter region upstream the *mexCD-oprJ* operon, thus blocking its transcription. External stimuli, such as the presence of disinfectants (for instance chlorhexidine) that alter the membrane integrity, can cause the detachment of NfxB, resulting in expression of the efflux pump, in order to extrude the toxic compounds (Morita *et al*., 2003). A complementary repressor is EsrC, that is involved in the envelope stress response and acts similarly to NfxB. Together with the *mexCD-oprJ* operon, *esrC* is regulated by NfxB, thus providing a second repressor that comes into play only when NfxB is no longer active, to avoid an excessive MexCD-OprJ expression (Purssell *et al*., 2015).

1.4.6.4.3 MexX-MexY/OprM

MexX-MexY/OprM is the second constitutive efflux pump expressed by *P. aeruginosa*. It specifically recognizes aminoglycosides, to which it represents one the most important resistance determinants (Morita *et al*., 2012). Indeed, a mutant strain with an inactivating insertion into *mexX* was shown to exhibit an aminoglycoside susceptibility phenotype (Aires *et al*., 1999). In addition, it can also expel fluoroquinolones, macrolides, tetracyclines and zwitterionic cephalosporins. It has a narrower β-lactam spectrum than MexCD-OprJ, since it is not able to accommodate aztreonam, even if it has a moderate activity on cefepime (Morita *et al*., 2012). The system is encoded by an operon lacking a specific OMP and, for this reason, it has been assumed to be generally associated with OprM, although complexes with OMPs OprA, OpmB, OpmG, OpmH, and OpmI have been described (Chuanchuen *et al*., 2008). Interestingly, when MexXY is paired with OprA, the efflux pump turns out to be more efficient for the extrusion of antibiotics and its activity spectrum is extended to carbenicillin (Singh *et al*., 2020). Besides its constitutive expression, the presence of antibiotics targeting the ribosome can induce the MexXY expression that is thus the only efflux pump that

responds to aminoglycosides presence. The regulator MexZ performs a transcriptional repression by ligating to the specific promoter region; its release leads to transcription, as a response to the presence of ribosome-targeting agents (Morita *et al*., 2012). Additionally, the functioning of MexZ depends on a second regulator, also responding to the protein synthesis perturbation, mediated by the presence of aminoglycoside antibiotics. This is the anti-repressor ArmR that operates by destabilizing the MexZ bound to the promoter region, thus inducing the *mexXY* transcription (Cao *et al*., 2004; Yamamoto *et al*., 2009). Among the other regulators that can influence MexXY expression, we report the two-component signal transduction system ParR-ParS, consisting of an IM transmembrane histidine kinase sensor (ParS) and a cytoplasmic signal transducer (ParR). This system was first described as being involved in LPS modification conferring resistance to polymyxins. Successively, it was demonstrated that the ParRS activation in response to LPS stress is also involved in MexXY upregulation and, in addition, in OprD downregulation (Muller *et al*., 2011).

1.4.6.4.4 MexE-MexF-OprN

MexE-MexF-OprN is another quiescent efflux pump that is regulated by the MexT repressor. When expressed, it is involved in the extrusion of fluoroquinolones, chloramphenicol, and trimethoprim but, in contrast to the above-mentioned systems, it does not recognize β-lactams as substrates. Moreover, it can also mediate the extrusion of toxic compounds, like triclosan. Transcription of MexEF-OprN is activated by the binding of the global regulator MexT in the promoter region, that turns out to be nonfunctional in wild-type strains. Interestingly, mutations in *mexT* that restore its activity, lead to the *nfxC* phenotype (Maseda *et al*., 2000). These mutants overproduce MexEF-OprN which thus reduces the susceptibility to the target antibiotics and also exhibit a decreased expression of both MexAB-OprM efflux pump and porin OprD. In consequence this increases their resistance to imipenem (Maseda *et al*., 2000; Köhler T. *et al*., 1999b; Ochs *et al*., 1999a; Sobel *et al*., 2005a). A similar result can also be due to mutations in the oxidoreductase *mexS,* a *mexT* negative regulator, and this mechanism appears to be the most frequently found in *nfxC* phenotypes (Uwate *et al*., 2013; Maseda *et al*., 2010). Various other regulators have been proposed to have an impact on MexEF-OprN expression. Among them, let us mention the MexEF-OprN downregulation driven by the global regulator AmpR (Balasubramanian *et al*., 2012), and its overexpression mediated by ParR, through the MexS-MexT pathway (Wang *et al*., 2013). This finding adds a further element to the role of ParRS in antibiotic resistance, in addition to those mentioned above concerning MexXY regulation.

1.4.6.4.5 Other RND efflux pump systems

The other RND efflux pump systems produced by *P. aeruginosa* are poorly expressed and have a minimal role in antibiotic resistance. They allow the extrusion of different chemotherapeutic substrates, with a marginal impact on β-lactams. We therefore provide a brief list of these systems, focusing on their relevant characteristics.

Similarly to MexXY, **MexJ-MexK/OprM** is encoded by an operon that lacks a specific OMF and is usually associated with OprM (Chuanchuen *et al*., 2002). Nevertheless, an association with OpmH has been reported and the replacement of one OMF by another modifies the substrate specificity (Chuanchuen *et al*., 2005). The presence of OprM allows the systems to extrude some antibiotics, such as erythromycin, while the association with OpmH makes it efficient in the extrusion of triclosan, a biocide for which MexJK turns out to be the specific elimination pathway (Chuanchuen *et al*., 2002). The operon *mexJK* is negatively regulated by a TetR repressor, also known as MexL, in a way completely similar to the RNDs described above (Chuanchuen *et al*., 2002).

MexG-MexH-MexI-OpmD is responsible for the extrusion of phenazine, an endogenous antibiotic that is an intermediate in the synthesis of pyocyanin (Aendekerk *et al*., 2002; Sakhtah *et al*., 2016). It is encoded by a specific operon and, notably, it requires an additional MFP (MexG) whose functionality has not been fully elucidated yet. MexGHI-OpmD is expressed in response to the increasing concentration of cytoplasmic phenazine. In this way, the resulting system avoids excessive intracellular accumulation of this compound that might become toxic for the bacterium (Sakhtah *et al*., 2016). Concerning antibiotic resistance, MexGHI-OpmD was shown to facilitate the detoxification of the fluoroquinolone antibiotic norfloxacin, due to a decrease in the MIC value observed for a strain lacking this pump (Sekiya *et al*., 2003).

MexM-MexN/OprM is encoded by a further operon (*mexMN*) lacking the specific OMF, and for this reason it is generally associated to the highly expressed OprM (Mima *et al*., 2005). Notably, the pump presents some selectivity for antibiotics such as chloramphenicol and some β-lactams (*i.e.,* carbenicillin, ticarcillin and aztreonam), without causing a marked resistance phenotype (Mima *et al*., 2005; Ranjitkar *et al*., 2019). MexMN expression is mediated by MmnRS, a two-component regulatory system with an uncertain function, but probably involved in the response to copper stress. In particular, a MexMN-OprM upregulation was highlighted in a strain where the major MexAB-OprM was blocked, thus compensating the loss of function (Ranjitkar *et al*., 2019). The same MmnRS regulator was also implicated in OprD downregulation, and its activation, in fact, caused increased carbapenems MICs (Ranjitkar *et al*., 2019). Notably, the MexMN nomenclature refers to an efflux

pump produced in the *P. aeruginosa* PAK strain, while the system in the annotated *P. aeruginosa* PAO1 is known as PA1435-PA1436 (Liu *et al*., 2022).

The **MexP-MexQ-OpmE** efflux pump presents a selectivity for fluoroquinolones, macrolides, and tetracycline (Mima *et al*., 2005). Little information is available on this efflux pump, except that its regulation is mediated by the copper regulator CueR. However, MexPQ involvement in copper extrusion, as first assumed, is to be excluded (Mima *et al*., 2005).

MexV-MexW/OprM is a poorly studied RND that enables the extrusion of a wide set of antibiotics like fluoroquinolones, tetracycline, erythromycin, and chloramphenicol, although no evidence of clinical multi-resistance has been found. Due to the lack of a co-transcribed OMF, it is most likely associated with OprM (Li *et al*., 2003).

MuxA-MuxB-MuxC-OpmB is a quadripartite system, and all its components are encoded by the same operon (Mima *et al*., 2009). MuxABC-OpmB shares a homology with the *E. coli* MdtABC efflux pump and other similar systems produced by different Enterobacterales (Nagakubo *et al*., 2002). All these systems include two IMPs (MuxB and MuxC in *P. aeruginosa*), both essential for their functionality (Mima *et al*., 2009). MuxABC-OpmB extrusion is mainly directed against novobiocin, an antibiotic that acts against the DNA gyrase, contributing to the *P. aeruginosa* intrinsic resistance to this drug. It also allows the ejection of other antibiotics such as macrolides, tetracycline and aztreonam (Mima *et al*., 2009).

The **TriA-TriB-TriC-OpmH** efflux pump was identified as specific for the extrusion of the biocide triclosan. Remarkably, it is a quadripartite system, the only one composed of two MFPs (TriA and TriB), both necessary for the functioning of the pump and co-transcribed with the IMP TriC in an operon. The gene encoding OpmH is somewhat distant from the *triABC* operon (Mima *et al*., 2007). The regulation of the operon has not been fully clarified. The presence of a repressor, like many RNDs, is understandable, but the involvement of two regulators adjacent to *triABC* operon was excluded (Mima *et al*., 2007). The TriABC-OpmH was reported to be strongly expressed when a mutant deprived of the other systems responsible for triclosan clearance (MexAB-OprM, MexCD-OprJ, MexEF-OprN, and MexJK-OpmH) was exposed to this biocide (Mima *et al*., 2007). In the literature this efflux pump has not been described to expel any antibiotic.

Finally, the RND family includes **CzcCBA**, the only HME efflux pump known to be produced by *P. aeruginosa,* that is not apparently involved in the extrusion of antibiotics or toxic compounds. It is one of the systems responsible for the regulation of zinc, cadmium, or cobalt, allowing the metal extrusion from the cytoplasm or the periplasm to the extracellular medium, when their concentrations reach an excessive level. Remarkably, CzcA is the IMP component, CzcG the MFP and CzcC, also

known as OpmN represents the OMF and they assemble in a way similar to that of the HAE1 efflux pumps (Ducret *et al*., 2020).

Although this pump does not promote the extrusion of any antibiotic, its expression is closely related to carbapenems resistance, due to the concomitant action that their regulators have on OprD expression. In particular, CzcCBA expression is controlled by the two-component system CzcR-CzcS, a cytoplasmic signal transducer and an inner transmembrane sensor, respectively. CzcS can detect the increased periplasmic zinc concentration, thus activating CzcR. The CzcR activation, together with the chaperone Hfq, allows CzcR to bind on the *oprD* promoter, causing the porin's downregulation (Perron *et al*., 2004; Ducret *et al*., 2016). Like CzcRS, the periplasmic copper accumulation activates the two-component system CopR-CopS. Once activated after copper detection by CopS, CopR promotes the synthesis of CzcCBA. Moreover, CopR and Hfq interact to target the *oprD* promoter, thus repressing *oprD* transcription (Caille *et al*., 2007; Ducret *et al*., 2016). Both systems are therefore involved in switching the bacterium to a "state of emergency", as a response to metal accumulation stress. This is achieved by enhancing the main metal extrusion system and, at the same time, by repressing one of the most expressed porins involved in the uptake of various substrates.

1.5 β-lactam antibiotics

In 1928 Alexander Fleming observed that the mold *Penicillium notatum* (later known as *Penicillium chrysogenum*) that had contaminated a *S. aureus* culture produced a compound causing the bacterial lysis; in this way he discovered the molecule progenitor of the β-lactam family and named penicillin, but he did not directly propose a clinical use (Fleming, 1929).
It was in fact only in 1940 that the therapeutic properties of penicillin were studied in a clinical trial and the compound was massively used for the treatment of infected war wounds in the US army after 1943.
We do not know how much this discovery has influenced the fate of the II World War, but we can certainly affirm that penicillin represented one of the first "bullet" used to successfully fight bacterial infections.
It was only in 1945 that the chemical structure of penicillin was solved by X-ray crystallography (Figure 11) and the characteristic β-lactam ring was firstly described (Crowfoot *et al*., 1949).
The β-lactam family presently represents 60 % of the antibiotics used worldwide and, despite the emergence of several resistance mechanisms, remains generally effective for antibacterial treatment (Öztürk *et al*., 2015).

1.5.1 Mechanism of action

Despite its massive clinical use, the exact mechanism of β-lactam action remained unclear for several decades.
It was only in 1965 that it was first hypothesized that, thanks to the steric similarity between the D-ala-D-ala dipeptide and penicillins, this class of antibiotics might act as a suicide inhibitor of the specific DD-carboxypeptidase-transpeptidase (Tipper and Strominger, 1965); the study of the acylation of a serine residue in the *Streptomyces* R61 DD-peptidase that confirmed the assumed penicillin mechanism of action is worth mentioning (Frère *et al*., 1976).
On this basis, it was confirmed that penicillin interferes with the formation of cross links, the last step of PG synthesis, and compromises the structural integrity of the bacterial cell wall.
In broader terms, for this reason all DD-peptidases have been described as PBPs due to their property of being acylated by penicillin.

1.5.2 β-lactam classification

Despite the initial lack of information about its exact mechanism of action, after penicillin introduction, different studies identified other natural compounds, derived from molds (*i.e.*, cephalosporins) or bacteria (*i.e.*, nocardicine, monobactams and carbapenems) or chemically modified other molecules (Abraham *et al.*, 1953; Hashimoto *et al.*, 1976; Sykes *et al.*, 1981; Kahan *et al.*, 1979).

β-lactam antibiotics are characterized by the presence of the 4-atom β-lactam ring, containing an amide bond and this class of bactericidal molecules can be subdivided into 4 families and 13 sub-families distinguished by different spectra of action and different capacities to circumvent the resistance mechanisms evolved by bacteria. The structures of different compounds belonging to the β-lactam subfamilies that will be discussed within this chapter is reported in Figure 11.

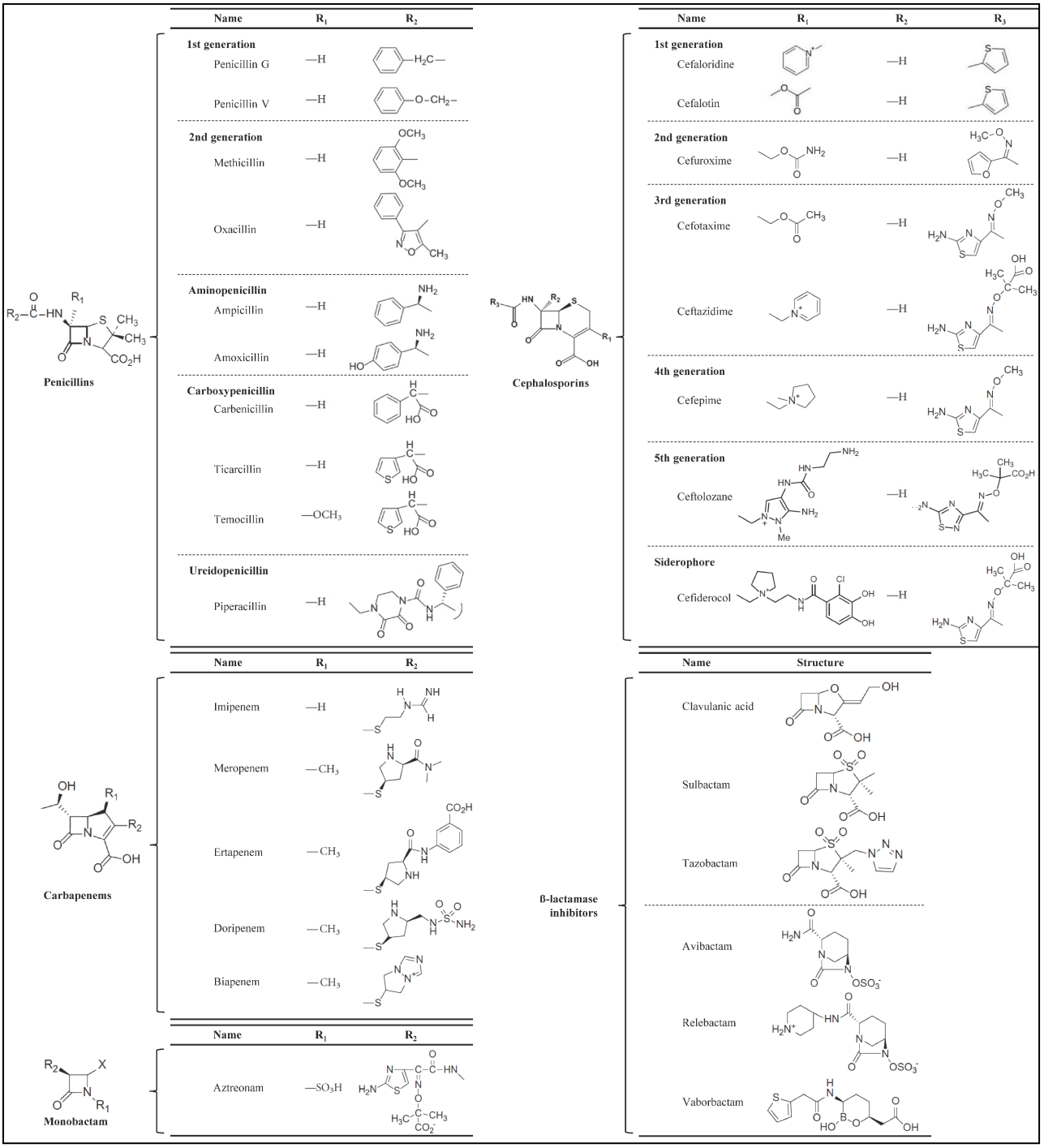

Figure 11: Structures of different β-lactam subfamilies listed in the text; β-lactamase inhibitors structures are also reported (adapted from Bush *et al*., 2016).

1.5.2.1 Penicillins

Penicillin was the first compound to be isolated, but the same term may also refer to a β-lactam family, that includes the penicillin G, also known as benzylpenicillin, very similar to the compound discovered by Fleming.

All these molecules are characterized by the presence of a penam, a bicyclic system containing a β-lactam moiety attached to a thiazoline ring (a five-membered ring containing a sulfur atom). These molecules differ by their specific R substituents.

This is a very wide family of compounds, exhibiting different activities, antimicrobial spectra, stability and susceptibility to inactivating enzymes (β-lactamases).

The β-lactam family can be further divided into 6 subfamilies:

I. First generation (or natural) penicillins (*i.e.*, penicillin G, penicillin V), that include compounds derived from *P. chrysogenum* and active only against non-β-lactamase producing Gram-positive cocci, including group A streptococci, such as *viridans streptococci* and *S. pneumoniae*.

These penicillins are also generally active against non-penicillinase producing *Staphylococcus spp.*, but their use is no longer recommended, due to the high likelihood of emerging resistance profiles.

Benzylpenicillin is the only compound belonging to this subfamily that is still used clinically as a valid option to treat life-threatening infections.

II. Second generation penicillins (*i.e.*, methicillin, oxacillin), which have been synthesized from the backbone of mold-produced antibiotics by substituting side chains to confer resistance to some β-lactamases, even though this modification led to decreased efficiency of the compounds.

Methicillin was introduced for clinical uses in 1959 but as soon as 1961 *S. aureus* resistant strains were reported (Jevons, 1961). The resistance is mediated by the synthesis of an alternative PBP target, named PBP2a that is encoded by the *mecA* gene.

This gene is carried on mobile genetic elements, thus facilitating the spread of this resistance.

Strains producing the alternative PBP target are defined as **m**ethicillin **r**esistant ***S***. ***a****ureus* (MRSA) and are characterized by resistance to different β-lactam subclasses. Oxacillin, due to its higher stability compared to methicillin, is currently used to screen MRSA strains (Chambers, 1997).

III. Aminopenicillins (*i.e.*, ampicillin, amoxicillin) were synthesized with the addition of a positively charged amino group, helping the translocation through bacterial porins (Danelon *et al*., 2006). This feature made it also adequate for oral administration (no hydrolysis under acidic conditions) and extended their use against different Gram-negative bacteria including *E. coli* but not *P. aeruginosa*.

These compounds, however, are quite sensitive to β-lactamases and, for this reason, are nowadays

usually prescribed in association with β-lactamase inhibitors, such as clavulanate or sulbactams, that are essential for therapeutic efficiency (Geddes *et al*., 2007).

IV. Carboxypenicillins (*i.e*., carbenicillin, ticarcillin, temocillin), which are characterized by the presence of a carboxylic acid or a carboxylic acid ester group in their variable side chain; this feature enlarged their activity spectrum against *P. aeruginosa* or *Proteus spp*., but the compounds remained sensitive to β-lactamases. For this reason, their administrations in association with β-lactamase inhibitors is recommended.

Importantly, temocillin, a methoxy-derivative of ticarcillin, is characterized by its stability to AmpC and different Extended-Spectrum β-Lactamases (ESBLs), including TEM, SHV, and CTX-M (Glupczynski *et al*., 2007).

However, temocillin is inactive against Gram-positive and *P. aeruginosa*, in contrast with the other members of this subgroup. After a first phase when its use was limited due to its narrow activity spectrum, this antibiotic has been reconsidered as a valid therapeutic option for some resistant Enterobacterales (Livermore and Tulkens, 2009).

In the case of *P. aeruginosa,* its intrinsic resistance has been correlated with efflux pump expression, or in a broader term with OM permeation, but the point is still debated.

A recent study has remarkably revealed that *P. aeruginosa* strains, isolated from CF patients and carrying mutations in the MexAB-OprM machinery, exhibited a restored susceptibility to temocillin (Buyck *et al*., 2012; Chalhoub *et al*., 2017).

V. Ureidopenicillins (*i.e*., mezlocillin, piperacillin) differ from penicillins by the substitution of the amino acid side chain with a variety of cyclic ureas, conferring a broad activity spectrum against Gram-positive and Gram-negative bacteria, including *P. aeruginosa*, and a favorable pharmacokinetic profile.

They are characterized by a better penetration through the bacterial cell wall, and a higher affinity for the PBPs but, as other penicillins subclasses, they are susceptible to β-lactamase inactivation.

For this reason, piperacillin, a specific ureidopenicillin, is commonly administered in association with the β-lactamase inhibitor tazobactam.

1.5.2.2 Cephalosporins

The discovery of the cephalosporins was similar to that of penicillins and resulted from an environmental monitoring. In the 1940s, the Italian scientist Giuseppe Brotzu observed a decreased incidence of salmonellosis in Cagliari's port wastewater, compared to other similar environments.

He hypothesized the presence of some bactericidal agent, isolated a *Cephalosporium acremonium* strain and managed to produce an antibacterial extract, called "mycetin".

The subsequent identification of cephalosporin C from this extract was achieved in 1953 (Abraham *et al*., 1953) and this molecule is considered as the progenitor of a wide number of antibiotic compounds.

Cephalosporins share the same structure of a six-membered dihydrothiazine ring, bound to the β-lactam ring yielding the cephems nucleus. This wide group of compounds is characterized by a moderate activity against penicillin-resistant strains.

Based on their discovery, they are traditionally divided into at least five different generations, according also to their properties and antibacterial activities.

First-generation cephalosporins (*i.e*., cefalotin, cefaloridine) are very active against Gram-positive cocci except for *Enterococcus spp*., methicillin-resistant staphylococci or *Listeria spp*. but can also be efficient against some Gram-negative, including *E. coli*, *K. pneumoniae* and *Proteus spp*..

Second-generation cephalosporins (*i.e*., cefuroxime, cefaclor) possess a similar spectrum of action to that of the first-generation cephalosporins, although less active against Gram-positive bacteria, but they can also be used to treat infections caused by *Haemophilus influenzae* and *Klebsiella aerogenes*. In particular, cefuroxime is widely used to successfully treat urinary and respiratory tract infections (Perry and Brogden, 1996).

Traditionally, due to their clinical properties, the cephamycin compounds cefoxitin and cefotetan are included in this subgroup.

Third-generation cephalosporins (*i.e*., cefotaxime, ceftriaxone, ceftazidime) have a weaker activity against Gram-positive bacteria but, with the exception of ceftazidime, can be successfully used against staphylococcal infections; their main property is a higher activity in cases of infections due to Gram-negative bacteria.

Moreover, they are able to cross the blood-brain barrier and are effective against central nervous system infections or sepsis caused by Gram-negative bacteria.

Of particular interest is ceftazidime, an efficient therapeutic option to treat infections due to Enterobacterales and *P. aeruginosa*.

However, the expression of ESBLs or AmpC β-lactamases has compromised its efficacy, subsequently restored by the co-administration of avibactam, a non-β-lactam β-lactamase inactivator (van Duin and Bonomo, 2016).

Fourth-generation cephalosporins (*i.e*., cefepime, cefpirome), due to their zwitterionic nature, possess a higher capacity to cross the Gram-negative OM and are characterized by their resistance to β-lactamases that can hydrolyze third-generation cephalosporins.

For instance, cefepime possesses a quaternary ammonium group that facilitates translocation across the Gram-negative OM. It has a broad antibacterial activity spectrum, and its antipseudomonal properties are similar to those of ceftazidime (Kessler, 2001).

Fifth-generation cephalosporins (*i.e*., ceftaroline, ceftolozane, ceftobiprole) have been designed to treat particularly drug-resistant strains. For example, ceftobiprole is active against MRSA, while ceftolozane, in combination with the β-lactamase inhibitor tazobactam, is used for complicated urinary tract infections caused by β-lactamases producing Gram-negative bacteria (van Duin and Bonomo, 2016).

Siderophore cephalosporin. The traditional cephalosporins classification by generation does not fit all recently approved compounds. Notably, cefiderocol is the first siderophore cephalosporin, approved in Europe in 2020, that exploits the properties of the chlorocatechol group linked to the C-3 side chain (Sato *et al*., 2019). This structure allows the uptake of the compound by the siderophore transport systems of Gram-negative bacteria and confers resistance to β-lactamase hydrolysis, including different carbapenemases.

The permeation via active iron transporters, which has so far remained untapped, has made siderophores a Trojan horse against pathogens that are currently resistant to almost all available compounds (Rayner *et al*., 2023).

1.5.2.3 Monobactams

This group possesses a peculiar β-lactam structure, defined by a monocyclic ring lacking the second ring.

Firstly isolated from *Chromobacterium violaceum,* aztreonam is the only member of this subclass to be used in clinical practice (Sykes *et al*., 1981).

Aztreonam presents a low toxicity and has activity against aerobic Gram-negative bacilli, including *P. aeruginosa*. Moreover, it has a good stability towards metallo-β-lactamases (MBL), but can be hydrolyzed by other β-lactamases, such as the CTX-M type.

The urgent search for valid options to treat MDR strains has made aztreonam a good candidate to be administrated in combination with avibactam, to ensure its activity against different inactivating enzymes (Crandon and Nicolau, 2013).

Although the combination aztreonam-avibactam is not available yet, different studies have encouraged the utilization of an association therapy with aztreonam and ceftazidime/avibactam to successfully fight Gram-negative bacteria producing various β-lactamase classes (Lee *et al*., 2021).

1.5.2.4 Carbapenems

Among β-lactams, carbapenems are the most potent broad-spectrum compounds and are resistant to most Ambler class A and C β-lactamases but are nevertheless susceptible to MBLs hydrolysis, like L1 produced by *Stenotrophomonas maltophilia*. However, *E. faecium* and MRSA are resistant to carbapenems due to low affinity of modified PBPs.

They are considered as the last resort therapeutic strategy, and they should be carefully utilized only against MDR strains.

Carbapenems have a penicillin-like five-membered ring but the sulfur atom in position 1 of the five-membered ring is replaced by a carbon atom, and a double bond is found between C2 and C3; this structure is known as penem.

Unlike, penicillins and cephalosporins, they have a hydroxyethyl side chain in trans configuration that makes them stable to inactivating enzymes.

The first member of this subfamily to be discovered was thienamycin, a natural compound produced by *Streptomyces cattleya* (Kahan *et al*., 1979). Despite its encouraging properties, thienamycin was found to be unstable in aqueous solutions and therefore unsuitable for *in vivo* therapies. A *N*-formimidoyl chemical modification to thienamycin structure increased its stability and the new molecule was named imipenem (Miyadera *et al*., 1983).

Imipenem was the first clinically approved carbapenem but presented a rapid degradation by renal tubular brush border dehydropeptidase I (DPH I), that was prevented by the co-administration of cilastatin, a DPHI I inhibitor (Norrby, 1985).

The imipenem lateral chain is conformationally and structurally identical to that of arginine, and this feature appears to be crucial for the drug penetration through specific basic amino acids channels (Figure 8).

The association of relebactam, a β-lactamases inhibitor, to imipenem/cilastatin has recently enlarged the arsenal for the treatment of complicated infections (*i.e*., pneumonia, bacteriemia or urinary infections) caused by MDR Gram-negative bacteria with limited treatment options, including *P. aeruginosa* (O'Donnel and Lodise, 2022).

The research of a higher stability to renal degradation led to the addition of a methyl group to the 1-β position and almost all other carbapenems share this feature.

One of these compounds, meropenem, is also characterized by a wider antibacterial spectrum, exhibiting better results against infections mediated by Enterobacterales and *P. aeruginosa*. Meropenem, due to its broad-spectrum antibacterial activity, is indicated for empirical therapy and can be prescribed, for example, in case of septicemia or meningitis before exact bacterial

identification. However, susceptibility tests, including manual ones, must always be performed, as it is not uncommon to find strains resistant to meropenem and susceptible to imipenem (Harino *et al*., 2013).

In addition, meropenem is also widely used to treat complicated infections affecting different areas such as abdomen, skin, respiratory or urinary tracts (Baldwin *et al*., 2008).

Its recent association with vaborbactam, a β-lactamases inhibitor, enhances its efficiency against Ambler class A β-lactamases producing organisms, especially for the extremely diffused KPC-producing *K. pneumoniae* strains (Novelli *et al*., 2020).

Ertapenem, that differs from meropenem in its 2′ substituent, carrying a *meta*-substituted benzoic acid group (Köhler J. *et al*., 1999), is active against different Gram-positive and Gram-negative bacteria but has a marginal activity against important non-fermenters pathogens, such as *Acinetobacter spp*. or *P. aeruginosa*, thus limiting its empirical prescription for nosocomial infections (Livermore *et al*., 2003).

Another member of this family, biapenem, characterized by a 2-substituted triazolium moiety, was approved in Japan in 2001 and its use was approved only in some Asiatic nations.

Biapenem has been described to be highly effective against *P. aeruginosa*, including strains growing in adherent biofilms or exhibiting MexCD-OprJ efflux pump overexpression (Vora and Tiwaskar, 2022).

Doripenem is a broad-spectrum carbapenem with enhanced affinity for *P. aeruginosa* PBP2 and PBP3, giving this compound antipseudomonal properties (Fritsche *et al*., 2005; Davies *et al*., 2008).

1.5.2.5 β-lactamase inhibitors

We have mentioned several times various β-lactamase inhibitors that allow the continued utilization of compounds that are sensitive to inactivating enzymes. We will focus in this section on these compounds that share structural similarities with β-lactams and are increasingly at the center of studies searching for new therapeutic solutions.

β-lactamase inhibitors can broadly be divided on the basis of their mechanism of action: *i)* they can act as β-lactamase suicide inhibitors by binding to the enzyme active site or *ii)* they can create sterically unfavorable interactions.

Clavulanic acid, a β-lactam with a modest antibacterial activity, was discovered in 1977 in *Streptomyces clavuligerus* (Reading and Cole, 1977) and behaves as a suicide inhibitor. It is characterized by a clavam core, a β-lactam structure where an oxygen atom replaces the sulfur in

the 5-member ring and devoid of acylamino side chain. The ability to block the hydrolyzing activity is mediated by the acylation of the serine residue in the active site of the enzyme, resulting in the inactivation of many β-lactamases (almost only Ambler classes A), including different TEM and SHV variants and CTX-M (Chen and Herzberg, 1992; Drawz and Bonomo, 2010).

Sulbactam and tazobactam, two penicillin sulfones derivates, were successively synthetized respectively in 1978 and 1980, with the aim of inactivating a large number of β-lactamases. Sulbactam has an enhanced activity against class C β-lactamases, exhibits a modest antibacterial activity against *Acinetobacter spp*., and, compared to clavulanic acid, is less prone to induce β-lactamase production (Akova, 2008).

Tazobactam has an activity similar to that of sulbactam, but its association with piperacillin was shown to have a better synergic activity against MDR Gram-negative infections (Kuck *et al*., 1989).

The second group includes the non β-lactams β-lactamase inhibitors, a heterogeneous family of compounds which exploits various mechanisms to inactivate clinically relevant enzymes.

Avibactam is a diazabicyclooctane (DBO) compound that forms a covalent carbamate bond with the enzyme active serine. It is characterized by a reversible acylation, thus enabling its re-cyclization and allowing its successive binding to additional enzymes (Ehmann *et al*., 2012). Avibactam is used to restore the antibiotic activity against different Ambler class A (in particular KPC), class C and some class D β-lactamases (especially OXA-48-like enzymes), and in 2015 it has been approved by Food and Drug Administration (FDA) for clinical administration with ceftazidime.

Relebactam is another DBO with an added piperidine ring. Its mechanism and spectrum of action is similar to those of avibactam, differing, however, for its limited activity against class D carbapenemases (Blizzard *et al*., 2014). It has been approved in 2019 by FDA for clinical use in association with imipenem/cilastatin, to improve their antibacterial activities against complicated urinary and intra-abdominal infections. Notably, resistance to imipenem/cilastatin/relebactam have been reported associated to mutations in porins and efflux pump systems (Karaiskos *et al*., 2025).

Vaborbactam is a cyclic boronic acid β-lactamase inhibitor that exploits the already known properties of boronic acid to hamper enzyme activity by forming a transient adduct with the catalytic serine, a reaction that blocks the active site responsible for antibiotic degradation (Werner *et al*., 2017). For this reason, it only inhibits enzymes that contain an active site serine, in particular against KPC enzymes, and remains inactive against MBLs. It is the first boronic acid derivative inhibitor approved in 2017 by the FDA in combination with meropenem, with an indication in the case of complicated urinary tract infections, and it is currently utilized to treat the extremely widespread KPC-producing *K. pneumoniae* (Dhillon *et al*., 2018; Giacobbe *et al*., 2023).

Although it is effectively used for MDR infections, resistances mediated by mutations in OmpK35 and OmpK36 porins have been described in *K. pneumoniae*. These studies highlight how, in this case as well, resistance may depend on a different porin expression that alters outer membrane permeability (Karaiskos *et al*., 2025).

1.6 β-lactam resistance

The antibacterial activity of β-lactams is challenged by the emergence of bacteria resistant to antibiotics. In Gram-negative bacteria this phenomenon is caused by the interplay between four independent factors: *i)* the sensitivity of the target enzymes, the PBPs *ii)* the properties and concentration of enzymes capable of inactivating β-lactams *i.e.*, periplasmic β-lactamases and alterations of the traffic through the OM mediated by *iii)* the overexpression of active efflux systems or iv) a reduced expression of the OM porins (Figure 12) (Poole, 2011).

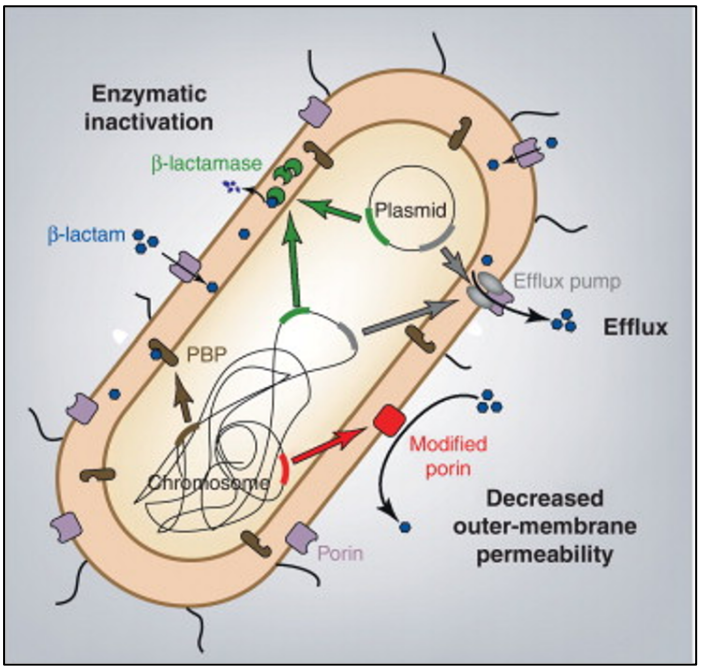

Figure 12: Graphical representation of the main mechanisms involved in bacterial resistance to β-lactams. The antibiotic efficacy depends on the bind between β-lactam and the PBP target and this can be modified by the synthesis of an alternative target; the production of inactivating enzymes (β-lactamases) can be mediated by constitutive or acquired genes, thus leading to antibiotic degradation; the β-lactam need to reach and adequate periplasmic concentration to perpetuate its activity, and this can be altered by a decreased/modified porin expression, or by efflux pumps overexpression (Nordmann *et al*., 2012).

A fifth and more recent element that influences the OM reduced permeability mechanism is the LPS thickening (Alvarez-Ortega *et al*., 2010).

All these mechanisms can be found in *P. aeruginosa* resistant strains, with a notably different incidence. In particular, in *P. aeruginosa* it is very common to find different simultaneous resistance mechanisms. As many different pieces of a complex jigsaw puzzle, this phenomenon generates many distinct phenotypic profiles.

We will now describe the different alterations that could change the antibiotic susceptibility, with a particular focus on *P. aeruginosa* β-lactam resistome.

1.6.1 Target modifications

The synthesis of alternative PBP targets is prevalently found in Gram-positive cocci, but some Gram-negative, such as *Neisseria* spp. and *Haemophilus* spp., are well known to produce modified PBPs that can confer resistance to β-lactams (Zapun *et al*., 2008).
The relevance of this mechanism has long remained controversial for *Pseudomonadaceae* and, although some PBP alterations have been associated with β-lactams increased resistance, their role is marginal.
In any case, the first correlation found was an indirect one, since mutations in *dacB* gene, encoding the non-essential PBP4, are the cause of AmpC β-lactamase overexpression, and consequently an increased resistance to some β-lactams (Moya *et al*., 2009).
A second observation was the reduced expression of the PBP pattern, correlated to antibiotic resistance, but not sufficient to result in a resistance phenotype by itself (Giske *et al*., 2008).
The third piece of evidence was revealed by the association of PBP1a/b modifications to some cephalosporin and carbapenem resistance (Moyá *et al*., 2012).
Another example is the adaptative PBP3 polymorphisms, derived from exposure to β-lactams, that are associated with a reduced susceptibility not only to cephalosporins but also to meropenem (Clark *et al*., 2019).
PBP modification is therefore a mechanism not widely present in *P. aeruginosa* clinical isolates, but to be anyway taken into consideration, especially as a possible response to the new generation cephalosporins.

1.6.2 Production of inactivating enzymes

β-lactamase-mediated resistance is undoubtedly the most developed mechanism in Gram-negative bacteria. It is the main cause of the rising incidence rate of antibiotic resistance in clinical settings, although the interplay with other mutations, like efflux pumps overexpression, can enhance the final phenotype.
In Gram-negative bacteria these enzymes are produced in the periplasm and are responsible for the hydrolysis of the amide bond in the β-lactam ring resulting in the production of an inactive derivative (Frère, *et al*., 2016).

These enzymes can be constitutively expressed in Gram-negative bacteria, but their emergence is mainly due to the localization of the corresponding genes in mobile DNA elements, such as plasmids and transposons, thus facilitating their spread through horizontal gene transfer.

Since the first report in 1940 of an "enzyme able to destroy penicillin" more than 1500 different β-lactamases have been identified (Frère *et al*., 2016) and a description of them, constantly updated, can be found in the online available database (http://www.bldb.eu) (Naas *et al*., 2017). The first broad classification can be made on the basis of their structures and hydrolysis mechanisms resulting in *i)* serine β-lactamases (SBLs) and *ii)* metallo-β-lactamases (MBLs) enzymes (Bush and Jacoby, 2010).

SBLs hydrolysis occurs via the formation of a covalent intermediate between the side-chain oxygen of the active site serine residue and the C=O carbon atom of the β-lactam ring. The acyl-enzyme product is then usually rapidly hydrolyzed, and the enzyme is ready for a successive reaction, unless a β-lactamase inhibitor is present.

MBLs are characterized by the presence in their catalytic site of at least one zinc cofactor participating in antibiotic hydrolysis. Due to their dependence on metal ions availability, their activity is inhibited by the presence of metal chelating agents, like ethylenediaminetetraacetic acid (EDTA) or dipicolinic acid (DPA). These compounds decrease β-lactam MIC values, but no clinical application is possible due to their intrinsic effect as membranes destabilizers and their general toxicity (Prachayasittikul *et al*., 2007; Bahr *et al*., 2017). Notably, variations in MIC values, must also take account of the membrane fluidification that would facilitate antibiotic diffusion.

The discovery of a metal chelator with low or no toxicity would certainly be a milestone in the treatment of infections caused by MBL-producing bacteria, but this seems to be presently an impossible dream.

A second classification, based on amino acid sequence similarities was proposed by Ambler and presently distinguishes four different classes, named A, B, C or D (Ambler, 1980). Class B represents MBLs while the other three classes include different SBLs.

It is worth mentioning that based on the very different kinetic properties of the enzymes, another classification has been proposed that defines four groups and multiple major subgroups (Bush, 2023). Nevertheless, the following discussion will be based on the Ambler classification, that we consider an adequate starting point to discuss the *P. aeruginosa* resistance mechanisms.

1.6.2.1 Class A β-lactamases

This class includes a wide range of enzymes, characterized by very diverse spectrum of antibiotic hydrolysis.

Among the most widespread, we can mention the TEM-1 and SHV-1 variants, enzymes with a strong propensity to hydrolyse penicillins and early generation cephalosporins, such as cephaloridine and cephalothin.

However, the introduction of third generation cephalosporins has resulted in the appearance of new TEM- and SHV-derived enzymes. These are characterized by one to three specific amino acid substitutions that enlarge their activity spectra, conferring resistance to third generation cephalosporins and monobactams (Livermore, 1995). For this reason, these enzymes have been defined as ESBLs.

Successively, CTX-M β-lactamases, that hydrolyze cefotaxime, ceftazidime and ceftriaxone, have emerged in clinical settings. CTX-M are generally found in *E. coli* and *K. pneumoniae* while detection of *P. aeruginosa* strains producing these β-lactamases is sporadic (Al Naiemi *et al*., 2006).

The GES enzyme, defined as an ESBL, is worth mentioning. Some variants are characterized by a carbapenemase activity. In particular, GES-5, that has been isolated from *P. aeruginosa* strains, is able to confer resistance to imipenem (Matlock *et al*., 2024).

In addition, among class A β-lactamases, the most worrisome enzyme is KPC that confers resistance to all β-lactams, including carbapenems. It is generally carried by mobile genetic elements, and is increasingly found in *K. pneumoniae* clinical isolates, but also in *P. aeruginosa* (Gali *et al*., 2023).

Finally, *P. aeruginosa* possesses a constitutive Class A imipenemase, named PIB-1, recently described to confer intrinsic resistance to carbapenems (Fajardo *et al*., 2014). However, this enzyme is not highly expressed in the laboratory reference strain PAO1 (Zincke *et al*., 2015).

Despite the concerns that these enzymes represent in clinical settings, Class A β-lactamases, including ESBLs, are generally susceptible to β-lactamase inactivators such as clavulanic acid, sulbactam, or tazobactam. In addition, KPC type enzymes are generally susceptible to non β-lactams β-lactamase inhibitors, such as vaborbactam or relebactam that restore the antibiotic activity, except for some KPC variants carrying specific mutations in the omega loop region (Findlay *et al*., 2021).

1.6.2.2 Class B β-lactamases (MBL)

The first enzyme belonging to this class was identified in 1966 in *Bacillus cereus* and, for many years, was not considered to have a significant clinical impact. However, the ability of MBLs to

inactivate both third and fourth generation cephalosporins and carbapenems has made them currently one of the most worrisome problems in the fight against bacterial resistance.

MBLs constitute a heterogeneous group with high variations in sequence identities, that can be lower than 23 %. In many cases several allelic variants have been documented (Queenan and Bush, 2007). Among the most prevalent, we can mention the VIM, IMP, NDM enzymes, while GIM, SIM, DIM and SPM are sporadically isolated.

P. aeruginosa does not have any MBL in its genome but it can acquire the corresponding genes thanks to mobile genetic elements like plasmids, transposons or integrons.

Interestingly, two of the currently most prevalent MBL carbapenemases, the IMP imipenemase and the Verona Integron-encoded-MBL VIM were first isolated in *P. aeruginosa* (Watanabe *et al*., 1991; Lauretti *et al*., 1999). Remarkably, two others MBLs, SPM and GIM, that are associated to specific high-risk clones mostly widespread in clinical settings in Brazil and Germany, respectively, were also initially identified in *P. aeruginosa* (Toleman *et al*., 2002; Castanheira *et al*., 2004; Silveira *et al.*, 2016; Wendel *et al*., 2015).

A worldwide diffusion of MDR *P. aeruginosa* strains carrying different variants of bla_{VIM} has caused a large number of outbreaks, particularly in clinical settings (Hong *et al*., 2015). In particular, the European epidemiology considers VIM-2 as the most prevalent MBL, due to the proliferation of specific clones carrying this determinant (Fortunato *et al*., 2023).

MBLs are able to hydrolyze all β-lactams and are not inhibited by any of the currently available inhibitors. They are less active towards monobactams and, for this reason, the ceftazidime/avibactam combination together with aztreonam may sometimes be efficient (Falcone *et al*., 2021).

The real revolution was represented by the introduction of siderophore cephalosporins, that are currently not good substrates for MBLs. However, selective pressure is undoubtedly a factor that may facilitate the appearance of new allelic variants with activity against cefiderocol (Wang *et al*., 2024).

Despite these few available options, MBL producing *P. aeruginosa* represents an alarming challenge that almost exclude β-lactams from therapeutic choices against strains that often carry a large number of resistance determinants to other antibiotic classes. In particular, the simultaneous overexpression of efflux pump systems that can confer resistance to a wide range of antibiotics different from β-lactams, greatly restricts the range of efficient therapeutic options.

1.6.2.3 Class C β-lactamases

Class C β-lactamases are enzymes that are generally chromosomally encoded in different Enterobacterales, but also in *P. aeruginosa* and are generally more active against cephalosporins than penicillins; interestingly their activity is important against aztreonam and they are not inhibited by clavulanic acid.

In *P. aeruginosa* the presence of a chromosomal inducible AmpC, also known as *Pseudomonas*-derived cephalosporinase (PDC), is the leading cause of its intrinsic resistance to aminopenicillins, first- and second-generation cephalosporins (Jacoby, 2009).

Its induction is mediated by PG damage that cause the accumulation of large amounts of muropeptides that mediate an AmpR-dependent induction of AmpC. Some β-lactams, such as cefoxitin or imipenem, are strongly related to this activation pathway (Curtis *et al*., 1986; Tausk *et al*., 1985). For this reason, the efficiency of antipseudomonal β-lactams results from the poor AmpC induction mediated by antibiotics such as piperacillin or ceftazidime, although these molecules can be hydrolyzed by AmpC when overexpressed (López-Argüello *et al*., 2021).

However, AmpC hyperproduction may result from the mutational inactivation of *ampD* or *ampR*, two regulators involved in AmpC expression, altering the correct regulation of this mechanism (Juan *et al*., 2005).

Unlike what happens to Enterobacterales, in *P. aeruginosa* AmpC overexpression is the cause of an extended activity against third- and fourth- generation cephalosporins in a dose-dependent manner. For this reason, resistance to ceftazidime and cefepime may only result from an AmpC upregulation (Castanheira *et al*., 2014).

It has also been demonstrated that exposure to ceftazidime/avibactam and ceftolozane/tazobactam can induce AmpC mutations in the active site that confer resistance to these drug combinations (Ruedas-López *et al*., 2022). On the contrary, AmpC mutations or overexpression are not sufficient to provide resistance to carbapenems (Jacoby, 2009).

1.6.2.4 Class D β-lactamases

Class D β-lactamases are enzymes able to hydrolyze oxacillin and not affected by most of the currently available inhibitors, except for avibactam. These enzymes are often found in *A. baumannii* strains, where they were also first isolated in 1993, and more that 1100 allelic variants have been described up to now and can be retrieved on the β-lactamase data base (http://www.bldb.eu) (Paton *et al*., 1993; Bush, 2023; Naas *et al*., 2017).

Historically (and unfortunately) they have all been defined by the term OXA, followed by a number, but at least nine majors different OXA subgroups can be identified.

Class D includes enzymes with different substrate specificities, among which some have a profile limited to penicillins while other have acquired ESBL properties. In addition, some variants evolved to broaden their spectrum of action while exhibiting carbapenemase activity.

Notably, OXA-10, which confers resistance to cefotaxime and ceftriaxone, but not to ceftazidime, is frequently found in *P. aeruginosa* clinical strains thanks to the diffusion of specific plasmids. In the same subgroup, different allelic variants have been isolated in *P. aeruginosa* clinical strains with different spectra of action. For instance, we can mention OXA-14 that has an enlarged activity against ceftazidime (Danel *et al*., 1995).

Moreover OXA-40 and OXA-198, both with carbapenemases properties, have been isolated in *P. aeruginosa*, which contributes to the enlargement of its antibiotic resistance arsenal (Sevillano *et al*., 2009; El Garch *et al*., 2011).

Interestingly, OXA-48, a worldwide prevalent class D carbapenemase and its allelic variants are frequently found among Enterobacterales, while their detection in *P. aeruginosa* clinical strains is less frequent, although reported occurrences have been recently rising (Vatansever *et al*., 2020; Gondal *et al*., 2024).

Finally, in *P. aeruginosa* PAO1, a chromosomally encoded β-lactamase, named PoxB (OXA-50), has been reported to be constitutively expressed, and also has been speculated to be associated with the inactivation of some carbapenems (Zincke *et al*., 2015). However, it does not seem to significantly contribute to *P. aeruginosa* PAO1 intrinsic resistance, but a possible selective pressure mediated by the introduction of the new non β-lactams β-lactamase inhibitors may make this constitutive resistance mechanism progressively more relevant (Zincke *et al*., 2015).

1.6.3 Permeability modifications

In Gram-negative bacteria the efficiency of a β-lactam rests on its capacity of reaching the PBPs, the molecular targets of the antibiotic. This is influenced by the permeability of the OM, that can be extremely variable among different species. In particular, *P. aeruginosa* wild type strains are characterized by a marked impermeability when compared to Enterobacterales such as *E. coli* (Matsumura *et al*., 1999). Moreover, different mechanisms can enhance the inaccessibility of the PBPs to β-lactams.

We will now focus on the different mechanisms that can increase β-lactam resistance in *P. aeruginosa* clinical strains.

1.6.3.1 LPS modification

Alterations in the composition of the OM may change the membrane's properties, resulting in an increased impermeability to antibiotics.
This mechanism has been recently described and associated with β-lactam tolerance and/or resistance to certain molecules.
In particular, we can report the increase in the MIC for ceftazidime and meropenem after the appearance of mutation in *galU*, encoding a UDP-glucose pyrophosphorylase and *wapR*, a rhamnosyltransferase, both involved in the synthesis of the LPS core (Alvarez-Ortega *et al*., 2010). Remarkably, these modifications are frequently found after exposure to repeated cycles of antibiotic therapies, like in CF treatments.
Various other mutations in genes involved in LPS synthesis have been found to alter the susceptibility to ceftazidime and, although in a marginal way, they all contribute to the final resistome of the bacteria (Alvarez-Ortega *et al*., 2010).

1.6.3.2 Efflux pumps alterations

As already described, up to twelve different efflux pump systems are produced by *P. aeruginosa* and, although to a different extent, they all contribute to an intrinsic antibiotic resistance phenotype. Their expression is finely modulated by several regulator genes as a response to a multitude of external stimuli (Morita *et al*., 2003; Sivaneson *et al*., 2011; Morita *et al*., 2012; Liao *et al*., 2013; Tian *et al*., 2016). The antibiotic selective pressure is by far the most relevant event that may induce mutations in the repressor genes, resulting in an uncontrolled increased expression of these pumps.

MexAB-OprM is the main efflux pump system whose overexpression gives rise to pronounced resistance to a broad range of antibiotics, including nearly all β-lactams, with the exclusion of imipenem, imipenem/relebactam and ceftolozane/tazobactam. As already mentioned, MexAB-OprM are under the control of different negative regulators and mutations altering their activity result in an increased antibiotic resistance (Srikumar *et al*., 2000).
Historically, strains that carry a mutated *mexR* repressor are defined as having a *nalB* phenotype (Saito *et al*., 1999). Similarly, *nalD* mutants that present an increased efflux pump expression are defined as *nalD* phenotypes (Morita *et al*., 2006). These mutations generally imply a translational disruption or non-sense substitutions that hamper the repressors' DNA binding site.

Other mutations may involve a large number of various regulator genes, among which one of the most studied is *nalC,* which has an indirect activity on MexR expression, giving rise to the so-called *nalC* phenotype (Cao *et al*., 2004).
Whatever mutation the dysregulation is caused by, MexAB-OprM overexpression can confer a worrying resistance profile to multiple antibiotics.

Concerning others efflux pumps, MexXY/OprM overexpression poorly correlates with β-lactams resistance, since aminoglycosides represent its principal target, but it can confer resistance to some cephalosporins (cefepime and ceftolozane/tazobactam) and carbapenems (imipenem and meropenem) (Castanheira *et al*., 2022). This phenotype can be due to various mutations involving the repressor MexZ or its target, the *mexX-mexZ* intergenic region. Furthermore, overexpression has been associated with mutations affecting the two-component activator ParR-ParS, or with an impaired protein synthesis that is mediated by mutations in the *rplA* gene that encodes a ribosomal protein (Morita *et al*., 2012).
NfxB mutants, resulting in a MexCD-OprJ upregulation, are not widespread and are associated with an increased resistance to cefepime and also to fluroquinolones and chloramphenicol. However, these mutants are generally characterized by a higher susceptibility to ticarcillin, aztreonam, and imipenem due to a decreased expression of MexAB-OprM and/or mexXY (Poole *et al*., 1996; Jeannot *et al*., 2008). Interestingly, it has recently been shown that an additional mutation in MexD in a *nfxB* mutant can also confer resistance to ceftazidime/avibactam and to ceftolozane/tazobactam (Gomis-Font *et al*., 2021).

MexEF-OprN overexpression is mainly mediated by *mexS* or *mexT* inactivating mutations and these strains present an increased resistance to fluroquinolones, trimethoprim, and chloramphenicol but not to β-lactams (Köhler *et al*., 1997). However, the *mexT* mediated MexEF-OprN upregulation coincides with an OprD downregulation, causing an indirect increased resistance to carbapenems (Köhler *et al*., 1997; Ochs *et al*., 1999a).

1.6.3.3 Porin deletion and modification

The intrinsic low OM permeability is a consequence of the absence of non-specific large pores, but this feature can also be enhanced by specific alterations.
OprD mutations that result in downregulation or lack of expression of a functional porin are textbook examples of the imipenem resistance related to a single porin. As a result, the same mutations have

increased MICs for all the carbapenems, although below the breakpoints for resistance, without significantly affecting the others β-lactam subclasses.

This can be achieved in several ways, including *i)* mutations, *ii)* nucleotide insertions or deletions (*indel*), *iii)* integration of insertion sequences truncating *oprD*. Interestingly, all these mutations can be quite easily acquired during prolonged antibiotic therapies (Fang *et al*., 2014; Ocampo-Sosa *et al*., 2012; Rojo-Bezares *et al*., 2014; Sherrard *et al*., 2022).

Mutations may cause changes in the amino acid sequence, resulting in structural alterations that, when occurring in certain positions, may inhibit the porin's functionality (Alvarez-Ortega *et al*., 2010; Rojo-Bezares *et al*., 2014). The *indel* mutations may change the frameshift and/or introduce a premature stop codon, while the insertion sequence integration disrupts the gene. These events result in the inactivation of the porin.

It is also important to highlight that *oprD* frequently presents polymorphisms like, for example, between PAO1 and PA14, another laboratory strain, that only result in very small MIC differences (Alvarez-Ortega *et al*., 2010). For this reason, if frameshifts or insertions easily correlate with the loss of porin functionality, each mutation must be carefully correlated with the changes produced in the tertiary structure. Any mutation affecting *oprD* must be confirmed by MIC determinations and, if possible, by testing the porin insertion into the OM, to differentiate between polymorphisms and alterations inactivating OprD (González-Vázquez *et al*., 2021). The main evidence is that mutations in the external loops L2 and L3, both involved in basic amino acids and imipenem binding, increases resistance to carbapenems (Ochs *et al*., 2000; Li *et al*., 2012; Ocampo-Sosa *et al*., 2012). However, the substitution of 12 residues with a different sequence of 10 amino acids that shortens the external loop L7 induces an enlarged opening of the channel. This results in the usual resistance to imipenem, common to different *oprD* mutations but, at the same time, in an increased susceptibility to meropenem (Epp *et al*., 2001). A similar effect of meropenem increased activity was observed as a result of the deletion of 8 amino acids in loop L7 without affecting the imipenem MIC (Huang *et al*., 1995). To further complicate the understanding of OprD behaviour, a recent study contradicted the previous assumption made by Epp and coworkers, highlighting meropenem resistance in strains carrying the 8 amino acid substitutions in loop L7 (Abu Khadra *et al*., 2022).

An interesting study by Pirnay and co-workers took into consideration 55 different *P. aeruginosa* strains, both from hospital settings and the environment with different sensitivities to imipenem. They pointed out the great *oprD* variability between imipenem-sensitive strains and identified unique mutations in 12 imipenem-resistant strains (Pirnay *et al*., 2002). This evidence is in agreement with an antibiotic pressure that randomly selects mutations that decrease or prevent porin expression (Chalhoub *et al*., 2016).

Recently, a *P. aeruginosa* strain belonging to the sequence type 175 emerged as a high-risk clone due to multiple resistance mechanisms and reached a worldwide diffusion. Interestingly, these strains share the Q142X substitution that inactivate OprD and can be considered as one of the most prevalent OprD mutations (Cabot *et al*., 2016).

In addition to the modifications in the *oprD* gene sequence, it is important to emphasize that mutations in a wide number of regulator genes may cause a transcriptional repression of the porin. Among the most widespread we can report MexT, activator of MexEF-OprN expression, that negatively regulates OprD transcription (Ochs *et al*., 1999a). A similar effect is triggered by other regulators, including ParR-ParS, responsible for MexXY/OprM induction, but at the same time acting as an OprD repressor (Muller *et al*., 2011). The induction of the CzcCBA efflux pump, mediated by the transcriptional regulators CzcR-CzcS, can decrease OprD expression due to CzcR binding to the *oprD* promoter (Perron *et al*., 2004; Ducret *et al*., 2016). A similar effect is driven by the copper regulator CopR that, in addition to inducing CzcCBA can repress OprD expression by binding to its specific promoter (Caille *et al*., 2007; Ducret *et al*., 2016).

Finally, concerning OprD mediated resistance, it is important to highlight that, due to the porin specificity for arginine and other basic amino acids, carbapenems MICs increase in the presence of large amounts of the natural substrates (Muramatsu *et al*., 2003).

The involvement of other porins to antibiotic resistance is still a matter of debate, with different reports of antibiotic resistance in strains with various mutations that include one or more porins different from OprD.

Furthermore, different studies have determined the ability of specific porins to allow the diffusion of various β-lactams, but none of these porins appeared to play as important a role as OprD.

In the previous chapter we reported the current state of knowledge on *P. aeruginosa* porins and their correlations with antibiotic permeation and/or resistance. However, none of these correlations resulted in a resistance mechanism that can be frequently found in clinical settings. On the contrary, these may contribute to enhance resistant phenotypes caused by other mechanisms.

A recent study even put the contribution of other porins to antibiotic uptake in doubt and hypothesized a porin-independent permeation and therefore dismissed any kind of correlation between porin deletion and antibiotic resistance, except for the confirmed relation between OprD and carbapenems (Ude *et al*., 2021).

1.7 Outer membrane permeability determination

Since β-lactam efficiency in Gram-negative bacteria is dependent on their ability to reach to PBPs, various studies have investigated the OM permeability or the specific permeation properties of the porins. These studies aim at interpreting β-lactamase independent resistance and, possibly, to address the research of new compounds with improved permeability properties.
In addition, the determination of a permeability coefficient is useful to compare the effects of other compounds, including antibiotics, on OM stability. Moreover, these approaches may elucidate the roles of one or more porins in the permeation of a specific antibiotic.
We now summarize the various methods described in the literature (note that we do not include absolutely all the proposed techniques). We focus on their advantages and disadvantages and on the information that they can give on the permeability of *P. aeruginosa*.
These procedures can take account of *i)* the permeation properties of one single porin *ii)* the complexity of the whole bacterial cell.

1.7.1 Single porin studies

The study of single porin permeation properties has been made possible by various techniques that exploit liposomes, planar lipid bilayers or computational simulations.

1.7.1.1 Liposome based assay

Artificial micelles of various sizes, similar to the natural OMVs, can be synthetized to perform permeability studies. Specific porins can be inserted into the membranes of these vesicles, thus determining a selective gateway for internalization of the solute and allowing to determine the substrate specificity. The antibiotic is then added under iso-osmotic conditions to the solution containing the liposomes into which it can diffuse. The process of solute accumulation inside the vesicle induces the swelling of the liposome that can be followed thanks to the alteration of the light-scattering pattern, thus giving an idea of the relative permeability of the porin to the antibiotic (Nikaido and Rosenberg, 1983; Eren *et al*., 2012; Samanta *et al*., 2018; Kucharska *et al*., 2015).
The liposomes have also been used in multiple modified tests that exploit various systems to quantify the crossing of the lipidic membrane by antibiotics, such as liquid chromatography-mass spectrometry (LC-MS) or the addition of fluorescent dyes inside the liposomes (Richter *et al*., 2022).

These methods are useful to easily test a wide set of solutes, although to a limited extent, due to the altered lipid environment (Samanta *et al*., 2018). Moreover, results for charged molecules might be distorted by the counter-ion flow (Winterhalter and Ceccarelli, 2015).

1.7.1.2 Electrophysiology

The reconstitution of specific porin systems can also be achieved in planar lipid bilayers, that are constituted by two chambers separated by a thin partition subjected to an ionic current. Insertion of the channels induces a specific conductance that is altered by the passage of a specific solute. Ion current fluctuations, caused by the permeation of the antibiotic, can be monitored by electrophysiology, and can lead to the determination of translocation properties of a specific channel (Zakharian, 2013).

This procedure is very useful to characterize the contribution of a single porin to the internalization of various substrates at a single molecule level. In addition, it allows to easily investigate the effects that different external parameters, like temperature, pH and ionic strength may have on translocation (Nestorovich *et al*., 2002). Moreover, it is very useful to distinguish between the different possible channel open states and can be used to assess the contribution of specific mutations (Liu *et al*., 2012a; Liu *et al*., 2012b).

Regarding its limitations, it is quite difficult to set up functional bilayers and the presence of an important background noise that complicates the measurements cannot be ruled out (Zakharian, 2013). Moreover, due to its specific behavior, it cannot discriminate the effective passage of a solute from a simple external binding that does not result in a real translocation (Nestorovich *et al*., 2002).

1.7.1.3 Computer simulation

The feasibility of simulation-based computational predictions of dynamic information on molecules interactions has been explored from the beginning of computer science in the 1950's. Recently, the availability of increasingly powerful computing systems has made possible the *in-silico* analysis of porin specificities.

Molecular dynamic (MD) is a simulation technique used to predict movements and interactions between atoms and molecules at atomic resolution that has been applied to the study of the interactions that may occur between porins and solutes (Danelon *et al*., 2006). MD uses as input the high-resolution structure of porins and the information of charge distributions within the antibiotics,

and yields an evaluation of the energy of the system (Parkin and Khalid, 2014; Lee J. *et al*., 2018; Samanta *et al*., 2018).

The prospective usefulness of this kind of analysis is enormous, especially for designing new molecules, albeit the availability of good resolution crystal structures is necessary in order to produce reliable results.

Nevertheless, all these methods have so far undoubtedly failed to fully represent the complexity of bacterial response to antibiotics, since synergic effects are not noticeable. Moreover, the lack of a bacterial native environment may lead to biased results, rendering these techniques unsuitable for the study of possible physiological adjustments that bacteria typically implement.

1.7.2 Whole cell-based studies

The ability to determine internalization of the antibiotics in a living cell is undoubtedly a fascinating challenge and it might lead to further achievements in this field.

This aim has been achieved in various ways that involve the use of *i*) enzymatic reactions, *ii*) radiolabeled modified targets, *iii*) fluorescent compounds, *iv*) mass spectrometry *v*) drug susceptibility determination.

These methodologies have often been applied in combination with each other, due to the lack of any method to evaluate bacterial specific permeabilities widely recognized as reliable and robust.

In this regard, a useful tool might be to perform analyses based on whole cell permeation. This approach that most likely has not been fully exploited yet, might prove to be useful for the discovery of new permeation properties, even if the limits of these procedures should always carefully be considered.

We now provide some details on the methodologies that have been described as successful to reach this goal, with a particular focus on a protocol developed a few years ago by researchers affiliated to the University of Liège that has now been revisited and used within this PhD project.

1.7.2.1 Use of enzymatic reactions

One of the first attempts was the pioneering work by Zimmermann and Rosselet, in which they exploited the hydrolysis by a periplasmic β-lactamase and compared this reaction to that obtained with a bacterial lysate thanks to a micro-iodometric assay (Zimmermann and Rosselet, 1977). The rapid hydrolysis of the antibiotic by the β-lactamase results in a passive antibiotic diffusion mediated by the OM barrier as the rate-limiting step. The ensuing steady state is such that the antibiotic rate

of penetration that obeys Fick's first law of flux, is equal to that of the enzymatic hydrolysis that follows Henri-Michaelis kinetics.

This approach only allows to investigate those β-lactams that are good substrates for a β-lactamase and was used for the determination of cephalosporins permeability coefficients, in *E. coli* strains.

Moreover, the permeability properties of *E. coli* strains characterized by different patterns of porin deletions and of other Gram-negative bacteria have been evaluated (Yoshimura and Nikaido, 1980; Nikaido *et al*., 1983; Kojo *et al*., 1980; Zimmermann, 1980; Cornaglia *et al*., 1995). In particular, this approach was applied to *P. aeruginosa* and the availability of an MBL has also been used to determine the specific permeability coefficients of carbapenems (Zimmermann, 1980; Iyobe *et al*., 1999). However, the validity and the reproducibility of the method has been questioned for overexpressing efflux pump strains, like *P. aeruginosa*, due to a variable involvement of these systems in the antibiotic extrusion. Moreover, the low intrinsic OM permeability of *P. aeruginosa* amplifies the error resulting from the presence of disturbing factors such as the presence of β-lactamases in the extracellular medium (Livermore and Davy, 1991).

These difficulties are therefore serious obstacles in the attempts to reliably determine permeability coefficients for *P. aeruginosa*, casting a shadow on the efforts to study the mechanisms underlying the antibiotic influx in this bacterium.

1.7.2.2 Radiolabeled β-lactams

The use of radioactive-labeled β-lactams may provide an alternative and sensitive method for quantifying antibiotic permeation (Simonet *et al*., 2000). Bacteria are incubated in a medium containing an excess of radio-labelled antibiotic and, after elimination of the excess of external antibiotic, the measurement of the cell-associated radioactivity provides a reliable measurement of the internalized compound. Although this method has the advantage of being potentially applied to all classes of antibiotics, rather than only to β-lactams, it is however hampered by the high costs associated with using a wide set of radioactive compounds. Moreover, direct permeation measurements of radiolabeled antibiotics are complicated by the nonspecific adsorption that occurs on the bacterial surface. This effect makes impossible to distinguish between adsorption and true uptake, therefore requiring the use of indirect measurements (Richmond *et al*., 1976).

1.7.2.3 Fluorescent β-lactams

A similar approach can be followed by exploiting the natural fluorescence of some antibiotics (*i.e.*, fluoroquinolones and tetracyclines) or by attaching a fluorescent group to β-lactams. The fluorescent antibiotics may be used in a liposome swelling assay, but they can also be used to evaluate the permeation into intact bacterial cells. In this second case, the antibiotic that has diffused into the periplasm can be measured in two ways: *i*) measurement of the fluorescence after bacterial cell lysis; or *ii*) directly by either a microfluidic method or UV micro spectrofluorimetry (Vergalli *et al*., 2018; Allam *et al*., 2017). Compared to radioactive compounds, these compounds can be more easily synthetized and can therefore be adapted to a wider range of studies. By contrast their activity can be modified by the fluorescent group itself. In particular, the fluorescent group properties and volume may reduce the affinity for the PBP targets and/or cause an altered permeation through the OM (Miao *et al*., 2020).

1.7.2.4 Mass Spectrometry-based analysis

Mass Spectrometry (MS) based analysis is another approach used to quantify antibiotic accumulation inside the periplasm. Bacterial cultures are incubated with the tested antibiotic and its quantification inside bacterial cells can be performed in two ways: *i*) by evaluating the decrease of β-lactam concentration in the supernatant; or *ii*) the corresponding increase of β-lactam in the cell lysate (Six *et al*., 2018; Zhou *et al*., 2015).

An MS-based analysis can also be optimized by simultaneously screening several compounds, thus providing a high-throughput screening method (Widya *et al*., 2019).

MS-based analyses are often coupled with fluorescent or radiolabeled drugs. An example is the use of radiolabeled ciprofloxacin together with a LC-MS-based assay used to determine the uptake of quinolones by *P. aeruginosa* strains, characterized by a different efflux pumps expression (Cai *et al*., 2009).

This approach, despite the positive aspects already mentioned, is very time consuming and requires highly specific equipment that is not available in many laboratories worldwide. In addition, as already mentioned, the use of radiolabeled antibiotics has the disadvantage of the compound adsorption to the membrane, thus making very complicated the determination of the real antibiotic uptake (Richmond *et al*., 1976).

1.7.2.5 Permeability determined from drug susceptibility

The idea that one or more porins influence the permeation of a specific antibiotic implies as a direct consequence that the MIC must also be increased by the deletion of one or more porins.
This has for example been used to determine the influence of OprD expression in an *E. coli* strain in the so called "titratable OM permeability assay system" (Iyer *et al*., 2017). In brief, the authors of this study used an *E. coli* strain deprived of three of the most expressed natural porins and transformed with a plasmid carrying *oprD* under the control of an arabinose expression vector that regulates expression of the porin. The carbapenem MIC variations were correlated to the modulated OprD expression and therefore consistent with the permeation characteristics for the specific compound (Iyer *et al*., 2017). This experiment is clearly useful to correlate the OprD expression with the variation of periplasmic antibiotic accumulation and, for this purpose, it has been successfully used to study the OprD-mediated permeation of new compounds. However, this method is not appropriate for describing the natural adaptative response of *P. aeruginosa*, whose MICs are only marginally related to the expression of different porins, except in the case of absence or downregulation of OprD.

1.7.2.6 Permeability determined from periplasmic PBP expression

The various protocols described so far provide sound reasons to believe that MICs, β-lactamases kinetic properties and permeability features are closely related to each other, and that knowing two of them one can predict the unknown third variable.
An interesting study devised some years ago by researchers at the University of Liège (Lakaye *et al*., 2002) is a relevant development in this approach. The authors exploited the properties of the C terminal domain of the *Bacillus licheniformis* β-lactams receptor BlaR (BlaR-CTD), whose properties and specificities for β-lactams were topics of great interest at that time. The production of this "β-lactam sponge" in a Gram-negative periplasm as described in the paper allowed the team to directly quantify the BlaR-CTD-β-Lactam adduct as a function of time. It was shown in the paper that this adduct was directly quantifiable when a radioactive antibiotic was studied or, for non-radioactive antibiotics, by performing a counter-labeling of the residual BlaR-CTD with a radioactive β-lactam.
By doing so, the authors achieved the determination of permeability coefficients for six antibiotics in *Enterobacter cloacae* and *K. aerogenes* (previously known as *Enterobacter aerogenes*) and, in

particular, they evaluated the very low coefficient specific for aztreonam a compound with which the steady state described in the protocol of Zimmerman and Rosselet's could not have been reached. However, for *P. aeruginosa* only preliminary results were obtained, while an appropriate procedure for permeability estimation in this species appears to have been devised (Lakaye *et al*., 2002). Interestingly, the permeability results obtained with this procedure, combined with the possible presence of β-lactamases and efflux pump systems, led to the predictions of MICs that were roughly in line with the results obtained by direct measurements.

2 OBJECTIVES

P. aeruginosa is a versatile pathogen that can acquire antibiotic resistance in multiple ways, including a reduced OM permeability to external agents. Resistance can be achieved by an increased efflux pumps expression and/or a reduced porin expression, both resulting in a reduced susceptibility or an acquired resistance to carbapenems.

To date, the knowledge of the mechanisms underlying the antibiotic permeation is still limited.

A better understanding of the antibiotic translocation properties is fundamental for conducting research on new antibiotics and the WHO has inserted carbapenem-resistant *P. aeruginosa* as a high priority pathogen for which new molecules are urgently needed (WHO, 2024).

Given its relevance, the study of the OM properties of *P. aeruginosa* has been the principal aim of the project described in this Ph.D. thesis. The results have been obtained according to the following successive steps:

1. The first goal was the development of a system that would allow the determination of the outer membrane permeability of *P. aeruginosa* through the production of a periplasmic sensor. To achieve this objective, we decided to revisit a previously described methodology (Lakaye *et al*., 2002) and apply it to *P. aeruginosa* strains, verifying that all the interactions with the physiological response of the bacterium were minimal or absent.
2. The second goal was the determination of permeability coefficients of *P. aeruginosa* PAO1 and of a collection of isogenic porin deleted mutants for a wide set of β-lactam subclasses to assess each porin's role in the entry of different antibiotics.
3. Initially the project included a third goal: the *in vitro* determination of the MIC of porin mutant strains, on the basis of the determined permeability coefficients. However, since we obtained results which clearly indicated the absence of a correlation between MIC and rate of antibiotic entry, we broadened the scope of our analysis to unravel the mechanisms behind this discrepancy.
4. We consequently decided to quantify the expression of various porins as a function of cellular growth, to highlight the different physiological conditions that occurred between MIC and permeability determinations that could determine a divergent response to some carbapenems. This analysis was performed on different porin mutants, with the purpose of detecting compensatory effects implemented by *P. aeruginosa* as a result of the absence of a porin.
5. Finally, we sought to determine whether the OpdP porin could acquire a direct role in antibiotic resistance, a function not previously clearly demonstrated. To this end, we

performed an experiment involving the selection of resistant mutants under sub-MIC antibiotic pressure, and subsequently examined several derived strains for mutations that conferred stable resistance to carbapenems.

3 MATERIALS AND METHODS

3.1 Bacterial strains

3.1.1 *P. aeruginosa* strains

In this project we also studied strains not reported in the article.

Prof. Hiroshi Yoneyama (Tohoku University, Japan) kindly provided us with a complete collection of eight strains (Table 3) characterized by deletions in the main expressed porins OprC, OprD and OprE. The collection included single, double and triple porin mutants.

Prof. Françoise Van Bambeke (Catholic University of Louvain, Belgium) provided us with *P. aeruginosa* PAO509 (*ΔmexAB-oprM, ΔmexCD-oprJ, ΔmexJK, ΔmexXY, ΔmexEF-oprN*), a strain where the main efflux pumps MexAB-oprM, MexCD-OprJ, MexJK, MexXY and MexEF-OprN where deleted (Mima *et al.,* 2007).

Table 3 resume all the strains used during the study.

P. aeruginosa	Relevant characteristics	Reference	Deposited sequence
ATCC 15692	PAO1 Wild type (WT)	BCCM	
ATCC 27853	PAO1 WT	CLSI	
PAO1-Jap	PAO1 WT	Satake *et al.,* 1991	SAMN35794375
TNP004	↓*oprD*	Satake *et al.,* 1991	SAMN35794376
TNP064	*ΔoprC*	Yoneyama *et al.,* 1995	
YY100	*ΔoprE*	Yoneyama *et al.,* 1995	
TNP065	*ΔoprC,* ↓*oprD*	Yoneyama *et al.,* 1995	
TNP066	*ΔoprC, ΔoprE*	Yoneyama *et al.,* 1995	
YY200	↓*oprD, ΔoprE*	Yoneyama *et al.,* 1995	
TNP067	*ΔoprC,* ↓*oprD, ΔoprE*	Yoneyama *et al.,* 1995	
ARC545	WT	Isabella *et al.,* 2015	SAMN35794377
ARC5990	*ΔoprD*	Isabella *et al.,* 2015	
ARC5170	*ΔopdP*	Isabella *et al.,* 2015	
ARC5782	*ΔoprD, ΔopdP*	Isabella *et al.,* 2015	
ARC5998	*ΔoprD, ΔopdP, ΔopdB, ΔopdC, ΔopdT*	Isabella *et al.,* 2015	
PAO509	*ΔmexAB-oprM, ΔmexCD-oprJ, ΔmexJK, ΔmexXY, ΔmexEF-oprN*	Mima *et al.,* 2007	
LG01	Resistance to carbapenems derived from PAO1	This study	
LG02	Resistance to carbapenems derived from ARC5170	This study	
LG03	Resistance to carbapenems derived from ARC5170	This study	SAMN35794378
LG04	Resistance to carbapenems derived from ARC5170	This study	
LG05	Resistance to carbapenems derived from ARC5170	This study	
LG06	Resistance to carbapenems derived from ARC5170	This study	
LG07	Resistance to carbapenems derived from ARC5170	This study	

Table 3: Collection of *P. aeruginosa* mutant strains used in the study; ↓ indicate a downregulation expression of specific gene coding for OprD porin. The genome BioSample number is reported for the strains for which this information is available.

3.2 Antibiotics and other reagents

Antibiotics and growth medium used in this study were mainly purchased from Sigma-Aldrich (Belgium). Exceptions were:

Bocillin FL, a boron-dipyrromethene fluorescent derivative of penicillin V (Gee *et al*., 2001), was purchased from Invitrogen (Waltham, MA, USA). Nitrocefin, a chromogenic cephalosporin β-lactamases substrate, was purchased from Unipath Oxoid (UK).
Dipicolinic acid (DPA) was purchased from Sigma-Aldrich (Belgium).

3.3 Determination of MIC values

MICs were performed, using the broth microdilution method as described by CLSI. *P. aeruginosa* ATCC 27853 strain was used as a reference strain.
Cellstar 48-wells polypropene microplates (Greiner BioOne, Belgium) were used and 200 µl of Mueller Hinton II (MHB II) broth was dispensed in each well.
A stock of each antibiotic was prepared 40 times more concentrated than the highest concentration we wanted to test (Solution A) and then was filtered using a 0.2 µm pore size syringe filter. Then the solution A was diluted 1:10 in MHB II broth and 200 µL were distributed in the first column of the plate. Then, serial dilutions were made with 200 µL in each well. The bacterial concentration needed was prepared by suspending some fresh colonies in physiological solution until a turbidity of 0.5 McFarland (OD_{625} =0.15) was reached. Then the bacterial suspension was diluted 1:200 in MHB II (Solution B), obtaining a concentration of 5*10 unit forming colony (CFU)/mL. Finally, 200 µL were distributed in each well, obtaining a final concentration of 4*10 CFU/ml in each well. The plates were incubated at 37°C for 18 hours.
The obtained MIC values were the result of a biological independent triplicate.

3.4 Molecular biology

3.4.1 PCR amplifications

We routinely used Polymerase Chain Reaction (PCR) for the *in vitro* amplification of DNA fragments (templates) not only to detect the presence of specific genes, but also to make the DNA product available for other applications (for example cloning or sequencing).
The PCR were realized starting from bacterial colonies picked up from freshly grown agar plates, diluted in 500 µL of sterile H_2O, followed by boiling at 100 ºC for 10 minutes. The lysed bacteria were then pelleted in a bench-top centrifuge at 16000 x *g* for 10 minutes and the supernatants were

used as template for the PCR. Specific oligonucleotides used in this thesis were ordered from Eurogentec (Liège, Belgium) and the complete list is reported in Annex, Table S1 (page 217).
PCR amplifications were performed using different polymerases, depending on the application, using the Thermal Cycler T100 (Bio-Rad, Hercules, CA, USA).

OneTaq® Quick-Load® 2X Master Mix with Standard Buffer (NEB, New England BioLabs, Ipswich, MA, USA) contains a polymerase without proofreading activity and was used to assess the presence/absence of a specific target in a wide variety of samples. Reactions were carried out in a volume of 25 µL, which consisted of 12.5 µL of Master Mix, 0.5 µL of each of the primers (10 µM), 9.5 µL of sterile distilled H_2O, and 2 µL of DNA template prepared as above described. The cycling conditions were set as follows: initial denaturation at 94 ºC for 30 seconds, followed by 35 cycles of 94 ºC for 30 seconds, hybridation at the specific primer's couple temperature for 45 seconds, and the amplification at 68 ºC for a period of 1 minute and 20 seconds each Kb, with a final extension at 72 ºC for 10 minutes.

Q5® High-Fidelity 2X Master Mix (NEB) contains a polymerase with proofreading activity that was used for successive cloning or sequencing applications. Reactions were carried out in a volume of 50 µL of which 25 µL of Master Mix, 2.5 µL of each of the primers (10 µM) 18 µL of sterile distilled H_2O and 2 µL of DNA template prepared as above described; in the case of amplification from plasmids or purified PCR fragments, the DNA template was 0.5 µL and the sterile distilled H_2O was 19.5 µL. The cycling conditions were: initial denaturation at 94 ºC for 30 seconds, followed by 35 cycles of 94 ºC for 30 seconds, hybridation at the specific primer's couple temperature for 45 seconds and the amplification at 68 ºC for a period of 1 minute each Kb and 20 seconds, with a final extension at 72 ºC for 10 minutes.

3.4.2 Agarose gel electrophoresis

Nucleic acids electrophoresis allows the separation of DNA fragments in accordance with their length. It was performed in agarose gel, generally at the concentration of 1.0 % (w/v), although lower or higher agar concentrations were used, on the basis of different fragments' length. Agarose gels were supplemented with Midori Green (Nippon Genetics Europe, Düren, Germany), diluted 1:10000, in 40 mM Tris-acetate, 1 mM EDTA, pH 8.0 (TAE) buffer. Samples were loaded adding the 6 X Orange DNA loading dye (Thermo Fisher Scientific).

Different DNA ladders were used in line with the fragment sizes. In particular, O'GeneRuler 1 kb DNA ladder was generally used, while the O'GeneRuler 50 bp DNA Ladder was used to discriminate the small size fragments, and the O'GeneRuler 1 kb plus DNA ladder was preferred in the case of long fragments; All three ladders are commercialized by Thermo Fisher Scientific.
The electrophoresis runs have been carried out using 5 µL of each sample with a constant voltage (5-7 V/cm).
Gels were scanned using the Gel Doc™ EZ Imager (Bio-Rad) that allows the Midori Green's fluorescence revelation.

3.4.3 Nucleic acids quantification

The NanoVue **Plus** spectrophotometer (GE Healthcare, Little Chalfont, UK) was used to measure the DNA and RNA concentration and purity (Abs_{260nm}/Abs_{280nm} and Abs_{260nm}/Abs_{230nm} ratios) values.

3.4.4 Nucleic acid purification

3.4.4.1 Gel Extraction and PCR product purification

Purification of DNA was performed from samples directly resulting from PCR amplification, but also from an excised band derived from agarose gel migration. In both cases it was carried out using the NucleoSpin® Gel and PCR Clean-up (Macherey-Nagel), according to the protocol of the supplier.

3.4.4.2 Genomic DNA extraction and purification

The genomic DNA of *P. aeruginosa* strains to be sequenced were extracted using the NucleoSpin® Microbial DNA Mini kit (Macherey-Nagel) The kit allows the isolation of genomic DNA of an adequate purity for successive whole genome sequencing. Bacterial samples were vortex-mixed with the supplied glass beads to perform cell wall mechanical disruption and, subsequently, the protocol indicated in the user guide was followed.

3.4.4.3 Plasmid DNA extraction and purification

Extraction and purification of plasmids solutions were obtained through purification commercial kits.

Depending on the bacterial culture volume used, minipreps or maxipreps were performed using a NucleoSpin Plasmid, Mini kit for plasmid DNA (Macherey-Nagel) or NucleoBond Xtra Maxi kit (Macherey-Nagel), respectively.

The colonies containing the interested plasmid were cultivated overnight in LB, added with the appropriate antibiotic; in particular, bacterial culture of 5 mL and 100 mL were used for miniprep or maxiprep, respectively. Bacterial pellets were collected through centrifugation at 1600 x *g* for 5 minutes at 4°C and then samples were processed according to the manufacturer's instructions.

3.4.5 Plasmids

The complete list of plasmids used in this work is available in Table 4.

We received pDML309 and pKT240 vectors from Prof. B. Lakaye (Giga Neurosciences, ULiège). The pDML309 is a derivative plasmid from pBR322 and was used in a previous study for BlaR-CTD expression in *E. cloacae* (Lakaye *et al*., 2002). The pKT240 is a 12.9 kb broad spectrum plasmid belonging to the IncQ/P4 incompatibility group.

We received pME6001 plasmid (Blumer *et al*., 1999) from Prof. M.C. Thaller (Tor Vergata, University of Rome), previously used for protein expression in *P. aeruginosa*.

Finally, the pET28b vector was used for protein's expression.

Plasmid	Resistance	Reference
pDML309	TET	Lakaye *et al*., 2002
pKT240	AMP; KAN	Lakaye *et al*., 2002
pME6001	GEN	Blumer *et al*., 1999
pKT240blaR	TET	This study
pKT240neg	TET	This study
pKT240blaR-gen	TET; GEN	This study
pET28b	KAN	
pET28b-opdP-fw2	KAN	This study

Table 4: list of plasmids used in this study.

3.4.6 Vector construction

3.4.6.1 Cloning through Gibson Assembly protocol

Gibson assembly is a method that enables the assembly in the correct order of linear large-scale DNA fragments (Gibson *et al*., 2009). It exploits the properties of three enzymes: *i)* an exonuclease that chews back DNA from the 5' end, allowing the fragments anneal; *ii)* a polymerase that incorporates nucleotides in the remaining gaps, and *iii)* a DNA ligase that promotes covalent bounds between adjacent DNA segments and that also removes possible nicks in the DNA.
At different times, in our laboratory we used two commercial kits for Gibson assembly: the Gibson Assembly® Master Mix and NEBuilder® HiFi DNA Assembly, both distributed by New England Biolabs. In particular, NEBuilder® is an improved Gibson Assembly® version, with a higher fidelity polymerase.
Both kits share the same procedure described as follows: DNA fragments containing identic ~20 base pairs extremities were obtained by PCR amplification or enzymatic digestion; successively, 0.2–1.0 pmoles of DNA fragments were added to 10 µL of the 2X master mix and distilled H_2O was added to reach the final volume of 20 µL. The mixture was then incubated for 30 minutes at 50 ºC.
Gibson assembly products were transformed in *E. coli* DH5α; the correct ligation was verified trough specific PCR amplification on adjacent fragments.

3.4.6.1.1 pKT240blaR

The goal was to recreate the vector used by Lakaye and coworkers (Lakaye *et al*., 2002).
A portion of the pDML309 plasmid was amplified trough PCR with 309-inf-fw and 309-inf-rev primers to obtain a 6204 kB fragment, containing the *tetA(C)* gene for tetracycline resistance and the BlaR-CTD expression system (*blaR-CTD* gene under the control of the lpp^p promoter of the *E. coli* lipoprotein, controlled by the *lac*-UV5 promoter-operator). A fragment derived from the pKT240 plasmid was PCR-amplified with pkt-fw-1 and pkt-rev-2 primers to obtain a 5953 kB fragment, containing the broad-host range origin of replication RSF1010.
The two segments were purified and merged using the Gibson Assembly® Master Mix to obtain the pKT240blaR vector (Figure 13).

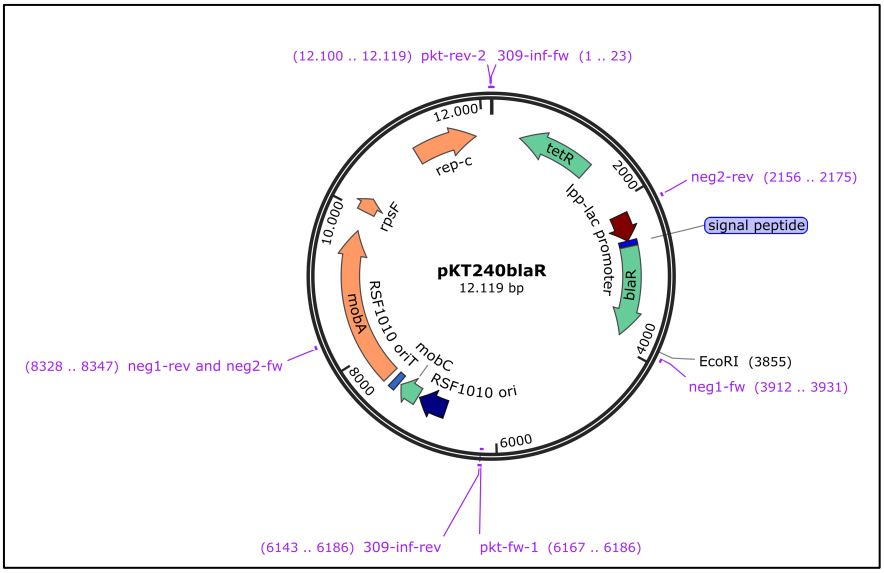

Figure 13: pKT240blaR plasmid map. The main genes and promoters are reported.

3.4.6.1.2 pKT240neg

The plasmid excised from *blaR-CTD* was obtained by PCR amplification of two fragments from pKT240blaR.

In particular, fragment 1 of 4460 bp resulted from the amplification of neg1-fw and neg1-rev while fragment 2 of 5966 bp was obtained with neg2-fw and neg2-rev.

Both fragments were purified and ligated using Gibson assembly to obtain the pKT240blaRneg plasmid (Figure 14).

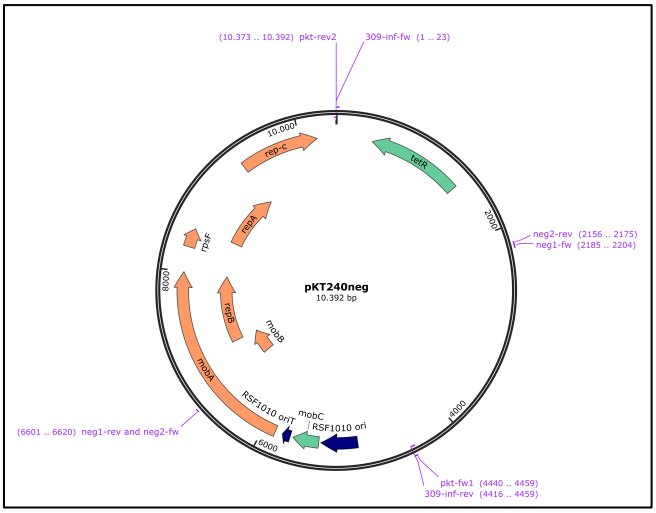

Figure 14: pKT240neg plasmid map. The main genes and promoters are reported.

3.4.6.1.3 pKT240blaR-gen

The *aac1* gene for gentamicin resistance, derived from pME6001 plasmid, was inserted in pKT240blaR to enable plasmid transformation in strains already resistant to tetracycline.

Briefly, pKT240blaR plasmid was digested with EcoRI (New England Biolabs). The *aac1* gene was PCR-amplified from pME6001 using gmr-eco-fw and gmr-eco-rev primers.

The fragments were purified and successively ligated using the Gibson assembly, in this way producing the pKT240blaR-gen vector (Figure 15).

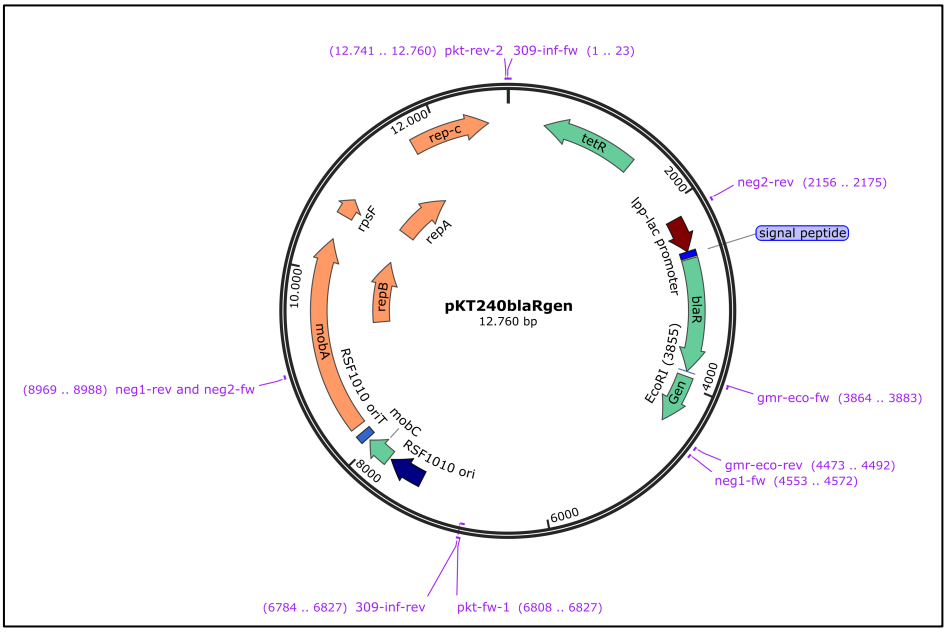

Figure 15: pKT240blaR-gen plasmid map. The main genes and promoters are reported.

3.4.6.1.4 pET28b-opdP-fw2

The plasmid was designed to insert *opdP*, including its signal peptide, under the control of the lac promoter and to enable an in-frame translation of the polyhistidine tag.

The pET28b plasmid was digested with NcoI and BamHI restriction enzymes (New England Biolabs).

The *opdP* sequence was amplified from *P. aeruginosa* PAO1 with opdP-gib-fw2 and opdP-gib-rev2 primers.

Both plasmid and PCR fragments were purified and subjected to ligation with NEBuilder® HiFi DNA assembly (Figure 16).

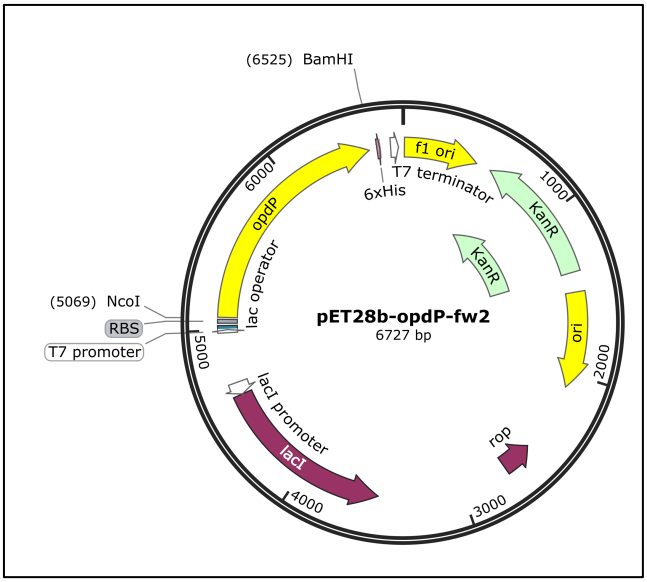

Figure 16: pET28b-opdP-fw2 plasmid map. The main genes and promoter are reported.

3.4.7 RT-qPCR

Reverse transcription quantitative (real time) PCR (RT-qPCR) is an extremely powerful technique that we used to quantify porins (and efflux pumps) gene expression.
This method requires different steps that are reported below.

3.4.7.1 RNA extraction

Total RNA isolation of different *P. aeruginosa* strains was performed using the NucleoSpin® RNA Plus kit. The obtained samples were subsequently processed via enzymatic digestion with a deoxyribonuclease, rDNase, to eliminate any DNA trace. The deoxyribonuclease was removed from the samples using the NucleoSpin® RNA Clean-up XS kit. Elutions were performed using RNase/DNase-free water. All the kits were commercialized by Macherey-Nagel and were used according to the manufacturer's recommendations.

3.4.7.2 Reverse transcription

The mRNA reverse transcription allows the synthesis into complementary DNA (cDNA) of all the mRNA present in the total RNA extract. It was performed using the SuperScript III® Reverse Transcriptase (Invitrogen), triggered by random hexamers and supplemented with Ribosafe RNase

Inhibitor (Bioline, USA). First-strand cDNA synthesis reactions consisted in two steps *i)*: 1 µg of total RNA was added to 1 µL of dNTPs (10 mM), 1 µL of random hexamers (50 ng/µL) in a total volume of 13 µL, reached with RNase/DNase-free water. The reaction was processed at 65°C for 5 minutes and was subsequently stopped by cooling it on ice for 5 minutes. *ii)* the samples were added with 7 µL of an enzyme mixture so composed: 4 µL of first-strand buffer, 1 µL of dithiothreitol (DTT) (0.1 M), 1 µL Superscript III enzyme (200 U/µL) and 1 µL of Ribosafe RNase Inhibitor (40 U/µL).

The 20 µL of the obtained mixture was processed at 25°C for 5 minutes, 50°C for 60 minutes, and the reactions were stopped by heating at 70°C for 15 minutes. The newly synthetized cDNA was diluted to 1:50 in RNase/DNase-free water and used as target for qRT-PCR.

3.4.7.3 RT-qPCR amplification

RT-qPCR amplifications were performed using Takyon Low Rox SYBR Master Mix (Eurogentec, Belgium) in 384-well plates. Primers used were both found in the literature and designed in the course of this project, and the list with references is reported in Annex, Table S2 (page 218).

Each well contained 5 µL of polymerase master mix, 4 µL of cDNA (dilution 1:50 after reverse transcription) and 1 µL of primer mix (2.5 µM each primer). The QuantStudio 5 Real-Time PCR system (Thermo Fisher Scientific) was used to set up the following conditions: 2 minutes at 95°C, followed by 40 cycles, each of them made by 15 seconds at 95°C, and 1 minute at 60°C.

A negative control reaction was performed for each sample by using the original RNA mixture, prior to the reverse transcription, to verify the absence of residual DNA. Experiments were reproduced in four biological replicates and three technical replicates for each target gene. An equivalent threshold was set-up and preferred to the automated value in order to adequately compare all RT-qPCR replicates.

3.4.7.4 Statistical analysis

The quality of the quantitative PCR was checked by analyzing the dissociation and amplification curves. For each primer pair, the mean reaction efficiencies were calculated using the LinRegPCR software (Ruijter *et al*., 2009) The obtained values were used to quantify relative gene expression levels by normalization using selected reference genes, known to have stable expression during the different experimental conditions. Analyses were performed with the qBase software (Biogazelle; Hellemans *et al*., 2007). The adequacy of the reference genes to normalize gene expression in the

experimental conditions was checked using the geNorm module in qBase (Vandesompele *et al*., 2002). Graphical results were obtained using GraphPad Prism software version 7 (GraphPad Software, Inc., San Diego, CA, USA).

3.4.8 DNA sequencing

Both Sanger and whole genome sequencing were carried out at a sequence facility (GIGA-Genomics, Liège, Belgium).

3.4.8.1 Sanger sequencing

The dideoxy chain-termination sequencing method (Sanger *et al*., 1977) was performed on PCR or plasmid DNA samples. DNA fragments were sequenced in pairs, using as primers both the original forward and reverse primers; occasionally, internal primers were used to cover with high score internal regions of long fragments (> 1000 base pairs). Plasmids were sequenced using specific primers. All the primers are reported in Annex, Table S1 (page 217).
The software Vector NTI 10.0 (Informax, Bethesda, MD, USA) was used to process raw sequences; comparisons were performed with the online tool BLAST (http://www.ncbi.nlm.nih.gov/BLAST/).

3.4.8.2 Whole genome sequencing

Whole genome sequences were performed on genomic DNA samples on a NovaSeq (Illumina, USA) sequencer, generating paired end reads (2*150). Reads corrections and assembly were made in collaboration with Olivier Verlaine (InBioS – CIP, ULiège). Raw reads were corrected by a homemade workflow, performing various step of analysis, using software included in the BBTools package (Bushnell *et al*., 2017) (https://sourceforge.net/projects/bbmap/). In synthesis, reads were overlapped with BBMerge and afterwards quality-trimmed and any remaining adapters were removed by the BBduk function. Tadpole and BBMap were in sequence used to perform a quick assembly and BBduk was used for a quality calibration; finally, BBNorm was used to normalize the coverage, and Tadpole was used for a final process of error-correction.
The sequence mapping was carried out with the Geneious (v10.2.6) software (Kearse *et al*., 2012). Genome assembly was achieved by mapping single verified reads to a reference *P. aeruginosa*

genome sequence (strain PAO1, GenBank accession number AE004091) and the resulting variations have been applied to the reference to generate the strains sequences.

3.4.9 Bacterial transformation methods

3.4.9.1 *E. coli* heat-shock transformation

Competent *E. coli* DH5α and BL21 (DE3) cells were prepared by treatment with calcium chloride (Sambrook and Russell, 2001) and transformed with the specific plasmid by a heat-shock protocol (20 minutes at 4°C, 1 minute at 42°C, 5 minutes at 4°C). Subsequently, 1 mL of super-optimal broth with catabolite repression (SOC) was added, and bacteria were allowed to grow for 1 hour, at 37°C with shaking. Finally, transformed cells were spread onto LB agar (LBA) plates containing the appropriate antibiotic and incubated at 37°C, overnight. Depending on the strain and plasmid used, the LBA was supplemented with tetracycline (10 μg/mL) or gentamycin (10 μg/mL).

3.4.9.2 *P. aeruginosa* electroporation

Electroporation was used to transform *P. aeruginosa* strains with the respective plasmids. First of all, a protocol to prepare electrocompetent cells was performed. Starting from an overnight culture in LB, cells were grown in super-optimal broth (SOB) until an OD_{600} of 0.6 was reached. Cells were successively washed three times with 10 % ice-cold glycerol and finally resuspended with in 100 μL of 10 % ice-cold glycerol (corresponding to 1:100 of the initial volume). The transformation by electroporation was carried out in an ice-cold 0.2 cm electroporation cuvette with the following parameters: 200 Ω, 25 μF, 2.5 kV on a Gene Pulser Xcell Electroporation System (Bio-Rad). Subsequently, 1 mL of SOC was added and the then cells were then incubated in a shaking incubator (250 rpm) for 1 hour at 37°C. Finally, shocked *P. aeruginosa* cells were spread onto LBA additionated with tetracycline (50 μg/mL) or gentamycin (10 μg/mL), according to the used plasmid, and incubated overnight to select transformant cells.

3.5 Protein analysis

3.5.1 Protein concentration determination

The specific sample's protein concentration has been determined using the bicinchoninic acid assay (BCA), also known as Smith assay (Thermo Fisher Scientific). This method is based Cu^{2+} reduction in an alkaline solution by means of peptide bonds and amino acid residues (cysteine, tyrosine, and tryptophan). The Cu^{1+}, in presence of bicinchoninic acid, forms a complex that absorbs at 562 nm. Tests were performed using a 96-well microplate (Greiner Bio One), using the manufacturer's protocol, and the absorbances were measured using the plate reader Tecan Infinite 200 Pro to (Tecan Group Ltd., Switzerland).

3.5.2 Polyacrylamide gel electrophoresis (SDS-PAGE)

Sodium Dodecyl Sulphate-PolyAcrylamide Gel Electrophoresis (SDS-PAGE) was carried out according to the Laemmli protocol (Laemmli, 1970). Samples were treated with Loading Dye (Tris-HCl 50 mM, pH 6.8, β-mercaptoethanol 5 %, SDS 2 %, Glycerol 10 %, Bromophenol Blue 0.1 %) and further denatured by heating (5 minutes at 100 ºC). Denatured samples were loaded on Mini-PROTEAN TGX precast 4-20 % acrylamide gel (Bio-Rad). The electrophoresis was carried at 120-160 V, in TGS pH 8.3 (Tris-HCl 25 mM, Glycine 192 mM, SDS 0.1 %) running buffer.

The protein markers used were Pierce Unstained Protein MW Thermo Fisher Scientific (Rockford, IL, USA) or Protein marker V (pre-stained) VWR (Radnor, PA, USA) in the case of a subsequent membrane transfer.

The gels were stained with PageBlue protein staining solution (Fermentas, St. Leon-Rot, Germany). In the case of fluorescence detection (*i.e.*, permeability determinations performed with Bocillin FL) or Western blot analyses, gels were stained after the respective analyses/procedures to assess the protein's contained in the samples, or the correct transfer of proteins on the membrane, respectively. The excess of staining was eliminated through washes with water and gels were scanned using the ImageQuant™ LAS 4000 GE Healthcare.

3.5.3 Anti-OpdP antibodies production and purification

3.5.3.1 OpdP production

OpdP production was performed in *E. coli* BL21 cells, using the plasmid pET28b-opdP-fw2. Bacterial growth was performed in 800 mL LB + 50 µg/mL of kanamycin, added with approximatively 25 mL of overnight preculture, in agitation at 37 ºC. The OpdP production in inclusion bodies was achieved by inducing the culture at OD_{600} ~ 0.6 with 500 µM isopropil-β-D-1-thiogalactopyranoside (IPTG) for 3 hours at 37 ºC.

Bacterial pellets were isolated by centrifugation for 15 minutes at 5000 x *g* at 4 ºC, using the Avanti J-E (Beckman Coulter, Brea, CA, USA).

Bacterial pellets were solubilized in 40 mL of a chaotropic solubilization buffer, composed of 8 M urea, 50 mM NaCl 50 mM phosphate buffer, pH 7.0 and incubated overnight in agitation at 20 ºC.

The sample was firstly centrifuged at 10000 x *g* for 20 minutes at 20 ºC and the supernatant, corresponding to the solubilized fraction, was collected. Successively, the solution was recovered and filtered with a 0.45 µm syringe filter.

3.5.3.2 OpdP purification by affinity chromatography

The production of OpdP containing a 6-Histidine tag at their c-terminal enabled the purification trough Immobilized Metal Affinity Chromatography (IMAC).

Purification was performed on bench with a 5 mL IMAC Ni NTA (HiTrap IMAC FF, GE Healthcare) column with the help of a peristaltic pump. The column was firstly charged with metal ions by passing 5 column volume (CV) of 0.1 M $NiSO_4$ and successively equilibrated with 5 CV of water and 5 CV of solubilization buffer. The solubilized inclusion bodies were then loaded on the column at 0.8 mL/min. The washing steps were realized with 5 CV of the equilibration buffer to eliminate contaminants and a successive 5 CV of 20 mM imidazole (20 mM HEPES buffer, 100 mM NaCl and 20 mM imidazole, pH 8.0). Finally, 2 CV of 500 mM imidazole (20 mM HEPES buffer, 100 mM NaCl and 500 mM imidazole, pH 8.0) were passed into the column to perform OpdP elution.

Different fractions of washing and elution were collected, and the presence of the protein was assessed by SDS-PAGE.

All fractions containing OpdP were pooled, concentrated until 500 µL with an Amicon 30 KDa (Merck, Germany) and successively dialyzed against an 8 M urea pH buffer overnight at 4 ºC.
A rough estimation of the protein concentration was performed using the BCA test and by assessing the protein concentration on SDS-PAGE.
The correctness of the protein was verified through mass spectrometry, performed by an external facility (GIGA-Proteomics, Liège, Belgium).
OpdP isolation for the following immunization purpose was performed excising the protein band from SDS-PAGE gels.

3.5.3.3 Polyclonal antibodies production and purification

Polyclonal antibodies were obtained by immunizing a rabbit with four subcutaneous injections of 200 µg of OpdP, performed at days 0, 14, 28 and 56. The protocol was performed by an external facility, the CER group (Marloie, Belgium). The obtained sera were conditioned in 50 mM phosphate-buffered saline (PBS) pH 7.5 buffer. The polyclonal antibodies were purified using a HiTrap Protein A HP 1 mL column (Cytiva, formerly GE Healthcare, Uppsala, Sweden) with the help of a bench peristaltic pump. The column was equilibrated with 10 CV PBS pH 7.5 and the sera, previously clarified via a 10-minute centrifugation at 1600 x *g*, were loaded on the column; 10 CV PBS pH 7.5 were charged to wash the column and antibodies were eluted in 10 fractions (1 mL each) with 100 mM glycine pH 2.2 and directly neutralized with 100 µL of 1.5 M TRIS-HCl pH 8.5.
Different samples were subjected to SDS-PAGE, fractions containing antibodies were pooled and dialyzed against a 50 mM PBS pH 7.5 buffer over night at 4°C.
The concentration of the polyclonal antibodies was measured by BCA.

3.5.4 Outer membrane profile

The outer membrane profiling of the proteins expressed by different *P. aeruginosa* strains was performed modifying a previous described protocol (Kolayli *et al*., 2004): accordingly, bacteria were grown in LB broth in agitation at 37 ºC, harvested at OD_{600} 1.6 and 250 mL of the cultures were pelleted for 20 minutes at 1600 x *g* at the temperature of 4 ºC. The pellets were washed two times with 10 mL of lysis buffer (NaCl 50 mM, Tris-HCl 50 mM pH 8.0) by centrifuging 20 minutes at 1600 x *g* at 4 ºC.
Cells were subsequently disrupted using the French press Emulsiflex C3 homogenizer (Avestin, Mannheim, Germany), passing the samples four times in the apparatus with a pressure ranging from

1000 to 1500 psi; cellular debris, collected on ice, were pelleted by centrifugation for 30 minutes at 1600 x *g* at 4 ºC. The supernatants were then ultra-centrifuged on an Avanti J-E (Beckman Coulter) centrifuge one hour at 150000 x *g* at 4 ºC.
The obtained pellets, that contain the outer membranes, were resolubilized in 8 mL of resuspension buffer (Tris-HCl 30 mM pH 8.0, *N*-lauroylsarcosinate 1 %) with the aid of a mortar and pestle Potter-Elvehjem homogenizer, and then kept in agitation at room temperature for one hour.
A successive ultra-centrifugation of 30 minutes at 150000 x *g* was performed and the pellets were resuspended in 2 mL of the above-mentioned resuspension buffer.
After one hour of agitation at room temperature to facilitate the resuspension of the proteins, the samples contained the outer membrane proteins and were then used for SDS-PAGE and/or Western blot analysis.

3.5.5 Periplasmic extraction

Periplasmic proteins were extracted following the "spheroplasting by lysozyme and sucrose" method, described by Imperi and coworkers as the most efficient extraction protocol for successive proteomic analysis (Imperi *et al.,* 2009). In essence, bacterial pellet derived from 1 L culture was resuspended in 30 mL of TES (30 mM Tris-HCl, 4 mM EDTA, sucrose 20 % 0.5 mg/mL lysozyme pH 8.0), preincubated at 30°C; after 2 minutes $MgCl_2$ was added to reach a final 10 mM concentration, and the suspension was incubated while gently shaking it for 60 minutes. The suspension was then centrifuged at 11000 x *g* for 15 minutes at 4 ºC and the periplasmic content was recovered from the supernatant.

3.5.6 Western blot

Western blot analyses were used to verify the presence of specific proteins in our samples and to relative quantify their production.
The polyclonal, rabbit derived primary antibodies used were: *i)* anti-BlaR-CTD received from Dr. A. Amoroso (InBios CIP, Uliège), (Duval *et al*., 2003), *ii)* anti-OprD, received from Dr. Thilo Köhler (University of Geneva, Switzerland) (Köhler *et al*., 1999a), *iii)* anti-OpdP, obtained during this study.
The protein transfer from SDS-PAGE gel to PolyVinyliDene Fluoride membrane (PVDF) was performed, after methanol activation, using the Trans-Blot Turbo Transfer System (Bio-Rad), using

the Trans-Blot Turbo RTA Mini 0.2 µm PVDF Transfer kit (Bio-Rad), following the manufacturer's protocol.

After transfer, the membrane was incubated 2 hours in agitation at room temperature with the blocking solution (Tris-HCl 200 mM, NaCl 1.5 M), the so-called Tris-Buffered Saline (TBS) solution, added with 3 % of milk powder.

The membrane was then washed three times in TTBS (TBS added with Tween-20 0.05 %) in agitation at room temperature for 15 minutes each wash.

The membrane was then incubated overnight (approximatively 16 hours) in agitation at 4 ºC in a solution of 5 mL of TTBS, 1 % of milk powder, and 1 µL of the specific primary antibody.

The membrane was washed three times in TTBS as above described and incubated for one hour at room temperature in a TTBS solution added with 1:2000 diluted goat anti-rabbit secondary antibody, conjugated to horseradish peroxidase (HRP) (Bio-Rad).

The membrane was again washed three times in TTBS, in agitation, 5 minutes each wash and the revelation was performed with the Clarity Western ECL substrate kit (Bio-Rad), following the manufacturer's protocol.

Chemiluminescence detection was performed using the ImageQuant^{TM} LAS 4000 GE Healthcare.

3.5.7 Two-dimensional gel electrophoresis

Two-dimensional gel electrophoresis (2-DE) is a technique that enables the separation of proteins according to their isoelectric point (first dimension) and based on their molecular mass (second dimension). This feature allows the comparison of proteins extracts between different samples, allowing the identification of differentially expressed targets.

During this project, we compared different periplasmic proteomes to assess the differences induced by plasmid transformation, BlaR-CTD production or multiple porins deletions.

Experiences were performed at the Department of Life Sciences, University of Siena, Italy in collaboration with Dr. A. Gagliardi of the proteomics laboratory, directed by Prof. L. Bini.

The protocol used took inspiration from previous works on Gram-negative bacteria proteome (Gagliardi *et al*., 2016).

Samples were processed in biological triplicate.

3.5.7.1 Isoelectric focusing (IEF)

Isoelectric focusing (IEF) on the periplasmic extracts were performed on a precast, 18-cm long non-linear Immobiline™ Dry-Strip, with a 3-10 range of immobilized pH gradient (Cytiva). Runs were performed using the Ettan™ IPGphor™ system (Cytiva). Immobilized pH gradient (IPG) strips for analytic runs were rehydrated following the manufacturer's indications with 350 µL of lysis buffer, added with bromophenol blue in trace, carrier ampholytes 0.2 % (v/v) and 60 µg of proteins for 1 hour at 0 V and for 8 hours at 30 V, at 16 ºC. Proteins were focused at 16°C, according to the following voltage program: 200 V for 1 hour, from 300 V to 3500 V for 30 minutes, 3500 V for 3 hours, from 3500 V to 8000 V for 30 minutes, 8000 V for 3 hours, 10000 V, and finally 10000 V for a total volt-hours accumulated during the run of 80000 VhT.

In the case of MS-preparative runs, strips were rehydrated for 12 hours at 20 ºC with 350 µL lysis buffer added with bromophenol blue in trace, carrier ampholytes 2 % (v/v). The protein samples, 600 µg, were added through a cup loading in the IPGphor Cup Loading Strip Holders (Cytiva) and were applied at the cathodic end of the strip. Proteins were then focused at 16°C, according to the following voltage program: 30 V for 30 minutes, 200 V for 2 hours, 500 V for 2 hours, from 500 V to 3500 V in 30 minutes, 3500 V for 5 hours, from 3500 V to 5000 V in 30 minutes, 5000 V for 4 hours, from 5000 V to 8000 V in 30 minutes, 8000 V for 3 hours, and finally10000 V for a total volt-hours accumulated during the run of 100000 VhT.

After IEF, the IPG strips were equilibrated into two buffers whose compositions were as follows: *i)* buffer 1: 6 M urea, 2 % (w/v) SDS, 2 % (w/v) DTE, 30 % (v/v) glycerol and 0.05 M Tris-HCl pH 6.8 for 12 minutes; *ii)* buffer 2: 6 M urea, 2 % (w/v) SDS, 2.5 % (w/v) iodoacetamide, 30 % (v/v) glycerol, 0.05 M Tris-HCl pH 6.8 and a trace of bromophenol blue for further 5 minutes.

3.5.7.2 Second-dimension run

The second-dimension runs were performed on house-made 9-16 % polyacrylamide linear gradient gels (18 x 20 cm x 1.5 mm) and carried out at 40 mA/gel constant current at 9°C. The runs were performed as long as the dye front reached the bottom of the gel.

Ammoniacal silver staining was used for analytical gels (Oakley *et al*., 1980) and the scans were performed using the ImageScanner III densitometer (Cytiva).

In the case of MS-preparative gels, they were previously attached covalently to a glass surface using Bind-Silane (γ-methacryloxypropyltrimethoxysilane) (LKB-Produkter AB, Bromma, Sweden); SYPRO Ruby staining (Bio-Rad) was successively performed, following manufacturer's protocol.

MS-preparative gels were digitalized with a Typhoon 9400 laser densitometer (Cytiva), at 532 nm wavelength.

3.5.7.3 Image and statistical analysis of proteomic data

Analytic gels were analyzed using the Image Master 2D Platinum v 6.0 software (Cytiva).
Briefly, for each tested condition, the biological triplicates were merged on a master reference gel that was used to perform comparisons between different samples.
Statistically significant quantitative and qualitative differences were identified on the basis of a fold change of at least ± 2.0 in relative volume (%V) ratio and on the basis of statistically analysis with two-tailed Student's *t*-test score less than 0.05.

3.5.7.4 Mass spectrometry

Matrix-Assisted Laser Desorption/Ionization Time-Of-flight (MALDI-TOF) was used to identify spots that statistical analysis flagged as differentially expressed.
Selected spots were automatically excised from MS preparative gels by means of an ETTAN™ Spot-picker (GE Healthcare) and minced into < 1 mm^3 fragments. Samples were destained twice with a solution composed of 2.5 mM ammonium bicarbonate and 50 % (v/v) acetonitrile at 37 ºC, with shaking for 30 minutes. Afterwards they were dehydrated in acetonitrile at 20 ºC for 10 minutes and acetonitrile by the means of a vacuum centrifuge (SpeedVac™, Thermo Fischer Scientific, Waltham, MA, USA). Subsequently, spot rehydration was performed on ice for 60 minutes with 10 ng/µL trypsin solution (Sigma Aldrich, St. Louis, MO, USA), and protein digestion was performed by an overnight incubation at 37 ºC.
The digested protein samples (1.25 µL) were directly spotted onto the MALDI-TOF target, air-dried, covered with 1 µL of matrix solution (5 mg/mL α-cyano-4-hydroxycinnamic acid, dissolved in 50 % (v/v) of acetonitrile and 5 % (v/v) of trifluoroacetic acid), and subsequently air-dried.
Mass spectra were acquired using an Ultraflex III MALDI-TOF/TOF mass spectrometer (Bruker Daltonics, Billerica, MA, USA), armed with a 200 Hz smartbeam I laser. Spectra were acquired by delayed extraction technology with reflectron in positive mode (laser frequency: 100 Hz), and then analyzed with the Flex Analysis software v.3.0 (Bruker). Auto-proteolytic trypsin peptides were used to calibrate internal standards of the acquired spectra. Filtering of the resulting mass lists was performed to remove contaminants, such as mass matrix-related ions, keratin-derived peaks, and trypsin auto-lysis peptides peaks. Protein identification was carried out by using the peptide mass

fingerprinting database, with the online available software MASCOT (Matrix Science Ltd., London, UK), searching on Swiss-Prot/TrEMBL database. The define searching parameters were the following: *P. aeruginosa* as taxonomy, 100 ppm as mass tolerance, one admissible missed cleavage site, carbamidomethylation (iodoacetamide alkylation) of cysteine as fixed modification, and oxidation of methionine as a variable modification.

3.6 Development of a protocol for the outer membrane permeability determination

The antibiotic flux passing through the *P. aeruginosa* outer membrane can be described by the Fick's first law of flux (1) that is:

$$\mathbf{J = - D \cdot A \cdot \frac{\Delta C}{\Delta x}} \quad (1)$$

Where J denotes the flux of the antibiotic through the outer membrane; D is the diffusion coefficient of the antibiotic; A is the outer membrane area (that can be assumed as 132 cm^2); ΔC is the concentration gradient of the antibiotic, and Δx indicates the membrane's thickness.

Given that the β-lactam flux in *P. aeruginosa* is influenced by specific porins expression, rather than only passive diffusion, we can introduce the permeability coefficient **P** (2), which is defined as the ratio between the diffusion coefficient and the membrane thickness:

$$\mathbf{P = - \frac{D}{\Delta x}} \quad (2)$$

As a result, the antibiotic flux can be expressed by equation 3:

$$\mathbf{J = P \cdot A \cdot \Delta C} \quad (3)$$

With these assumptions, the antibiotic flux can be estimated by expressing in the periplasm of *P. aeruginosa* a probe capable to rapidly and stably acylate any β-lactams entered in this compartment. This premise can lead to determine low permeability coefficients, as in the case of *P. aeruginosa*.
The C-terminal domain of BlaR (BlaR-CTD), a PBP derived from *B. licheniformis*, might be effective for this purpose (Lakaye *et al*., 2002). BlaR-CTD affinity for different β-lactams was previously assessed to be particularly elevated (Duval *et al*., 2003).
The periplasmic BlaR-CTD expression is therefore suitable to allow the direct quantification of the β-lactam concentration present in the periplasmic space, and, consequently, to measure the permeability coefficient (4) as shown in the following equation:

$$\mathbf{P = \frac{d(E_1I^*)/dt}{A \cdot [I_e]}} \quad (4)$$

where E_1I^* is the concentration of the acyl-enzyme complex BlaR-CTD/β-Lactam, and $[I_e]$ denotes the external β-lactam concentration. The $d(E_1I^*)/dt$ ratio was measurable and equal to the slope of the line which define the evolution of the concentration of the acyl-enzyme adduct in function of the incubation time (Figure 17B).
To validate this model, it must be confirmed that the BlaR-CTD sensor possesses a strong affinity for all the β-lactams tested and consequently rapidly reacts with the β-lactams entered in the periplasm. At the same time, β-lactams must not induce the constitutive Ambler Class C β-lactamase AmpC, which would then compete with BlaR-CTD for β-lactams' acylation.
To substantiate these two preconditions, specific experiences have been performed.

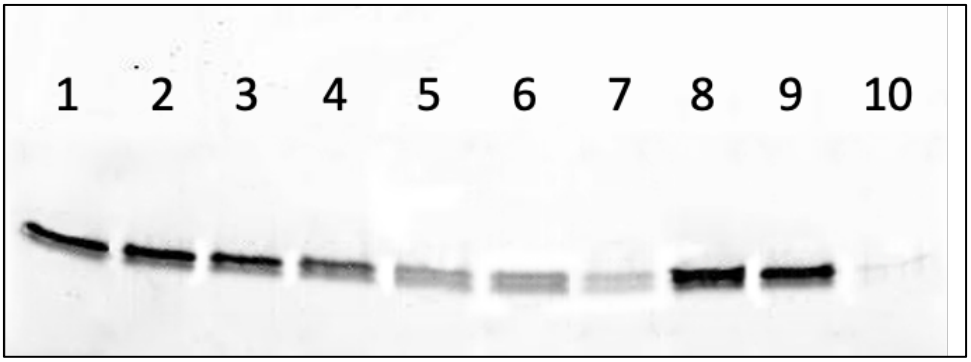

A

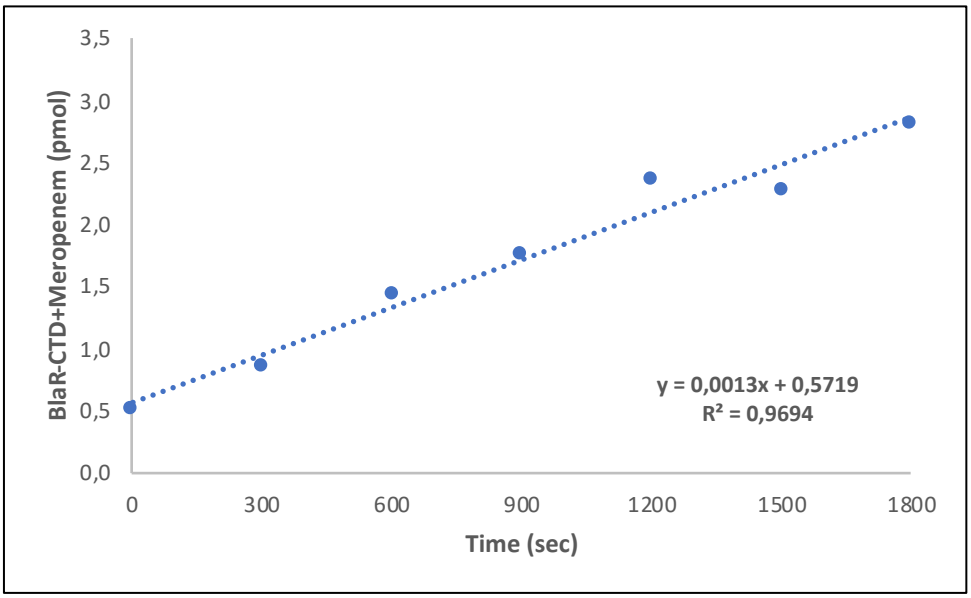

B

Figure 17: Example of densitometric analysis for β-lactam translocation measurement.
A): densitometric analysis of the fluorescence signal given by the complex BlaR-CTD-Bocillin FL, reported as an example; samples from 1 to 7 represent different aliquots, taken every 5 minutes for determining meropenem uptake in ARC5782 (PAO1*ΔoprD*, *ΔopdP*); samples 8 and 9 are aliquots taken before the addition of meropenem in the culture, representing the total quantity of BlaR-CTD produced and sample 10 is an aliquot not sonicated, used to quantify possible BlaR-CTD released in the medium.
B): graph representing the increase of the complex Meropenem+BlaR-CTD as a function of time; this quantification was possible by subtracting to the total BlaR-CTD produced in an aliquot (samples 8 or 9 of figure A) the values obtained during the experience (samples 1-7 of figure A). The slope of the line represents the antibiotic flux passing the outer membrane.

3.6.1 BlaR-CTD affinity

BlaR-CTD is a PBP derived from *B. licheniformis* that possess structural homologies with Class D β-lactamases (Joris *et al.*, 1990; Zhu *et al.*, 1990). BlaR-CTD has a high affinity for β-lactams but, unlike SBL, is less prone to catalyse the diacylation step. Generally, the reaction between β-lactams and β-lactamases can be described by Michaelis-Menten's kinetic (5) as:

$$E + C \underset{k_{-1}}{\overset{k_{+1}}{\rightleftarrows}} E.C \xrightarrow{k_2} E - C^* \xrightarrow{k_3} E + X \quad (5)$$

where E is the β-lactamase, C the β-lactam, E.C the Henri-Michaelis complex, E-C* the acyl-enzyme, and X the hydrolysed β-lactam, obtained via the addition of one H_2O molecule, k+1 is the foreword rate constant, k-1 is the reverse rate constant, k2 is the second-order rate constant and k3 is the first-order rate for deacylation constant.

Due to the incapacity of BlaR-CTD to catalyse the last diacylation step, the interaction of BlaR-CTD with β-lactams can be obtained as in equation (6):

$$E + C \underset{k_{-1}}{\overset{k_{+1}}{\rightleftarrows}} E.C \xrightarrow{k_2} E - C^* \quad (6)$$

where E, in this case, indicates BlaR-CTD.

The pseudo-first order rate constant for acylation (k_a) is given by (7):

$$\frac{k_2[C]}{K'} \text{ where } K' = \frac{k_{-1} + k_2}{k_{+1}} \quad (7)$$

PBPs are characterized by *k2* values that are much smaller than k_{-1}; these assumptions lead to the formulation of (8):

$$k_a = \frac{k_2[C]}{K + [C]} \text{ where } K = \frac{k_{-1}}{k_{+1}} \quad (8)$$

However, high acylation rates are found when [C]<<K and, for this reason, the PBP's acylation constant might be described by (9):

$$\frac{k_2}{K} \quad (9)$$

The (k_2/K′) ratio corresponds to the second-order rate constant for the formation of the acyl-enzyme complex and refers to the acylation step efficiency (Frère and Joris, 1985).

This parameter is determined by simultaneously incubating a known concentration of antibiotic whose k_2/K is to be measured with a known concentration of reporter antibiotic (r), whose kinetic parameters are known. The proportion of each acyl-enzyme formed at saturation is dependent on the concentration and on the k_2/K ratio of the antibiotics (equation 10) (Frère *et al*., 1992). In our case, we firstly used ampicillin ($\Delta\varepsilon^{482}$ = 13000 M^{-1} cm^{-1}) as a reporter molecule to determine k_2/K ratio for nitrocefin ($\Delta\varepsilon^{482}$ = 15000 M^{-1} cm^{-1}) ($k_2/K_{Nitrocefin}$ = 3.6 ± 0.3 μM^{-1} s^{-1}).

Successively, nitrocefin was used as reporter molecule to determine cefalotin, ceftazidime, imipenem, meropenem, ertapenem, biapenem and doripenem k_2/K values.

The assay can be described as:

$$\frac{[EC^*]r}{[EC^*]} = \frac{\left(\frac{k_2}{K'}\right)r * [C]r}{\left(\frac{k_2}{K'}\right) * [C]} \quad (10) \qquad \text{and} \quad [EC^*]r + [EC^*] = [E_0]$$

$$\frac{[EC]_r}{[E_0] - [EC]_r} = \frac{\left(\frac{k_2}{K'}\right) r * [C]r}{\left(\frac{k_2}{K'}\right) * [C]}$$

Where [EC*]r and [EC*] are, respectively, the concentrations of BlaR-nitrocefin and BlaR-antibiotic acyl-enzymes, [C]r and [C] correspond to the concentration of the nitrocefin and of the tested antibiotic respectively. (k_2/K')r and (k_2/K') represent the acylation rate constant of the antibiotic for BlaR-CTD for reporter and the antibiotic.

Reactions were carried out in PBS pH 7.5 and the absorbance at 482 nm was measured using the Specord 50 plus spectrophotometer (Analytic Jena, Jena, Germany). BlaR-CTD (20 μM) previously

produced and purified (Duval *et al*., 2003) was added to a solution containing nitrocefin (80 µM) and variable concentrations (25 - 1000 µM) of tested antibiotics.

3.6.2 β-Lactamase assays

The level of expression of the AmpC β-lactamase was measured in crude cell extracts from the different *P. aeruginosa* PAO1 cultures as follows. The growth of the bacteria was monitored by measuring OD_{600}. At an absorbance value of 1.6, the culture was divided into two aliquots of 10 mL. One culture corresponded to the control. The second culture was obtained by adding the different antibiotic tested at a final concentration equal to the maximum concentration of the antibiotic tested in the permeability assay. The cultures were then incubated for a time that corresponds to the time of incubation with the selected antibiotic in the permeability test. 1 mL of each culture was centrifuged at 13000 x *g* for 10 minutes, the pellet was washed twice and resuspended in 1 mL of 10 mM PBS buffer pH 7.4. Cells were then disrupted by sonication with the refrigerated and automated Bioruptor® Plus (Diagenode, Liège, Belgium), thus minimizing the variability in this step. The cellular extract was then clarified by centrifugation at 13000 x *g* for 30 minutes at 4°C.
The protein concentration of each extract was measured with the help of a BCA protein assay kit (Pierce, Rockford, IL, USA).
The β-lactamase activity of the crude extracts was determined by measuring the initial rate of hydrolysis of a 100 µM nitrocefin solution in 10 mM PBS buffer pH 7.4 at 30°C as reporter substrate. The Hanes-Wolf linearization and the Henri-Michaelis equation were used to determine the sample's AmpC concentration. The wave lengths and the molar extinction coefficient variations are reported in Annex, Table S3 (page 219). The absorbances were measured on the Specord 50 plus spectrophotometer.
Positive controls for AmpC induction in *P. aeruginosa* PAO1 were analysed as previously described and incubated for six hours with 50 µM ampicillin and 50 µM cefoxitin; the negative controls were obtained as the culture without antibiotic, grown for the different incubation times tested.
Specific activity, expressed in micromoles per minute per milligram of protein, resulted from dividing AmpC quantification by total protein amount, thus expressing the rate of hydrolysis of each substrate.

3.6.3 Permeability determination

Antibiotic diffusion in the periplasmic space was analysed in planktonic cultures. The different *P. aeruginosa* strains, previously transformed with pKT240blaR or pKT40blaR-gen in the case of TNP004, were precultured overnight in LB medium added with antibiotic selection (tetracycline 50 µg/mL or gentamicin 10 µg/mL, respectively). Successively, the culture was scaled up in 100 mL LB medium additionated with 1:50 reached the late exponential phase ($OD_{600} \simeq 1.6$) a prefixed β-lactam concentration was added in the medium and aliquots (1 mL) were harvested at different incubation times. All the antibiotics tested, their concentrations and the time frame of sampling, are reported in Table 5.

Antibiotics	Tested concentrations (µM)		
Benzylpenicillin	40	20	10
Cefoxitin	30	15	7.5
Cefuroxime	60	30	15
Cefotaxime	60	30	15
Ampicillin	20	10	5
Cephaloridin	8	4	2
Imipenem	0.02	0.01	0.005
Imipenem*	4	2	1
Meropenem	8	4	2
Meropenem^	20	10	5
Ertapenem	7.5	5	2.5
Doripenem	4	2	1
Biapenem	0.04	0.02	0.01
Biapenem^	4	2	1

Table 5: Different antibiotic concentrations tested for the determination of the permeability coefficients. The asterisk indicates the concentrations tested on strains deprived of OprD, while the circumflex denotes the concentrations tested on strains both deprived of OprD and OpdP.

The MBL VIM-4, produced and purified in a previous study (Lassaux *et al*., 2011) was used with the purpose of hydrolysing all the antibiotic present outside the cells and consequently interrupting its permeation in an active form. In particular, 2 µL of VIM-4 (1 mg/mL) was added to the bacterial culture to immediately stop the antibiotic permeation. EDTA (1 mM) was successively added to the medium in order to chelate the metal ions, thus inactivating the MBL VIM-4. The crude extract was obtained by means of ten cycles of refrigerated sonication at 4°C, performed with the Bioruptor® Plus Diagenode. The BlaR-CTD acylation with the tested antibiotics was assessed by counter-

marking experiments with the fluorescent reporter antibiotic Bocillin FL. The crude extract was incubated at 37 ºC for 5 minutes with 2 µL of Bocillin FL (2.5 µM), and the reaction was stopped by the addition of SDS-loading buffer.

Two positive controls for BlaR-CTD production were harvested on the culture before the antibiotic addition; a negative control was obtained from the supernatant culture, to ensure low concentrations of BlaR-CTD released into the medium.

Samples were submitted to SDS-PAGE and the fluorescence intensity of BlaR-CTD labeled with Bocillin FL was revealed using the Typhoon Trio+ imager (GE Healthcare) (excitation at 488 nm and emission at 650 nm). The quantification of the decrease of BlaR-CTD acylated with Bocillin FL as a function of time, and consequently the increase of BlaR-CTD acylated with the unlabelled antibiotic, was performed by densitometry with the Image Quant TL software (GE Healthcare) (Figure 17A). An assumed value of 100 ng was given to one of the two positive controls, to represent the initial concentration of BlaR-CTD produced by the culture taken into consideration.

The obtained densitometric data were plotted on a graph where on the horizontal axis the time is reported in second, while the vertical axis reports the quantity of the BlaR-CTD complex acylated with Bocillin FL, expressed in picomoles. The slope of the resulting straight line is estimated and the associated R^2 should be larger that 0.9 to be considered adequate, as shown in Figure 17B.

Analyses were performed in duplicate at three different antibiotic concentrations, that are reported in Table 5.

3.6.4 Complementary permeability experience

The fine-tuned protocol was suitable to determine the effect of different conditions on membrane stability. Dipicolinic acid (DPA), a metal ions chelator, was studied for its involvement on membrane integrity. In essence, DPA at different concentrations (1 mM, 750, 500, 250, 100 and 50 µM) was added to 5 µM ampicillin and submitted to the permeability coefficient determination.

Any variation in antibiotic penetration is to be considered caused by DPA effect on membrane integrity.

4 RESULTS

This paper summarizes the main results obtained in the course of this thesis project with respect to the set objectives. Specifically, it describes the studies carried out to validate the use of BlaR-CTD as a periplasmic sensor for determining the permeability coefficients of the outer membrane of *P. aeruginosa*, with minimal or no interaction with the physiological response. Permeability coefficients were successively determined for a large number of β-lactams in *P. aeruginosa* PAO1 and a series of isogenic mutants deleted for various porins.

The paper also highlights the different expression of porins depending on the bacterial growth phase and in response to the absence of OprD, a phenomenon that partly explains the lack of correlation between the increase in MICs for carbapenems and the pretty unaltered (except for imipenem) outer membrane permeability coefficients obtained in the absence of the OprD porin.

The RT-PCR results are reported in Figures 4, 5 and S2 of the paper, and are also presented in the annexes of this thesis—Figure S1 (Annex, page 220), Figure S2 (Annex, page 220) and Figure S3 (Annex, page 221) with additional details of the statistical analyses performed.

The role of the OpdP porin is further analyzed in a different setting, shown by exposing a mutant lacking this porin to sub-MIC concentrations of meropenem. This experiment revealed an increased propensity, under this condition, to select mutants deleted for (or downregulating) OprD, in the absence of OpdP.

Finally, whole-genome sequencing revealed previously undocumented mutations associated with carbapenem resistance profiles. Together with the content of the paper, the raw sequencing data from these experiments have been uploaded under the same Bioproject (PRJNA985251).

AMERICAN SOCIETY FOR MICROBIOLOGY | Microbiology Spectrum

| Open Peer Review | Bacteriology | Research Article

Outer membrane permeability of *Pseudomonas aeruginosa* through β-lactams: new evidence on the role of OprD and OpdP porins in antibiotic resistance

Francesco Amisano,[1] Paola Mercuri,[1] Steven Fanara,[2] Olivier Verlaine,[1] Patrick Motte,[2] Jean Marie Frère,[1] Marc Hanikenne,[2,3] Moreno Galleni[1]

AUTHOR AFFILIATIONS See affiliation list on p. 20.

ABSTRACT Gram-negative bacteria are a major concern for public health, particularly due to the continuous rise of antibiotic resistance. A major factor that helps the development of resistance is the outer membrane that is essential since it acts as a strong permeability barrier to many antibiotics that are effective against other bacteria. In this study, we determine the specific permeability coefficients for various antibiotics in *Pseudomonas aeruginosa* strains, which differ from each other for their porin expressions. We showed that OprD and OpdP porins contribute both to internalize meropenem and biapenem. Using qRT-PCR, we demonstrated that their expression is dependent of the various phases of cellular growth. We were able to show how the OpdP porin is less expressed in exponential growth phases, while it tends to be produced when the bacterial culture enters into the latent phase, in an inversely proportional way compared to the OprD porin. The deletion of the OpdP porin, in the presence of meropenem at concentrations equivalent to the MIC values, contributes to the selection of carbapenem-resistant strains. Therefore, the presence of mutations/deletions of the OpdP porin should receive greater consideration from a clinical point of view as the use of meropenem at nonoptimal concentrations could lead to the appearance of resistance phenotypes.

IMPORTANCE Carbapenem-resistant strains of *Pseudomonas aeruginosa* are among the major threats to public health. The permeability of the outer membrane for the β-lactam antibiotics is one of the major factors that reduce the activity of the antibiotics. In this study, we measure the low permeability coefficient of the *P. aeruginosa* outer membrane to β-lactams. The methodology we develop to determine the permeability can be applied to other antibiotic families and/or pathogens.

KEYWORDS OpdP porin, external membrane permeability, *Pseudomonas aeruginosa*, porins

The gram-negative rod-shaped γ-proteobacterium *Pseudomonas aeruginosa* (*P. aeruginosa*) is a ubiquitous and opportunistic pathogen responsible for life-threatening infections, especially in immune-compromised patients, such as those with ventilator-associated pneumonia (VAP) or with urinary tract infections (UTIs) and is the leading cause of respiratory tract infections (RTIs) in cystic fibrosis patients (1–4). It is intrinsically resistant to different classes of antibiotics, and the few available therapeutical options include some β-lactam compounds, often delivered in combination with β-lactamase inhibitors, such as piperacillin/tazobactam, ceftazidime/avibactam, and imipenem/relebactam (5–8). Unfortunately, this bacterium has developed different mechanisms of resistance. In the case of β-lactam antibiotics, the major resistance

Editor Mariagrazia Perilli, University of L'Aquila, L'Aquila, Italy

Address correspondence to Moreno Galleni, mgalleni@uliege.be.

The authors declare no conflict of interest.

See the funding table on p. 20.

Received 22 February 2024
Accepted 19 October 2024
Published 4 March 2025

mechanism is the production of enzymes (β-lactamases) that can hydrolyze the β-lactam ring (3, 9). *P. aeruginosa* carries a chromosomally encoded and inducible AmpC β-lactamase (10). In addition, it can acquire extended-spectrum β-lactamases (ESBLs) and/or metallo-β-lactamases (MBLs), which confer resistance to carbapenems (11–13).

Moreover, *P. aeruginosa* is characterized by a low outer membrane permeability to β-lactams, due to the presence of OprF, a nonspecific pore, homologous to OmpC and OmpF from *Escherichia coli*. This porin is, indeed, present into two conformers, and the closed fraction represents approximatively 95% of the total OprF expressed by the bacteria, leaving a minority in the open state, and its involvement in the permeation is still debated (14, 15).

As a consequence, hydrophilic nutrients and antibiotic internalization are mediated by a wide number of substrate selective channels (15).

Interplay with other resistance mechanisms, like the efflux pump upregulation, can extrude a wide variety of antibiotics present in the cytoplasmic or periplasmic space of the bacteria. In particular, increased expression of MexAB-OprM contributes to β-lactam resistance, as commonly found in clinical multiresistant isolates (16–18).

It is well documented that a decrease in the outer membrane permeability can be mediated by an altered expression of OprD. This porin facilitates basic amino acid uptake and influences antibiotic sensitivity, primarily to imipenem, due to the structural homology between arginine and the C2 antibiotic lateral chain (19, 20).

P. aeruginosa possesses 18 OprD homologs, characterized by their structural similarities and substrate specificities. They belong to the family of outer membrane carboxylate channel (Occ).

Within this family, two subgroups are identified: the OprD (or OccD) and the OpdK (or OccK) subfamilies (15, 21, 22).

OpdP (OccD3) shows the highest sequence identity with OprD (51%). It is associated with glycine–glutamate dipeptide translocation, and it has been assumed to be involved in meropenem uptake, although a clear phenotypic resistance profile in deletion mutants has not been determined (21, 23–26). This porin belongs to the *dppA4BCDF* operon, encoding the ABC machinery responsible for the utilization of dipeptides during the stationary phase, increasing the bacterial metabolic versatility. Its expression is controlled by the PsdR regulator (27, 28). Recent studies have shown that *psdR* is prone to acquire mutations, but their impact on the OpdP expression has not yet been described (29–31).

The research for antibiotic-specific channels has been directed to other porins belonging to the Occ family. For instance, in the study by Isabella and coworkers, porins selected for their expression quantified by RNAseq analysis after growth in minimal medium were hypothesized to be involved in the entry of antibiotics. The study identified the OpdC (OccD2), OpdT (OccD4), and OpdB (OccD7) porins as possible candidates. However, a *P. aeruginosa* isogenic mutant where the genes encoding three porins were deleted, together with *opdP* and *oprD,* did not display a modification of the antibiotic resistance profile compared to the single *oprD* mutant (24). Even a *P. aeruginosa* strain stripped of 40 porins resulted in MICs comparable to those of the single *oprD* knockout, suggesting the presence of alternative translocation pathways, independent of porins (32). For this reason, the MIC determination of *P. aeruginosa* isolates does not reflect the real pattern of porin expression and does not exhibit a reliable predictive value for bacterial permeability.

Therefore, an improved understanding of β-lactam translocation mechanisms in gram-negative bacteria might help in the design of new molecules, formulated also on the basis of their abilities to cross the outer membrane barrier.

Different methods have been proposed to study the outer membrane permeability in *P. aeruginosa*, starting from the pioneering work by Zimmermann and Rosselet (33). Comparing the periplasmic β-lactam hydrolysis of intact cells with the one obtained by a lysate made it possible to determine the outer membrane permeability coefficients for *P.*

aeruginosa (34). Unfortunately, this method turned out to be poorly reproducible due to the contribution of efflux pumps that interfere with antibiotic accumulation (35).

The use of radio-labeled β-lactams has been proposed as an alternative method for the quantification of the antibiotic periplasmic concentration (36). However, this method is limited by the difficulty of obtaining a wide set of radioactive compounds.

Whole-cell analytical techniques, including mass spectrometry-based analysis, allow the quantification of the variation in extracellular antibiotics or the measurement of the direct accumulation in the periplasm (37–39), but they are highly time-consuming.

Another approach being pursued was the study of single porin permeation properties using different techniques such as the liposome swelling assay, electrophysiology, or molecular dynamics simulations. They have importantly contributed to the definition of the specific role of single porins, the determination of their specific conductance, and have identified the consequences that mutations may have on translocation properties (40–44). Nevertheless, the study of the single porin properties undoubtedly failed to comprehend the complexity of the bacterial response to antibiotics, given that synergic effects are not noticeable.

In a first approach, we determined the *P. aeruginosa* outer membrane permeability toward β-lactam, as described below. This method exploits the property of BlaR-CTD, a soluble penicillin-binding protein that displays a high affinity for β-lactams. Its expression in the periplasm allows an accurate estimation of the quantity of the antibiotic that permeates through the outer membrane (45).

Unlike the previously mentioned methods, the study of single or multiple porin(s) isogenic mutants can elucidate the role of a single porin or the presence of any synergic effect in double or multiple knockout strains for a broad variety of β-lactams, and this was the first aim of our research.

The second goal of this study was to ascertain the real contribution of OpdP in carbapenem resistance, especially under stress conditions. To the best of our knowledge, we were the first to investigate the expression of different porins during different bacterial growth phases by means of qRT-PCR, and we believe that this is a useful tool to broaden our understanding of the response to antibiotic therapy.

Our third goal was to verify whether the single deletion of the OpdP porin confers a selective advantage in developing a phenotype of carbapenem resistance. To this end, we performed a multistep resistance experiment using meropenem at sub-minimum inhibitory concentrations and subsequently analyzed the resistant mutants thus obtained.

Finally, we performed whole-genome sequencing on selected strains to clarify the specific resistance genotype.

RESULTS AND DISCUSSION

Antibiotic resistance determination and mutant selection

Different subclasses of β-lactams were tested to evaluate the MIC variations associated to porin deletions, and the resistance profiles of *P. aeruginosa* strains are reported in Table 1.

MIC values for carbapenems were increased in all the strains where OprD was deleted and also in TNP004, described to downregulate OprD expression (47). The deletions of the other porins did not change the resistance phenotype and did not suggest any synergic effect for the antibiotic tested.

We further obtained *P. aeruginosa* mutant strains, derived from *P. aeruginosa* PAO1 and *P. aeruginosa* ARC5170 (PAO1*ΔopdP*), with the help of a multistep resistance experiment.

Colonies were cultured and then plated at different growth phases at sub-MIC meropenem concentrations. We registered the appearance of resistant colonies for both strains and at the different growth phases tested, but ARC5170 proved to be the most adept at acquiring the ability to grow in the presence of meropenem, 30 times more frequently than for the other strain; in particular, we found approximatily 600 colonies derived from ARC5170, while only 20 were derived from PAO1.

TABLE 1 MIC values for the different *P. aeruginosa* strains[a,b]

Antibiotics (µg/mL)	*P. aeruginosa* MICs (µg/mL)																	
	CLSI Standard	CLSI Susc.	ATCC 27853	PAO1	PAO1-Jap	TNP004	ARC545	ARC5990 (*Δoprd*)	ARC5170 (*Δopdp*)	ARC5782 (*Δoprd, ΔopdP*)	ARC5998 (Δ5porins)	LG01	LG02	LG03	LG04	LG05	LG06	LG07
Ampicillin	NA	NA	2,000	2,000	2,000	1,000	2,000	1,000	1,000	1,000	1,000	2,000	2,000	2,000	ND	ND	ND	ND
Benzylpenicillin	NA	NA	>2,000	>2,000	>2,000	>2,000	>2,000	>2,000	>2,000	>2,000	>2,000	>2,000	>2,000	>2,000	ND	ND	ND	ND
Piperacillin	1–8	≤16	2	2	2	2	2	2	2	2	2	8	4	8	ND	ND	ND	ND
Cefalotin	NA	NA	>2,000	>2,000	>2,000	>2,000	>2,000	>2,000	>2,000	>2,000	>2,000	ND	ND	ND	ND	ND	ND	ND
Cephaloridine	NA	NA	>2,000	>2,000	>2,000	>2,000	>2,000	>2,000	>2,000	>2,000	>2,000	ND	ND	ND	ND	ND	ND	ND
Cefoxitin	NA	NA	1,000	1,000	1,000	500	1,000	1,000	1,000	1,000	1,000	ND	ND	ND	ND	ND	ND	ND
Cefuroxime	NA	NA	250	250	250	250	250	500	500	500	500	>500	>500	>500	ND	ND	ND	ND
Cefotaxime	8–32	NA	16	16	16	8	16	16	16	16	16	32	16	32	ND	ND	ND	ND
Ceftazidime	1–4	≤8	1	1	1	2	1	1	1	1	1	2	1	2	ND	ND	ND	ND
Cefepime	0.5–4	≤8	1	1	1	0.5	1	1	1	1	1	2	2	2	ND	ND	ND	ND
Imipenem	1–4	≤2	1	1	1	**8**	1	**8**	1	**8**	**8**	**16**	**16**	**8**	**16**	**16**	**16**	**16**
Meropenem	0.12–1	≤2	0.5	0.5	0.5	**2**	0.5	**4**	0.5	**4**	**4**	**8**	**4**	**8**	**4**	**4**	**4**	**4**
Ertapenem	2–8	NA	8	8	8	**32**	8	**32**	8	**32**	**32**	**64**	**64**	**64**	**64**	**64**	**64**	**64**
Biapenem	0.5–2	NA	0.5	0.5	0.5	**4**	0.5	**4**	0.5	**4**	**4**	**4**	**4**	**4**	**4**	**4**	**4**	**4**
Doripenem	0.12–0.5	≤2	0.25	0.25	0.25	**1**	0.25	**1**	0.25	**1**	**1**	**2**	**2**	**2**	**2**	**2**	**2**	**2**
Tetracycline	8–32	≤4	8	8	8	8	8	8	8	8	8	16	8	16	ND	ND	ND	ND
Gentamicin	0.5–2	≤4	1	1	1	2	1	2	2	2	2	ND	ND	ND	ND	ND	ND	ND

[a]CLSI standard refers to acceptable limits for quality control strains used to monitor the accuracy of MICs. CLSI susc. refers to the MIC susceptibility breakpoints interpreted by CLSI (46). NA: not available, ND not determined.
[b]The bold characters represent the names of the *Pseudomonas* strains utilized in this study.

We selected *P. aeruginosa* LG01, derived from PAO1, and six mutants derived from ARC5170 named *P. aeruginosa* LG02-LG07; determined their MICs; and observed that all the strains presented a stable resistance profile characterized by a reduced sensitivity to carbapenems, identical to that of the strains deprived of OprD (Table 1).

OprD sequencing and whole-genome sequencing

P. aeruginosa TNP004 was described to produce an undetectable amount of OprD (47), but the cause underlying this downregulation has not been elucidated yet. For this reason, we sequenced the *oprD* gene and observed that it contained a single-nucleotide mutation (T1301C) yielding the Leu434Pro mutation in OprD, a modification in a transmembrane domain that increases the instability of the porin (GenBank accession number OR069747).

We were also interested in assessing whether the carbapenem resistance found in the strains selected under meropenem pressure was attributable to *oprD* mutations and consequently performed Sanger sequencing. For *P. aeruginosa* LG01, the insertion of one cytosine between positions 1,205 and 1,206 was found to induce a frameshift in the *oprD* open reading frame (GenBank accession number OR069748). LG02 is characterized by a single-nucleotide substitution (G1017A), introducing a premature STOP codon (GenBank accession number OR069749). The strains LG04, LG05, LG06, and LG07 shared the same nucleotide deletion in position 1,291 (G), resulting in a frameshift and in the synthesis of a truncated porin (GenBank accession number OR069750). Figure S3 summarizes the alignments of the different *oprD* mutated genes. Interestingly, *P. aeruginosa* LG03 did not exhibit any mutation when compared to the *oprD* wild-type gene, despite a carbapenem resistance profile similar to that of the other *oprD* mutants.

The whole-genome sequences of *P. aeruginosa* TNP004 and LG03 were determined to identify other mutations that could lead to the carbapenem resistance genotype associated to those strains. Due to the report of many polymorphisms in different PAO1 reference strains diffused worldwide (48), PAO1-Jap and ARC545, parental strains of TNP004 and ARC5170, respectively, were sequenced in order to exclude the role of mutations already present in these strains for carbapenem resistance observed in TNP004 and LG03.

The nucleotide sequences were deposited in the GenBank database, Bioproject PRJNA985251 under accession number SAMN35794375-8, while the observed mutations are reported in Fig. 1.

TNP004, besides the nucleotide substitution in *oprD*, presented other mutations including a deletion in *fliF* and two point mutations in *lasR* and *pilR*. However, these genes have not been described to be involved in the regulation of OprD expression, and so we concluded that the mere amino acid substitution in OprD causes the lack of porin's expression.

We also observed that, when compared to the reference PAO1, LG03 exhibited two single-nucleotide polymorphisms in *nalD* and *dsbS* in addition to the *opdP* deletion.

dsbS was recently described as a histidine-kinase sensor that acts together with the cognate response regulator *dsbR* in copper homeostasis (49). The copper-induced response has been previously shown to reduce the OprD expression through a regulation mediated by different two-component systems, such as *czcRS* and *copRS* (50, 51). It is reasonable to speculate that also this third copper regulation system might govern OprD expression. *nalD* is a transcriptional repressor of cellular efflux whose mutations have been correlated with MexAB-OprM overexpression (52); the upregulation of another efflux pump system, MexEF-OprN, mediated by the regulator *mexT* is known to decrease OprD expression (53). However, although many strains have been described to exhibit mutations in *nalD* causing MexAB-OprM overexpression, there is no evidence in the literature that these mutations could directly influence OprD.

The sequencing has therefore revealed that a single mutation can cause carbapenem resistance in TNP004, while *oprD* mutations for six of the seven mutants selected under meropenem pressure alter the correct OprD synthesis, giving rise to increased resistance

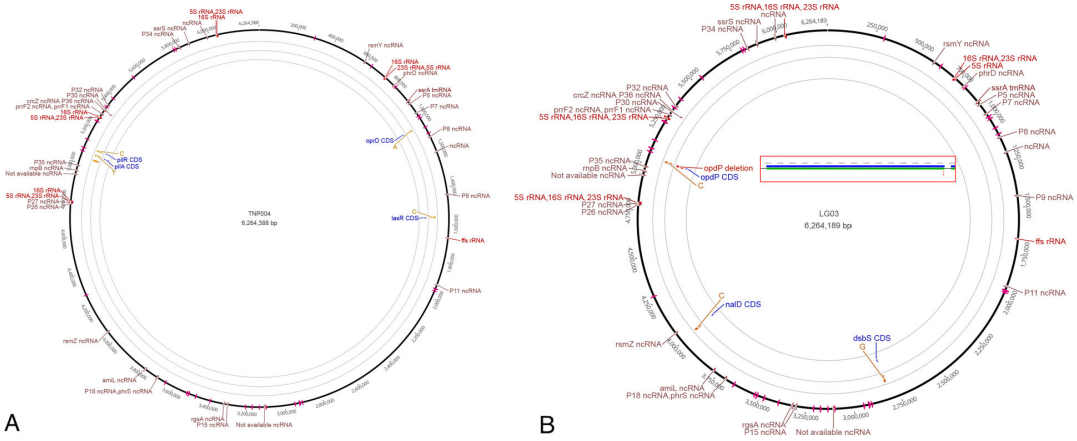

FIG 1 Circular visualization of the genome assembly obtained using the software Geneious (version R10). (A) The genome sequence of TNP004 was compared to that of its parental strain PAO1-Jap. The mutations between the genomes are shown. (B) Genome sequence of LG03 was compared with that of its parental strain ARC545. The opdP deletion is highlighted, and the other observed mutations are shown.

to carbapenems. Furthermore, the whole-genome sequencing has revealed the presence in LG03 of two mutations that contribute to carbapenem resistance, but their actual contribution requires further investigations.

Western blot

The expression of OprD in different mutant strains was verified by means of Western Blot (Fig. 2). As assumed, we confirmed the absence of the porin not only in the deleted mutants but also in the *oprD* mutant TNP004 and in the LG01, LG02, and LG04-LG07 strains, confirming the sequencing results. Interestingly, we could observe that LG03 was characterized by a downregulation of OprD, thus resulting in a consistent resistance profile to carbapenems.

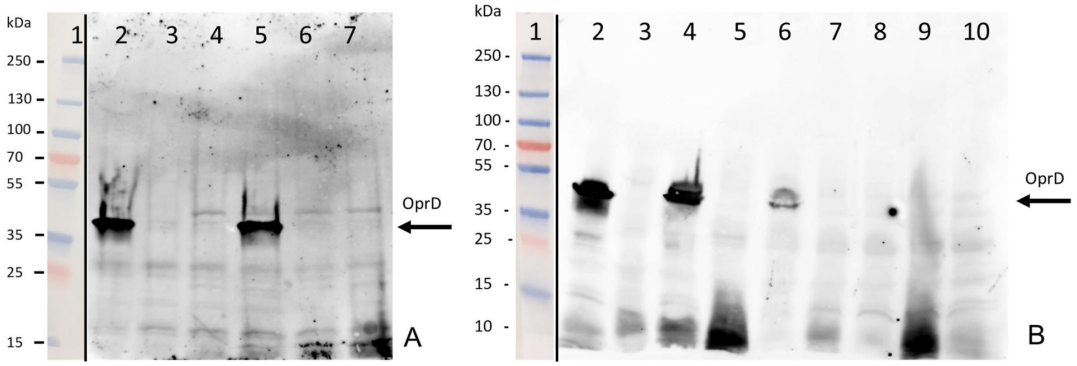

FIG 2 OprD detection performed by Western Blot in the following strains: (A). 1, protein marker; **2**,PAO1; 3,TNP004; **4**, ARC5990 (PAO1.ΔoprD); **5**, ARC5170 (PAO1ΔopdP); **6**, ARC5782 (PAO1ΔoprD, ΔopdP) and **7**, ARC5998 (PAO1ΔoprD, ΔopdP,ΔopaB, ΔopdC, and ΔopdT). (B). **1**, protein marker; **2**, PAO1; 3, LG01; **4**, ARC5170 (PAO1ΔopdP); **5**, LG02; **6**, LG03; **7**, LG04; **8**, LG05; **9**, LG06 and **10**, LG07. The porin OprD is marked by an arrow. Protein markers' pictures were put aside the chemiluminescence scans.

Growth curves

The planktonic growth in the LB medium of different porin mutants was compared to that of the wild-type PAO1 (Fig. 3). Remarkably, we did not observe an important delay in the growth of the different tested mutants compared to *P. aeruginosa* PAO1. Even ARC5998, with five different porins deleted, was able to grow in the LB medium at a rate similar to that of the PAO1 wild-type strain.

A possibly relevant difference is shown only in TNP004 where the cell density is slightly larger compared to the other strains. We could so assess that the lack of one or more porins does not influence bacterial growth, at least in the LB medium.

Permeability coefficient determination

A better understanding of the permeability of gram-negative bacteria, and in particular of *P. aeruginosa*, is an important factor for better directing the search for new antibiotics (54, 55).

While the role of the OprD porin in imipenem resistance is now widely understood (20, 56), the permeation of other antibiotics through the outer membrane remains difficult to interpret (15, 26, 57); indeed, antibiotic diffusion due to other porins does not seem to be sufficient to explain their uptake (32).

With this aim in mind, we adapted a previously described protocol (45) to quantify the β-lactam translocation into *P. aeruginosa* periplasm in order to determine the permeability coefficients of the outer membrane to different β-lactams. We performed validations to exclude major interfering events that could occur during measurements that include the following: i) the absence of MIC variation as a consequence of BlaR-CTD periplasmic production, ii) the verification of BlaR-CTD high affinity for the β-lactams tested, and iii) the absence of significant AmpC induction in the presence of β-lactams.

We transformed *P. aeruginosa* PAO1, ARC5990 (PAO1*ΔoprD*), ARC5170 (PAO1*ΔopdP*), ARC5782 (PAO1*ΔoprD*, *ΔopdP*), ARC5998 (PAO1 five porins mutant) with plasmid pKT240blaR, and TNP004 (PAO1 ↓OprD) with pKT240blaR-gen, a derived plasmid carrying gentamicin resistance, to produce BlaR-CTD in the periplasm of these strains.

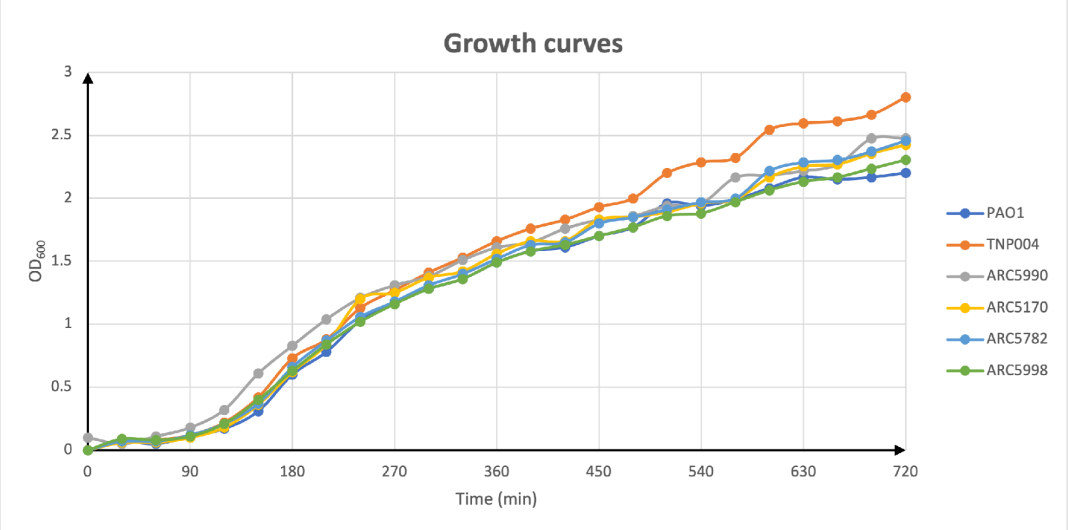

FIG 3 Growth curves of *P. aeruginosa* strains in LB cultures.

We compared the MIC profiles of the strains producing BlaR-CTD or not. We also transformed PAO1 with an empty vector (pKT240neg) as a control to compare the effects induced by the plasmid alone to those caused by BlaR-CTD expression.

As reported in Table 2, the presence of BlaR in the periplasmic space did not alter the MIC values of the host bacteria with the exception of three compounds, piperacillin, ceftazidime, and cefepime, that presented unexpected MIC increases ranging from twofold to fourfold dilutions when compared to the *blaR*-devoid strain.

This phenomenon could be explained by a lower affinity of these three antibiotics for natural PBPs compared to the other antibiotics tested. A similar conclusion was made by Montaner and coworkers studying the effect of AmpC hyperexpression (58). The periplasmic BlaR-CTD production, similarly to AmpC hydrolysis, might reduce the intracellular concentration of these three antibiotics to a limit level that would change the PBP occupancy causing increases in MICs, or, equivalently, might induce AmpC expression. However, whatever the exact cause, we excluded these antibiotics from our permeability study and preferred to concentrate on antibiotics whose MICs were not altered by BlaR-CTD expression.

We successively measured the acylation constants of BlaR-CTD with the different β-lactam antibiotics (Table 3). Our data confirmed that the formation of a stable acyl-enzyme was not a rate-limiting step in our experiments ($k_2/K' > 0.02\ \mu M^{-1}\ s^{-1}$).

We finally verified that the expression of the chromosome-encoded AmpC β-lactamase did not affect the detection of labeled BlaR-CTD. To do so, we determined the level of production of the AmpC β-lactamase in the different *P. aeruginosa* PAO1 cultures. The concentration of the antibiotic added to the culture was identical to its maximum concentration used during the permeability assay, and the incubation times for different β-lactams were equal to the maximum duration of the permeability measurements for the specific antibiotic. We, therefore, determined the AmpC concentration in the function of the incubation time (Table 4).

We showed that the specific activity of the chromosome-encoded AmpC remained similar to those obtained for the negative controls. Nevertheless, ertapenem showed a minor increase in the AmpC activity (fourfold compared to the negative control). The validity of the assay to detect increased expression of the β-lactamase was demonstrated by verifying the strong AmpC induction after a longer incubation (6 hours) in the presence of ampicillin and cefoxitin, known to be good AmpC inductors (59).

Antibiotic penetration was assessed in planktonic cultures grown in LB, and the assay was performed during the late exponential growth phase (A_{600} approximatively 1.6), thus excluding an increase in periplasmic BlaR-CTD due to bacterial duplication during the short duration of the analysis (maximum 40 minutes).

We first determined the permeability coefficients for different β-lactams in *P. aeruginosa* PAO1, and the results are reported in Table 5 (60–62). One can immediately notice the lower outer membrane permeability of *P. aeruginosa* when compared to that of *E. coli*.

We then selected a penicillin (ampicillin), a first-generation cephalosporin (cephaloridine) and five carbapenems (imipenem, meropenem, ertapenem, doripenem, and biapenem) and determined their permeability coefficients in different mutant strains (Table 6). As expected, decreased values for imipenem uptake were detected in all the strains where OprD was deleted or mutated. The OprD mutants exhibited a 130-fold reduction in the permeability coefficient when compared to PAO1. The values obtained for the TNP004 mutant are similar to those for ARC5990 (PAO1Δ*oprD*), confirming that the porin is not expressed in TNP004.

This result is in accordance with the specific role of OprD in imipenem uptake, due to the structural identity between the C2 side-chain of imipenem and that of arginine, the natural substrate of the porin. For the other tested carbapenems, the increase in MIC values does not clearly map into a marked permeability decrease since we only measured a twofold difference between the single OprD mutants and the wild-type.

TABLE 2 MIC values of the different *P. aeruginosa* strains producing or not BlaR-CTD[a,b]

Antibiotics (µg/mL)	*P. aeruginosa* MICs (µg/mL)														
	CLSI Standard	CLSI Susc.	PAO1	PAO1 pKT240neg	PAO1 pKT240blaR	TNP004	TNP004 pKT240blaR	ARC5990 (*Δoprd*)	ARC5990 pKT240blaR	ARC5170 (*Δopdp*)	ARC5170 pKT240blaR	ARC5782 (*Δoprd, ΔopdP*)	ARC5782 pKT240blaR	ARC5998 (Δ5porins)	ARC5998 pKT240blaR
Ampicillin	NA	NA	2,000	1,000	1,000	1,000	500	1,000	1,000	1,000	1,000	1,000	1,000	1,000	1,000
Benzylpenicillin	NA	NA	>2,000	>2,000	2,000	>2,000	>2,000	>2,000	>2,000	>2,000	>2,000	>2,000	>2,000	>2,000	>2,000
Piperacillin	1–8	≤16	2	1	4	2	4	2	**8**	2	**8**	2	**8**	2	**8**
Cefalotin	NA	NA	>2,000	>2,000	>2,000	>2,000	2,000	>2,000	>2,000	>2,000	>2,000	>2,000	>2,000	>2,000	>2,000
Cephaloridine	NA	NA	>2,000	>2,000	>2,000	>2,000	2,000	>2,000	>2,000	>2,000	>2,000	>2,000	>2,000	>2,000	>2,000
Cefoxitin	NA	NA	1,000	1,000	500	500	500	1,000	1,000	1,000	1,000	1,000	1,000	1,000	1,000
Cefuroxime	NA	NA	250	250	250	250	250	500	500	500	500	500	500	500	500
Cefotaxime	8–32	NA	16	16	16	8	16	16	16	16	16	16	16	16	16
Ceftazidime	1–4	≤8	1	1	**16**	2	**32**	1	**16**	1	**16**	1	**16**	1	**16**
Cefepime	0.5–4	≤8	1	1	**4**	1	**4**	1	**4**	1	**4**	1	**4**	1	**4**
Imipenem	1–4	≤2	1	1	1	8	8	8	8	1	1	8	8	8	8
Meropenem	0.12–1	≤2	0.5	0.5	0.5	2	2	4	4	0.5	0.5	4	4	4	4
Ertapenem	2–8	NA	8	8	8	32	32	32	32	8	8	32	32	32	32
Biapenem	0.5–2	NA	0.5	0.5	0.5	4	4	4	4	0.5	0.5	4	4	4	4
Doripenem	0.12–0.5	≤2	0.25	0.25	0.25	1	1	1	1	0.25	0.25	1	1	1	1
Tetracycline	8–32	≤4	8	>128	>128	8	>128	8	>128	8	>128	8	>128	8	>128
Gentamicin	0.5–2	≤4	1	1	2	2	16	2	2	2	2	2	2	2	2

[a]The values previously obtained for the non-transformed strains are reported. The CLSI standard refers to acceptable limits for quality control strains used to monitor the accuracy of MICs. CLSI susc. refers to the MIC susceptibility breakpoints interpreted by CLSI (46). NA: not available, ND not determined.
[b]The bold characters represent the names of the Pseudomonas strains utilized in this study.

TABLE 3 Acylation rate constant (K_2/K) for the different tested antibiotics

Antibiotic	k_2/K ($\mu M^{-1} \cdot s^{-1}$)	Reference
Nitrocefin	3.6 ± 0.3	This study
Benzylpenicillin	8.7 ± 1.1	(57)
Ampicillin	1.3 ± 0.1	(57)
Cephaloridine	5.9 ± 0.2	(57)
Cefoxitin	0.06 ± 0.02	(57)
Cefuroxime	0.02 ± 0.005	(57)
Cefotaxime	0.04 ± 0.003	(57)
Imipenem	0.8 ± 0.2	This study
Meropenem	0.8 ± 0.2	This study
Ertapenem	1.1 ± 0.2	This study
Biapenem	1.4 ± 0.3	This study
Doripenem	1.7 ± 0.3	This study

The permeability coefficients of ARC5170 (PAO1*ΔopdP*) were similar to those of the reference strain PAO1, suggesting that OpdP was not involved in antibiotic uptake.

Interestingly, a different result was noticed in the analysis of the mutant ARC5782, that lacks both OprD and OpdP. The imipenem permeability coefficient was similar to that of ARC5990 (PAO1*ΔoprD*), while, for meropenem and biapenem, the permeability coefficients were respectively tenfold and 30-fold lower than that of the wild-type PAO1.

These data underline a synergistic role of the OprD and OpdP porins in meropenem and biapenem uptake. An involvement of OpdP in meropenem permeation had already been suggested in the literature (24), but the diffusion of biapenem through this porin had never been described before.

We performed the same analysis on ARC5998 and obtained data similar to those observed with the double OprD and OpdP mutants, indicating that OpdB, OpdC, and OpdT are not primarily involved in the uptake of the tested antibiotics.

This approach allowed the evaluation of the specific permeability coefficients for various antibiotics in a series of *P. aeruginosa* strains (Table 6), which exhibit different levels of porin expressions.

TABLE 4 Periplasmic AmpC concentration and specific activity of the AmpC β-lactamase in the presence or absence (/) of β-lactams for the different *P. aeruginosa* cultures[a]

Incubation time (min)	Antibiotic (final concentration μM)	Periplasmic AmpC (mg/L)	Specific activity ($\mu mol \cdot min^{-1} \cdot mg^{-1}$)
12	Imipenem (0.02)	0.029	0.07
	Doripenem (1)	0.024	0.06
	Biapenem (0.04)	0.020	0.05
	/	0.026	0.06
20	Meropenem (2)	0.020	0.05
	/	0.042	0.10
30	Ampicillin (20)	0.026	0.05
	Benzylpenicillin (40)	0.027	0.08
	Cephaloridine (7.5)	0.024	0.08
	Ertapenem (7.5)	0.073	0.25
	/	0.029	0.06
40	Cefoxitin (30)	0.49	1.25
	Cefuroxime (60)	0.018	0.03
	Cefotaxime (60)	0.021	0.03
	/	0.017	0.03
360	Ampicillin (50)	22.6	1.43
	Cefoxitin (30)	90.4	5.76
	/	4.88	0.31

[a]The activity was followed by nitrocefin hydrolysis. (/) refers to a negative culture where no antibiotic was added.

TABLE 5 Permeability coefficients determined in *P. aeruginosa* PAO1 for a set of different β-lactams, belonging to penicillin, cephalosporin (1st, 2nd, and 3rd generation), and carbapenem families[a]

Permeability coefficients (nm/sec)		
Antibiotic	***P. aeruginosa* PAO1**	***E. coli***
Ampicillin	0.008 ± 0.004	28 (70)
Benzylpenicillin	0.006 ± 0.002	
Cephaloridine	0.03 ± 0.01	
Cefoxitin	0.002 ± 0.0006	
Cefuroxime	0.001 ± 0.0004	
Cefotaxime	0.001 ± 0.0005	180 (72)
Imipenem	20 ± 9	1800 (71)
Meropenem	0.06 ± 0.01	300 (71)
Ertapenem	0.06 ± 0.02	
Doripenem	0.56 ± 0.38	
Biapenem	4.7 ± 1.4	

[a]Values reported in the literature for *E. coli* are shown for comparison.

We also highlighted the presence of compensatory effects in the permeation of antibiotics, in particular, the contribution of both OprD and OpdP porins in the internalization of meropenem and biapenem. Deleting each of these porins individually does not alter the entry rate of these antibiotics in the respective mutants, while in the mutant deprived of both porins, a marked decrease in permeability for both antibiotics is observed (tenfold and 30-fold, respectively). This outcome could not have been inferred from the MIC values, which are in fact identical in all mutants for the antibiotics mentioned above (Table 1).

The method described here can, in principle, be extended to other antibiotics and also to other gram-negative pathogens of clinical interest, representing a useful tool to study porin's functionality.

qRT-PCR

The relative expression of *oprD*, together with four other porins (*opdP*, *opdB*, *opdC*, and *opdT*) at four different time points of cellular growth was quantified by qRT-PCR. Total mRNAs were so extracted at OD_{600} of 0.6, 1.2, 1.6, and 2.0, corresponding, respectively, to the early, mid and late exponential, and early stationary phase.

PA3340, *gyrA*, and *cysG* genes, due to their relative stable expressions, were chosen as reference genes, and the exact protocol that results in their selection is reported in the Supplementary Material.

The relative *oprD* expression in *P. aeruginosa* PAO1, TNP004, and ARC5170 (PAO1*ΔopdP*) is reported in Fig. 4A. We confirmed that, as previously assumed, the expression of *oprD* mRNA is inversely proportional to cell density (53); as a consequence, the decreased expression of *oprD* observed at OD_{600} 1.6, compared to the early

TABLE 6 Permeability coefficients for different β-lactams determined for *P. aeruginosa* PAO1 and other porin(s) or efflux pump mutants[a]

Permeability coefficients (nm/sec)						
Antibiotic	**PAO1**	**TNP004**	**ARC5990**	**ARC5170**	**ARC5782**	**ARC5998**
Relevant characteristics		**↓OprD**	***ΔoprD***	***ΔopdP***	***ΔoprD, ΔopdP***	***ΔoprD, ΔopdP, ΔopdB, ΔopdC,* and *ΔopdT***
Ampicillin	0.008 ± 0.005	0.008 ± 0.003	0.02 ± 0.01	0.01 ± 0.002	0.01 ± 0.002	0.02 ± 0.005
Cephaloridine	0.03 ± 0.02	0.02 ± 0.004	ND	0.03 ± 0.01	0.03 ± 0.01	0.04 ± 0.01
Imipenem	20 ± 9	0.13 ± 0.07	0.14 ± 0.07	15 ± 5.8	0.13 ± 0.05	0.12 ± 0.06
Meropenem	0.06 ± 0.01	0.03 ± 0.02	0.03 ± 0.01	0.1 ± 0.05	0.006 ± 0.002	0.01 ± 0.005
Ertapenem	0.06 ± 0.02	0.03 ± 0.01	0.04 ± 0.02	0.02 ± 0.01	0.02 ± 0.01	0.02 ± 0.01
Doripenem	0.51 ± 0.35	0.16 ± 0.06	0.07 ± 0.03	0.11 ± 0.02	0.14 ± 0.11	0.11 ± 0.05
Biapenem	4.7 ± 1.4	3.4 ± 1.9	4.2 ± 2.7	7.2 ± 2.9	0.21 ± 0.13	0.12 ± 0.03

[a]ND refers to a coefficient not determined.

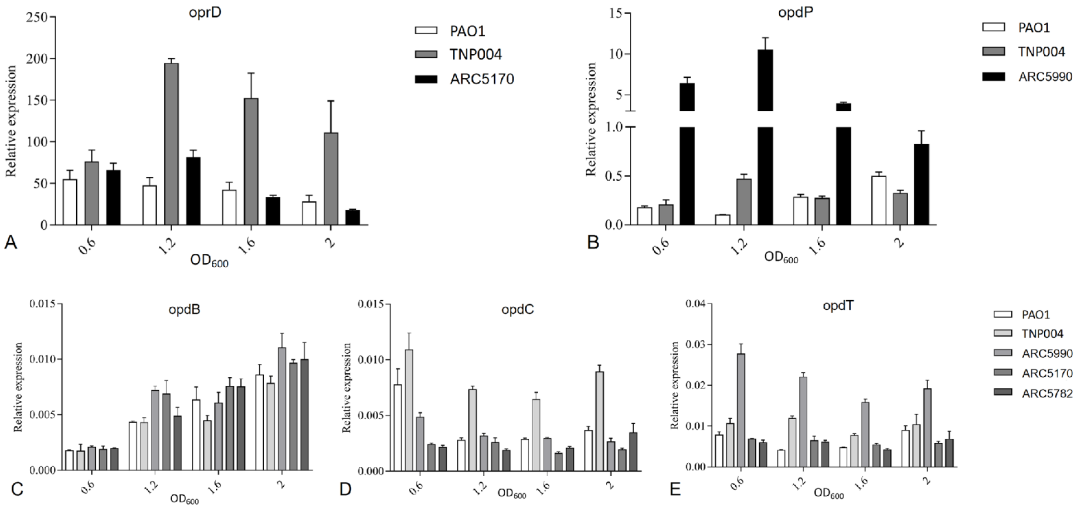

FIG 4 Relative expressions of (A) oprD, (B) opdP, (C) opdB, (D) opdC, and (E) opdT mRNAs in *P. aeruginosa* PAOI and four porin(s) mutant strains; mRNAs were extracted at four different points of bacterial growth, reported in the x-axis as the absorbance at 600 nm, and the relative expression reported on the y-axis is the mean of the transcription of three indipendent reference genes (PA3340, gyrA, and cysG). Data were analyzed by two-way analysis of variance (ANOVA), followed by Bonferroni multiple comparison *post-test*.

exponential phase (OD_{600} 0.6), might explain the differences found between carbapenem MICs and the permeability coefficients obtained in this study.

During our permeability measurements performed during the late exponential growth phase, as a consequence of the low physiological expression of OprD, the deletion of this porin does not produce a strong decrease in permeability for carbapenems, except for imipenem. In contrast, the MICs, whose determination involves the passage through the exponential phase in the overnight culture, show the effect of OprD's higher expression in the early growth phase.

Interestingly, in TNP004, *oprD* mRNA appeared to be upregulated, but this did not reflect in the insertion of a functional porin in the outer membrane, as demonstrated by Western blot analysis. The bacteria are, therefore, able to respond to the lack of the functional porin by overexpressing *oprD* mRNA transcription, suggesting that the expression of this porin is controlled by a precise regulatory mechanism.

We performed the same screening on *opdP* mRNA in *P. aeruginosa* PAO1, TNP004, and ARC5990 (PAO1*ΔoprD*), and the results are shown in Fig. 4B.

In *P. aeruginosa* PAO1 the expression of OpdP does not seem to be regulated by cell density, but, in contrast to OprD, its expression is slightly increased during the early stationary phase. Moreover, its expression is increased 20-fold when *oprD* mRNA is not expressed as in the case of ARC5990 (PAO1*ΔoprD*). In TNP004, in fact, the relative *opdP* expression remains similar to that in PAO1, probably due to the simultaneous over-transcription of *oprD* mRNA. This finding highlights how the absence of a porin can be compensated for, but it does not fully elucidate the mechanism that prevails in the TNP004 strain.

It is important to notice that the relative mRNA expression of *opdP* in ARC5990 (PAO1*ΔoprD*) is ten times less than that of *oprD* in ARC5170 (PAO1*ΔopdP*); nevertheless, the permeability coefficients for all carbapenems, except for imipenem, are similar in the two considered strains.

However, OpdP has been described to exhibit a 30-fold higher conductance than OprD (30), and this can explain how a lower expression of this porin allows the uptake of all carbapenems at the same rate, with the exception of imipenem.

We finally quantified the relative mRNA expression of the *oprB, oprC,* and *oprT* porin genes, previously chosen for their high relative expression in minimal medium (24), in *P. aeruginosa* PAO1, TNP004, ARC5990 (PAO1*ΔoprD*), ARC5170 (PAO1*ΔopdP*), and ARC5782 (PAO1*ΔoprD, ΔopdP*).

The results for these porins are reported in Fig. 4C through E, respectively, and show that all three porins have a basal expression level, while only that of *opdB* mRNA seems to be directly proportional to cell density. However, their low expression does not seem to be crucial for antibiotic uptake, as shown by the MICs and the permeability coefficient determinations.

We also quantified the relative expression of *oprD* mRNA in two strains selected during the multistep resistance experiment. We chose LG01, derived from *P. aeruginosa* PAO1, carrying a mutated *oprD* sequence, and LG03, derived from ARC5170 (PAO1*ΔopdP*) that possesses an intact *oprD,* and we compared the relative expression of the porin at A_{600} = 1.6, using the reference genes mentioned above.

The results reported in Fig. 5 show an increased expression of *oprD* mRNA, similarly to TNP004, in LG01 when compared to the wild-type, most likely due to the synthesis of a mutated unstable porin.

Interestingly, *oprD* mRNA expression in LG03 appears to be tenfold downregulated compared to PAO1, probably as a consequence of the already mentioned mutations found in the *nalD* or *dsbS* genes.

Thus, the so far undocumented mechanism results in a downregulation of the porin (verified by qRT-PCR and Western blot), which causes carbapenem resistance highlighted by the MIC values.

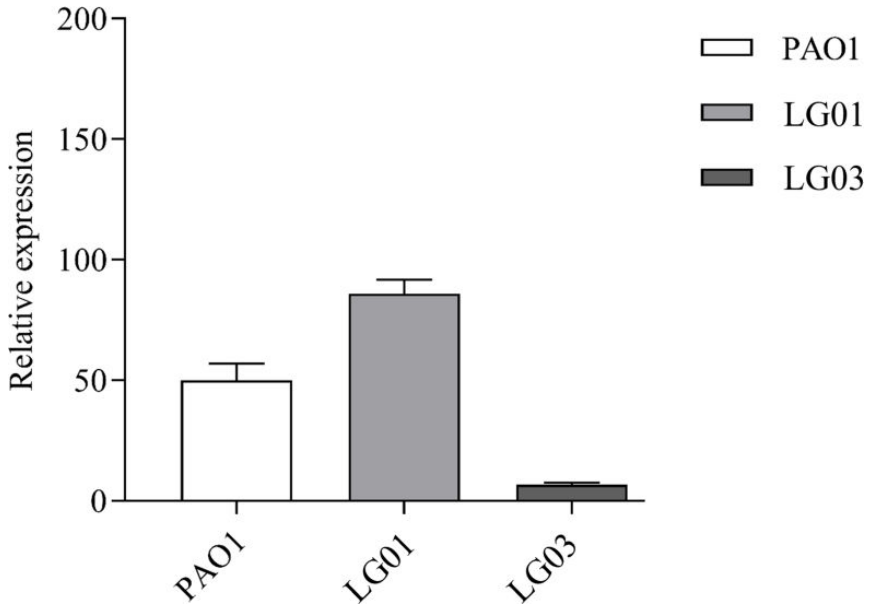

FIG 5 Relative expression of oprD mRNA in *P. aeruginosa* PAOI, LG01, and LG03; mRNAS were extracted at A600 = 1.6, and the relative expression reported on the y axis is the mean of the transcriptions of three indipendent reference genes (PA3340, gyrA, and cysG) mentioned above. Data were analyzed by two-way analysis of variance (ANOVA), followed by Bonferroni multiple comparison *post-test*.

These experiments shed further light on OpdP, demonstrating that this porin is less expressed during the exponential growth phase, while its production increases when the bacterial culture enters the latent phase. This phenomenon turns out to be of particular importance during the permeability determinations, which were performed with cultures in the late exponential growth phase, but also during an *in vivo* infection. Conversely, the production of OprD follows an inverse pathway (Fig. 5A and B), and this mechanism contributes to explain why the MIC values appear to be mostly influenced by OprD. The determination of the MICs necessarily requires an exponential growth phase and, therefore, more affected by the presence/absence of the OprD porin in *P. aeruginosa*.

Besides this experimental evidence, it is, therefore, important to highlight how the simultaneous absence of OprD and OpdP porins might determine the poor efficacy of meropenem and biapenem during an antibiotic therapy, while the single deletion of OpdP can favor the appearance of a carbapenem resistance phenotype after exposure to meropenem in a concentration close to the MIC value.

Therefore, the presence of mutations/deletions of the OpdP porin should receive greater consideration from a clinical point of view, and further studies on the expression of this porin in clinical strains could lead to a better understanding of the resistance mechanisms mediated by this porin.

MATERIALS AND METHODS

Bacterial strains, growth conditions, plasmids, and antibiotics

Antibiotics were purchased from Sigma-Aldrich and nitrocefin from Oxoid Ltd. (Basingstoke, UK).

Biapenem was kindly provided by Dr. O. Lomovskaya from The Medicines Company (San Diego, CA, USA).

Bacterial strains are listed in Table 7, and the porin(s) deletion assessment is reported in supplemental data. Plasmids are reported in Table S1. Bacteria were grown aerobically at 37°C in LB, purchased from Sigma-Aldrich.

To perform planktonic cultures, a single colony was inoculated into liquid medium and incubated overnight (14–16 hours). Cultures were then diluted 1:20 into fresh media, and bacterial growth was monitored by following the absorbance at 600 nm using an Ultrospec 10 spectrophotometer (BioChrom, St Albans, UK).

TABLE 7 Collection of *P. aeruginosa* strains used in the study[a]

P. aeruginosa	Relevant characteristics	Reference
PAO1	Wild-type	BCCM
PAO1-Jap	Presumptive TNP004 parental strain	(47)
TNP004	↓OprD	(47)
ARC545	ARC presumptive parental strain	(24)
ARC5990	*ΔoprD*	(24)
ARC5170	*ΔopdP*	(24)
ARC5782	*ΔoprD*, *ΔopdP*	(24)
ARC5998	*ΔoprD*, *ΔopdC*, *ΔopdP*, *ΔopdT*, and *ΔopdB*	(24)
LG01	*oprD* mutant, derived from PAO1	This study
LG02	*oprD* mutant, derived from ARC5170	This study
LG03	*oprD* mutant, derived from ARC5170	This study
LG04	*oprD* mutant, derived from ARC5170	This study
LG05	*oprD* mutant, derived from ARC5170	This study
LG06	*oprD* mutant, derived from ARC5170	This study
LG07	*oprD* mutant, derived from ARC5170	This study

[a]↓OprD indicates a downregulated expression of OprD.

The pKT240blaR shuttle vector (45) includes the *B. licheniformis blaR-CTD* gene under the control of the *lpp-lac* fusion promoter. The pKT240neg vector was derived from pKT240blaR where *blaR-CTD* was excised. Finally, pKT240blaR-gen was obtained by the addition of the *aac1* gene, in order to confer resistance to gentamicin. Both latter constructs were produced using the Gibson assembly technology (63), by amplifying fragments of the pKT240blaR plasmid and the *aac1* gene in the case of pKT240blaR-gen. Primers are listed in Table S2. The different plasmids were transformed in *E. coli* DH5α-Proteobacterium *Pseudomonas aeruginosa*. They were purified using the NucleoBond Xtra Maxi kit (Macharey-Nagel, Bethlehem, PA) and used to transform *P. aeruginosa* strains by electroporation using the Gene Pulser Xcell Electroporation System (Bio-Rad, Hercules, CA, USA), in an ice-cold 0.2 cm cuvette with the following parameters: 200 Ω, 25 µF, and 2.5 kV.

We further selected new *P. aeruginosa* mutant strains where the permeability of the outer membrane is affected. Those strains were obtained with the help of a multistep resistance experiment. Briefly, *P. aeruginosa* PAO1 and *P. aeruginosa* ARC5170 (PAO1*ΔopdP*), grown in liquid LB medium, were harvested in the mid- and late-exponential growth phase (A_{600} ~1.2 and 1.6) and streaked (10^9 CFU) onto Petri plates containing two different meropenem concentrations (1 and 2 µg/mL), higher than the MICs determined for both parental strains (0.5 µg/mL). The plates were incubated for 16 hours at 37°C. Seven colonies (*P. aeruginosa* LG01, derived from *P. aeruginosa* PAO1, and *P. aeruginosa* LG02-LG07 derived from *P. aeruginosa* ARC5170) were then randomly selected for further characterizations.

Susceptibility testing

Antimicrobial susceptibility was evaluated by broth microdilutions in cation-adjusted Mueller–Hinton broth (MHBII), purchased from Sigma-Aldrich, according to the Clinical and Laboratory Standards Institute guidelines (46). *P. aeruginosa* ATCC 27853 was used as a control strain, and data were collected in triplicate independent experiences.

PCR amplification, DNA sequencing, and whole-genome sequencing (wgs)

PCR screenings on different targets were performed on crude extracts using OneTaq polymerase (New England Biolabs, Ipswich, MA, USA), while Q5 High-Fidelity enzyme (New England Biolabs) was used in case of a successive Sanger sequencing analysis.

The *oprD* sequence was determined by Sanger sequencing of PCR products, obtained using the pair of primers oprD_flankF and oprD_flankR (Table S2).

The nucleotide and protein sequences were analyzed using the blastn and blastp algorithms, available on the National Center of Biotechnology Information website (http://www.ncbi.nlm.nih.gov), and the alignments of the translated amino acid sequences of OprD were performed using the software Alignx (InforMax, Bethesda, MD, USA).

To perform whole-genome sequencing, genomic DNA was extracted using the NucleoSpin DNA Plus kit (Macherey-Nagel). Samples were then processed on a NovaSeq (Illumina, Inc., San Diego, CA, USA) sequencer, generating paired-end reads (2 × 150); raw reads were corrected by a homemade workflow, performing various steps of analysis, using software included in the BBTools package (64); briefly, reads were overlapped with BBMerge and subsequently quality-trimmed, and any remaining adapters were removed by the BBduk function. Tadpole and BBMap were in sequence used to perform a quick assembly, and BBduk was used for quality calibration; finally, BBNorm was used to normalize the coverage, and Tadpole was used for a final process of error-correction.

The sequence mapping was carried out with the Geneious (v10.2.6) software (65). Genome assembly was achieved by mapping single verified reads to a reference *P. aeruginosa* genome sequence (strain PAO1, GenBank accession number AE004091), and the resulting variations have been applied to the reference to generate the strain sequences.

Both Sanger and whole-genome sequencing were carried out at the GIGA-Genomics platform (GIGA-Genomics, Liège, Belgium).

RNA extraction, cDNA synthesis, and quantitative qRT-PCR

Quantitative real-time PCR (qRT-PCR) was used to compare the expressions of porins genes, at four different moments of cellular growth (A_{600} = 0.6, 1.2, 1.6, and 2.0).

Total RNA isolation of the different aliquots was performed using the NucleoSpin RNA Plus kit (Macherey-Nagel), and rDNase (Macherey-Nagel) digestion was subsequently performed to eliminate any DNA trace. The samples were finally purified using the NucleoSpin RNA Clean-up XS kit (Macherey-Nagel) according to the manufacturer's recommendations.

RNA quantification was performed by measuring the absorbance at 260 nm with the help of a NanoVue spectrophotometer (GE Healthcare, Little Chalfont, UK). Then, 1 µg of RNA was retrotranscribed using the SuperScript III reverse transcriptase (Invitrogen, Waltham, MA, USA), triggered by random hexamers and supplemented with 0.4 U/µL of Ribosafe RNase Inhibitor (Bioline, USA). The reaction was carried out at 25°C for 5 minutes, 50°C for 60 minutes, and stopped by heating to 70°C for 15 minutes. The newly synthesized cDNA was diluted to 1:50 in RNase/DNase-free water and used as a target for qRT-PCR.

Amplifications were performed in 384-well plates with a QuantStudio 5 Real-Time PCR system (Thermo Fisher Scientific, Waltham, MA, USA) using Takyon Low Rox SYBR MasterMix Eurogentec (Seraing, Belgium); the list of primers used is reported in Table S3.

A control reaction was performed for each sample by using the original RNA mixture to verify the absence of residual DNA. Experiments were reproduced in four biological replicates and three technical replicates for each target gene.

The quality of the quantitative PCR was checked by the analysis of dissociation and amplification curves. For each primer pair, the mean reaction efficiencies were calculated using the LinRegPCR software (66) (Table S3). Those values were used to quantify relative gene expression levels by normalization using three reference genes (*PA3340*, *gyrA,* and *cysG*) with the qBase software (Biogazelle) (67). The reference genes were chosen because they were similarly expressed in the various growth phases. The adequacy of the reference genes to normalize gene expression in the experimental conditions was checked using the geNorm module in qBase (68).

BlaR-CTD affinity

BlaR-CTD is the soluble C-terminal domain of the BlaR transmembrane protein that displays a high affinity for β-lactams characterized by the acylation constant (k_2/K′), the second-order rate constant for the formation of the acyl-enzyme adduct characterizing the acylation step efficiency. This rate constant can be determined by incubating a known concentration of the antibiotic, whose k_2/K′ is to be measured, together with a known concentration of a reporter antibiotic (r), whose kinetic parameters are known. The proportion of each acyl-enzyme formed at saturation depends on the concentration and k_2/K′ value of each antibiotic (equation 1) (69). Our reporter molecule was nitrocefin ($\Delta\varepsilon^{482}$ = 15,000 M^{-1} cm^{-1}).

The assay can be described as follows:

$$\frac{[\mathrm{EC}^*]\mathrm{r}}{[\mathrm{EC}^*]} = \frac{\left(\frac{k_2}{K'}\right)\mathrm{r} * [C]\mathrm{r}}{\left(\frac{k_2}{K'}\right) * [C]} \text{ and } [\mathrm{EC}^*]\mathrm{r} + [\mathrm{EC}^*] = [\mathrm{E}_0] \quad , \qquad (1)$$
$$\frac{[EC]_r}{[E_0] - [EC]_r} = \frac{(k_2/K')_r[C]_r}{(k_2/K')[C]}$$

where [EC*]r and [EC*] are the concentrations of BlaR-nitrocefin and BlaR-antibiotic acyl-enzymes, respectively. [C]r and [C] correspond to the concentrations of nitrocefin

and of the tested antibiotic, respectively. (k_2/K')r and (k_2/K') represent the acylation rate constants of BlaR-CTD for the nitrocefin and the tested antibiotic.

We first determined the acylation rate constant of BlaR-CTD for nitrocefin. Purified BlaR-CTD was previously purified at the CIP (70). BlaR-CTD (20 µM), was added to a solution of nitrocefin (80 µM) containing increasing concentrations (25–600 µM) of ampicillin, whose k_2/K' is known (1.3 10^6 $M^{-1}\cdot s^{-1}$) (70). The variation of A_{482} is directly proportional to the concentration of the BlaR-CTD-nitrocefin adduct. The k_2/K' for nitrocefin was then calculated (3.6 10^6 $M^{-1}\cdot s^{-1}$) and used as a competitor to determine the other affinity values. The acylation rate constants were so determined for cefalotin, ceftazidime, imipenem, meropenem, ertapenem, biapenem, and doripenem.

β-Lactamase assays

The production of the class C AmpC β-lactamases was measured in crude cell extracts from the different *P. aeruginosa* PAO1 cultures as follows. The growth of the bacteria in LB at 37°C was monitored by measuring A_{600}. At a value of 1.6, the culture was divided into two 10 mL aliquots. One aliquot was used as a control. Antibiotic was added to the second aliquot at a final concentration equal to the maximum concentration of the antibiotic tested in the permeability assay (Table 8). The cultures were then incubated for a time corresponding to the incubation time with the selected antibiotic in the permeability test. One mL of each culture was then centrifuged at 13,000 *g* for 10 minutes. The pellet was washed twice and resuspended in 1 mL of 10 mM PBS buffer pH 7.4. Cells were lysed by sonication with the Bioruptor Plus Diagenode (Seraing, Belgium). The cellular extract was clarified by centrifugation at 13,000 *g* for 30 minutes at 4°C.

Positive controls for AmpC induction in *P. aeruginosa* PAO1 were analysed as previously described and incubated for six hours in presence of 50 µM ampicillin and 50 µM cefoxitin. The negative controls were made by the culture without antibiotic, grown for the different tested incubation times.

The protein concentration in each extract was measured with the help of a BCA protein assay kit (Pierce, Rockford, IL). The β-lactamase activity of the extract was determined by measuring the initial rate of hydrolysis of 100 µM nitrocefin. All the enzymatic assays were performed in 10 mM PBS buffer pH 7.4 at 30°C. The specific activity of the different samples was the rate of hydrolysis of each substrate expressed in nmoles per minute per milligram of protein.

TABLE 8 Different antibiotics concentrations tested during permeability experiments

Antibiotics	Concentrations tested (µM)		
Benzylpenicillin	40	20	10
Cefoxitin	30	15	7.5
Cefuroxime	60	30	15
Cefotaxime	60	30	15
Ampicillin	20	10	5
Cephaloridine	8	4	2
Imipenem	0.02	0.01	0.005
Imipenem[a]	4	2	1
Meropenem	8	4	2
Meropenem[b]	20	10	5
Ertapenem	7.5	5	2.5
Doripenem	4	2	1
Biapenem	0.04	0.02	0.01
Biapenem[b]	4	2	1

[a]* refers to tests performed on strains lacking the OprD porin.
[b]while ^ refers to tests performed on strains deprived of both OprD and OpdP porins.

Permeability determination

The antibiotic flux passing through the outer membrane can be described by the Flick's first law of flux (2).

$$\mathrm{J} = -\mathrm{D} \cdot \mathrm{A} \cdot \frac{\Delta C}{\Delta x}, \tag{2}$$

where J is the flux of the antibiotic through the outer membrane OM, D the diffusion coefficient of the antibiotic, A the OM area (assumed as 132 cm^2), ΔC the concentration gradient of the antibiotic, and Δx the OM thickness.

β-lactam flux in *P. aeruginosa* can be characterized by the permeability coefficient P (3), that is defined as the ratio between the diffusion coefficient and the OM thickness. It can be defined as:

$$\mathrm{P} = -\frac{\mathrm{D}}{\Delta x}. \tag{3}$$

The antibiotic flux is defined by equation 4:

$$\mathrm{J} = \mathrm{P} \cdot \mathrm{A} \cdot \Delta \mathrm{C}. \tag{4}$$

The estimation of the antibiotic flux can be achieved by expressing the high affinity BlaR-CTD in the bacterial periplasm, allowing the direct quantification of the β-lactam concentration present in the periplasmic space, and consequently to measure the permeability coefficient (5)

$$P = \frac{d(EC^*)/dt}{A \cdot [C_e]} \tag{5}$$

where EC* is the concentration of the BlaR-CTD-β-lactam adduct and $[C_e]$ the external β-lactam concentration.

d(EC*)/dt is equal to the slope of the line reflecting the increase of the acyl-enzyme concentration *vs* the incubation time (Fig. 6B).

Antibiotic diffusion in the periplasmic space was analyzed in planktonic cultures. The different *P. aeruginosa* strains, previously transformed with pKT240blaR (or pKT40blaR-gen in the case of TNP004), were grown in LB medium added with selection antibiotic (50 µg/mL tetracycline or 10 µg/mL gentamicin, respectively). When the culture reached the late exponential phase (A_{600} ≃ 1.6) a prefixed β-lactam concentration was added to the medium and aliquots (1 mL) were harvested at different incubation times. Two microliters of the metallo-β-lactamase VIM-2 (1 mg/mL) was added to the bacterial culture to hydrolyze all the antibiotics present outside the cells and consequently interrupt its permeation in an active form. EDTA (1 mM) was then added in order to chelate the metal ions and inactivate the metallo-β-lactamase. The crude extract was obtained by means of ten cycles of refrigerated sonication at 4°C, performed with the Bioruptor Plus Diagenode. The quantification of BlaR-CTD acylated by the tested antibiotic was performed by adding 2.5 µM Bocillin FL (Invitrogen), a fluorescent derivative of penicillin V, to the crude extracts. The proteins of the different cell extracts were separated by SDS-PAGE, and the fluorescence intensity of BlaR-CTD recorded using a Typhoon Trio +imager and Image Quant TL software (GE Healthcare) (Fig. 6A). The quantification of the BlaR-CTD-Bocillin adduct *vs* the incubation time in presence of an unlabeled β-lactam allowed the determination of the quantity of BlaR-CTD acylated with the unlabelled compound. Analyses were performed in duplicate at three different antibiotic concentrations as reported in Table 8.

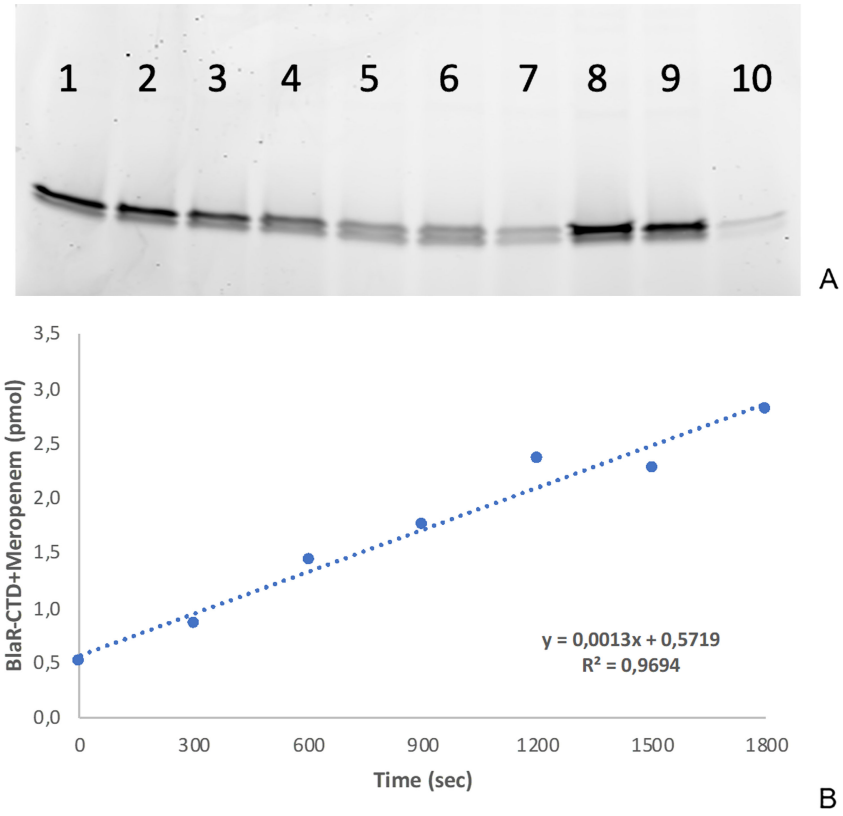

FIG 6 (A) Densitometric analysis of the fluorescence signal of the BlaR-CTD-Bocillin adduct, shown as an example; samples from 1 to 7 represent different aliquots, taken every 5 minutes for determining meropenem uptake in ARC5782 (PAO1ΔoprD, ΔopdP); samples 8 and 9 are aliquots taken before the addition of meropenem to the culture, representing the total quantity of produced BlaR-CTD; sample 10 is a not sonicated aliquot, used to quantify possible BlaR-CTD release in the medium. (B) Graph representing the increase of the meropenem-BlaR-CTD adduct as a function of time; this quantification was made possible by subtracting the values obtained during the experiment (samples 1-7 of panel A) from the total BlaR-CTD produced in an aliquot (samples 8 or 9 of panel A). The slope of the line represents the antibiotic flux passing through the outer membran.

Protein extraction, SDS, and Western Blot

The outer membrane profiling was performed on LB cultures as previously described (71).

SDS-PAGE was carried out according to the Laemmli protocol, using 4%–20% Mini-Protean (Bio-Rad) gels and Coomassie blue staining.

For Western blot analysis, proteins were electroblotted onto a PVDF membrane, using a commercial kit (Bio-Rad), and the protein marker V (pre-stained) VWR (Radnor, PA, USA) was used.

The membranes were then incubated with 1:2,000 rabbit-derived anti-OprD polyclonal antibody (72), kindly provided us by Dr Thilo Köhler (University of Geneva, Switzerland) and finally with the secondary antibody 1:5,000 goat anti-rabbit HRP antibody (Bio-Rad).

For the revelation, Clarity Western ECL substrate kit (Bio-Rad) was added, and signals were detected using an ImageQuant LAS 4000 camera (GE Healthcare).

ACKNOWLEDGMENTS

We thank Prof. H. Yoneyama and Dr. A. Miller for the kind gifts of *P. aeruginosa* porin mutant strains.

We thank Dr O. Lomovskaya for the kind gift of biapenem.

Amisano F. was supported by the Excellence grants in WBI (Grant ID 2015/242329, Wallonie Bruxelles International) and the work was supported by Fund for Scientific Research (FRS-FNRS) Belgium.

AUTHOR AFFILIATIONS

[1]InBioS, Center for Protein Engineering, Biological Macromolecules, Department of Life Sciences, University of Liège, Liège, Belgium
[2]InBioS - PhytoSystems, Functional Genomics and Plant Molecular Imaging and Centre for Assistance in Technology of Microscopy (CAREm), University of Liège, Liège, Belgium
[3]InBioS-PhytoSystems, Translational Plant Biology, University of Liège, Liège, Belgium

AUTHOR ORCIDs

Francesco Amisano http://orcid.org/0000-0003-0822-4909
Moreno Galleni http://orcid.org/0000-0003-0992-0391

FUNDING

Funder	Grant(s)	Author(s)
Wallonie Bruxelles International - WBI	2015/242329	Francesco Amisano
Fonds De La Recherche Scientifique - FNRS (FNRS)	J0081.20	Moreno Galleni

AUTHOR CONTRIBUTIONS

Francesco Amisano, Data curation, Investigation, Methodology, Validation, Visualization, Writing – original draft | Paola Mercuri, Conceptualization, Formal analysis, Methodology, Project administration, Resources, Supervision, Validation, Visualization, Writing – original draft, Writing – review and editing | Steven Fanara, Conceptualization, Formal analysis, Investigation, Methodology, Writing – review and editing | Olivier Verlaine, Conceptualization, Data curation, Methodology, Software, Supervision, Validation, Writing – review and editing | Patrick Motte, Resources, Writing – review and editing | Jean Marie Frère, Conceptualization, Supervision, Writing – original draft, Writing – review and editing | Marc Hanikenne, Methodology, Supervision, Writing – original draft, Writing – review and editing | Moreno Galleni, Conceptualization, Data curation, Funding acquisition, Investigation, Methodology, Project administration, Resources, Supervision, Validation, Writing – original draft, Writing – review and editing

DATA AVAILABILITY

The assembled genomic sequences of P. aeruginosa isolates were deposited under the Bioproject number PRJNA985251 in the NCBI database (https://www.ncbi.nlm.nih.gov/bioproject/)
Sanger sequencing data have been deposited on Genbank, under the accession numbers OR069747, OR069748, OR069749 and OR069750.

ADDITIONAL FILES

The following material is available online.

Supplemental Material

Fig. S1 (Spectrum00495-24-s0001.tiff). Supplemental figure 1.

Fig. S2 (Spectrum00495-24-s0002.tiff). Supplemental figure 2.
Fig. S3 (Spectrum00495-24-s0003.tiff). Supplemental figure 3.
Supplemental material (Spectrum00495-24-s0004.docx). Porin(s) deletion assessment; RT-PCR reference genes.
Table S1 (Spectrum00495-24-s0005.docx). Collection of plasmids used in this study.
Table S2 (Spectrum00495-24-s0006.docx). Collection of primers used in this study for PCR amplification and sequencing.
Table S3 (Spectrum00495-24-s0007.docx). Sequences and reaction efficiencies of quantitative RT-PCR primer pairs.

Open Peer Review

PEER REVIEW HISTORY (review-history.pdf). An accounting of the reviewer comments and feedback.

REFERENCES

1. Weber DJ, Rutala WA, Sickbert-Bennett EE, Samsa GP, Brown V, Niederman MS. 2007. Microbiology of ventilator-associated pneumonia compared with that of hospital-acquired pneumonia. Infect Control Hosp Epidemiol 28:825–831. https://doi.org/10.1086/518460
2. Lamas Ferreiro JL, Álvarez Otero J, González González L, Novoa Lamazares L, Arca Blanco A, Bermúdez Sanjurjo JR, Rodríguez Conde I, Fernández Soneira M, de la Fuente Aguado J. 2017. *Pseudomonas aeruginosa* urinary tract infections in hospitalized patients: mortality and prognostic factors. PLoS One 12:e0178178. https://doi.org/10.1371/journal.pone.0178178
3. Jurado-Martín I, Sainz-Mejías M, McClean S. 2021. *Pseudomonas aeruginosa*: an audacious pathogen with an adaptable Arsenal of virulence factors. Int J Mol Sci 22:3128. https://doi.org/10.3390/ijms22063128
4. Staudinger BJ, Muller JF, Halldórsson S, Boles B, Angermeyer A, Nguyen D, Rosen H, Baldursson O, Gottfreðsson M, Guðmundsson GH, Singh PK. 2014. Conditions associated with the cystic fibrosis defect promote chronic *Pseudomonas aeruginosa* infection. Am J Respir Crit Care Med 189:812–824. https://doi.org/10.1164/rccm.201312-2142OC
5. Angrill N, Gallego M, Font J, Vallés J, Morón A, Monsó E, Rello J. 2020. Determinants of empirical antipseudomonal antibiotic prescription for adults with pneumonia in the emergency department. BMC Pulm Med 20:83. https://doi.org/10.1186/s12890-020-1115-0
6. Curran CS, Bolig T, Torabi-Parizi P. 2018. Mechanisms and targeted therapies for *Pseudomonas aeruginosa* lung infection. Am J Respir Crit Care Med 197:708–727. https://doi.org/10.1164/rccm.201705-1043SO
7. Zhanel GG, Lawrence CK, Adam H, Schweizer F, Zelenitsky S, Zhanel M, Lagacé-Wiens PRS, Walkty A, Denisuik A, Golden A, Gin AS, Hoban DJ, Lynch JP III, Karlowsky JA. 2018. Imipenem-relebactam and meropenem-vaborbactam: two novel carbapenem-β-lactamase inhibitor combinations. Drugs (Abingdon Engl) 78:65–98. https://doi.org/10.1007/s40265-017-0851-9
8. Sader HS, Castanheira M, Duncan LR, Mendes RE. 2021. Antimicrobial activities of ceftazidime/avibactam, ceftolozane/tazobactam, imipenem/relebactam, meropenem/vaborbactam, and comparators against *Pseudomonas aeruginosa* from patients with skin and soft tissue infections. Int J Infect Dis 113:279–281. https://doi.org/10.1016/j.ijid.2021.10.022
9. Mesaros N, Nordmann P, Plésiat P, Roussel-Delvallez M, Van Eldere J, Glupczynski Y, Van Laethem Y, Jacobs F, Lebecque P, Malfroot A, Tulkens PM, Van Bambeke F. 2007. *Pseudomonas aeruginosa*: resistance and therapeutic options at the turn of the new millennium. Clin Microbiol Infect 13:560–578. https://doi.org/10.1111/j.1469-0691.2007.01681.x
10. Campbell JI, Ciofu O, Høiby N. 1997. *Pseudomonas aeruginosa* isolates from patients with cystic fibrosis have different beta-lactamase expression phenotypes but are homogeneous in the ampC-ampR genetic region. Antimicrob Agents Chemother 41:1380–1384. https://doi.org/10.1128/AAC.41.6.1380
11. Luzzaro F, Endimiani A, Docquier JD, Mugnaioli C, Bonsignori M, Amicosante G, Rossolini GM, Toniolo A. 2004. Prevalence and characterization of metallo-beta-lactamases in clinical isolates of *Pseudomonas aeruginosa*. Diagn Microbiol Infect Dis 48:131–135. https://doi.org/10.1016/j.diagmicrobio.2003.09.005
12. Zavascki AP, Carvalhaes CG, Picão RC, Gales AC. 2010. Multidrug-resistant *Pseudomonas aeruginosa* and *Acinetobacter baumannii*: resistance mechanisms and implications for therapy. Expert Rev Anti Infect Ther 8:71–93. https://doi.org/10.1586/eri.09.108
13. Hong DJ, Bae IK, Jang IH, Jeong SH, Kang HK, Lee K. 2015. Epidemiology and Characteristics of Metallo-β-Lactamase-Producing *Pseudomonas aeruginosa*. Infect Chemother 47:81–97. https://doi.org/10.3947/ic.2015.47.2.81
14. Sugawara E, Nestorovich EM, Bezrukov SM, Nikaido H. 2006. *Pseudomonas aeruginosa* porin OprF exists in two different conformations. J Biol Chem 281:16220–16229. https://doi.org/10.1074/jbc.M600680200
15. Chevalier S, Bouffartigues E, Bodilis J, Maillot O, Lesouhaitier O, Feuilloley MGJ, Orange N, Dufour A, Cornelis P. 2017. Structure, function and regulation of *Pseudomonas aeruginosa* porins. FEMS Microbiol Rev 41:698–722. https://doi.org/10.1093/femsre/fux020
16. Nakae T, Nakajima A, Ono T, Saito K, Yoneyama H. 1999. Resistance to beta-lactam antibiotics in *Pseudomonas aeruginosa* due to interplay between the MexAB-OprM efflux pump and beta-lactamase. Antimicrob Agents Chemother 43:1301–1303. https://doi.org/10.1128/AAC.43.5.1301
17. Li XZ, Plésiat P, Nikaido H. 2015. The challenge of efflux-mediated antibiotic resistance in Gram-negative bacteria. Clin Microbiol Rev 28:337–418. https://doi.org/10.1128/CMR.00117-14
18. Castanheira M, Doyle TB, Smith CJ, Mendes RE, Sader HS. 2019. Combination of MexAB-OprM overexpression and mutations in efflux regulators, PBPs and chaperone proteins is responsible for ceftazidime/avibactam resistance in *Pseudomonas aeruginosa* clinical isolates from US hospitals. J Antimicrob Chemother 74:2588–2595. https://doi.org/10.1093/jac/dkz243
19. Trias J, Nikaido H. 1990. Outer membrane protein D2 catalyzes facilitated diffusion of carbapenems and penems through the outer membrane of *Pseudomonas aeruginosa*. Antimicrob Agents Chemother 34:52–57. https://doi.org/10.1128/AAC.34.1.52
20. Lister PD, Wolter DJ, Hanson ND. 2009. Antibacterial-resistant *Pseudomonas aeruginosa*: clinical impact and complex regulation of chromosomally encoded resistance mechanisms. Clin Microbiol Rev 22:582–610. https://doi.org/10.1128/CMR.00040-09
21. Tamber S, Ochs MM, Hancock REW. 2006. Role of the novel OprD family of porins in nutrient uptake in *Pseudomonas aeruginosa*. J Bacteriol 188:45–54. https://doi.org/10.1128/JB.188.1.45-54.2006
22. Eren E, Vijayaraghavan J, Liu J, Cheneke BR, Touw DS, Lepore BW, Indic M, Movileanu L, van den Berg B. 2012. Substrate specificity within a family of outer membrane carboxylate channels. PLoS Biol 10:e1001242. https://doi.org/10.1371/journal.pbio.1001242
23. Tamber S, Hancock REW. 2006. Involvement of two related porins, OprD and OpdP, in the uptake of arginine by *Pseudomonas aeruginosa*. FEMS Microbiol Lett 260:23–29. https://doi.org/10.1111/j.1574-6968.2006.00293.x
24. Isabella VM, Campbell AJ, Manchester J, Sylvester M, Nayar AS, Ferguson KE, Tommasi R, Miller AA. 2015. Toward the rational design of carbapenem uptake in *Pseudomonas aeruginosa*. Chem Biol 22:535–547. https://doi.org/10.1016/j.chembiol.2015.03.018

25. Chalhoub H, Sáenz Y, Rodriguez-Villalobos H, Denis O, Kahl BC, Tulkens PM, Van Bambeke F. 2016. High-level resistance to meropenem in clinical isolates of *Pseudomonas aeruginosa* in the absence of carbapenemases: role of active efflux and porin alterations. Int J Antimicrob Agents 48:740–743. https://doi.org/10.1016/j.ijantimicag.2016.09.012
26. Atrissi J, Milan A, Bressan R, Lucafò M, Petix V, Busetti M, Dolzani L, Lagatolla C. 2021. Interplay of OpdP porin and chromosomal carbapenemases in the determination of carbapenem resistance/susceptibility in *Pseudomonas aeruginosa*. Microbiol Spectr 9:e0118621. https://doi.org/10.1128/Spectrum.01186-21
27. Kiely PD, O'Callaghan J, Abbas A, O'Gara F. 2008. Genetic analysis of genes involved in dipeptide metabolism and cytotoxicity in *Pseudomonas aeruginosa* PAO1. Microbiology (Reading, Engl) 154:2209–2218. https://doi.org/10.1099/mic.0.2007/015032-0
28. Pletzer D, Lafon C, Braun Y, Köhler T, Page MGP, Mourez M, Weingart H. 2014. High-throughput screening of dipeptide utilization mediated by the ABC transporter DppBCDF and its substrate-binding proteins DppA1-A5 in *Pseudomonas aeruginosa*. PLoS One 9:e111311. https://doi.org/10.1371/journal.pone.0111311
29. Asfahl KL, Walsh J, Gilbert K, Schuster M. 2015. Non-social adaptation defers a tragedy of the commons in *Pseudomonas aeruginosa* quorum sensing. ISME J 9:1734–1746. https://doi.org/10.1038/ismej.2014.259
30. Liu J, Wolfe AJ, Eren E, Vijayaraghavan J, Indic M, van den Berg B, Movileanu L. 2012. Cation selectivity is a conserved feature in the OccD subfamily of *Pseudomonas aeruginosa*. Biochim Biophys Acta 1818:2908–2916. https://doi.org/10.1016/j.bbamem.2012.07.009
31. Smalley NE, Schaefer AL, Asfahl KL, Perez C, Greenberg EP, Dandekar AA. 2022. Evolution of the quorum sensing regulon in cooperating populations of *Pseudomonas aeruginosa*. MBio 13:e0016122. https://doi.org/10.1128/mbio.00161-22
32. Ude J, Tripathi V, Buyck JM, Söderholm S, Cunrath O, Fanous J, Claudi B, Egli A, Schleberger C, Hiller S, Bumann D. 2021. Outer membrane permeability: antimicrobials and diverse nutrients bypass porins in *Pseudomonas aeruginosa*. Proc Natl Acad Sci U S A 118:e2107644118. https://doi.org/10.1073/pnas.2107644118
33. Zimmermann W. 1980. Penetration of beta-lactam antibiotics into their target enzymes in *Pseudomonas aeruginosa*: comparison of a highly sensitive mutant with its parent strain. Antimicrob Agents Chemother 18:94–100. https://doi.org/10.1128/AAC.18.1.94
34. Yoshimura F, Nikaido H. 1982. Permeability of *Pseudomonas aeruginosa* outer membrane to hydrophilic solutes. J Bacteriol 152:636–642. https://doi.org/10.1128/jb.152.2.636-642.1982
35. Livermore DM, Davy KW. 1991. Invalidity for *Pseudomonas aeruginosa* of an accepted model of bacterial permeability to beta-lactam antibiotics. Antimicrob Agents Chemother 35:916–921. https://doi.org/10.1128/AAC.35.5.916
36. Simonet V, Malléa M, Pagès JM. 2000. Substitutions in the eyelet region disrupt cefepime diffusion through the *Escherichia coli* OmpF channel. Antimicrob Agents Chemother 44:311–315. https://doi.org/10.1128/AAC.44.2.311-315.2000
37. Cai H, Rose K, Liang LH, Dunham S, Stover C. 2009. Development of a liquid chromatography/mass spectrometry-based drug accumulation assay in *Pseudomonas aeruginosa*. Anal Biochem 385:321–325. https://doi.org/10.1016/j.ab.2008.10.041
38. Zhou Y, Joubran C, Miller-Vedam L, Isabella V, Nayar A, Tentarelli S, Miller A. 2015. Thinking outside the "bug": a unique assay to measure intracellular drug penetration in gram-negative bacteria. Anal Chem 87:3579–3584. https://doi.org/10.1021/ac504880r
39. Iyer R, Ye Z, Ferrari A, Duncan L, Tanudra MA, Tsao H, Wang T, Gao H, Brummel CL, Erwin AL. 2018. Evaluating LC-MS/MS to measure accumulation of compounds within bacteria. ACS Infect Dis 4:1336–1345. https://doi.org/10.1021/acsinfecdis.8b00083
40. Modi N, Ganguly S, Bárcena-Uribarri I, Benz R, van den Berg B, Kleinekathöfer U. 2015. Structure, dynamics, and substrate specificity of the OprO porin from *Pseudomonas aeruginosa*. Biophys J 109:1429–1438. https://doi.org/10.1016/j.bpj.2015.07.035
41. Soundararajan G, Bhamidimarri SP, Winterhalter M. 2017. Understanding carbapenem translocation through OccD3 (OpdP) of *Pseudomonas aeruginosa*. ACS Chem Biol 12:1656–1664. https://doi.org/10.1021/acschembio.6b01150
42. Dogan Guzel F, Pletzer D, Norouz Dizaji A, Al-Nahas K, Bajrai M, Winterhalter M. 2021. Towards understanding single-channel characteristics of OccK8 purified from *Pseudomonas aeruginosa*. Eur Biophys J 50:87–98. https://doi.org/10.1007/s00249-021-01498-5
43. Golla VK, Prajapati JD, Joshi M, Kleinekathöfer U. 2020. Exploration of free energy surfaces across a membrane channel using metadynamics and umbrella sampling. J Chem Theory Comput 16:2751–2765. https://doi.org/10.1021/acs.jctc.9b00992
44. Piselli C, Benz R. 2021. Fosmidomycin transport through the phosphate-specific porins OprO and OprP of *Pseudomonas aeruginosa*. Mol Microbiol 116:97–108. https://doi.org/10.1111/mmi.14693
45. Lakaye B, Dubus A, Joris B, Frère JM. 2002. Method for estimation of low outer membrane permeability to beta-lactam antibiotics. Antimicrob Agents Chemother 46:2901–2907. https://doi.org/10.1128/AAC.46.9.2901-2907.2002
46. National Committee for Clinical Laboratory Standards. 2020. Performance standards for antimicrobial susceptibility testing. In CLSI supplement M100, 30th ed. NCCLS, Wayne, PA, USA.
47. Satake S, Yoneyama H, Nakae T. 1991. Role of OmpD2 and chromosomal beta-lactamase in carbapenem resistance in clinical isolates of *Pseudomonas aeruginosa*. J Antimicrob Chemother 28:199–207. https://doi.org/10.1093/jac/28.2.199
48. Chandler CE, Horspool AM, Hill PJ, Wozniak DJ, Schertzer JW, Rasko DA, Ernst RK. 2019. Genomic and phenotypic diversity among ten laboratory isolates of *Pseudomonas aeruginosa* PAO1. J Bacteriol 201:e00595-18. https://doi.org/10.1128/JB.00595-18
49. Yu L, Cao Q, Chen W, Yang N, Yang CG, Ji Q, Wu M, Bae T, Lan L. 2022. A novel copper-sensing two-component system for inducing Dsb gene expression in bacteria. Sci Bull Sci Found Philipp 67:198–212. https://doi.org/10.1016/j.scib.2021.03.003
50. Perron K, Caille O, Rossier C, Van Delden C, Dumas J-L, Köhler T. 2004. CzcR-CzcS, a two-component system involved in heavy metal and carbapenem resistance in *Pseudomonas aeruginosa*. J Biol Chem 279:8761–8768. https://doi.org/10.1074/jbc.M312080200
51. Caille O, Rossier C, Perron K. 2007. A copper-activated two-component system interacts with zinc and imipenem resistance in *Pseudomonas aeruginosa*. J Bacteriol 189:4561–4568. https://doi.org/10.1128/JB.00095-07
52. Sobel ML, Hocquet D, Cao L, Plesiat P, Poole K. 2005. Mutations in PA3574 (nalD) lead to increased MexAB-OprM expression and multidrug resistance in laboratory and clinical isolates of *Pseudomonas aeruginosa*. Antimicrob Agents Chemother 49:1782–1786. https://doi.org/10.1128/AAC.49.5.1782-1786.2005
53. Ochs MM, McCusker MP, Bains M, Hancock RE. 1999. Negative regulation of the *Pseudomonas aeruginosa* outer membrane porin OprD selective for imipenem and basic amino acids. Antimicrob Agents Chemother 43:1085–1090. https://doi.org/10.1128/AAC.43.5.1085
54. Acosta-Gutiérrez S, Bodrenko I, Ceccarelli M. 2021. The influence of permeability through bacterial porins in whole-cell compound accumulation. Antibiotics (Basel) 10:635. https://doi.org/10.3390/antibiotics10060635
55. Tommasi R, Iyer R, Miller AA. 2018. Antibacterial drug discovery: some assembly required. ACS Infect Dis 4:686–695. https://doi.org/10.1021/acsinfecdis.8b00027
56. Glen KA, Lamont IL. 2021. β-lactam resistance in *Pseudomonas aeruginosa*: current status, future prospects. Pathogens 10:1638. https://doi.org/10.3390/pathogens10121638
57. Samanta S, Bodrenko I, Acosta-Gutiérrez S, D'Agostino T, Pathania M, Ghai I, Schleberger C, Bumann D, Wagner R, Winterhalter M, van den Berg B, Ceccarelli M. 2018. Getting drugs through small pores: exploiting the porins pathway in *Pseudomonas aeruginosa*. ACS Infect Dis 4:1519–1528. https://doi.org/10.1021/acsinfecdis.8b00149
58. Montaner M, Lopez-Argüello S, Oliver A, Moya B. 2023. PBP target profiling by β-lactam and β-lactamase inhibitors in intact *Pseudomonas aeruginosa*: effects of the intrinsic and acquired resistance determinants on the periplasmic drug availability. Microbiol Spectr 11:e0303822. https://doi.org/10.1128/spectrum.03038-22
59. Jacoby GA. 2009. AmpC beta-lactamases. Clin Microbiol Rev 22:161–182, https://doi.org/10.1128/CMR.00036-08
60. Kojima S, Nikaido H. 2013. Permeation rates of penicillins indicate that *Escherichia coli* porins function principally as nonspecific channels. Proc Natl Acad Sci U S A 110:E2629–E2634. https://doi.org/10.1073/pnas.1310333110
61. Matsumura N, Minami S, Watanabe Y, Iyobe S, Mitsuhashi S. 1999. Role of permeability in the activities of beta-lactams against gram-negative bacteria which produce a group 3 beta-lactamase. Antimicrob Agents Chemother 43:2084–2086. https://doi.org/10.1128/AAC.43.8.2084

62. Nikaido H. 1985. Role of permeability barriers in resistance to beta-lactam antibiotics. Pharmacol Ther 27:197–231. https://doi.org/10.1016/0163-7258(85)90069-5
63. Gibson DG, Young L, Chuang R-Y, Venter JC, Hutchison CA III, Smith HO. 2009. Enzymatic assembly of DNA molecules up to several hundred kilobases. Nat Methods 6:343–345. https://doi.org/10.1038/nmeth.1318
64. Bushnell B, Rood J, Singer E. 2017. BBMerge - accurate paired shotgun read merging via overlap. PLoS One 12:e0185056. https://doi.org/10.1371/journal.pone.0185056
65. Kearse M, Moir R, Wilson A, Stones-Havas S, Cheung M, Sturrock S, Buxton S, Cooper A, Markowitz S, Duran C, Thierer T, Ashton B, Meintjes P, Drummond A. 2012. Geneious Basic: an integrated and extendable desktop software platform for the organization and analysis of sequence data. Bioinformatics 28:1647–1649. https://doi.org/10.1093/bioinformatics/bts199
66. Ruijter JM, Ramakers C, Hoogaars WMH, Karlen Y, Bakker O, van den Hoff MJB, Moorman AFM. 2009. Amplification efficiency: linking baseline and bias in the analysis of quantitative PCR data. Nucleic Acids Res 37:e45. https://doi.org/10.1093/nar/gkp045
67. Hellemans J, Mortier G, De Paepe A, Speleman F, Vandesompele J. 2007. qBase relative quantification framework and software for management and automated analysis of real-time quantitative PCR data. Genome Biol 8:R19. https://doi.org/10.1186/gb-2007-8-2-r19
68. Vandesompele J, De Preter K, Pattyn F, Poppe B, Van Roy N, De Paepe A, Speleman F. 2002. Accurate normalization of real-time quantitative RT-PCR data by geometric averaging of multiple internal control genes. Genome Biol 3:RESEARCH0034. https://doi.org/10.1186/gb-2002-3-7-research0034
69. Frère J-M, Nguyen-Distèche M, Coyette J, Joris B. 1992. Mode of action: interaction with the penicillin binding proteins, p 148–195. In Page M (ed), The chemistry of beta-lactams. Chapman and Hall, Glasgow, Scotland.
70. Duval V, Swinnen M, Lepage S, Brans A, Granier B, Franssen C, Frère JM, Joris B. 2003. The kinetic properties of the carboxy terminal domain of the *Bacillus licheniformis* 749/I BlaR penicillin-receptor shed a new light on the derepression of beta-lactamase synthesis. Mol Microbiol 48:1553–1564. https://doi.org/10.1046/j.1365-2958.2003.03520.x
71. Kolayli F, Karadenizli A, Savli H, Ergen K, Hatirnaz O, Balikci E, Budak F, Vahaboglu H. 2004. Effect of carbapenems on the transcriptional expression of the *oprD*, *oprM* and *oprN* genes in *Pseudomonas aeruginosa*. J Med Microbiol 53:915–920. https://doi.org/10.1099/jmm.0.45692-0
72. Epp SF, Pechère J, Kok M. 2001. Raising antibodies against OprD, an outer membrane protein of *Pseudomonas aeruginosa* using translational fusions to MalE. J Microbiol Methods 46:1–8. https://doi.org/10.1016/s0167-7012(01)00236-6

Supplemental information for: "Outer membrane permeability of *Pseudomonas aeruginosa*: elucidating the role of OprD and OpdP porins in antibiotic resistance"

Porin(s) deletion assessment

A PCR-based screening was carried out on porin mutant strains to verify the presence/absence of the porins as previously described. Results are shown in Figure S1.

RT-PCR reference genes

The first goal to perform RT-PCRs was the determination of the most reliable reference genes for their stability at the different growth phases; we selected ten genes (*PA2875*, *PA3340*, *gyrA*, *recA*, *rho*, *proC*, *mreB cysG*, *gapA* and *mutL*), previously reported to be used as reference for qRT-PCR experiments and we analysed their relative expression in PAO1 in the early and late exponential phase and also during the stationary phase.

The quantification result is reported in figure S2.

We selected as references genes for the successive analysis *PA3340*, *gyrA* and *cysG* genes, on the basis of their stability during the bacterial growth and for their different relative expression. They have been in fact used as qRT-PCR internal controls.

References (for tables S2 and S3)

1. Shen J, Pan Y, Fang Y. 2015. Role of the Outer Membrane Protein OprD2 in Carbapenem-Resistance Mechanisms of *Pseudomonas aeruginosa*. PLoS One 10:e0139995.
2. Ocampo-Sosa AA, Cabot G, Rodríguez C, Roman E, Tubau F, Macia MD, Moya B, Zamorano L, Suárez C, Peña C, Domínguez MA, Moncalián G, Oliver A, Martínez-Martínez L; Spanish Network for Research in Infectious Diseases (REIPI). 2012. Alterations of OprD in carbapenem-intermediate and -susceptible strains of *Pseudomonas aeruginosa* isolated from patients with bacteremia in a Spanish multicenter study. Antimicrob Agents Chemother 56:1703-1713.
3. Caille O, Rossier C, Perron K. 2007. A copper-activated two-component system interacts with zinc and imipenem resistance in *Pseudomonas aeruginosa*. J Bacteriol 189:4561-4568.
4. Costaglioli P, Barthe C, Fayon M, Christoflour N, Bui S, Derlich L, Domblides P, Crouzet M, Vilain S, Garbay B. 2014. Selection of *Pseudomonas aeruginosa* reference genes for RT-qPCR analysis from sputum of cystic fibrosis patients. Mol Cell Probes 28:10-12.
5. Bragonzi A, Worlitzsch D, Pier GB, Timpert P, Ulrich M, Hentzer M, Andersen JB, Givskov M, Conese M, Doring G. 2005. Nonmucoid *Pseudomonas aeruginosa* expresses alginate in the lungs of patients with cystic fibrosis and in a mouse model. J Infect Dis 192:410-419.
6. Dumas JL, van Delden C, Perron K, Köhler T. 2006. Analysis of antibiotic resistance gene expression in *Pseudomonas aeruginosa* by quantitative real-time-PCR. FEMS Microbiol Lett 254:217-225.
7. Savli H, Karadenizli A, Kolayli F, Gundes S, Ozbek U, Vahaboglu H. 2003. Expression stability of six housekeeping genes: A proposal for resistance gene quantification studies of *Pseudomonas aeruginosa* by real-time quantitative RT-PCR. J Med Microbiol 52:403-408.
8. Gupta K, Marques CN, Petrova OE, Sauer K. 2013. Antimicrobial tolerance of *Pseudomonas aeruginosa* biofilms is activated during an early developmental stage and requires the two-component hybrid SagS. J Bacteriol 195:4975-4987.
9. Costaglioli P, Barthe C, Fayon M, Christoflour N, Bui S, Derlich L, Domblides P, Crouzet M, Vilain S, Garbay B. 2014. Selection of *Pseudomonas aeruginosa* reference genes for RT-qPCR analysis from sputum of cystic fibrosis patients. Mol Cell Probes 28:10-12.

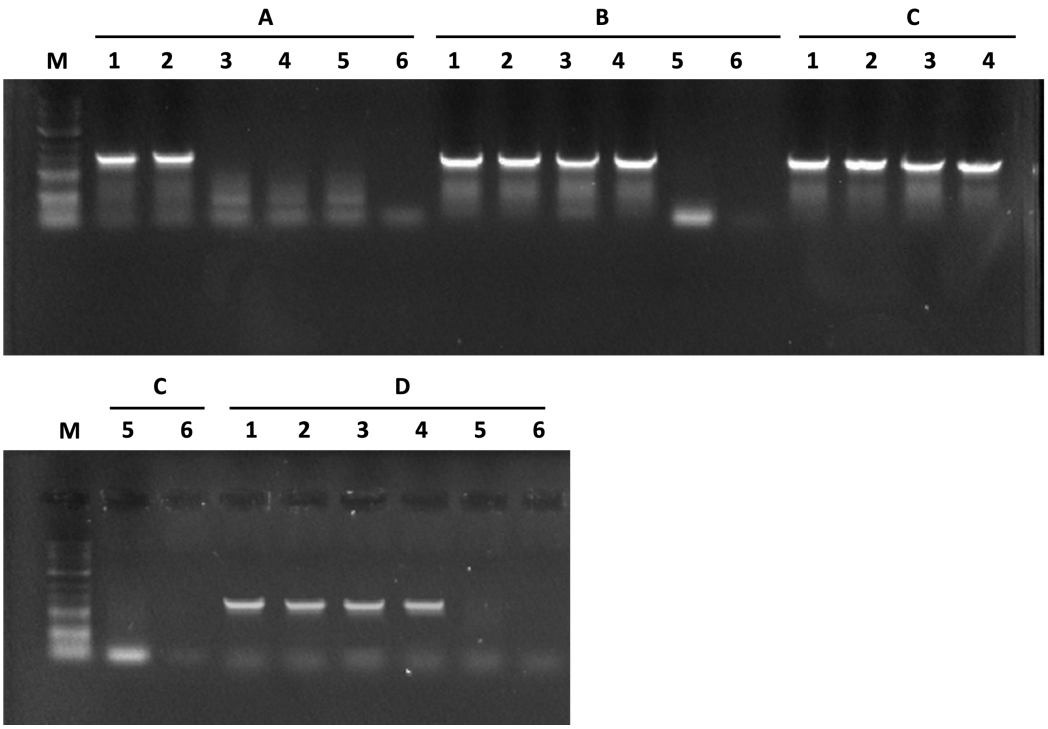

Figure S1: PCR amplifications for the following different targets: A *opdP*, B *opdC*, C *opdT* and D *opdB*. The corresponding sample are the following: 1 ARC545, 2 ARC5990, 3 ARC5170, 4 ARC5782, 5 ARC5998, 6 negative controls. M corresponds to 1 Kb DNA ladder.

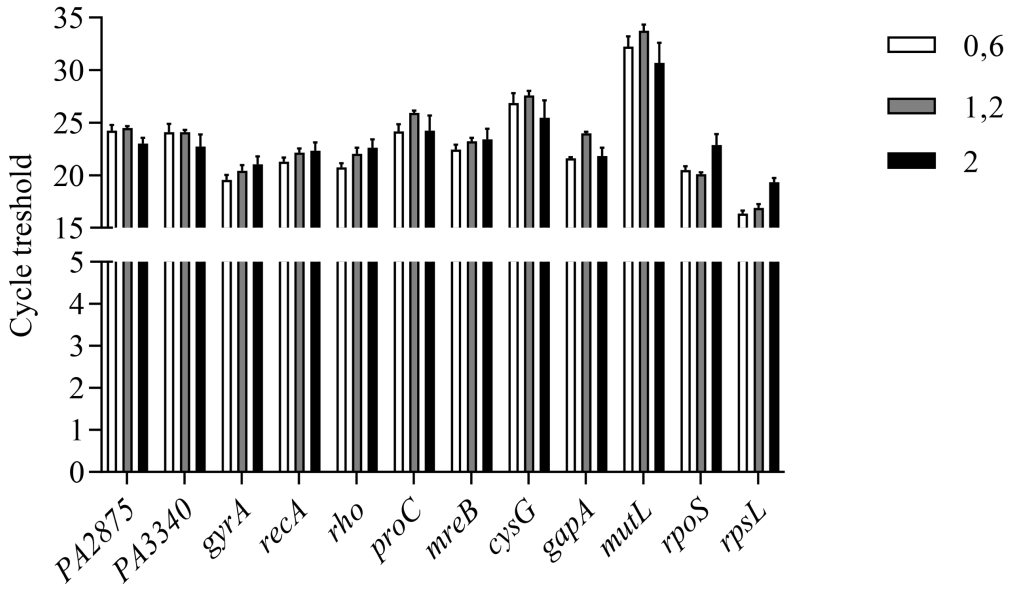

Figure S2: Relative expression of *PA2875*, *PA3340*, *gyrA*, *recA*, *rho*, *proC*, *mreB, cysG*, *gapA* and *mutL* in *P. aeruginosa* PAO1; the relative expression reported on the y axis is the expression of the target gene relative to the mean expression level of two genes used as reference (*rpoS* and *rpsL*). Data were analyzed by two-way analysis of variance (ANOVA) followed by Bonferroni multiple comparison post-test.

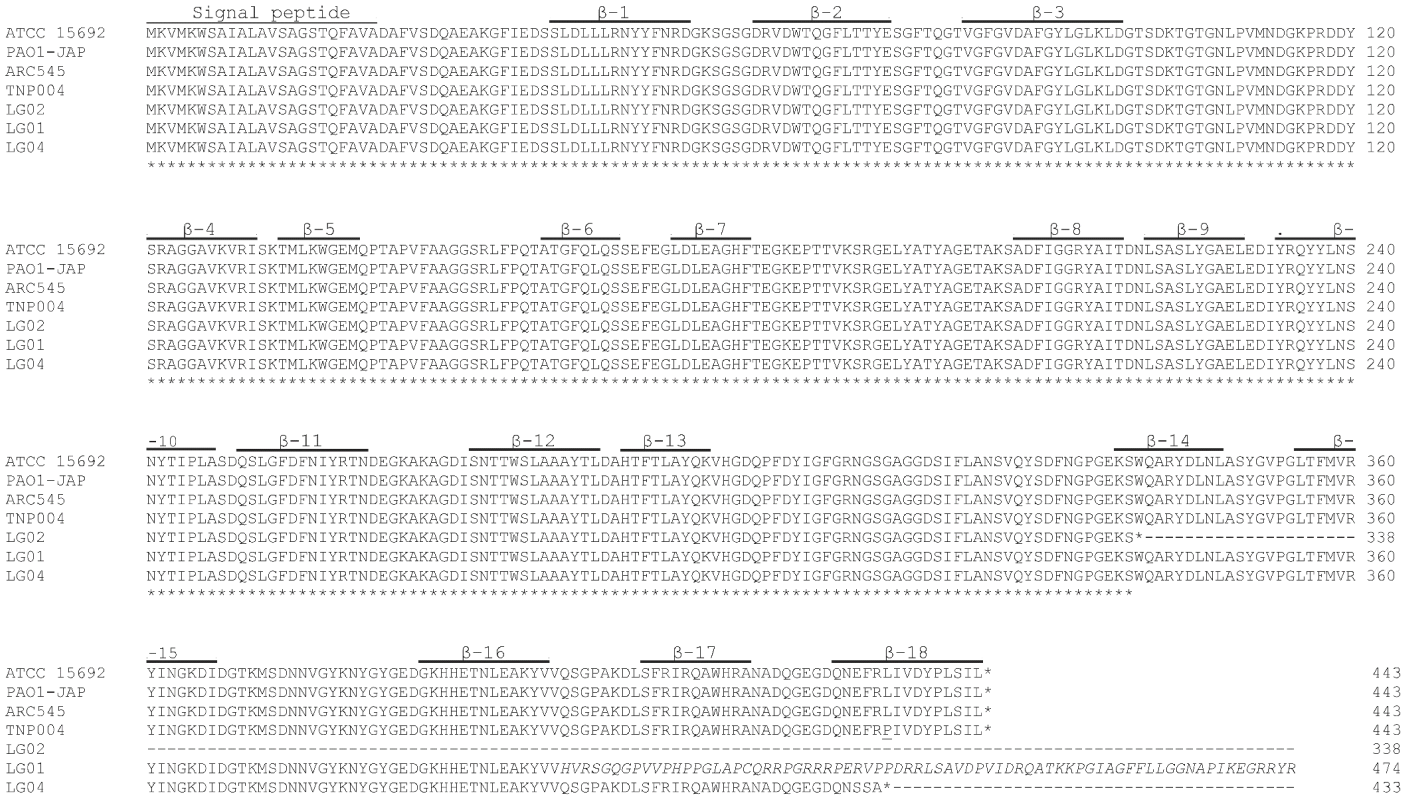

Figure S3: *oprD* CLUSTAL O (1.2.4) multiple sequence alignments of the reference strains *P. aeruginosa* PAO1 ATCC 15692, *P. aeruginosa* PAO1-Jap, *P. aeruginosa* PAO1 ARC545 and the mutants *P. aeruginosa* TNP004, *P. aeruginosa* LG02, LG01 and LG04.

Table S1: Collection of plasmids used in this study.

Plasmid	Description	Resistance	Reference
pKT240blaR	Shuttle vector for BlaR-CTD expression in *E. coli* and *P. aeruginosa*	TET	(45)
pKT240neg	pKT240blaR depleted of *blaR-CTD* gene	TET	This study
pKT240blaR-gen	pKT240blaR added with *aac1* gene	TET, GEN	This study

Table S2: Collection of primers used in this study for PCR amplification and sequencing.

Primer	Sequence 5'=>3'	Reference	Use
blaR-fw	CCATGCAAAAAGAAACACGC	This study	*blaR-CTD* amplification and sequencing
blaR-rev	TTCTTGCCTCCAAGTTCCGT	This study	
blaR-seq-rev	ACAGGACAAAGCCCCCTGAGGCTG	This study	*blaR-CTD* sequencing
oprD-fw	ATGAAAGTGATGAAGTGGAGCG	1	*oprD* detection
oprD-rev	TTACAGGATCGACAGCGGATAG	1	
oprD_flankF	CGGCTGAGGGGAAAGTCGCC	2	*oprD* sequencing
oprD_flankR	TACGCGGTCATTCTCGGGCG	2	
opdB-fw	ATGATCCGCGTTCGACCGGTCG	This study	*opdB* detection
opdB-rev	TCAGAGCGAGCCTTTGAGTGGG	This study	
opdC-fw	ATGAGGAATCTGTTCGCCTTGA	This study	*opdC* detection
opdC-rev	TCAGAACACGTCGATGGGATAG	This study	
opdP-fw	GTGATGAGAAACCAACGTGTGA	This study	*opdP* detection
opdP-rev	TTACAGCAGGTTGAAGGGGAAG	This study	
opdT-fw	ATGCAAGGGGATGGAAAGAAAC	This study	*opdT* detection
opdT-rev	TCAGAGGACTTGCAGCGGGTAT	This study	
neg1-fw	AATAGGCGTATCACGAGGCCCTTTGCGTTCAGGCTGCTAAAGATG	This study	pKT240neg construction
neg1-rev	TCATGGTCTATTGCCTCCCG	This study	
neg2-fw	CGGGAGGCAATAGACCATGA	This study	pKT240neg construction
neg2-rev	CAAAGGGCCTCGTGATACGC	This study	
gmr_fw	GTTACGCCGTGGGTCGATGT	This study	pKT240blaR-gen construction
gmr_rev	AATTTACCGAACAACTCCGC	This study	
gmr-inf-fw1	GCGGAGTTGTTCGGTAAATTAGAAATTGCATCAACGCATA	This study	pKT240blaR-gen construction
gmr-inf-rev1	GCGGGGTTTGGTGTGGGGTT	This study	
gmr-inf-fw2	AACCCCACACCAAACCCCGC	This study	pKT240blaR-gen construction
gmr-inf-rev2	ACATCGACCCACGGCGTAACATGGAAGCCGGCGGCACCTC	This study	

Table S3. Sequences and reaction efficiencies of quantitative RT-PCR primer pairs.

Primer	Sequence 5'-3'	Reference	Reaction efficiency (RE)	Standard deviation (SD)
oprD-rt-fw	ATCTACCGCACAAACGATGAAGG	3	1.925	0.0247
oprD-rt-rev	GCCGAAGCCGATATAATCAAACG	3		
opdB-rt-fw	GCTCAACCGCAACTACTTCC	This study	1.753	0.0164
opdB-rt-rev	GCGTCGGAATACTCGCTGGC	This study		
opdC-rt-fw	GCTGAAGATCCGCGCCTTC	This study	1.835	0.0178
opdC-rt-rev	GCTGAGATGATGGCTGTCGC	This study		
opdP-rt-fw	CAACACCGAATTCAAGGCC	This study	1.923	0.0195
opdP-rt-rev	CCGTACTCGGTGGTCATGTC	This study		
opdT-rt-fw	GCTTCACCCTGGTCAACGAC	This study	1.853	0.0181
opdT-rt-rev	GAAGCTGGTGCCGGCGTAGT	This study		
PA3340-rt-fw	GCTTGCAGTTCCTCAACGAG	4	1.933	0.0229
PA3340-rt-rev	CACCAGGAAATTCAGGTAGGG	4		
gyrA-rt-fw	TGTGCTTTATGCCATGAGCGA	5	1.934	0.0188
gyrA-rt-rev	TCCACCGAACCGAAGTTGC	5		
cysG-rt-fw	GCAGCAGCGCCGGGTGTTC	This study	1.856	0.0223
cysG-rt-rev	ACGTCGGCCTGCTGCATC	This study		
rpsL-rt-fw	GCAAGCGCATGGTCGACAAGA	6	1.883	0.0214
rpsL-rt-rev	CGCTGTGCTCTTGCAGGTTGTGA	6		
proC-rt-fw	CAGGCCGGGCAGTTGCTGTC	7	1.919	0.0267
proC-rt-rev	GGTCAGGCGCGAGGCTGTCT	7		
gapA-rt-fw	CAACGACCAGAACCTCTCCG	This study	1.884	0.0208
gapA-rt-rev	ACCTGCACGGTGAGATCGAC	This study		
mreB-rt-fw	CTGTCGATCGACCTGGG	8	1.877	0.0184
mreB-rt-rev	GATCACGCCGTCTTTCATCG	This study		
rho-rt-fw	GCAACGGCTCCACCGAAGAC	This study	1.901	0.0185
rho-rt-rev	GTCACTTCCTCAGGGCGCTC	This study		
recA-rt-fw	GAATCCTCGGGCAAGACCAC	This study	1.910	0.0203
recA-rt-rev	CACGTCGACCGCGTTGGAGC	This study		
mutL-rt-fw	CAAGTTCCTGCGTGCCGAGA	This study	1.651	0.0176
mutL-rt-rev	CAGCGCCTGCTCGAGGAATG	This study		
PA2875-rt-fw	AGTTTCCAGCGCATCCAGTT	9	1.903	0.0205
PA2875-rt-rev	CGGGATGGAAGACGAATTG	9		
rpoS-rt-fw	CTCCCCGGGCAACTCCAAAAG	7	1.898	0.0225
rpoS-rt-rev	CGATCATCCGCTTCCGACCAG	7		

4.2 Complementary results

In this section, we present results obtained during this Ph.D. project that, for various reasons, were not included in the paper.

A wider set of strains were considered only in an initial phase, or not used for the results reported in the paper. Their MIC values are reported below.

The proteomics results, obtained in collaboration with a laboratory at the University of Siena (Italy), provided an overall view of the alterations caused by the lack of OprD expression and by the production of BlaR-CTD. However, we did not consider these results complete enough to be published.

We decided to include in this section also the results regarding the determination of permeability in a strain deprived of the main efflux pump systems. Additionally, we report here a collateral use of the outer membrane permeability determination methodology to assess potential alterations that various substances might cause to outer membrane integrity.

We also thought worth reporting the presence of different PAO1 lineages obtained from genome sequencing, which, by pure serendipity, led to the discovery of strains that appeared to be OpdP overexpressors.

Finally, we report the results obtained thanks to Western blot quantification of OpdP expression, despite its limitations due to the non-specificity of the anti-OpdP antibodies raised during this project.

4.2.1 Antibiotic resistance patterns

All the strains received during the study were characterized for MIC for a subset of β-lactams, in order to detect the possible role of porins or efflux pumps deletion in antibiotic resistance. The results obtained for the strains not included in the paper are reported in Table 6.

Antibiotics	**CLSI Std.**	**PAO1**	**TNP004**	**TNP064**	**YY100**	**TNP065**	**TNP066**	**YY200**	**TNP067**	**PA0509**	**PA0509 +blaR**
Characteristics		**wild type**	**(↓OprD)**	**(*ΔoprC*)**	**(*ΔoprE*)**	**(*ΔoprC*, ↓OprD)**	**(*ΔoprC*, *ΔoprE*)**	**(↓OprD, *ΔoprE*)**	**(*ΔoprC*, ↓OprD, *ΔoprE*)**	***ΔmexAB-oprM, ΔmexCD-oprJ, ΔmexJK, ΔmexXY, ΔmexEF-oprN***	
Benzylpenicillin	**NA**	>2000	>2000	2000	>2000	2000	>2000	>2000	>2000	1000	500
Ampicillin	**NA**	2000	1000	1000	2000	1000	2000	2000	2000	**125**	62.5
Piperacillin	**1-8**	2	2	2	2	2	2	2	2	**0.25**	4
Cefalotin	**NA**	> 2000	> 2000	> 2000	> 2000	> 2000	> 2000	> 2000	> 2000	ND	ND
Cephaloridine	**NA**	> 2000	> 2000	> 2000	> 2000	> 2000	> 2000	> 2000	> 2000	ND	ND
Cefoxitin	**NA**	1000	500	500	500	500	500	500	500	ND	ND
Cefuroxime	**NA**	250	250	250	250	250	250	250	250	500	250
Cefotaxime	**8-32**	16	8	16	16	16	16	16	16	**0.5**	0.5
Ceftazidime	**1-4**	1	2	2	2	2	2	0.5	2	0.5	16
Cefepime	**0.5-4**	1	0.5	1	1	1	1	1	1	**0.12**	4
Imipenem	**1-4**	1	**8**	1	1	**8**	1	**8**	**8**	1	1
Meropenem	**0.12-1**	0.5	**2**	0.5	0.5	**2**	0.5	**2**	**2**	**0.12**	0.25
Ertapenem	**2-8**	8	**32**	8	8	**16**	8	**16**	**16**	**2**	4
Biapenem	**0.5-2**	0.5	**4**	0.5	0.5	**4**	0.5	**4**	**4**	0.5	0.25
Doripenem	**0.12-0.5**	0.25	**1**	0.25	0.25	**1**	0.25	**1**	**0.5**	0.12	0.12
Tetracycline	**8-32**	8	8	>128	128	>128	128	128	128	<0.25	>32
Gentamicin	**0.5-2**	1	2	1	2	1	2	2	2	1	1

Table 6: MIC values for the different *P. aeruginosa* strains. CLSI standard refers to acceptable limits for quality control strains used to monitor the accuracy of MICs. NA: not available, ND not determined.

One can notice that the strains belonging to the porin mutant collection provided by Prof. Yoneyama present an increased MIC for carbapenems only for the strains derived from TNP004, that have a mutated *oprD* (*i.e.* TNP065, YY200 and TNP067). The other porin mutant strains, deleted of *oprC* and/or *oprE*, show MIC values similar to those of the reference strain PAO1. We highlighted a two-fold dilution difference for some antibiotics such as ampicillin, cefoxitin, ceftazidime but this divergence can be ascribed to the experimental variability.

A close correlation between the deletion of a porin and an increase in MIC could not be demonstrated, except for the already known porin OprD. We can also notice that all the porin deleted strains derived

from TNP004 presented an increased MIC for tetracycline, due to the use of this resistance determinant for gene suppression (Yoneyama *et al*., 1995).

In order to standardize the experimental variability, we constructed the pKT240blaR-gen plasmid, to be used for TNP004, that is not resistant to tetracycline, and for all its derived strains.

However, concerning this strain collection, we only performed our study on TNP004, and we were more interested in studying the effect of the lack of OpdP, rather than focusing on OprC or OprE. We did not have the opportunity to determine permeability coefficients for these strains, but this is the reason why TNP004 is the only strain we transformed with pKT240blaR-gen.

We kindly received from Prof. Van Bambeke the strain PAO509, characterized by the deletion of the five main efflux pump systems (*mexAB-oprM*, *mexCD-oprJ*, *mexJK*, *mexXY*, *mexEF-oprN*) (Mima *et al*., 2007). We first proceeded with a phenotypic resistance characterization by MIC analysis, and we highlighted as expected a strong MIC decrease for several antibiotics, including ampicillin, piperacillin, cefotaxime, cefepime, meropenem and ertapenem (Table 6). The general MIC reduction is consistent with the absence of a constitutive expression of the five efflux pumps, and in particular with the absence of MexAB-OprM, which has the wider spectrum of action (Morita *et al*., 2001). Further proof of the most relevant role of MexAB-OprM across the other efflux systems is that the imipenem MIC remains unchanged between PAO1 and PAO509, due to the poor affinity of MexB for this antibiotic (Collu *et al*., 2012). However, a similar consideration made for imipenem can be done also for biapenem and doripenem, probably for a poor capability of MexAB-OprM to extrude these compounds. Interestingly, the absence of the other efflux pumps does not reflect a difference in susceptibility for imipenem, biapenem and doripenem, suggesting a marginal role for this antibiotic when the other pumps are not overexpressed.

We also verified the PAO509 strain transformed with the pKT240blaR plasmid. We noted increased MIC values for piperacillin, ceftazidime and cefepime, similarly to the other strains, as already reported in the paper and we did not use these antibiotics in permeability determinations.

We finally ascribed all the other MIC values increases to experimental variability, considering that they are limited to a two-fold variation.

4.2.2 Proteomic analysis

4.2.2.1 Influence of BlaR-CTD expression on periplasmic proteome

The proteomic content of the periplasm of *P. aeruginosa* strains was extracted according to the protocol described by Imperi and colleagues (Imperi *et al*., 2009). *P. aeruginosa* PAO1 was compared to the strains transformed with the BlaR-CTD producing vector (pKT240blaR) and with the same plasmid deprived of *blaR-CTD* (pKT240neg), respectively. This analysis was performed to make sure that the periplasmic production of BlaR-CTD was not the cause of an altered proteomic profile, and this claim was investigated with a two-dimensional gel electrophoresis (2-DE). Image analysis identified 1465 spots for PAO1 gel, 981 spots for PAO1+pKT240blaR gel and 984 spots for PAO1+pKT240neg gel.

The comparative analysis between *P. aeruginosa* PAO1 and *P. aeruginosa* PAO1+pKT240blaR uncovered 31 statistically relevant differences. The spots were subjected to mass spectrometry and 19 were identified as reported in Table 7.

Spot N.	Protein name	Accession number	Mascot search results			PAO1vsBlaR		
			Score	N. of matched peptides	Sequence coverage (%)	PAO1/ BlaR	BlaR/ PAO1	T-test PAO1vsBlaR
378	Chaperone protein ClpB (PA4542)	CLPB_PSEAE	245	20/22	30	0.428	2.339	0.008
395	Non identified					2.485	0.402	0.032
480	Fe(3+)-pyochelin receptor FptA (PA4221)	FPTA_PSEAE	167	12/13	21	0.489	2.043	0.041
623	Glucans biosynthesis protein G OpgG (PA5078)	OPGG_PSEA8	102	8/11	15	only in PAO1		0.001
694	ABC transporter substrate-binding protein DppA3 (PA4500)	WP_057388431.1	199	18/28	35	only in PAO1		0.100
723	Non identified					2.183	0.458	0.001
911	Non identified					2.774	0.360	0.012
913	Non identified					2.010	0.498	0.022
1088	Non identified					5.279	0.189	0.003
1096	Polyamine transporter PotD (PA3610)	EJZ73984.1	245	22/38	66	only in PAO1		0.005
1121	Non identified					0.392	2.553	0.001
1319	Tol-pal system protein YbgF (PA0974)	AGV59417.1	139	8/11	42	2.368	0.422	0.023
1374	Short-chain dehydrogenase (PA1828)	WP_062838333.1	155	8/8	30	2.102	0.476	0.017
1463	Hydrolase YcaC (PA1202)	WP_031799024.1	135	9/16	71	2.028	0.493	0.040
1484	2-dehydro-3-deoxyphosphogluconate aldolase EdaB (PA3131)	WP_074253171.1	109	7/14	46	0.224	4.474	0.019
1507	Protease PasP (PA0423)	Y421_PSEA8	100	5/5	26	only in PAO1		0.031
1510	ATP-dependent Clp protease proteolytic subunit 2 ClpP2 (PA3326)	CLPP2_PSEAE	110	6/7	39 C-fragment	only in PAO1		0.111
1512	Glutamine amidotransferase (PA4336)	WP_033941094.1	169	9/11	52	0.217	4.61	0.015
1513	Non identified					only in PAO1		0.004
1580	Non identified					4.416	0.226	0.050
1648	Non identified					only in PAO1		0.006
1650	Appr-1-p processing protein (PA1746)	WP_038828181.1	103	8/12	36	2.857	0.350	0.020
1656	Aspartokinase LysC (PA0904)	AK_PSEAE	118	10/16	21	only in PAO1		0.010
1702	Non identified					only in PAO1		0.007
1707	Non identified					only in PAO1		0.019
1768	Peroxiredoxin (PA1203)	WP_034022270.1	153	9/17	60	only in PAO1		0.006
1966	Immunomodulating metalloprotease (PA0572)	IMPA_PSEAE	189	16/19	21	4.477	0.223	0.053
2022	Hypothetical protein (PA2450)	WP_047925318.1	169	11/15	41	only in PAO1		0.001
2172	Methylmalonate-semialdehyde dehydrogenase MmsA (PA3570)	MMSA_PSEAE	156	11/14	30	only in PAO1		0.026
2273	Non identified					0.353	2.831	0.043
BlaR	Regulatory protein BlaR-CTD	BLAR_BACLI	178	16/25	26 C-fragment	only in PAO1		0.015

Table 7: MALDI-TOF identification of the spots exhibiting a different abundance in *P. aeruginosa* PAO1 *vs P. aeruginosa* PAO1+pKT240blaR. The table reports the associated spot number during the gel analysis, protein name, UniProt Accession number, Mascot search results including score, number of matched peptides and sequence coverage, fold-change in both PAO1 and PAO1 producing BlaR-CTD, and T-test value.

The same analysis was performed for the comparison between *P. aeruginosa* PAO1 and *P. aeruginosa* PAO1+pKT240neg, highlighting 20 differently abundant spots, 13 of which were identified (Table 8).

Spot N.	Protein name	Accession number	Mascot search results			PAO1vsneg		
			Score	N. of matched peptides	Sequence coverage (%)	PAO1/ neg	neg/ PAO1	T-test PAO1vsneg
480	Fe(3+)-pyochelin receptor (PA4221) FptA	FPTA_PSEAE	167	12/13	21	only in PAO1		0.001
492	Nitrous-oxide reductase (PA3392)	NOSZ_PSEAE	177	14/17	27	2.097	0.477	0.041
587	Gluconate 2-dehydrogenase, membrane-bound, flavoprotein (PA2265)	EYT98518.1	154	12/16	22	2.913	0.343	0.050
607	60 kDa chaperonin (PA4385) GroEL	CH60_PSEA8	209	19/27	43	0.479	2.088	0.010
616	Not identified					only in PAO1		0.0001
647	ABC transporter substrate-binding protein DppA4 (PA4502)	WP_031768557.1	118	8/10	22	6.456	0.155	0.034
873	X-Pro dipeptidase (PA4498) MdpA	WP_031754074.1	266	17/20	53	2.054	0.487	0.005
894	1-deoxy-D-xylulose 5-phosphate reductoisomerase (PA3650) YaeM	DXR_PSEA8	171	13/18	35	2.233	0.448	0.020
913	Not identified					2.881	0.347	0.039
1096	polyamine transporter PotD (PA3610)	EJZ73984.1	245	22/38	66	only in PAO1		0.005
1283	Not identified					0.256	3.901	0.043
1354	amino acid ABC transporter substrate-binding protein (PA5076)	WP_031766234.1	172	11/15	56	0.416	2.406	0.029
1373	Not identified					0.284	3.515	0.032
1405	Not identified					0.204	4.905	0.004
1455	MexE family multidrug efflux RND transporter periplasmic adaptor subunit	WP_046054090.1	96	6/7	20	2.913	0.343	0.030
1648	Not identified					only in PAO1		0.006
1656	Aspartokinase LysC (PA0904)	AK_PSEAE	118	10/16	21	only in PAO1		0.010
1702	Not identified					only in PAO1		0.007
2022	hypothetical protein (PA2450)	WP_047925318.1	169	11/15	41	only in PAO1		0.001
2174	N-succinylglutamate 5-semialdehyde dehydrogenase (PA0898) AruD	ASTD_PSEAE	152	10/11	22	0.409	2.445	0.031

Table 8: MALDI-TOF identification of the spots exhibiting a different abundance in *P. aeruginosa* PAO1 *vs P. aeruginosa* PAO1+pKT240neg. The table reports the associated spot number during the gel analysis, protein name, UniProt Accession number, Mascot search results including score, number of matched peptides and sequence coverage, fold-change in both PAO1 and PAO1 transformed with pKT240neg, and T-test value.
Spots 480, 913, 1096, 1702 and 2022 were already described in PAO1vsBlaR.

Finally, the comparison between PAO1+pKT240blaR and PAO1+pKT240neg revealed only 8 differently expressed spots, 2 of which were specific to this comparison, while the remaining 6 were already found in the two above-mentioned 2-DE investigations (Table 9).

Spot N.	Protein name	Accession number	Mascot search results			BlaRvsneg		
			Score	N. of matched peptides	Sequence coverage (%)	BlaR/ neg	neg/ BlaR	T-test BlaRvsneg
931	Non identified					2.625	0.381	0.045
1088	Non identified					0.154	6.491	0.011
1319	Tol-pal system protein YbgF (PA0974)	AGV59417.1	139	8/11	42	0.413	2.420	0.022
1374	Short-chain dehydrogenase (PA1828)	WP_062838333.1	155	8/8	30	0.457	2.188	0.046
1484	2-dehydro-3-deoxyphosphogluconate aldolase EdaB (PA3131)	WP_074253171.1	109	7/14	46	only in BlaR		0.007
1512	Glutamine amidotransferase (PA4336)	WP_033941094.1	169	9/11	52	7.507	0.133	0.012
1584	Gamma-glutamyltranspeptidase (PA1338)	GGT_PSEAE	111	10/12	15 C-fragment	0.139	7.183	0.005
BlaR	Regulatory protein BlaR-CTD	BLAR_BACLI	178	16/25	26 C-fragment	only in BlaR		0.015

Table 9: MALDI-TOF identification of the spots exhibiting a different abundance in *P. aeruginosa* PAO1+pKT240blaR *vs P. aeruginosa* PAO1+pKT240neg. The table reports the associated spot number during the gel analysis, protein name, UniProt Accession number, Mascot search results including score, number of matched peptides and sequence coverage, fold-change in both PAO1 producing BlaR and PAO1 transformed with pKT240neg, and T-test value.
Spots 1088,1319,1374,1484,1512 and BlaR were already described in PAO1vsBlaR; only spots 931 and 1584 are specific to this analysis.

Despite the lack of identification of some spots, the preliminary results obtained did not indicate a clear and univocal increase of some protein pathways that would be responsible for antibiotic resistance or permeability adaptations. Consequently, we decided to rest with the obtained results, and we did not attempt to identify the other spots. We demonstrated that the changes induced by the plasmid and the periplasmic BlaR-CTD production were minor, thus validating our method for this variable.

4.2.2.2 Influence of OprD deletion on periplasmic proteome

TNP065, a strain derived from TNP004, characterized by the deletion of *oprC* porin, in addition to the *oprD* mutation described in TNP004 (Yoneyama *et al*., 1995) was available.
TNP065 periplasmic content was extracted as for the other strains and was compared to that obtained for *P. aeruginosa* PAO1.
The image analysis identified 1176 spots on the TNP065 gel, and the comparative analysis showed 24 differently expressed spots between the two strains, 16 of which were identified by mass spectrometry (Figure 18, Table 10).
The first interesting result is the presence of OprD as a different expressed spot. At the time of the experiment, we believed that this porin was deleted in TNP004 and its derivative strain TNP065.
However, the subsequent identification of the nucleotide substitution in *oprD*, previously exposed in the paper, provided an explanation for the presence of OprD in TNP065. The mutated non-functional porin, whose mRNA was demonstrated to be overexpressed in TNP004, and thus probably in the same way in TNP065, somehow manages to reach the periplasm, but the mutation does not allow OprD to be inserted in the outer membrane, as suggested by the western-blot analysis. Moreover, the fraction that has been isolated in the periplasm is also very small when compared to the reference PAO1.
Secondly, we notice that OprC, deleted in TNP065, is identified in two spots, and, as expected, is only expressed in the wild type PAO1.
The third result highlighted by this analysis is the absence of any identified porin among the spots that are upregulated in TNP065. However, one can notice that 4 spots are more expressed in TNP065 compared to PAO1 are identified as DppA3 and DppA4, two dipeptide-binding proteins included in the network of the DppBCDF transporter, of which OpdP is the associated outer membrane porin.
Between the eight non identified spots only one (named 2222) was overexpressed in TNP065. This isolated protein upregulation allowed us to exclude a massive expression of other porins as a response to the absence of OprD and OprC, two of the most highly expressed porins.
The identification of DppA4 as one of the proteins with differential expression in other conditions (*i.e*. PAO1*vs* neg) might be related to the samples collection time at the beginning of the stationary phase, when OpdP increased expression was described by RT-PCR in the paper.
We cannot be sure that the 2222 spot corresponds to the OpdP porin, but the differential expression of DppA3 and DppA4 was the alarm bell which subsequently led us to investigate the OpdP porin.
In order to obtain a general view of the different expressed proteins, we tried without success to define specific pathways. From this attempt, we can tentatively conclude that the absence of two porins

induced some changes in the bacterial metabolism, increasing for example the expression of the Clp2 protease and the dipeptide transporters DppA3 and DppA4. We should not be surprised if the absence of such important porins could cause some minor metabolic adaptations.

Spot N.	Protein name	Accession number	Mascot search results			BlaRvsTNP065		
			Score	N. of matched peptides	Sequence coverage (%)	PAO1/ TNP065	TNP065/ PAO1	T-test PAO1vs TNP065
418	Not identified					2.268	0.441	0.009
457	Not identified					only in PAO1		0.045
481	Fe(3+)-pyochelin receptor FptA(PA4221)	FPTA_PSEAE	321	25/30	41	4.264	0.235	0.033
482	Not identified					only in PAO1		0.001
483	TonB-dependent copper receptor OprC (PA3790)	EOT19083.1	112	8/9	15	only in PAO1		0.013
485	TonB-dependent copper receptor OprC (PA3790)	EOT19083.1	229	19/27	36	only in PAO1		0.017
571	2-isopropylmalate synthase LeuA (PA3792)	LEU1_PSEAE	223	19/31	45	0.458	2.185	0.026
587	Gluconate 2-dehydrogenase, membrane-bound, flavoprotein (PA2265)	EYT98518.1	154	12/16	22	4.307	0.232	0.016
616	Not identified					only in PAO1		0.0001
647	ABC transporter substrate-binding protein DppA4 (PA4502)	WP_031768557.1	118	8/10	22	0.275	3.636	0.050
648	Peptide ABC transporter substrate-binding protein DppA4 (PA4502)	WP_069954591.1	171	14/23	33	0.199	5.014	0.001
649	ABC transporter DppA4 (PA4502)	WP_021264151.1	223	22/40	53	0.270	3.707	0.006
694	ABC transporter substrate-binding protein DppA3 (PA4500)	WP_057388431.1	199	18/28	35	0.217	4.617	0.002
851	OprD	PORD_PSEAE	223	19/30	57	5.703	0.175	0.023
1510	ATP-dependent Clp protease proteolytic subunit 2 ClpP2 (PA3326)	CLPP2_PSEAE	110	6/7	39 C-fragment	0.097	10.334	0.001
1643	AsnC family transcriptional regulator (PA3965)	WP_034044015.1	138	7/7	42	0.368	2.720	0.036
1707	Not identified					0.409	2.444	0.048
1726	Not identified					3.272	0.306	0.028
1757	Not identified					2.908	0.344	0.046
1768	peroxiredoxin	WP_034022270.1	153	9/17	60	2.253	0.444	0.050
2043	Rubredoxin-NAD(+) reductase RubB (PA5349)	RURE_PSEAE	129	8/9	25	0.374	2.671	0.050
2172	Methylmalonate-semialdehyde dehydrogenase [acylating] MmsA (PA3570)	MMSA_PSEAE	156	11/14	30	0.465	2.151	0.036
2222	Not identified					0.358	2.792	0.0032
2251	Probable binding protein component of ABC iron transporter (PA5217)	P5217_PSEAE	76	8/31	28	0.379	2.638	0.046

Table 10: MALDI-TOF identification of spots exhibiting a different abundance in *P. aeruginosa* PAO1 *vs P. aeruginosa* TNP065. The table reports the associated spot number during the gel analysis, protein name, UniProt Accession number, Mascot search results including score, number of matched peptides and sequence coverage, fold-change in both PAO1 and TNP065, and T-test value.

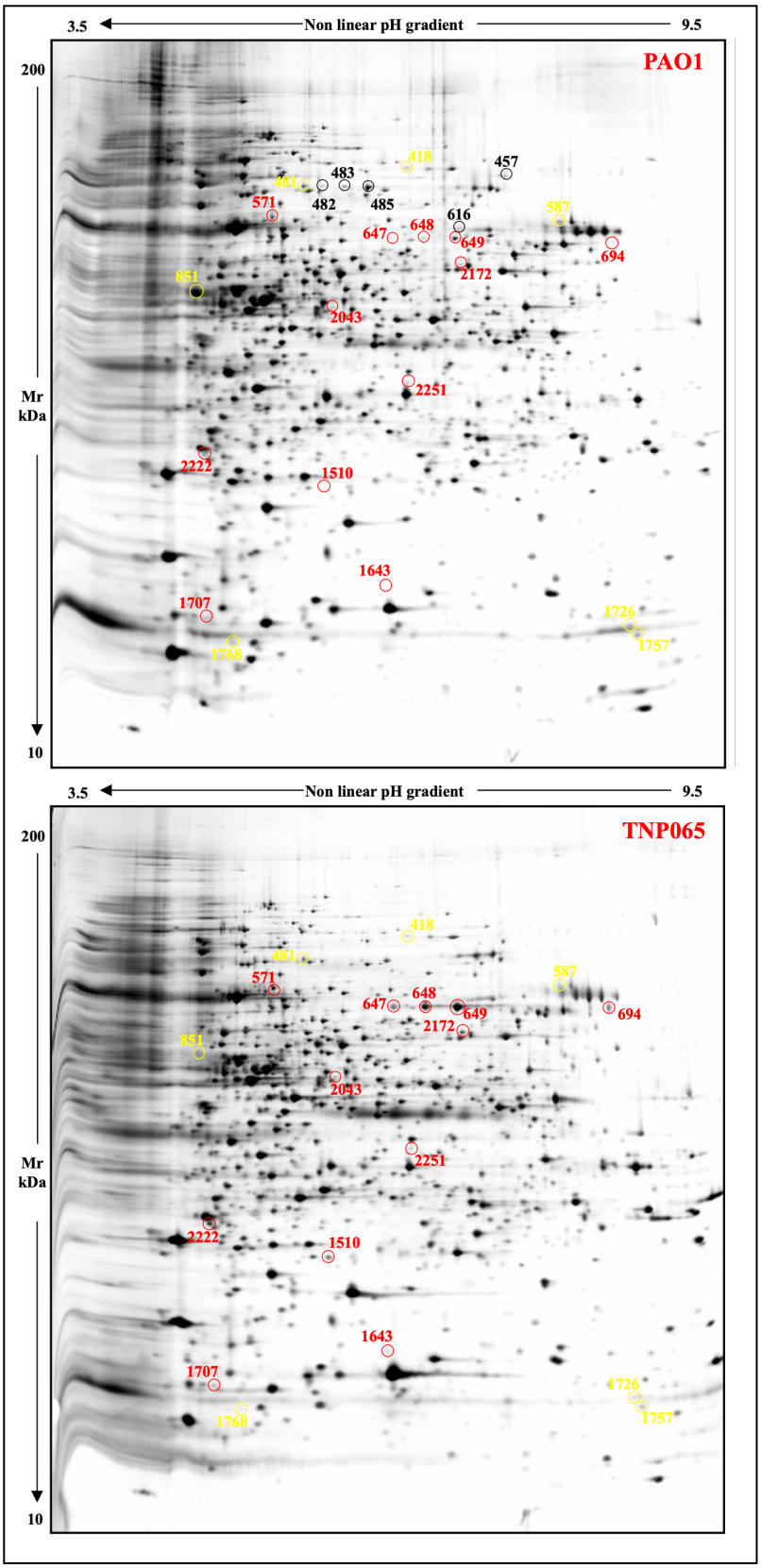

Figure 18: Representative silver stained electropherograms of *P. aeruginosa* PAO1 and TNP065 periplasm; two-dimensional gels that show patterns of proteins ranging from 200 to 10 kDa molecular masses and isoelectric points ranging from 3.5 to 10 pH. Black circles highlight 5 spots only present in PAO1; yellow spots indicate 7 spots that are quantitatively more expressed in PAO1; red spots point out 12 spots that are quantitatively more expressed in TNP065.

4.2.3 Outer membrane permeability determinations

The measurements of antibiotic influx in *P. aeruginosa* PAO1 and different isogenic mutants are described in the paper. The availability of the protocol described in the paper gave us the possibility to measure permeability coefficients also in other conditions, thus allowing the determination of the influence that these may have on permeation. The relevant variables include: *i*) the presence of molecules described to enhance antibiotic activity; *ii*) the deletion of the main efflux pump systems.

4.2.3.1 Membrane stability analysis

Dipicolinic Acid (DPA) is a metal ions chelator, thus possessing the ability to inhibit Metallo-β-lactamases activity and, consequently, to minimize their contribution to β-lactams resistance. This property has been exploited in a research performed by A. Vila's group, aiming at determining the influence of zinc deprivation on NDM-1 activity (Bahr *et al.,* 2017). These researchers stated that DPA is not lethal for bacteria and, starting from this assumption, we decided to investigate whether DPA could otherwise interfere with outer membrane stability, thus enhancing antibiotic permeation and adding a determinant to the decreased MIC observed in their experiments (Bahr *et al.,* 2017).
For this purpose, we determined the permeability to ampicillin, whose permeability coefficient for *P. aeruginosa* PAO1 was previously fixed at 0.008 ± 0.004 nm/sec, in presence of different concentration of DPA.
We tested DPA concentrations ranging from 1 mM to 50 μM (in details: 1000, 750, 500, 250, 100, 50 μM). The first result was that concentrations greater or equal to 500 μM did not allow the determination of any permeability coefficient; in fact, the test performed in presence of 5 μM ampicillin showed a complete acylation of BlaR-CTD by ampicillin already in the first sample collected at time 0. This evidence highlighted a sort of membrane disruption, mediated by DPA, that promoted a massive entry of antibiotic which was therefore no longer mediated by porins or any other permeation mechanisms consistently with what shown by Ude and colleagues (Ude *et al*., 2021).
On the contrary, when the entry of 5 μM ampicillin was performed with 250 μM, 100 μM or 50 μM DPA we succeeded in determining a permeability coefficient by measuring the decrease of periplasmic BlaR-CTD not acylated by the antibiotic. The result was 0.03 ± 0.004 nm/sec, an approximatively 4-fold increase of the permeability coefficient previously measured for ampicillin alone.

The ampicillin permeation coefficient was amongst the most easily reproducible ones, across the different antibiotic tested on *P. aeruginosa* PAO1, suggesting that the observed variation has to be due to the presence of DPA.

This result confirms the hypothesis that DPA plays also a role in the membrane stability and that the MIC decrease, that could be observed in MBL producing bacteria, might be the result of both an enzyme inhibition and a membrane destabilization that increases antibiotic internalization.

We therefore suggest that the decrease in MICs reported by Vila and colleagues was attributable not only to an enzyme inhibition but also to a membrane destabilization induced by DPA.

4.2.3.2 Permeability in an efflux pumps deprived strains

Our method proved sufficiently robust to detect permeability differences due to the lack of porins and gave interesting results concerning the capacity of *P. aeruginosa* to compensate for the absence of a porin.

We were interested in determining the role of a constitutive antibiotic extrusion mediated by efflux pumps in *P. aeruginosa* PAO1, by comparison with the results obtained for PAO509, deprived of the five major efflux pump systems. The results are reported in Table 11, but one can immediately notice that the permeability coefficients results obtained for PAO509 are generally similar to those previously determined for the reference strain PAO1.

Antibiotic	Permeability coefficients (nm/sec)	
	PAO1	PAO509
Ampicillin	0.008 ± 0.004	0.03 ± 0.007
Cephaloridin	0.03 ± 0.01	0.06 ± 0.02
Imipenem	20 ± 9	18 ± 9
Meropenem	0.06 ± 0.01	0.07 ± 0.02
Ertapenem	0.06 ± 0.02	0.03 ± 0.01
Doripenem	0.56 ± 0.38	0.13 ± 0.03
Biapenem	4.7 ± 1.4	4.0 ± 1.4

Table 11: Permeability coefficients determined in *P. aeruginosa* PAO1 and PAO509, deprived of the five main efflux pump systems. A penicillin, a cephalosporin and five carbapenems were tested.

This aspect of the results can be explained by the high affinity of BlaR-CTD for the different β-lactams (paper, Table 3); the acylation rate constants were high enough to ensure that the efflux pumps expressed in the wild type PAO1 and in the porin(s) mutants were able to play their extrusion role solely with the excess of antibiotic that has not acylated BlaR-CTD.

The efflux pumps action can therefore be appreciated when MICs are determined while the shortest time in which permeability determinations are performed only allows to evaluate the instantaneous bond that is formed between BlaR-CTD and the antibiotic. As a consequence, we must retreat from our expected goal of determining the influence of efflux pumps on periplasmic antibiotic accumulation in a wild type strain (PAO1), or in any other strain described to overexpress these systems.

4.2.4 Different *P. aeruginosa* PAO1 lineages

The presence of different lineages of *P. aeruginosa* PAO1, previously available in several distinct laboratories across the world has been widely documented (Klockgether *et al*., 2010). For this reason, when we received the two porin mutant collections provided with their parental strains PAO1-Jap and ARC545 respectively, we first proceeded to store them in our laboratory collection at -80ºC, and every passage was performed from the frozen stock to minimize the risk of accumulation of mutations. We characterized the antibiotic susceptibility of all the mutants, as reported in the article, but also the two reference strains.

Here we report the results obtained for the reference strains that have not been shown in the paper (Table 12). The reference strains showed the same resistance profile as the *P. aeruginosa* PAO1 strain that we obtained from the Belgian Co-ordinated Collections of Micro-organisms (BCCM), and with which we started the determination of permeability coefficients. Moreover, the three strains presented the same MIC values as the *P. aeruginosa* ATCC 27853 strain, that is mentioned in the CLSI guidelines as the reference quality control for *P. aeruginosa* MICs determinations and that was present in our laboratory strain collection.

Antibiotics (µg/mL)	CLSI Standard	ATCC 27853	PAO1	PAO1-Jap	ARC545
Ampicillin	**NA**	2000	2000	2000	2000
Benzylpenicillin	**NA**	>2000	>2000	>2000	>2000
Piperacillin	**1-8**	2	2	2	2
Cefalotin	**NA**	>2000	>2000	>2000	>2000
Cephaloridine	**NA**	>2000	>2000	>2000	>2000
Cefoxitin	**NA**	1000	1000	1000	1000
Cefuroxime	**NA**	250	250	250	250
Cefotaxime	**8-32**	16	16	16	16
Ceftazidime	**1-4**	1	1	1	1
Cefepime	**1-8**	1	1	1	1
Aztreonam	**2-8**	4	4	4	4
Imipenem	**1-4**	1	1	1	1
Meropenem	**0.25-1**	0.5	0.5	0.5	0.5
Ertapenem	**2-8**	8	8	8	8
Biapenem	**0.5-2**	0.5	0.5	0.5	0.5
Doripenem	**0.12-0.5**	0.25	0.25	0.25	0.25
Tetracycline	**8-32**	8	8	8	8
Gentamicin	**0.5-2**	1	1	1	1

Table 12: MIC values of three different *P. aeruginosa* PAO1 and *P. aeruginosa* ATCC 27853 reference strains; CLSI standard refers to acceptable limits for quality control strains (ATCC 27853) used to monitor the accuracy of MICs.

MIC results supported our assumption that the three *P. aeruginosa* PAO1 strains, despite their different origins, could be considered for our permeability experiments as the same reference strain. For this reason, permeability measurements were only performed on the reference *P. aeruginosa* PAO1 strain obtained from BCCM, although the porin mutant strains for which we characterized the permeation properties were characterized as obtained from both PAO1-Jap and ARC545.

4.2.4.1 Searching for mutations

As previously reported in the paper, a whole genome sequencing was performed in order to find mutations in two strains (TNP004 and LG03) characterized by increased carbapenems MICs. To simplify the analysis, we assumed that the inclusion of the two parental strains, PAO1-Jap and ARC545 from which TNP004 and LG03 had been derived respectively, would have facilitated the search of specific mutations.

For this reason, the sequencing of two strains, strictly correlated with each other would have easily highlighted mutations involved in the phenotypic resistance profile, excluding variations due to different lineages. As a proof of that, we found that the (supposed) reference strains PAO1-Jap and ARC545, formerly both *P. aeruginosa* PAO1 strains, carried some different mutations compared to the reference PAO1 (GenBank accession number AE004091). Interestingly, the mutations found were not limited to single nucleotide polymorphisms that could have been generated in the various passages performed in the laboratories of origin, or during the few passages we performed in order to stock the strains in our bacterial collection. Indeed, we found two different deletions that were curiously located in the same *locus* for both strains, *i.e.* the dipeptide-binding protein *dppA3* gene and an adjacent intragenic region. Notably, the intergenic region separates *dppA3* from *opdP*, the porin we contributed to characterized for antibiotic permeation specificity and its role in antibiotic resistance (Figure 19).

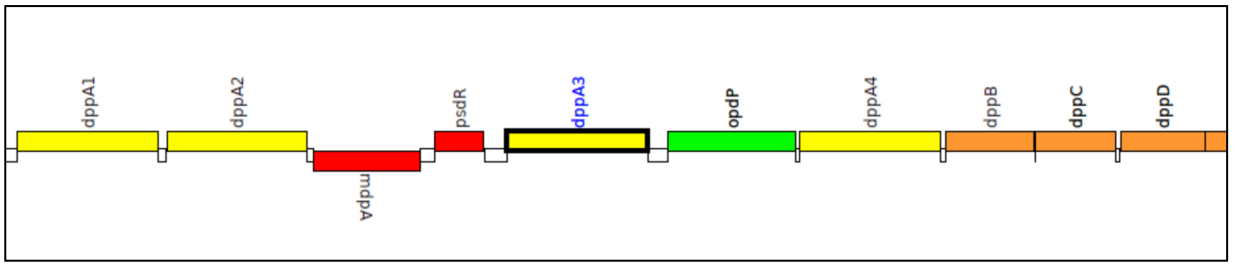

Figure 19: Graphic representation of the genome fragment including *opdP, dppA3* and the intergenic region located between these genes.

In particular, both strains exhibited a 6-nucleotide deletion (CCCTGA) in *dppA3* after G 1596, resulting in the deletion of its TGA stop codon and of the successive 2 nucleotides (TG) in the following intergenic region. In addition, ARC545 was deleted of 2 nucleotides (AG) after C 1594 that precede the above mentioned 8 bp deletion, while PAO1-Jap contained a 10 nucleotides deletion (CCGACGCCGC) in the intergenic non-coding region located between *dppA3* and *opdP*, that followed the 8bp common deletions (Figure 20).

```
PAO1 BCCM     CTTCTATGGCGTAGCCAACCAGCCCTGATGCCGACGCCGCCCCGGTCGTGAAACGACCGG    60
PAO1-Jap      CTTCTATGGCGTAGCCAACCAG----------------CCCGGTCGTGAAACGACCGG    42
ARC545        CTTCTATGGCGTAGCCAACC----------CCGACGCCGCCCCGGTCGTGAAACGACCGG    50
TNP004        CTTCTATGGCGTAGCCAACCAGCCCTGATGCCGACGCCGCCCCGGTCGTGAAACGACCGG    60
LG03          CTTCTATGGCGTAGCCAACCAGCCCTGATGCCGACGCCGCCCCGGTCGTGAAACGACCGG    60
ARC5170       CTTCTATGGCGTAGCCAACCAGCCCTGATGCCGACGCCGCCCCGGTCGTGAAACGACCGG    60
```

Figure 20: Alignments of *dppA3* and the adjacent intragenic region for three different PAO1 strains (PAO1 obtained from BCCM, PAO1-Jap, ARC545), TNP004 derived from PAO1-Jap, ARC5170 and LG03 derived from ARC545. The *dppA3* TGA stop codon is highlighted in green.

Moreover, these mutations found in PAO1-Jap and ARC545 were not present in the derived strains TNP004 and LG03, thus indicating that the reference strains had been propagated several times (and maybe subjected to some selective pressure) after the completion of the experiments where porin deletion mutants were obtained (Satake *et al*., 1991; Isabella *et al*., 2015).
The same region was verified by Sanger sequencing on *P. aeruginosa* PAO1 obtained from the BCCM collection and on ARC5170, the strain from which we derived the LG03 mutant, confirming that they were homologous to the reference PAO1 (GenBank accession number AE004091) (Figure 20).
We can therefore speculate that PAO1-Jap and ARC545 would have somehow accumulated these mutations not found in TNP004 and ARC5170 and, as a consequence, we cannot really consider them as parental strains.

4.2.4.2 Is OpdP expression affected?

The proximity of these mutations with the studied *opdP* gene made us suspect that these might somehow affect OpdP expression. As previously mentioned, an operon, regulated by the repressor PsdR, determines the expression of *dppBCDF*, while the inclusion of *opdP* and *dppA4* in such an operon is a debated question (Kiely *et al*., 2008; Pletzer *et al*., 2014). For this reason, we wondered whether these mutations could have somehow altered the operon organization and consequently OpdP expression.
An in-silico analysis performed using operon-mapper, a web server tool for operon prediction was performed (Taboada *et al*., 2018). It predicted that these deletions were responsible for the change of the operon organization, by eliminating the function of a transcription terminator, located before the *opdP* gene. In particular, in *P. aeruginosa* PAO1-Jap, *dppA3* and *opdP* are supposed to be co-transcribed in a unique 1088 amino acid fusion protein. However, the specific porin signal peptide has been predicted to be recognised, despite the synthesis of OpdP as a fusion protein. In consequence, it is reasonable to conclude that the expression of the porin is no longer influenced by the repressor located between *dppA3* and *opdP*, thus resulting in upregulation.
On the contrary, in ARC545 the deletion caused the synthesis of a 73 amino acid longer DppA3, thus changing the *opdP* operon organization. Accordingly, the mutated *dppA3* seems to be included in the downstream operon and, by consequence, also in this case, OpdP is no longer regulated by the

transcription terminator. In conclusion, both mutations seem to alter OpdP expression and give rise to an overexpression of this porin.
These are the only main mutations that we found in PAO-Jap and ARC545 and we were very surprised that these mutations seemed to alter the expression of OpdP, resulting in two hypothetical OpdP overexpressors.

4.2.5 OpdP quantification

The relative *opdP* expression has been investigated by means of RT-PCR, demonstrating the increased expression of the porin in the late exponential phase, but also its positive regulation mediated by the lack of expression of OprD, as in the case of ARC5990.
We were interested in validating this result through the quantification of the increased expression of the synthesized porin and its insertion in the outer membrane. Moreover, we were intrigued by the prediction that assumed an OpdP overexpression in PAO1-Jap and ARC545.
We will now expose the results obtained in this regard.

4.2.5.1 Outer membrane profiles

The outer membrane profiling, as reported in the paper concerning OprD western-blot, was performed by adapting a previously reported protocol (Kolayli *et al*., 2004). We were careful to collect all the samples at the same point of the growth phase, in order to correctly compare results. This approach allowed us to visually appreciate the proteins associated to the outer membrane in an SDS-PAGE, removing several proteins that are not related, thus supporting the possibility to evaluate the presence/absence of specific porins. This potentiality is limited to highly expressed porins, such as OprD or OprF. For example, it is possible to demonstrate the absence of OprD in TNP004, ARC5990, ARC5782 and ARC5998 (Figure 21).
However, it turned out to be impossible to recognize the absence of the 53 kDa OpdP porin in ARC5170, ARC5782 and ARC5998. As a consequence, the method we used turned out not to be valid in order to detect any variations in OpdP expression.

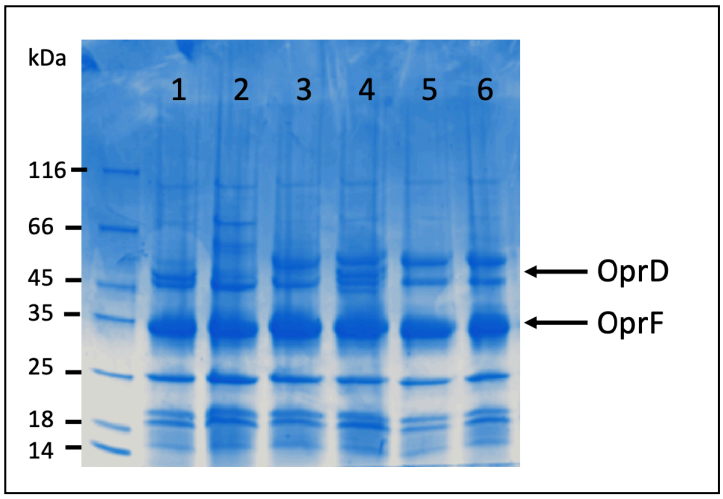

Figure 21: Outer membrane profiles of the following strains: 1) PAO1, 2) TNP004, 3) ARC5990 (*ΔoprD*), 4) ARC5170 (*ΔopdP*) 5) ARC5782 (*ΔoprD*, *ΔopdP*) 6) ARC5998 (*ΔoprD*, *ΔopdP*, *ΔopdB*, *ΔopdC*, *ΔopdT*); the porins OprD (45.9 kDa) and OprF (37.6 kDa) are identified by an arrow.

4.2.5.2 Setting up OpdP western-blot

Western-blot is clearly a validated method to detect variations in the expression of a selected protein. In the case of OprD, we easily obtained a previously raised antibody (Epp *et al.*, 2001) and, as reported in the paper, we demonstrated the absence of functional OprD in TNP004, ARC5990 and in the other *oprD*-deleted strains, but also a decreased expression in LG03 (*Ibid.*, Figure 2). However, the lack of availability of an already used antibody against OpdP made the direct quantification of OpdP expression more laborious.

We now describe the various steps that resulted in the development of a western-blot protocol for OpdP quantification.

4.2.5.2.1 OpdP production and purification

OpdP production was obtained in inclusion bodies in LB medium. OpdP expression was performed with an His_6 tag to facilitate its purification by affinity chromatography using a Ni-NTA HisTrap column.

The purification of the solubilized inclusion bodies was achieved on a bench column. The collected different fractions of washing and elution were analyzed on an SDS-PAGE (Figure 22). Note that the majority of contaminants did not bind to the column and were not retained.

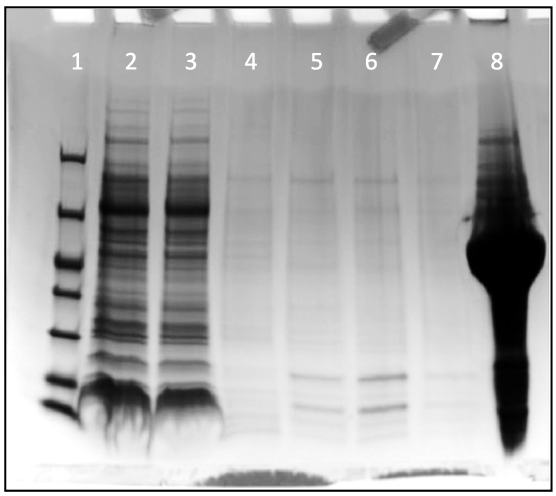

Figure 22: Purification of OpdP porin; 1) marker, 2) load, 3) not retained, 4-5) two fractions of washing with equilibration buffer, 6-7) two fractions of washing with 20 mM imidazole, 8) eluted protein.

The fraction containing the porin was concentrated and dialyzed against 8 M urea, and a porin concentration of approximatively 2 mg/mL was obtained.

For further confirmation, the produced protein was identified as OpdP by mass spectrometry. Since it turned difficult to correctly refold the porin, we decided that using the denatured porin would be the easiest way to provide the antigen for rabbit immunization.

4.2.5.2.2 OpdP immunization

The rabbit immunization was performed by an external facility, where the possibility to use SDS-PAGE-slices as a starting material to be injected was tested. Different fractions of rabbit serum were provided following a specific scheduled timing.

4.2.5.2.3 Purification of polyclonal antibodies by affinity chromatography

The polyclonal antibodies were purified by affinity chromatography using a HiTrap Protein A HP antibody purification column (Cytiva). This chromatography allows to bind the antibodies to the protein A on the matrix by the fragment crystallizable region of the antibodies. Elution of the polyclonal antibodies was performed under acid condition (20 mM glycine buffer, pH 2.2).

The polyclonal antibodies purification was performed on different sera samples obtained at different collection times. In particular, we purified the zero-time serum (pre-immunization) and the sera collected at day 38, 66 and 87.

The different elution fractions were collected and loaded onto an SDS-PAGE to identify those containing antibodies. The Coomassie-stained SDS-PAGE demonstrated the presence in the first elution fraction of two bands of approximatively 25 and 50 kDa. These correspond, respectively, to the light and heavy chain of polyclonal antibodies (Figure 23).

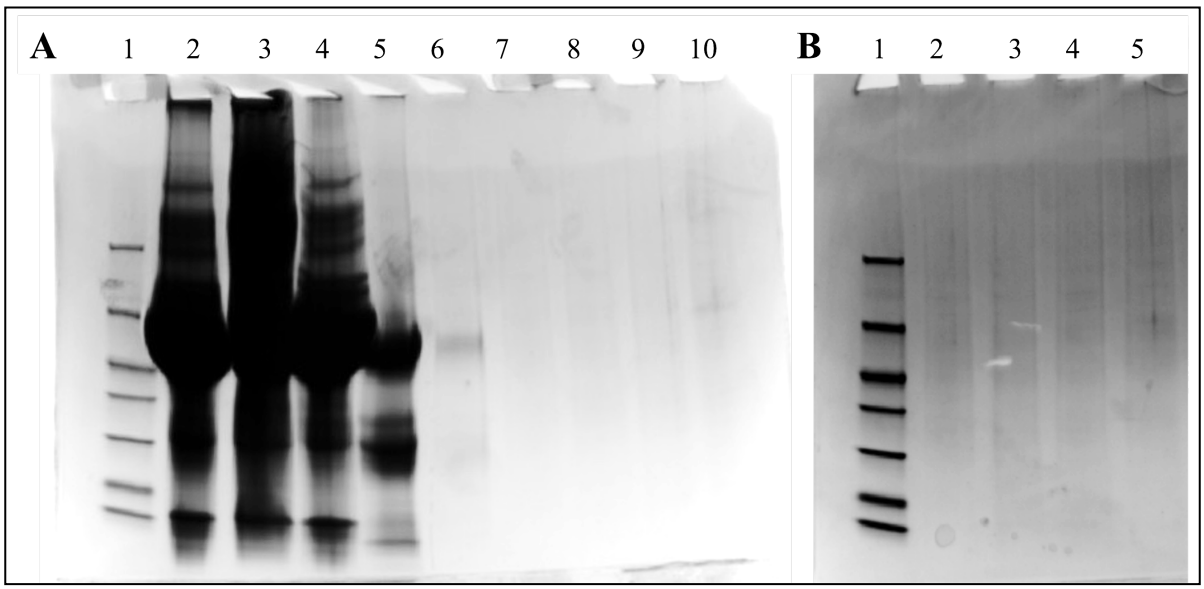

Figure 23: Coomassie-stained SDS-PAGE used to assess the efficiency of the affinity purification. **Gel A**: 1) marker, 2) loading, 3) wash 1st fraction, 4) wash 2nd fraction, 5-10) elutions, fractions 1 to 6; **Gel B** 1) marker, 2-5) elutions, fractions 7 to 10.

4.2.5.2.4 OpdP western blot

We had originally decided to verify the absence in the rabbit serum of any antibody that could recognize OpdP, formerly an outer membrane protein, with domains shared with other bacterial outer membrane proteins. Unfortunately, we noticed that at the initial time, the rabbit already possessed an immunization status which led it to recognize proteins collected in the outer membrane extract.

The wester-blot shown in Figure 24 highlighted a signal present in all the strains, including ARC5170 that lack OpdP suggesting the presence in the outer membrane extracts of some proteins containing epitopes recognized by antibodies present in rabbit serum.

We were not able to identify which proteins were recognized, but we excluded a previously raised response against OpdP, considering the negative result in the sample containing the purified porin.

Moreover, as shown in Figure 24, the nonspecific proteins exhibit a molecular mass not far from the 53 kDa of the OpdP porin.

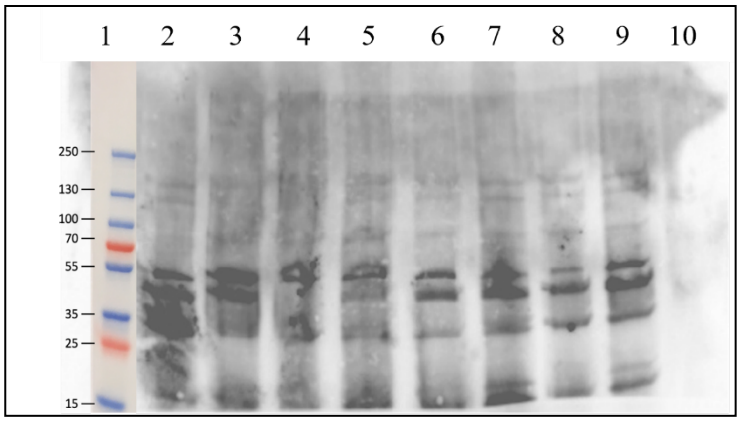

Figure 24: Western-blot using antibodies purified from pre-injection serum. 1) marker, 2) PAO1 BCCM, 3) PAO1-Jap, 4) TNP004, 5) ARC545, 6) ARC5990 (*ΔoprD*), 7) ARC5170 (*ΔopdP*), 8) ARC5782 (*ΔoprD, ΔopdP*), 9) ARC5998 (Δ5porins), 10) OpdP purified.

Confident that the nonspecific signal would have decreased (and not being able to do otherwise, considering the already started immunization protocol), we performed western-blot using the antibodies raised from the three-bleeding points. Several attempts were made to obtain evaluable results. However, the antibodies obtained at the three times were all characterized by the presence of nonspecific signals.

We show here what we believe to be the best result obtained on this topic (Figure 25). The recognition of the purified OpdP confirmed the presence of specific antibodies, but the nonspecific bands did not allow us to consider them as an adequate result to be included in the paper. One can notice that the highest OpdP expression was in ARC545, consistent with the porin overexpression suggested by the operon prediction.

The absence of OpdP in ARC5170 was a result similar to that obtained with the double mutant ARC5782 (*ΔoprD, ΔopdP*) and with the five porin mutants ARC4567, but also with PAO1 derived from BCCM for which RT-PCR exhibited a basal expression. Compared to *P. aeruginosa* PAO1 BCCM, ARC5990, the strain lacking OprD showed an increased OpdP expression, consistent with the increased mRNA expression observed by RT-PCR. Despite the transcription of a nonfunctional

oprD, TNP004 did not show an OpdP increased expression. This result is in agreement with what found through RT-PCR, which showed an *opdP* transcription similar to that in PAO1 BCCM.
Finally, PAO1-jap showed an OpdP expression which is between those in PAO1-Jap and ARC545. This evidence can be rationalized as the result of the expression of a DppA3-OpdP fusion protein and the consequent lack of OpdP repressor activity. In contrast, ARC545 mutations appear to induce a single OpdP protein overexpression, thus resulting in a more abundant OpdP expression.
The analysis of small amounts of expressed porin, in particular in comparison with OprD, and the presence of nonspecific bands did not allow us to obtain a precise quantification of the increased ratio between *P. aeruginosa* PAO1 (BCCM) and the isogenic *oprD* mutant ARC5990. However, our results confirmed what we had shown by RT-PCR *i.e.* that the absence of *oprD*, but not the transcription of a nonfunctional porin, caused an OpdP upregulation.
Interestingly, this experiment allowed us to verify what the operon-mapper suggested *i.e.* that the mutations found in ARC545 and PAO1-Jap are indeed the cause of an OpdP overexpression.

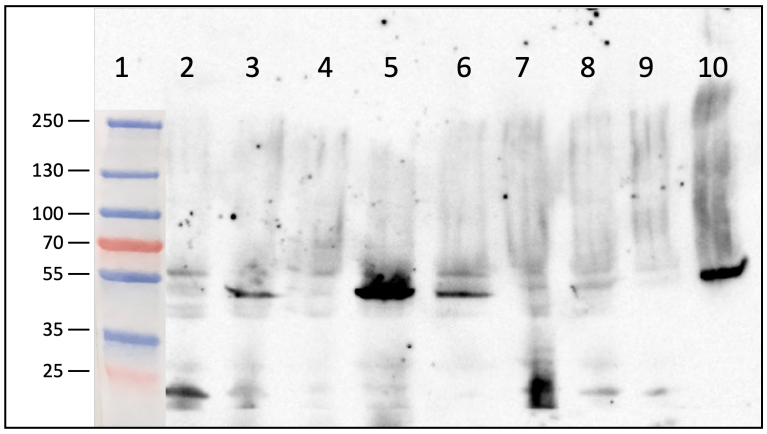

Figure 25: OpdP detection by western-blot. 1) marker, 2) PAO1 BCCM, 3) PAO1-Jap, 4) TNP004, 5) ARC545, 6) ARC5990 (*ΔoprD*), 7) ARC5170 (*ΔopdP*), 8) ARC5782 (*ΔoprD, ΔopdP*), 9) ARC5998 (Δ5porins), 10) OpdP purified.

5 DISCUSSION

In this thesis we studied the permeability of the outer membrane of *P. aeruginosa* by analyzing the role of some porins in the entry of β-lactams. The intrinsic resistance of *P. aeruginosa* to many antibiotics is well known, as is the fact that it is mediated, among other factors, by low permeability of the outer membrane. Furthermore, the involvement of the porin OprD in the uptake of imipenem is well known, particularly the presence of resistance profiles to this antibiotic when the porin is not properly expressed. The inclusion of *P. aeruginosa* in the so-called ESKAPE pathogens, for which the development of new therapeutic alternatives is required, also necessitates a better understanding of the intrinsic permeation properties of the bacterium. To highlight this interest, during this doctoral project, a consortium of European universities participated in the "New Drugs 4 Bad Bugs" program. One of the challenges of this program was the study of translocation properties, directing efforts to understand the penetration of antibiotics through the double membrane of Gram-negative bacteria. Considering the importance of this topic, and independently from other research centers -as we were initially unaware of their studies- we found it interesting to revisit a study conducted at the University of Liège that had yielded intriguing preliminary results regarding the permeability characteristics of *P. aeruginosa*.

5.1 Validation of the analysis methodology

The objective of this study was to reproduce the method delineated by Lakaye and colleagues, who more than 20 years ago successfully determined permeability coefficients for *E. cloacae* and *K. aerogenes* and provided preliminary findings for *P. aeruginosa*. We also introduced appropriate modifications to keep the conditions that could potentially influence our measurements under control.

The commercial availability of Bocillin, a fluorescent penicillin, allowed us to avoid using radiolabeled antibiotics, which would have complicated the measurement process and also would have produced biased results due to the difficulty of distinguishing adsorption from uptake. In this way, any β-lactam could be evaluated with Bocillin as an indirect reporter molecule.

Moreover, during the development phase of the analysis, it was established that the utilization of a refrigerated and automated sonicator significantly increased the reproducibility of the isolation of the periplasmic content, compared to the previously described freeze-thaw method.

As outlined in the literature and summarized in the introductory chapter 1.7, all methodologies employed thus far to ascertain the permeation characteristics of compounds through biological

membranes have different strengths and limitations regarding the extrapolation of results. While we do not claim that the proposed method is devoid of challenges, we consider it a cautious way to minimize the influencing variables and to verify that the developed system closely reflects the physiological entry of the antibiotic.

5.1.1 Growth phase

First of all, our measurements were based on the periplasmic amount of BlaR-CTD in a given culture volume. The maximum time required to record the entry of an antibiotic in our measurements was 40 minutes. Considering this assumption, we had to face the fact that during exponential (log) phase for a *P. aeruginosa* culture, the bacterial doubling time is about 20-30 minutes. For this reason, we excluded to perform the measurement during the log phase, since bacterial growth during this time interval would have consequently resulted in increased synthesis of BlaR-CTD, interfering with the accuracy of the results.

For this reason, we decided to start our measurements when the bacterial culture exited the log growth phase, going into the stationary phase, at an OD of approximately 2. As shown in Figure 3 of the paper, all strains tested for permeability -despite the deletion of one or more porins- displayed similar growth patterns. In particular, around an OD of approximatively 2 and within the maximal 40-minute time frame used in our experiments, there was no significant increase in bacterial population that could have affected the results.

This choice allowed for good reproducibility of the experiments, but also confronted us with conditions that were initially unexpected. The role of the OpdP porin appeared to be marginal in the early log phases, being less expressed when compared to the initial stationary phase, as can be seen in Figure 4 of the paper. Conversely, the OprD porin was less expressed when the culture entered the stationary phase.

Therefore, performing our measurements at the onset of the stationary phase helped us to better highlight the role of the OpdP porin. Its deletion caused little to no changes in the MIC of meropenem and biapenem, two antibiotics for the uptake of which we found a significant involvement of OpdP during our experiments.

This observation also led us to a broader consideration: how MIC measurement may have limitations in predicting the behavior of the bacterium *in vivo*.

We can imagine that during an infection caused by a *P. aeruginosa* strain carrying an *oprD* deletion, a portion of the bacterial population -likely not marginal, given the tendency of the bacteria to form biofilms- might appear resistant to meropenem based on MIC values. However, this evidence could

be partially contradicted *in vivo*, due to a possible overexpression of OpdP that correlates with increased meropenem permeability.

5.1.2 Influence of efflux pumps

In 1991 Livermore and Davy pointed out that the method developed by Zimmermann and Rosselet, which was efficiently used to determine permeability coefficients in *E. coli*, was not suitable for bacteria expressing a high number of efflux pumps, such as *P. aeruginosa* (Livermore and Davy, 1991). This assumption first led Lakaye and collaborators, and later us, to use a different method for measuring specific permeability coefficients of β-lactams in *P. aeruginosa*.

The question of whether varying efflux pump expression could influence our measurements did arise. However, the idea that *P. aeruginosa* PAO1 and all the tested PAO1 derived-mutant strains expressed similar levels of efflux pumps initially allayed our concerns in this regard. In fact, the possibility to highlight the increased or decreased permeability due to the absence (or overexpression) of a porin was a matter of fact.

A clear answer regarding the reliability of our antibiotic permeability measurements came when we had to confront our inability to assess the role of the absence of the major efflux pumps in the PAO509 strain on the permeability coefficients. The different MIC values determined for the wild-type PAO1 and the PAO509 strain confirmed the role that these pumps play in antibiotic resistance. However, despite this significant difference, we obtained similar permeability coefficients for both strains. This indicates that our method allows to immediately detect the antibiotic entry *via* the acylation of BlaR-CTD. As a consequence, the antibiotics did not have time to be intercepted and expelled by efflux pumps, thus eliminating any possible effect of the efflux pumps.

On the other side, this also led us to conclude that our method does not allow to determine the amount of antibiotic expelled by the efflux pumps, and therefore cannot be used to better characterize their activity.

5.1.3 Study of the periplasm

One of the issues that concerned us from the outset was the evaluation of the impact that the expression of an additional PBP, such as BlaR-CTD, could have at the periplasmic level, or whether the presence of a plasmid might alter the composition of the periplasm. For this reason, we collaborated with the proteomics laboratory at the University of Siena (where I had previously completed an internship over several months). In this regard we thought that it would be interesting

to assess whether and how the periplasmic content might change depending on the presence of a plasmid containing the *blaR-CTD* gene, or the same plasmid but lacking this gene. To carry out this analysis, we replicated a method described in the literature to be highly effective in isolating the periplasm of *P. aeruginosa* (Imperi *et al*., 2009). By subjecting cells representing the three possibilities to 2-DE analysis, we found that the proteins differentially expressed according to the conditions were few, and none of them appeared to be related to systems that could affect permeability, or potentially the degradation of the antibiotic that had entered the periplasm. Of particular interest, the comparison between two strains transformed with the two plasmids, one carrying *blaR-CTD* and the other not, showed that, besides BlaR-CTD, only 7 proteins were differentially expressed. Of these, only 5 were identified, and the lack of metabolic correlation among them reassured us that the changes introduced by the plasmid as a consequence of the production of BlaR-CTD were minimal. As previously mentioned, any method used to measure membrane permeability represents a compromise between the measurement itself and any changes that the imposed conditions might have on the results. In any case, our system allowed us to detect variations in permeability in strains expressing different porin profiles, thereby making it possible to fully achieve the goal of our study.

5.1.4 MIC variations

To rule out any possible effect that the periplasmic production of BlaR-CTD might have on the bacteria, we found it necessary to compare the MICs for various strains with those of the corresponding ones transformed with the pKT240blaR plasmid (or with pKT240blaR-gen in the case of TNP004). As shown in Table 2 of the paper, for most antibiotics, no changes in MIC values were recorded between the parent strain and the corresponding derivative transformed with the plasmid containing the *blaR-CTD* gene. Obvious exceptions were tetracycline and gentamicin, that were the selective antibiotics for the utilized plasmids. This result allowed us to conclude that the presence of an additional PBP in the periplasm of *P. aeruginosa* did not alter its susceptibility to the various antibiotics tested. However, this conclusion did not hold for piperacillin, ceftazidime, and cefepime. In all tested conditions, the presence of BlaR-CTD, but not the presence of the empty plasmid pKT240neg, was associated with an increase of up to four serial dilutions in MIC values between the non-BlaR-CTD-producing strain and its BlaR-CTD-producing counterpart.
This finding led us to exclude these three antibiotics from the permeability experiments and raised questions about the real causes of such a change.

Although we were not able to conduct specific investigations on this matter, we believe that a possible explanation could be the lower affinity of the natural PBPs of *P. aeruginosa* for these three antibiotics (Montaner *et al*., 2023). During the overnight incubation, when the bacterial inoculum remains in contact with the antibiotics, after these antibiotics cross the outer membrane, they might bind more efficiently to BlaR-CTD than to their natural PBP targets. This difference, over the course of the incubation period, could result in the MIC-increased phenotype that we observed. However, this explanation remains a hypothesis that was not verified or further investigated, as we preferred to exclude these antibiotics from our measurements and rather focus on enlarging the range of tested carbapenems, with which we obtained interesting results.

5.1.5 Presence of inducible β-lactamase

P. aeruginosa PAO1 carries three genes coding for β-lactamases. Although PIB-1 and POX-B have been described as playing only a marginal role in the resistance mechanisms of the bacterium, with their expression limited to a constitutive basal level, the same cannot be said for AmpC.

AmpC is known to be inducible, and its expression is triggered by peptidoglycan degradation products in the presence of β-lactams, particularly imipenem and cefoxitin. Given the significant association between imipenem and OprD, and therefore the importance of comparing permeability coefficients between the wild-type and the porin-deleted strain, it was essential to verify that the presence of the antibiotic at the highest concentration tested during the experiment did not induce AmpC expression. This would have affected the measurement during the test. Equally important, we were concerned that other antibiotics, which were tested for a longer duration than imipenem, might also induce AmpC production. AmpC could then compete with BlaR-CTD for binding the antibiotic, leading to unreliable data over the course of the experiment. This possibility was ruled out by verifying that none of the antibiotics, at their highest concentrations and within the specific timeframes used in the permeability experiments, caused considerable AmpC induction. As shown in Table 4 of the paper, nearly all tested antibiotics induced specific AmpC activity to a level similar to that of the control, that was measured by assessing AmpC activity in the absence of any antibiotic. A slight induction was observed in the case of ertapenem (4-fold compared to the baseline value of cultures grown without antibiotics). However, we do not believe that this minimal induction significantly modified the observed data. Different considerations hold for cefoxitin, which is well known to be a strong inducer of AmpC. Indeed, we observed an approximately 40-fold increase in AmpC specific activity when 30 µM cefoxitin was incubated for 30 minutes in a culture of *P. aeruginosa* PAO1. This result highlights a potential limitation of the system used, namely that for

certain antibiotics, a strain deleted for AmpC should ideally be used to avoid competition between this enzyme and the expressed BlaR-CTD. However, the data related to cefoxitin were used only in the case of *P. aeruginosa* PAO1 and appeared consistent with other second- and third-generation cephalosporins, suggesting that the system is sufficiently robust to remain unaffected by AmpC induction. Moreover, the measurements were taken within time frames shorter than 40 minutes, the time interval within which AmpC induction was observed, which might nevertheless allow an accurate measurement.

5.1.6 BlaR-CTD affinity for β-lactams

The last variable we wanted to analyze was the affinity of various β-lactams for BlaR-CTD.
Since the first study conducted on BlaR-CTD, the high specificity of this water-soluble carboxy-terminal domain of the *B. licheniformis* receptor for a wide range of penicillins, cephalosporins, and monobactams had already been demonstrated (Duval *et al*., 2003).
The published kinetic parameters for BlaR-CTD were indeed significantly higher than those determined for the *B. licheniformis* PBP1 or for a wide set of PBPs expressed by other bacteria.
A complete list of the affinity parameters of *P. aeruginosa* PBPs for all the antibiotic tested has not been determined but, based on the available data, we believe that they cannot reach the high values published for BlaR-CTD (Smith *et al*., 2013; Montaner *et al*., 2023).
We therefore extended the determination of BlaR-CTD kinetic parameters to all the antibiotics considered in the permeability study. As expected, we were able to verify that, despite minor differences, all the antibiotics whose membrane permeability was analyzed formed a stable acyl-enzyme with BlaR-CTD. In this way, we were able to demonstrate that the BlaR-CTD produced in the periplasm could successfully compete with the antibiotic target, thus capturing almost instantaneously the β-lactam that crossed the outer membrane. This evidence thus supported our study model.

5.2 Determination of Permeability Coefficients

After having ruled out the possibility that any of the involved variables could alter the bacterial physiological uptake, the method relying on the expression of BlaR-CTD in the periplasm was used to determine the permeability coefficients of many β-lactams in *P. aeruginosa* PAO1. To our knowledge, this study is the first to characterize the translocation properties of a wide range of β-lactams in an in vivo model of *P. aeruginosa*.

Interestingly, we identified carbapenems as the antibiotics with the highest capacity to overcome the outer membrane barrier. We found that imipenem, with a coefficient of 20 ± 9 nm/sec, is the antibiotic with the fastest penetration rate, followed by biapenem (4.7 ± 1.4 nm/sec) and doripenem (0.56 ± 0.38 nm/sec). Their ability to reach the periplasm more easily than other β-lactams, combined with their moderate stability towards inactivating enzymes and good affinity for the bacterial PBPs, makes carbapenems a valid option in the treatment of these infections.

Penicillins and cephalosporins, although largely not considered valid therapeutic choices, were included in the study to determine their permeation characteristics. With the exception of cephaloridine, their permeability coefficients were at least 10 times lower than those of carbapenems.

The MICs for piperacillin, ceftazidime, and cefepime (that represent valid therapeutic options) increased in the presence of BlaR-CTD. For this reason, we did not consider the determination of their specific coefficients to be reliable. Furthermore, some preliminary experiments carried out to establish measurements with these three antibiotics and (in addition with cefotaxime) did not produce consistent and reproducible data to reliably determine permeability coefficients.

The inability to apply the method to all antibiotics, likely due to *in vivo* interactions, is undoubtedly a limitation of this study. However, this drawback must be weighed against the opportunity to investigate the characteristics of numerous antibiotics, including carbapenems.

The second goal of the study was to determine the changes that the absence of one or more porins could cause to the previously determined coefficients. We received two mutant strains with deletions of the OprD porin that, despite different underlying mechanisms (*i.e.,* deletion or synthesis of a structurally non-functional porin), showed rather similar permeability results. Specifically, although the MICs for all carbapenems increased, the only permeability coefficient that increased for both strains was that for imipenem (by about 130-fold). Notably coefficients for the other carbapenems remained stable (Paper, Table 6).

This result was partially expected on the basis of literature data describing the role of OprD in the permeation of imipenem that underlined the structural homology between arginine (the natural substrate of the porin) and the side chain of imipenem. The generalized increased MICs for all carbapenems in the absence of the OprD porin would instead have suggested some change in permeability that, however, was not noticeable. In a constructive way, this result led us to conclude that it is not possible to use our developed method to predict in vitro MIC values. In fact, initially, we speculated that the MIC variations resulting from an absence of a porin might directly correlate with a decrease in permeability, and consequently that the knowledge of the permeability coefficient could thus be used to predict *in vitro* MIC variations. This finding prompted us to focus on the

mechanism underlying this apparent incongruity and on the potential role of other porins in the permeation of the remaining carbapenems.

Although we had access to two different collections of porin mutant strains, we decided to focus only on the one that included the deletion of the OpdP porin, that according to the literature, showed the highest homology with OprD. Moreover, using a proteomic approach that compared TNP065 to the reference strain PAO1, we observed an increased expression of proteins encoded by a genomic region adjacent to the one containing *opdP*. This finding provided us with an additional rationale to investigate this porin.

The mutant strain with a single deletion of *opdP* did not display significant differences in MIC values. Similarly, the measured permeability coefficients were very close to those for the PAO1 wild type. Unexpectedly, strains with simultaneous deletions of both *oprD* and *opdP* and that phenotypically exhibited a resistance profile similar to that of the single *oprD* mutant, exhibited an unexpected permeability behavior.

The double deletion of these two porins led to significant drops in the permeability coefficients of meropenem and biapenem, 10-fold and 30-fold respectively, highlighting how both porins are associated with these antibiotics and how they exhibit a synergistic organization.

The single deletion of either *oprD* or *opdP* alone did not suggest their involvement in biapenem or meropenem uptake, due to the residual compensatory activity shown by the remaining porin. A 20-fold increase in *opdP* expression observed by RT-PCR in log phase in the strain deleted of *oprD* undoubtfully constitutes a valid explanation of the compensatory effect (Paper, Figure 4). However, the *opdP* expression in the log phase is only marginally increased in TNP004, while in the stationary phase both OprD mutated strains restored an OpdP expression level that does not markedly deviate from that of the wild-type PAO1. We therefore hypothesized that the correlation between permeability coefficients and porin expression levels in OprD mutant strains was related to the OpdP conductance, that has been determined as 30-fold high compared with OprD (Liu *et al*., 2012a). We concluded that the slight OpdP increased expression as a function of growth phase is sufficient in the early stationary phase to compensate for the absence of OprD in the uptake of meropenem and biapenem.

This result underscores the importance of characterizing permeation both *in vivo* and *in vitro,* allowing for the detection and elucidation of such compensatory phenomena.

In an attempt to determine the function of other porins in permeation, we repeated permeability coefficient measurements for strain ARC5998, deleted of three additional porins, as well as of OprD and OpdP. In this case, however, we observed coefficients comparable to those of the OprD, OpdP

double mutant, thereby excluding the involvement of OpdC, OpdB, and OpdT in the permeation of the studied antibiotics.

Despite having single porin mutants for *oprC* and *oprE* and various combinations of their deletions along with the *oprD* mutation, characteristic of TNP004, determining permeability coefficients for these strains was not deemed necessary for our study. In these strains, the absence of MIC changes between wild type and *oprC* and/or *oprE* mutants was one of the reasons for their exclusion from the study. However, the specificity of OprC for copper ion uptake, essentially functioning as a siderophore, did not suggest a particular involvement in carbapenem permeation. Moreover, the lack of overexpression of other porins in strain TNP065, verified through a proteomic approach, led us to consider the deletion of OprE as not particularly significant.

It would certainly be of interest in the future to characterize the permeability coefficients of these strains and of additional porin-deleted strains to assess their potential individual or combined role in β-lactam uptake. In this regard, it would be advisable to accordingly analyze the strain deleted of 40 porins (described by Ude and collaborators, 2021), to evaluate potential variations in permeability in addition to simple MIC measurements.

5.3 Other Possible Studies

In addition to determining coefficients and observing how they vary with the deletion of one or more porins, we wanted to assess the possibility of observing permeability changes caused by external factors. This includes evaluating the outer membrane destabilizing effects induced by the presence of DPA. We observed in fact a consistent increase in ampicillin permeability in the presence of low concentrations of DPA (250, 100, and 50 μM). This result can only be explained by an interaction between DPA and the outer membrane, thereby altering the ability of the bacteria to internalize antibiotics. Furthermore, the presence of DPA concentrations starting from 500 μM prevented the measurement of coefficients, as an immediate saturation of periplasmic BlaR-CTD was observed, suggesting a more extensive damage to membrane integrity. Possible extensions of the current study could therefore be exploited to determine the potential activity of various compounds to interact with the outer membrane of *P. aeruginosa*.

The existence of compounds that enhance outer membrane permeation, besides polymyxins, has already been described and we consider that other molecules belonging to this functional class may in the future potentially find some *in vivo* applications (Chan *et al*., 2021). In any case, our method could represent a valuable tool for evaluating the efficiency of these compounds.

5.4 Compensatory mechanisms for the loss of OprD

Prior to this study, no evidence had been provided on the involvement of porins other than OprD in the development of antibiotic resistance in *P. aeruginosa*. In this context, the work by Ude and coworkers demonstrated that a strain with 40 porin deletions exhibited a resistance phenotype similar to that of a single *oprD* mutant, suggesting that none of the non-expressed porins participated in antibiotic uptake.

At the outset of our investigation, before these findings were published, we considered it worthwhile to perform a proteomic analysis aimed at identifying potential alterations in the expression of other porins in the absence of OprD. We hypothesized that this approach, which to our knowledge had not previously been applied in this context, could allow to identify a candidate protein potentially compensating for OprD function.

When we focused on this subject, the only strain available to us was TNP065, which harbored both an *oprD* L434P point mutation and a deletion of *oprC*. Although this study should have been ideally performed using the single *oprD* mutant ARC5990, we believe that the results obtained with TNP065 are sufficient.

Proteomic analyses revealed the overexpression of 10 proteins in the absence of OprD and OprC, none of which could be clearly identified as a porin. The uncertainty concerning the detection of a porin upregulation was due to the failure to identify two protein spots whose expression was increased in the mutant strain compared to the wild-type. The collaborative nature of these experiments with another Unversitary laboratory and the lack of clear evidence for porin involvement limited the possibility of repeating the proteins identification.

Nevertheless, particular attention was drawn to the overexpression of two proteins involved in dipeptide transport, whose expression is closely linked to that of the OpdP porin. This finding prompted us to further investigate this pathway.

This preliminary result, on which subsequent analyses rested, was confirmed through transcriptomic studies. These investigations first characterized the increased expression of the *opdP* gene during different bacterial growth phases. Moreover, deletion of *oprD* led to a significant upregulation of *opdP* transcription, a phenomenon less evident in TNP004, in agreement with proteomic observations performed with the derivative TNP065 strain.

This was confirmed by permeability assays involving meropenem and biapenem in the *oprD*-deleted strain. Notably, the permeability coefficients for these antibiotics remained similar to those of the wild-type strain, due to the OpdP compensatory expression.

Finally, despite the known limitations related to the low specificity of the raised antibodies, the direct OpdP targeting trough Western blot confirmed the overexpression of this porin in the absence of OprD.

Together, these findings provide substantial evidence of a regulatory interplay between OprD and OpdP, thus highlighting the potential compensatory role of OpdP in maintaining carbapenem permeability in *P. aeruginosa* lacking OprD.

5.5 Involvement of OpdP deletion in mutant selection

The identification of an active role for OpdP in meropenem permeation, particularly in the absence of the OprD porin, raises the question of the significance of this porin. We therefore tried to determine if the single *opdP* deletion, that by itself did not produce any phenotypic effect (neither in terms of increased MIC nor in permeability coefficient variations) for any carbapenem, might nonetheless play a role in bacterial resistance.

Aware of the increased expression of OpdP during the stationary phase, we investigated the differential responses between the wild-type strain and the *opdP*-deleted strain in this specific growth phase.

On the basis of our previous demonstration of the dual involvement of OprD and OpdP in meropenem uptake, it was not surprising to observe that strains lacking OpdP expression were more prone to developing carbapenem resistance mediated by the loss of OprD expression.

Interestingly, in addition to detecting strains with various mutations within *oprD*, we also identified a downregulatory mechanism affecting OprD expression, mediated by a regulatory system that had not been previously described in the literature. We hypothesize that, in addition to the already known downregulation of OprD mediated by different two-component systems involved in copper homeostasis, the mutation found in *dsbR*, encoding the response regulator of a histidine kinase sensor, may be responsible for this regulatory effect on OprD expression. However, an in-depth study involving targeted mutagenesis of *dsbR,* followed by complementation assays, is required to clarify the precise role of this newly suggested regulatory mechanism, while excluding any potential contribution from the additional mutation detected in our mutant strain, particularly in the *nalD* gene.

In future research, it would also be of considerable interest to characterize the carbapenem permeability coefficients of the LG03 strain, that displays a feasible level of OprD expression to better understand the contribution of a downregulation to carbapenems uptake.

The multistep resistance experiment we performed served as a simple factual proof of the different behaviors of the *opdP*-deleted strain and the wild-type in the presence of meropenem.

We were thus able to report for the first time an active role for OpdP in antibiotic resistance and to demonstrate how its absence facilitates the emergence of better known *oprD* mutations when the bacterium is exposed to sub-MIC meropenem concentrations. It is important to consider that during antibiotic therapy, drug distribution may be suboptimal, and the mutant selection observed experimentally could possibly occur in specific organs *in vivo*.

There is no doubt that characterizing a larger number of strains selected in the presence of meropenem, or conducting additional selection cycles, might lead to the identification of further OprD downregulation mechanisms as well as additional gene mutations. A similar study performed using biapenem would also be of significant interest and could ideally provide further insight into the role of OpdP in carbapenem resistance.

It should be noted, however, that the results obtained in this area stem from a secondary experiment carried out during the final months of this doctoral project, that was specifically aimed at differentiating the *opdP*-deleted strain from its wild-type counterpart with respect to antibiotic resistance. We believe that this objective was successfully achieved, and we are confident that future reproduction and extension of this experimental approach will undoubtedly provide a solid basis for obtaining further meaningful results.

5.6 Different PAO1 Lineages

In the early stages of designing this study, we knew that, in order to better interpret variations in permeability, it would have been simpler to compare a wild-type strain with its isogenic mutants, without considering clinical isolates, at least initially.

For this reason, we obtained from BCCM PAO1, the worldwide reference strain for *P. aeruginosa*, extensively characterized under many aspects in numerous studies. However, the possibility of obtaining collections of PAO1 mutants with deletions in different porins already described in the literature was particularly appealing. As soon as we received them, we began to characterize these mutants in terms of permeability, setting aside the initial plan to generate gene deletions ourselves.

It was already known that different lineages of PAO1 are spread across various laboratories worldwide, but the permeability results we obtained were reassuring, showing outcomes consistent with what had been previously described (Klockgether *et al*., 2010).

After obtaining strain LG03, we decided to undertake a genomic approach on several strains, including the characterization of potential differences in the parental strains from which the two

collections of porin mutants had been derived. Ideally, we expected that identifying mutations in PAO1-Jap would be reflected in its derivative TNP004 and, in the same way, that ARC545 might carry mutations traceable in all its derivatives.

However, the results surprised and puzzled us. In both collections (obtained independently from two different continents!) we observed two similar issues. Neither collection, in fact, harbored the same mutations identified in their supposed parental strains. Moreover, the main mutation found in both parental strains was located in the same genomic region, albeit with distinct features.

Adding to the intrigue, the mutations identified were in a region of the genome close to *opdP*, and both were associated with promoting the overexpression of this porin. We do not know how many passages the parental strains we received may have undergone in their respective laboratories of origin over the years. Such a circumstance could explain the accumulation of mutations in the parental strains that were absent in their supposed derived strains.

Furthermore, considering that Yoneyama's work dates back to 1995, while Isabella's was published 20 years later, it would be interesting to determine whether sample of PAO1-Jap was used in Isabella's experiments, or whether PAO1-Jap and ARC545 independently derive from the original strain isolated in Melbourne in 1954 (Stover *et al*., 2000).

In any case, it would be of great interest to understand the possible selective pressures these strains were subjected to over time, or whether the similar mutations observed are merely the result of chance.

The observation of these differences also highlights the fact that, in experiments performed over several years, it is crucial to minimize plate passages and consistently restart from a frozen, stable strain to avoid the emergence of similar issues. As far as we are concerned, we can confidently state that the identified mutations likely did not originate in our laboratory, as we have always been mindful of this matter and minimized the number of culture passages after we received the various strains.

We regret that these genomic analyses were only performed at the end of the project, so that we did not have the opportunity to characterize the permeability profiles of PAO1-Jap and ARC545, that turn out to be OpdP overexpressors. In the future, this analysis would certainly be an interesting study to undertake, in order to describe the potential effects of OpdP overexpression on permeability.

6 CONCLUSIONS AND FUTURE PERSPECTIVES

The multidrug resistance of Gram-negative bacteria, and in particular *P. aeruginosa*, is the result of the interplay between multiple mechanisms, making the characterization of the various aspects of this phenomenon extremely important. The permeability of the outer membrane to a given antibiotic is a critical variable in determining its efficiency, yet studies addressing this subject in living bacterial cells remain scarce and fragmented. This gap has become even more apparent after the introduction of cefiderocol, the first siderophore cephalosporin, that exploits siderophore porins as entry channels into the periplasm.

The study we conducted was the first to measure *in vivo* the permeability coefficients of *P. aeruginosa* PAO1 and of various porin mutants for a wide range of β-lactams belonging to different subfamilies. This approach allowed to compare the effects that the deletion of one or more porins exerts on specific permeability coefficients, thus helping to define the synergistic role of OprD and OpdP in the permeation of some carbapenems, an interaction that would not have been detectable with conventional phenotypic drug susceptibility testing.

The validation of this approach through the results presented in our work represents only a starting point. In the future, we hope to characterize the permeability of additional *P. aeruginosa* strains, that either overexpress or are deleted for one or more porins, to further elucidate potential compensatory effects. Furthermore, applying this study to clinical isolates would be of great interest, providing a clearer picture of the adaptive response of the bacteria following prolonged antibiotic therapy.

An equally intriguing prospect would be to expand the panel of β-lactams examined, including cefiderocol, in order to investigate the resistance profiles associated with this drug. Moreover, it would be interesting to study the permeability variations induced by the presence of various other compounds, as already demonstrated in the case of DPA.

The same analytical strategy could also be successfully applied to characterize the permeability properties of other MDR Gram-negative pathogens, such as *K. pneumoniae* or *A. baumannii*, the latter representing a major challenge in terms of the spread of pan-drug-resistant strains.

For all these purposes, it would be valuable to automate the analytical procedures, for example, by performing BlaR-CTD quantification through fluorescence detection upon capillary electrophoresis, thereby simplifying the workflow.

Our interest in the various different behaviors of porin mutants also led us to focus on quantifying variations in porin expression as a function of bacterial growth phase. This result was achieved through RT-PCR, that, in any case, is limited to the analysis of the selected porins under investigation. We believe that a transcriptomic approach based on bacterial growth phases could still

yield valuable insights. Particularly, this could be achieved by performing RNA sequencing, which would allow the simultaneously quantification of protein expression, resulting in the identification of additional compensatory mechanisms.

Similarly, inducing mutagenesis through antibiotic exposure in strains deleted for one or more porins is a strategy that could lead to further significant findings. Future research may better characterize the novel OprD downregulation system identified in strain LG03, expand the genotypic characterization of mutants derived from meropenem exposure in the *opdP*-deleted strain. In addition, the same experiment could be performed with biapenem.

Finally, if one considers the rather small variations observed in the permeability coefficients of ertapenem and doripenem across the various mutants studied, it would be of interest to expose strain ARC5998, already deleted for five porins, to sub-MIC concentrations of these two antibiotics. We speculate that such conditions might select mutations in the residual porin(s) responsible for mediating the entry of these carbapenems.

7 REFERENCES

Abouhamad WN, Manson M, Gibson MM, Higgins CF. Peptide transport and chemotaxis in Escherichia coli and Salmonella typhimurium: characterization of the dipeptide permease (Dpp) and the dipeptide-binding protein. Mol Microbiol. 1991 May;5(5):1035-47. PMID: 1956284.

Abouhamad WN, Manson MD. The dipeptide permease of *Escherichia coli* closely resembles other bacterial transport systems and shows growth-phase-dependent expression. Mol Microbiol. 1994 Dec;14(5):1077-92. PMID: 7536291.

Abraham EP, Newton GG, Crawford K, Burton HS, Hale CW. Cephalosporin N: a new type of penicillin. Nature. 1953 Feb 21;171(4347):343. PMID: 13036884.

Abu Khadra KM, Al-Rabaia SY, Khalil AM, Abu-Qatouseh LF, Abussaud MJ. Molecular analysis for the OprD gene among *Pseudomonas aueroginosa* clinical isolates obtained from hospitals in Jordan. J Infect Dev Ctries. 2022 Apr 30;16(4):683-690. PMID: 35544631.

Aendekerk S, Ghysels B, Cornelis P, Baysse C. Characterization of a new efflux pump, MexGHI-OpmD, from *Pseudomonas aeruginosa* that confers resistance to vanadium. Microbiology (Reading). 2002 Aug;148(Pt 8):2371-2381. PMID: 12177331.

Aires JR, Köhler T, Nikaido H, Plésiat P. Involvement of an active efflux system in the natural resistance of *Pseudomonas aeruginosa* to aminoglycosides. Antimicrob Agents Chemother. 1999 Nov;43(11):2624-8. PMID: 10543738.

Akama H, Kanemaki M, Yoshimura M, Tsukihara T, Kashiwagi T, Yoneyama H, Narita S, Nakagawa A, Nakae T. Crystal structure of the drug discharge outer membrane protein, OprM, of *Pseudomonas aeruginosa:* dual modes of membrane anchoring and occluded cavity end. J Biol Chem. 2004**a** Dec 17;279(51):52816-9. PMID: 15507433.

Akama H, Matsuura T, Kashiwagi S, Yoneyama H, Narita S, Tsukihara T, Nakagawa A, Nakae T. Crystal structure of the membrane fusion protein, MexA, of the multidrug transporter in *Pseudomonas aeruginosa*. J Biol Chem. 2004**b** Jun 18;279(25):25939-42. PMID: 15117957.

Akova M. Sulbactam-containing beta-lactamase inhibitor combinations. Clin Microbiol Infect. 2008 Jan;14 Suppl 1:185-8. Erratum in: Clin Microbiol Infect. 2008 May;14 Suppl 5:21-4. PMID: 18154545.

Al Naiemi N, Duim B, Bart A. A CTX-M extended-spectrum beta-lactamase in *Pseudomonas aeruginosa* and *Stenotrophomonas maltophilia*. J Med Microbiol. 2006 Nov;55(Pt 11):1607-1608. PMID: 17030926.

Al-Thabhawee MHJ, Al-Dahmoshi HM. Molecular Investigation of Outer Membrane Channel Genes Among Multidrug Resistance Clinical *Pseudomonas Aeruginosa* Isolates. Rep Biochem Mol Biol. 2022 Apr;11(1):102-110. PMID: 35765529.

Alam F, Blair JMA, Hall RA. Transcriptional profiling of *Pseudomonas aeruginosa* mature single- and dual-species biofilms in response to meropenem. Microbiology (Reading). 2023 Jan;169(1):001271. PMID: 36748572.

Allam A, Maigre L, Vergalli J, Dumont E, Cinquin B, Alves de Sousa R, Pajovic J, Pinet E, Smith N, Herbeuval JP, Réfrégiers M, Artaud I, Pagès JM. Microspectrofluorimetry to dissect the permeation of ceftazidime in Gram-negative bacteria. Sci Rep. 2017 Apr 20;7(1):986. PMID: 28428543.

Allen WJ, Phan G, Waksman G. Structural biology of periplasmic chaperones. Adv Protein Chem Struct Biol. 2009;78:51-97. PMID: 20663484.

Alonso A, Rojo F, Martínez JL. Environmental and clinical isolates of *Pseudomonas aeruginosa* show pathogenic and biodegradative properties irrespective of their origin. Environ Microbiol. 1999 Oct;1(5):421-30. PMID: 11207762.

Alvarez-Ortega C, Wiegand I, Olivares J, Hancock RE, Martínez JL. Genetic determinants involved in the susceptibility of *Pseudomonas aeruginosa* to beta-lactam antibiotics. Antimicrob Agents Chemother. 2010 Oct;54(10):4159-67. PMID: 20679510.

Ambler RP. The structure of beta-lactamases. Philos Trans R Soc Lond B Biol Sci. 1980 May 16;289(1036):321-31. PMID: 6109327.

Ambreetha S, Zincke D, Balachandar D, Mathee K. Genomic and metabolic versatility of *Pseudomonas aeruginosa* contributes to its inter-kingdom transmission and survival. J Med Microbiol. 2024 Feb;73(2). PMID: 38362900.

Andrews SC, Robinson AK, Rodríguez-Quiñones F. Bacterial iron homeostasis. FEMS Microbiol Rev. 2003 Jun;27(2-3):215-37. PMID: 12829269.

Angrill N, Gallego M, Font J, Vallés J, Morón A, Monsó E, Rello J. Determinants of empirical antipseudomonal antibiotic prescription for adults with pneumonia in the emergency department. BMC Pulm Med. 2020 Apr 3;20(1):83. PMID: 32245452.

Arhin A, Boucher C. The outer membrane protein OprQ and adherence of *Pseudomonas aeruginosa* to human fibronectin. Microbiology (Reading). 2010 May;156(Pt 5):1415-1423. PMID: 20093292.

Asfahl KL, Walsh J, Gilbert K, Schuster M. Non-social adaptation defers a tragedy of the commons in *Pseudomonas aeruginosa* quorum sensing. ISME J. 2015 Aug;9(8):1734-46. PMID: 25615439.

Atrissi J, Milan A, Bressan R, Lucafò M, Petix V, Busetti M, Dolzani L, Lagatolla C. Interplay of OpdP Porin and Chromosomal Carbapenemases in the Determination of Carbapenem Resistance/Susceptibility in *Pseudomonas aeruginosa*. Microbiol Spectr. 2021 Oct 31;9(2):e0118621. PMID: 34585948.

Augustin DK, Song Y, Baek MS, Sawa Y, Singh G, Taylor B, Rubio-Mills A, Flanagan JL, Wiener-Kronish JP, Lynch SV. Presence or absence of lipopolysaccharide O antigens affects type III secretion by *Pseudomonas aeruginosa*. J Bacteriol. 2007 Mar;189(6):2203-9. PMID: 17209027.

Avakh A, Grant GD, Cheesman MJ, Kalkundri T, Hall S. The Art of War with *Pseudomonas aeruginosa*: Targeting Mex Efflux Pumps Directly to Strategically Enhance Antipseudomonal Drug Efficacy. Antibiotics (Basel). 2023 Aug 9;12(8):1304. PMID: 37627724.

Bahr G, Vitor-Horen L, Bethel CR, Bonomo RA, González LJ, Vila AJ. Clinical Evolution of New Delhi Metallo-β-Lactamase (NDM) Optimizes Resistance under Zn(II) Deprivation. Antimicrob Agents Chemother. 2017 Dec 21;62(1):e01849-17. PMID: 29038264.

Balasubramanian D, Kumari H, Mathee K. *Pseudomonas aeruginosa* AmpR: an acute-chronic switch regulator. Pathog Dis. 2015 Mar;73(2):1-14. PMID: 25066236.

Baldwin CM, Lyseng-Williamson KA, Keam SJ. Meropenem: a review of its use in the treatment of serious bacterial infections. Drugs. 2008;68(6):803-38. PMID: 18416587.

Ball G, Antelmann H, Imbert PR, Gimenez MR, Voulhoux R, Ize B. Contribution of the Twin Arginine Translocation system to the exoproteome of *Pseudomonas aeruginosa*. Sci Rep. 2016 Jun 9;6:27675. PMID: 27279369.

Ball J, Reis RAG, Agniswamy J, Weber IT, Gadda G. Steric hindrance controls pyridine nucleotide specificity of a flavin-dependent NADH:quinone oxidoreductase. Protein Sci. 2019 Jan;28(1):167-175. PMID: 30246917.

Barrow K, Kwon DH. Alterations in two-component regulatory systems of phoPQ and pmrAB are associated with polymyxin B resistance in clinical isolates of *Pseudomonas aeruginosa*. Antimicrob Agents Chemother. 2009 Dec;53(12):5150-4. PMID: 19752280.

Bassetti M, Vena A, Croxatto A, Righi E, Guery B. How to manage *Pseudomonas aeruginosa* infections. Drugs Context. 2018 May 29;7:212527. PMID: 29872449.

Bay DC, Rommens KL, Turner RJ. Small multidrug resistance proteins: a multidrug transporter family that continues to grow. Biochim Biophys Acta. 2008 Sep;1778(9):1814-38. PMID: 17942072.

Bellido F, Martin NL, Siehnel RJ, Hancock RE. Reevaluation, using intact cells, of the exclusion limit and role of porin OprF in *Pseudomonas aeruginosa* outer membrane permeability. J Bacteriol. 1992 Aug;174(16):5196-203. PMID: 1322882.

Benamara H, Rihouey C, Abbes I, Ben Mlouka MA, Hardouin J, Jouenne T, Alexandre S. Characterization of membrane lipidome changes in *Pseudomonas aeruginosa* during biofilm growth on glass wool. PLoS One. 2014 Sep 29;9(9):e108478. PMID: 25265483.

Bhamidimarri SP, Young TR, Shanmugam M, Soderholm S, Baslé A, Bumann D, van den Berg B. Acquisition of ionic copper by the bacterial outer membrane protein OprC through a novel binding site. PLoS Biol. 2021 Nov 11;19(11):e3001446. PMID: 34762655.

Bielecki P, Jensen V, Schulze W, Gödeke J, Strehmel J, Eckweiler D, Nicolai T, Bielecka A, Wille T, Gerlach RG, Häussler S. Cross talk between the response regulators PhoB and TctD allows for the integration of diverse environmental signals in *Pseudomonas aeruginosa*. Nucleic Acids Res. 2015 Jul 27;43(13):6413-25. PMID: 26082498.

Biró I, Pezeshki S, Weingart H, Winterhalter M, Kleinekathöfer U. Comparing the temperature-dependent conductance of the two structurally similar *E. coli* porins OmpC and OmpF. Biophys J. 2010 May 19;98(9):1830-9. PMID: 20441746.

Bissonnette L, Champetier S, Buisson JP, Roy PH. Characterization of the nonenzymatic chloramphenicol resistance (*cmlA*) gene of the In4 integron of Tn1696: similarity of the product to transmembrane transport proteins. J Bacteriol. 1991 Jul;173(14):4493-502. PMID: 1648560.

Biswas S, Mohammad MM, Movileanu L, van den Berg B. Crystal structure of the outer membrane protein OpdK from *Pseudomonas aeruginosa*. Structure. 2008 Jul;16(7):1027-35. PMID: 18611376.

Biswas S, Mohammad MM, Patel DR, Movileanu L, van den Berg B. Structural insight into OprD substrate specificity. Nat Struct Mol Biol. 2007 Nov;14(11):1108-9. PMID: 17952093.

Bitar I, Salloum T, Merhi G, Hrabak J, Araj GF, Tokajian S. Genomic Characterization of Mutli-Drug Resistant *Pseudomonas aeruginosa* Clinical Isolates: Evaluation and Determination of Ceftolozane/Tazobactam Activity and Resistance Mechanisms. Front Cell Infect Microbiol. 2022 Jun 15;12:922976. PMID: 35782142.

Bleves S, Viarre V, Salacha R, Michel GP, Filloux A, Voulhoux R. Protein secretion systems in *Pseudomonas aeruginosa*: A wealth of pathogenic weapons. Int J Med Microbiol. 2010 Dec;300(8):534-43. PMID: 20947426.

Blizzard TA, Chen H, Kim S, Wu J, Bodner R, Gude C, Imbriglio J, Young K, Park YW, Ogawa A, Raghoobar S, Hairston N, Painter RE, Wisniewski D, Scapin G, Fitzgerald P, Sharma N, Lu J, Ha S, Hermes J, Hammond ML. Discovery of MK-7655, a β-lactamase inhibitor for combination with Primaxin®. Bioorg Med Chem Lett. 2014 Feb 1;24(3):780-5. PMID: 24433862.

Blumer C, Heeb S, Pessi G, Haas D. Global GacA-steered control of cyanide and exoprotease production in *Pseudomonas fluorescens* involves specific ribosome binding sites. Proc Natl Acad Sci U S A. 1999 Nov 23;96(24):14073-8. PMID: 10570200.

Bouteiller M, Dupont C, Bourigault Y, Latour X, Barbey C, Konto-Ghiorghi Y, Merieau A. *Pseudomonas* Flagella: Generalities and Specificities. Int J Mol Sci. 2021 Mar 24;22(7):3337. PMID: 33805191.

Braun V, Braun M. Active transport of iron and siderophore antibiotics. Curr Opin Microbiol. 2002 Apr;5(2):194-201. PMID: 11934617.

Brinkman FS, Bains M, Hancock RE. The amino terminus of *Pseudomonas aeruginosa* outer membrane protein OprF forms channels in lipid bilayer membranes: correlation with a three-dimensional model. J Bacteriol. 2000 Sep;182(18):5251-5. PMID: 10960112.

Brisse, S., Grimont, F., Grimont, P.A.D. (2006). The Genus *Klebsiella*. In: Dworkin, M., Falkow, S., Rosenberg, E., Schleifer, KH., Stackebrandt, E. (eds) The Prokaryotes. Springer, New York, NY. https://doi.org/10.1007/0-387-30746-X_8

Brown MH, Paulsen IT, Skurray RA. The multidrug efflux protein NorM is a prototype of a new family of transporters. Mol Microbiol. 1999 Jan;31(1):394-5. PMID: 9987140.

Browne P, Barret M, O'Gara F, Morrissey JP. Computational prediction of the Crc regulon identifies genus-wide and species-specific targets of catabolite repression control in Pseudomonas bacteria. BMC Microbiol. 2010 Nov 25;10:300. PMID: 21108798.

Bush K, Jacoby GA. Updated functional classification of beta-lactamases. Antimicrob Agents Chemother. 2010 Mar;54(3):969-76. PMID: 19995920.

Bush K. Classification for β-lactamases: historical perspectives. Expert Rev Anti Infect Ther. 2023 May;21(5):513-522. PMID: 36951174.

Bushnell B, Rood J, Singer E. BBMerge - Accurate paired shotgun read merging via overlap. PLoS One. 2017 Oct 26;12(10):e0185056. PMID: 29073143.

Buyck JM, Guénard S, Plésiat P, Tulkens PM, Van Bambeke F. Role of MexAB-OprM in intrinsic resistance of *Pseudomonas aeruginosa* to temocillin and impact on the susceptibility of strains isolated from patients suffering from cystic fibrosis. J Antimicrob Chemother. 2012 Mar;67(3):771-5. PMID: 22218683.

Cabot G, López-Causapé C, Ocampo-Sosa AA, Sommer LM, Domínguez MÁ, Zamorano L, Juan C, Tubau F, Rodríguez C, Moyà B, Peña C, Martínez-Martínez L, Plesiat P, Oliver A. Deciphering the Resistome of the Widespread *Pseudomonas aeruginosa* Sequence Type 175 International High-Risk Clone through Whole-Genome Sequencing. Antimicrob Agents Chemother. 2016 Nov 21;60(12):7415-7423. PMID: 27736752.

Cai H, Rose K, Liang LH, Dunham S, Stover C. Development of a liquid chromatography/mass spectrometry-based drug accumulation assay in *Pseudomonas aeruginosa*. Anal Biochem. 2009 Feb 15;385(2):321-5. PMID: 19032927.

Caille O, Rossier C, Perron K. A copper-activated two-component system interacts with zinc and imipenem resistance in *Pseudomonas aeruginosa*. J Bacteriol. 2007 Jul;189(13):4561-8. PMID: 17449606.

Cao L, Srikumar R, Poole K. MexAB-OprM hyperexpression in NalC-type multidrug-resistant *Pseudomonas aeruginosa*: identification and characterization of the *nalC* gene encoding a repressor of PA3720-PA3719. Mol Microbiol. 2004 Sep;53(5):1423-36. PMID: 15387820.

Casabona MG, Vandenbrouck Y, Attree I, Couté Y. Proteomic characterization of *Pseudomonas aeruginosa* PAO1 inner membrane. Proteomics. 2013 Aug;13(16):2419-23. PMID: 23744604.

Castanheira M, Doyle TB, Hubler CM, Collingsworth TD, DeVries S, Mendes RE. The plethora of resistance mechanisms in *Pseudomonas aeruginosa*: transcriptome analysis reveals a potential role of lipopolysaccharide pathway proteins to novel β-lactam/β-lactamase inhibitor combinations. J Glob Antimicrob Resist. 2022 Dec;31:72-79. PMID: 35931381.

Castanheira M, Mills JC, Farrell DJ, Jones RN. Mutation-driven β-lactam resistance mechanisms among contemporary ceftazidime-nonsusceptible *Pseudomonas aeruginosa* isolates from U.S. hospitals. Antimicrob Agents Chemother. 2014 Nov;58(11):6844-50. PMID: 25182652.

Castanheira M, Toleman MA, Jones RN, Schmidt FJ, Walsh TR. Molecular characterization of a beta-lactamase gene, blaGIM-1, encoding a new subclass of metallo-beta-lactamase. Antimicrob Agents Chemother. 2004 Dec;48(12):4654-61. PMID: 15561840.

Catel-Ferreira M, Marti S, Guillon L, Jara L, Coadou G, Molle V, Bouffartigues E, Bou G, Shalk I, Jouenne T, Vila-Farrés X, Dé E. The outer membrane porin OmpW of *Acinetobacter baumannii* is involved in iron uptake and colistin binding. FEBS Lett. 2016 Jan;590(2):224-31. PMID: 26823169.

Catte A, K Ramaswamy V, Vargiu AV, Malloci G, Bosin A, Ruggerone P. Common recognition topology of mex transporters of *Pseudomonas aeruginosa* revealed by molecular modelling. Front Pharmacol. 2022 Nov 11;13:1021916. PMID: 36438787.

Cescutti P. 2010. Chapter 6 - Bacterial capsular polysaccharides and exopolysaccharides. In Microbial Glycobiology (pp. 93-108). Academic Press. https://doi.org/10.1016/B978-0-12-374546-0.00006-7

Chalhoub H, Pletzer D, Weingart H, Braun Y, Tunney MM, Elborn JS, Rodriguez-Villalobos H, Plésiat P, Kahl BC, Denis O, Winterhalter M, Tulkens PM, Van Bambeke F. Mechanisms of intrinsic resistance and acquired susceptibility of *Pseudomonas aeruginosa* isolated from cystic fibrosis patients to temocillin, a revived antibiotic. Sci Rep. 2017 Jan 16;7:40208. PMID: 28091521.

Chalhoub H, Sáenz Y, Rodriguez-Villalobos H, Denis O, Kahl BC, Tulkens PM, Van Bambeke F. High-level resistance to meropenem in clinical isolates of *Pseudomonas aeruginosa* in the absence of carbapenemases: role of active efflux and porin alterations. Int J Antimicrob Agents. 2016 Dec;48(6):740-743. PMID: 28128097.

Chambers HF. Methicillin resistance in staphylococci: molecular and biochemical basis and clinical implications. Clin Microbiol Rev. 1997 Oct;10(4):781-91. PMID: 9336672.

Chan DCK, Burrows LL. *Pseudomonas aeruginosa* FpvB Is a High-Affinity Transporter for Xenosiderophores Ferrichrome and Ferrioxamine B. mBio. 2023 Feb 28;14(1):e0314922. PMID: 36507834.

Chan LW, Hern KE, Ngambenjawong C, Lee K, Kwon EJ, Hung DT, Bhatia SN. Selective Permeabilization of Gram-Negative Bacterial Membranes Using Multivalent Peptide Constructs for Antibiotic Sensitization. ACS Infect Dis. 2021 Apr 9;7(4):721-732. PMID: 33689277.

Chang W, Small DA, Toghrol F, Bentley WE. Microarray analysis of toxicogenomic effects of peracetic acid on *Pseudomonas aeruginosa*. Environ Sci Technol. 2005 Aug 1;39(15):5893-9. PMID: 16124331.

Chen CC, Herzberg O. Inhibition of beta-lactamase by clavulanate. Trapped intermediates in cryocrystallographic studies. J Mol Biol. 1992 Apr 20;224(4):1103-13. Erratum in: J Mol Biol 1992 Jul 5;226(1):285. PMID: 1569569.

Chen L, Duan K. A PhoPQ-Regulated ABC Transporter System Exports Tetracycline in *Pseudomonas aeruginosa*. Antimicrob Agents Chemother. 2016 Apr 22;60(5):3016-24. PMID: 26953208.

Chen W, Zhang YM, Davies C. Penicillin-Binding Protein 3 Is Essential for Growth of *Pseudomonas aeruginosa*. Antimicrob Agents Chemother. 2016 Dec 27;61(1):e01651-16. PMID: 27821444.

Cheneke BR, van den Berg B, Movileanu L. Analysis of gating transitions among the three major open states of the OpdK channel. Biochemistry. 2011 Jun 7;50(22):4987-97. PMID: 21548584.

Cherak Z, Loucif L, Ben Khedher M, Moussi A, Benbouza A, Baron SA, Rolain JM. MCR-5-Producing Colistin-Resistant *Cupriavidus gilardii* Strain from Well Water in Batna, Algeria. mSphere. 2021 Oct 27;6(5):e0057521. PMID: 34468167.

Chevalier S, Bouffartigues E, Bodilis J, Maillot O, Lesouhaitier O, Feuilloley MGJ, Orange N, Dufour A, Cornelis P. Structure, function and regulation of *Pseudomonas aeruginosa* porins. FEMS Microbiol Rev. 2017 Sep 1;41(5):698-722. PMID: 28981745.

Chopra I, Roberts M. Tetracycline antibiotics: mode of action, applications, molecular biology, and epidemiology of bacterial resistance. Microbiol Mol Biol Rev. 2001 Jun;65(2):232-60; second page, table of contents. PMID: 11381101.

Chopra I. New developments in tetracycline antibiotics: glycylcyclines and tetracycline efflux pump inhibitors. Drug Resist Updat. 2002 Jul-Aug;5(3-4):119-25. PMID: 12237079.

Chuanchuen R, Murata T, Gotoh N, Schweizer HP. Substrate-dependent utilization of OprM or OpmH by the *Pseudomonas aeruginosa* MexJK efflux pump. Antimicrob Agents Chemother. 2005 May;49(5):2133-6. PMID: 15855547.

Chuanchuen R, Narasaki CT, Schweizer HP. The MexJK efflux pump of *Pseudomonas aeruginosa* requires OprM for antibiotic efflux but not for efflux of triclosan. J Bacteriol. 2002 Sep;184(18):5036-44. PMID: 12193619.

Chuanchuen R, Wannaprasat W, Schweizer HP. Functional characterization of MexXY and OpmG in aminoglycoside efflux in *Pseudomonas aeruginosa*. Southeast Asian J Trop Med Public Health. 2008 Jan;39(1):115-22. PMID: 18567450.

Citak F, Ghai I, Rosenkötter F, Benier L, Winterhalter M, Wagner R. Probing transport of fosfomycin through substrate specific OprO and OprP from *Pseudomonas aeruginosa*. Biochem Biophys Res Commun. 2018 Jan 1;495(1):1454-1460. PMID: 29198700.

Clamens T, Rosay T, Crépin A, Grandjean T, Kentache T, Hardouin J, Bortolotti P, Neidig A, Mooij M, Hillion M, Vieillard J, Cosette P, Overhage J, O'Gara F, Bouffartigues E, Dufour A, Chevalier S, Guery B, Cornelis P, Feuilloley MG, Lesouhaitier O. The aliphatic amidase AmiE is involved in regulation of *Pseudomonas aeruginosa* virulence. Sci Rep. 2017 Jan 24;7:41178. PMID: 28117457.

Clark ST, Sinha U, Zhang Y, Wang PW, Donaldson SL, Coburn B, Waters VJ, Yau YCW, Tullis DE, Guttman DS, Hwang DM. Penicillin-binding protein 3 is a common adaptive target among *Pseudomonas aeruginosa* isolates from adult cystic fibrosis patients treated with β-lactams. Int J Antimicrob Agents. 2019 May;53(5):620-628. PMID: 30664925.

Collu F, Vargiu AV, Dreier J, Cascella M, Ruggerone P. Recognition of imipenem and meropenem by the RND-transporter MexB studied by computer simulations. J Am Chem Soc. 2012 Nov 21;134(46):19146-58. PMID: 23146101.

Compagne N, Vieira Da Cruz A, Müller RT, Hartkoorn RC, Flipo M, Pos KM. Update on the Discovery of Efflux Pump Inhibitors against Critical Priority Gram-Negative Bacteria. Antibiotics (Basel). 2023 Jan 15;12(1):180. PMID: 36671381.

Cooper CJ, Krishnamoorthy G, Wolloscheck D, Walker JK, Rybenkov VV, Parks JM, Zgurskaya HI. Molecular Properties That Define the Activities of Antibiotics in *Escherichia coli* and *Pseudomonas aeruginosa*. ACS Infect Dis. 2018 Aug 10;4(8):1223-1234. PMID: 29756762.

Cornaglia G, Russell K, Satta G, Fontana R. Relative importances of outer membrane permeability and group 1 beta-lactamase as determinants of meropenem and imipenem activities against *Enterobacter cloacae*. Antimicrob Agents Chemother. 1995 Feb;39(2):350-5. PMID: 7726496.

Costerton JW, Irvin RT, Cheng KJ. The bacterial glycocalyx in nature and disease. Annu Rev Microbiol. 1981;35:299-324. PMID: 7027902.

Cowan SW, Schirmer T, Rummel G, Steiert M, Ghosh R, Pauptit RA, Jansonius JN, Rosenbusch JP. Crystal structures explain functional properties of two *E. coli* porins. Nature. 1992 Aug 27;358(6389):727-33. PMID: 1380671.

Cox CD, Parker J. Use of 2-aminoacetophenone production in identification of *Pseudomonas aeruginosa*. J Clin Microbiol. 1979 Apr;9(4):479-84. PMID: 110829.

Crandon JL, Nicolau DP. Human simulated studies of aztreonam and aztreonam-avibactam to evaluate activity against challenging Gram-negative organisms, including metallo-β-lactamase producers. Antimicrob Agents Chemother. 2013 Jul;57(7):3299-306. PMID: 23650162.

Crone S, Vives-Flórez M, Kvich L, Saunders AM, Malone M, Nicolaisen MH, Martínez-García E, Rojas-Acosta C, Catalina Gomez-Puerto M, Calum H, Whiteley M, Kolter R, Bjarnsholt T. The environmental occurrence of *Pseudomonas aeruginosa*. APMIS. 2020 Mar;128(3):220-231. PMID: 31709616.

Crowfoot D, Bunn C, Rogers-Low B, Turner-Jones. A X-ray crystallographic investigation of the structure of penicillin. In: Clarke HT, Johnson JR, Robinson SR, editors. The chemistry of penicillin. Princeton, New Jersey: Princeton University Press; 1949. pp. 310 – 367.

Curran CS, Bolig T, Torabi-Parizi P. Mechanisms and Targeted Therapies for *Pseudomonas aeruginosa* Lung Infection. Am J Respir Crit Care Med. 2018 Mar 15;197(6):708-727. PMID: 29087211.

Curtis NA, Eisenstadt RL, Rudd C, White AJ. Inducible type I beta-lactamases of Gram-negative bacteria and resistance to beta-lactam antibiotics. J Antimicrob Chemother. 1986 Jan;17(1):51-61. PMID: 3485092.

D'Andrea MM, Amisano F, Giani T, Conte V, Ciacci N, Ambretti S, Santoriello L, Rossolini GM. Diversity of capsular polysaccharide gene clusters in Kpc-producing *Klebsiella pneumoniae* clinical isolates of sequence type 258 involved in the Italian epidemic. PLoS One. 2014 May 13;9(5):e96827. PMID: 24823690.

Danel F, Hall LM, Gur D, Livermore DM. OXA-14, another extended-spectrum variant of OXA-10 (PSE-2) beta-lactamase from *Pseudomonas aeruginosa*. Antimicrob Agents Chemother. 1995 Aug;39(8):1881-4. PMID: 7486940.

Danelon C, Nestorovich EM, Winterhalter M, Ceccarelli M, Bezrukov SM. Interaction of zwitterionic penicillins with the OmpF channel facilitates their translocation. Biophys J. 2006 Mar 1;90(5):1617-27. PMID: 16339889.

Davies TA, Shang W, Bush K, Flamm RK. Affinity of doripenem and comparators to penicillin-binding proteins in *Escherichia coli* and *Pseudomonas aeruginosa*. Antimicrob Agents Chemother. 2008 Apr;52(4):1510-2. PMID: 18250190.

Dhillon S. Meropenem/Vaborbactam: A Review in Complicated Urinary Tract Infections. Drugs. 2018 Aug;78(12):1259-1270. Erratum in: Drugs. 2018 Sep;78(13):1383. PMID: 30128699.

Díez-Aguilar M, Cantón R. New microbiological aspects of fosfomycin. Rev Esp Quimioter. 2019 May;32 Suppl 1(Suppl 1):8-18. PMID: 31131587.

Dogan Guzel F, Pletzer D, Norouz Dizaji A, Al-Nahas K, Bajrai M, Winterhalter M. Towards understanding single-channel characteristics of OccK8 purified from *Pseudomonas aeruginosa*. Eur Biophys J. 2021 Jan;50(1):87-98. PMID: 33481046.

Dolan SK, Kohlstedt M, Trigg S, Vallejo Ramirez P, Kaminski CF, Wittmann C, Welch M. Contextual Flexibility in *Pseudomonas aeruginosa* Central Carbon Metabolism during Growth in Single Carbon Sources. mBio. 2020 Mar 17;11(2):e02684-19. PMID: 32184246.

Drawz SM, Bonomo RA. Three decades of beta-lactamase inhibitors. Clin Microbiol Rev. 2010 Jan;23(1):160-201.PMID: 20065329.

Dreier J, Ruggerone P. Interaction of antibacterial compounds with RND efflux pumps in *Pseudomonas aeruginosa*. Front Microbiol. 2015 Jul 8;6:660. PMID: 26217310.

Duan K, Dammel C, Stein J, Rabin H, Surette MG. Modulation of *Pseudomonas aeruginosa* gene expression by host microflora through interspecies communication. Mol Microbiol. 2003 Dec;50(5):1477-91. PMID: 14651632.

Duchêne M, Barron C, Schweizer A, von Specht BU, Domdey H. *Pseudomonas aeruginosa* outer membrane lipoprotein I gene: molecular cloning, sequence, and expression in *Escherichia coli*. J Bacteriol. 1989 Aug;171(8):4130-7. PMID: 2502533.

Ducret V, Gonzalez MR, Leoni S, Valentini M, Perron K. The CzcCBA Efflux System Requires the CadA P-Type ATPase for Timely Expression Upon Zinc Excess in *Pseudomonas aeruginosa*. Front Microbiol. 2020 May 15;11:911. PMID: 32477311.

Ducret V, Gonzalez MR, Scrignari T, Perron K. OprD Repression upon Metal Treatment Requires the RNA Chaperone Hfq in *Pseudomonas aeruginosa*. Genes (Basel). 2016 Oct 3;7(10):82. PMID: 27706108.

Dulyayangkul P, Satapoomin N, Avison MB, Charoenlap N, Vattanaviboon P, Mongkolsuk S. Over-Expression of Hypochlorite Inducible Major Facilitator Superfamily (MFS) Pumps Reduces Antimicrobial Drug Susceptibility by Increasing the Production of MexXY Mediated by ArmZ in *Pseudomonas aeruginosa*. Front Microbiol. 2021 Jan 12;11:592153. PMID: 33510718.

Duval V, Swinnen M, Lepage S, Brans A, Granier B, Franssen C, Frère JM, Joris B. The kinetic properties of the carboxy terminal domain of the *Bacillus licheniformis* 749/I BlaR penicillin-receptor shed a new light on the derepression of beta-lactamase synthesis. Mol Microbiol. 2003 Jun;48(6):1553-64. PMID: 12791138.

ECDC; 2023. European Centre for Disease Prevention and Control. Point prevalence survey of healthcare associated infections and antimicrobial use in European long-term care facilities: 2016–2017. Stockholm.

Ehmann DE, Jahić H, Ross PL, Gu RF, Hu J, Kern G, Walkup GK, Fisher SL. Avibactam is a covalent, reversible, non-β-lactam β-lactamase inhibitor. Proc Natl Acad Sci U S A. 2012 Jul 17;109(29):11663-8. PMID: 22753474.

El Garch F, Bogaerts P, Bebrone C, Galleni M, Glupczynski Y. OXA-198, an acquired carbapenem-hydrolyzing class D beta-lactamase from *Pseudomonas aeruginosa*. Antimicrob Agents Chemother. 2011 Oct;55(10):4828-33. PMID: 21788473.

El Khoury M, Swain J, Sautrey G, Zimmermann L, Van Der Smissen P, Décout JL, Mingeot-Leclercq MP. Targeting Bacterial Cardiolipin Enriched Microdomains: An Antimicrobial Strategy Used by Amphiphilic Aminoglycoside Antibiotics. Sci Rep. 2017 Sep 6;7(1):10697. PMID: 28878347.

Epp SF, Köhler T, Plésiat P, Michéa-Hamzehpour M, Frey J, Pechère JC. C-terminal region of *Pseudomonas aeruginosa* outer membrane porin OprD modulates susceptibility to meropenem. Antimicrob Agents Chemother. 2001 Jun;45(6):1780-7. PMID: 11353625.

Eren E, Parkin J, Adelanwa A, Cheneke B, Movileanu L, Khalid S, van den Berg B. Toward understanding the outer membrane uptake of small molecules by *Pseudomonas aeruginosa*. J Biol Chem. 2013 Apr 26;288(17):12042-53. PMID: 23467408.

Eren E, Vijayaraghavan J, Liu J, Cheneke BR, Touw DS, Lepore BW, Indic M, Movileanu L, van den Berg B. Substrate specificity within a family of outer membrane carboxylate channels. PLoS Biol. 2012 Jan;10(1):e1001242. PMID: 22272184.

Erickson HP. How Teichoic Acids Could Support a Periplasm in Gram-Positive Bacteria, and Let Cell Division Cheat Turgor Pressure. Front Microbiol. 2021 May 10;12:664704. PMID: 34040598.

Ernst RK, Adams KN, Moskowitz SM, Kraig GM, Kawasaki K, Stead CM, Trent MS, Miller SI. The *Pseudomonas aeruginosa* lipid A deacylase: selection for expression and loss within the cystic fibrosis airway. J Bacteriol. 2006 Jan;188(1):191-201. PMID: 16352835.

Evans K, Poole K. The MexA-MexB-OprM multidrug efflux system of *Pseudomonas aeruginosa* is growth-phase regulated. FEMS Microbiol Lett. 1999 Apr 1;173(1):35-9. PMID: 10220878.

Fajardo A, Hernando-Amado S, Oliver A, Ball G, Filloux A, Martinez JL. Characterization of a novel Zn^{2+}-dependent intrinsic imipenemase from *Pseudomonas aeruginosa*. J Antimicrob Chemother. 2014 Nov;69(11):2972-8. PMID: 25185138.

Falcone M, Daikos GL, Tiseo G, Bassoulis D, Giordano C, Galfo V, Leonildi A, Tagliaferri E, Barnini S, Sani S, Farcomeni A, Ghiadoni L, Menichetti F. Efficacy of Ceftazidime-avibactam Plus Aztreonam in Patients With Bloodstream Infections Caused by Metallo-β-lactamase-Producing Enterobacterales. Clin Infect Dis. 2021 Jun 1;72(11):1871-1878. PMID: 32427286.

Fang ZL, Zhang LY, Huang YM, Qing Y, Cao KY, Tian GB, Huang X. OprD mutations and inactivation in imipenem-resistant *Pseudomonas aeruginosa* isolates from China. Infect Genet Evol. 2014 Jan;21:124-8. PMID: 24211415.

Fernando DM, Kumar A. Resistance-Nodulation-Division Multidrug Efflux Pumps in Gram-Negative Bacteria: Role in Virulence. Antibiotics (Basel). 2013 Mar 18;2(1):163-81. PMID: 27029297.

Filloux A. Protein Secretion Systems in *Pseudomonas aeruginosa*: An Essay on Diversity, Evolution, and Function. Front Microbiol. 2011 Jul 18;2:155. PMID: 21811488.

Findlay J, Poirel L, Juhas M, Nordmann P. KPC-Mediated Resistance to Ceftazidime-Avibactam and Collateral Effects in *Klebsiella pneumoniae*. Antimicrob Agents Chemother. 2021 Aug 17;65(9):e0089021. PMID: 34228551.

Fito-Boncompte L, Chapalain A, Bouffartigues E, Chaker H, Lesouhaitier O, Gicquel G, Bazire A, Madi A, Connil N, Véron W, Taupin L, Toussaint B, Cornelis P, Wei Q, Shioya K, Déziel E, Feuilloley MG, Orange N, Dufour A, Chevalier S. Full virulence of *Pseudomonas aeruginosa* requires OprF. Infect Immun. 2011 Mar;79(3):1176-86. PMID: 21189321.

Fléchard M, Duchesne R, Tahrioui A, Bouffartigues E, Depayras S, Hardouin J, Lagy C, Maillot O, Tortuel D, Azuama CO, Clamens T, Duclairoir-Poc C, Catel-Ferreira M, Gicquel G, Feuilloley MGJ, Lesouhaitier O, Heipieper HJ, Groleau MC, Déziel É, Cornelis P, Chevalier S. The absence of SigX results in impaired carbon metabolism and membrane fluidity in *Pseudomonas aeruginosa*. Sci Rep. 2018 Nov 21;8(1):17212. PMID: 30464317.

Fleming A. On the antibacterial action of cultures of a penicillium, with special reference to their use in the isolation of *B. Influenzae*. Br J Exp Pathol 1929; 10:226–236.

Fortunato G, Vaz-Moreira I, Gajic I, Manaia CM. Insight into phylogenomic bias of blaVIM-2 or blaNDM-1 dissemination amongst carbapenem-resistant *Pseudomonas aeruginosa*. Int J Antimicrob Agents. 2023 May;61(5):106788. PMID: 36924802.

Fowler RC, Hanson ND. The OpdQ porin of *Pseudomonas aeruginosa* is regulated by environmental signals associated with cystic fibrosis including nitrate-induced regulation involving the NarXL two-component system. Microbiologyopen. 2015 Dec;4(6):967-82. PMID: 26459101.

Franklin MJ, Nivens DE, Weadge JT, Howell PL. Biosynthesis of the *Pseudomonas aeruginosa* Extracellular Polysaccharides, Alginate, Pel, and Psl. Front Microbiol. 2011 Aug 22;2:167. PMID: 21991261.

Frère JM, Duez C, Ghuysen JM, Vandekerkhove J. Occurrence of a serine residue in the penicillin-binding site of the exocellular DD-carboxy-peptidase-transpeptidase from *Streptomyces* R61. FEBS Lett. 1976 Nov;70(1):257-60. PMID: 992070.

Frère JM, Joris B. Penicillin-sensitive enzymes in peptidoglycan biosynthesis. Crit Rev Microbiol. 1985;11(4):299-396. PMID: 3888533.

Frère JM, Nguyen-Distèche M, Coyette J, Joris B. Mode of action: interaction with the penicillin binding proteins. *The Chemistry of β-lactams*. 1992. 148-197.

Frère JM, Sauvage E, Kerff F. From "An Enzyme Able to Destroy Penicillin" to Carbapenemases: 70 Years of Beta-lactamase Misbehaviour. Curr Drug Targets. 2016;17(9):974-82. PMID: 26424390.

Fritsche TR, Stilwell MG, Jones RN. Antimicrobial activity of doripenem (S-4661): a global surveillance report (2003). Clin Microbiol Infect. 2005 Dec;11(12):974-84. PMID: 16307551.

Fukuoka T, Ohya S, Narita T, Katsuta M, Iijima M, Masuda N, Yasuda H, Trias J, Nikaido H. Activity of the carbapenem panipenem and role of the OprD (D2) protein in its diffusion through the *Pseudomonas aeruginosa* outer membrane. Antimicrob Agents Chemother. 1993 Feb;37(2):322-7. PMID: 8452364.

Funken H, Bartels KM, Wilhelm S, Brocker M, Bott M, Bains M, Hancock RE, Rosenau F, Jaeger KE. Specific association of lectin LecB with the surface of *Pseudomonas aeruginosa*: role of outer membrane protein OprF. PLoS One. 2012;7(10):e46857. PMID: 23056489.

Gagliardi A, Lamboglia E, Bianchi L, Landi C, Armini A, Ciolfi S, Bini L, Marri L. Proteomics analysis of a long-term survival strain of *Escherichia coli* K-12 exhibiting a growth advantage in stationary-phase (GASP) phenotype. Proteomics. 2016 Mar;16(6):963-72. PMID: 26711811.

Gali KV, St Jacques RM, Daniels CID, O'Rourke A, Turner L. Surveillance of carbapenem-resistant organisms using next-generation sequencing. Front Public Health. 2023 May 15;11:1184045. PMID: 37255756.

Galle M, Carpentier I, Beyaert R. Structure and function of the Type III secretion system of *Pseudomonas aeruginosa*. Curr Protein Pept Sci. 2012 Dec;13(8):831-42. PMID: 23305368.

Gao C, Chen Y, Cheng X, Zhang Y, Zhang Y, Wang Y, Cui Z, Liao Y, Luo P, Wu W, Wang C, Zeng H, Zou Q, Gu J. A novel structurally identified epitope delivered by macrophage membrane-coated PLGA nanoparticles elicits protection against *Pseudomonas aeruginosa*. J Nanobiotechnology. 2022 Dec 14;20(1):532. PMID: 36517801.

Garrity GM, Bell JA, Lilburn T. 2005. Pseudomonadales. p 323–442. In Bergey's manual of systematic bacteriology. Springer, Boston, MA.

Geddes AM, Klugman KP, Rolinson GN. Introduction: historical perspective and development of amoxicillin/clavulanate. Int J Antimicrob Agents. 2007 Dec;30 Suppl 2:S109-12. PMID: 17900874.

Gee KR, Kang HC, Meier TI, Zhao G, Blaszcak LC. Fluorescent Bocillins: synthesis and application in the detection of penicillin-binding proteins. Electrophoresis. 2001 Mar;22(5):960-5. PMID: 11332764.

Geno KA, Saad JS, Nahm MH. Discovery of Novel Pneumococcal Serotype 35D, a Natural WciG-Deficient Variant of Serotype 35B. J Clin Microbiol. 2017 May;55(5):1416-1425. PMID: 28202800.

Gessard C. De la pyocyanine et de son microbe. Paris; 1882

Ghssein G, Ezzeddine Z. A Review of *Pseudomonas aeruginosa* Metallophores: Pyoverdine, Pyochelin and Pseudopaline. Biology (Basel). 2022 Nov 25;11(12):1711. PMID: 36552220.

Giacobbe DR, Di Pilato V, Karaiskos I, Giani T, Marchese A, Rossolini GM, Bassetti M. Treatment and diagnosis of severe KPC-producing *Klebsiella pneumoniae* infections: a perspective on what has changed over last decades. Ann Med. 2023 Dec;55(1):101-113. PMID: 36856521.

Gibson DG, Young L, Chuang RY, Venter JC, Hutchison CA 3rd, Smith HO. Enzymatic assembly of DNA molecules up to several hundred kilobases. Nat Methods. 2009 May;6(5):343-5. PMID: 19363495.

Gillis RJ, White KG, Choi KH, Wagner VE, Schweizer HP, Iglewski BH. Molecular basis of azithromycin-resistant *Pseudomonas aeruginosa* biofilms. Antimicrob Agents Chemother. 2005 Sep;49(9):3858-67. PMID: 16127063.

Giske CG, Buarø L, Sundsfjord A, Wretlind B. Alterations of porin, pumps, and penicillin-binding proteins in carbapenem resistant clinical isolates of *Pseudomonas aeruginosa*. Microb Drug Resist. 2008 Mar;14(1):23-30. PMID: 18321207.

Glen KA, Lamont IL. β-lactam Resistance in *Pseudomonas aeruginosa*: Current Status, Future Prospects. Pathogens. 2021 Dec 18;10(12):1638. PMID: 34959593.

Glupczynski Y, Huang TD, Berhin C, Claeys G, Delmée M, Ide L, Ieven G, Pierard D, Rodriguez-Villalobos H, Struelens M, Vaneldere J. In vitro activity of temocillin against prevalent extended-spectrum beta-lactamases producing *Enterobacteriaceae* from Belgian intensive care units. Eur J Clin Microbiol Infect Dis. 2007 Nov;26(11):777-83. PMID: 17668253.

Golla VK, Piselli C, Kleinekathöfer U, Benz R. Permeation of Fosfomycin through the Phosphate-Specific Channels OprP and OprO of *Pseudomonas aeruginosa*. J Phys Chem B. 2022 Feb 24;126(7):1388-1403. PMID: 35138863.

Gomi R, Sharma A, Wu W, Sung B, Worgall S. Post-exposure immunization by capsid-modified AdC7 vector expressing *Pseudomonas aeruginosa* OprF clears *P. aeruginosa* respiratory infection. Vaccine. 2017 Dec 18;35(51):7174-7180. PMID: 29126807.

Gomis-Font MA, Pitart C, Del Barrio-Tofiño E, Zboromyrska Y, Cortes-Lara S, Mulet X, Marco F, Vila J, López-Causapé C, Oliver A. Emergence of Resistance to Novel Cephalosporin-β-Lactamase Inhibitor Combinations through the Modification of the *Pseudomonas aeruginosa* MexCD-OprJ Efflux Pump. Antimicrob Agents Chemother. 2021 Jul 16;65(8):e0008921. PMID: 34060900.

Gondal AJ, Choudhry N, Niaz A, Yasmin N. Molecular Analysis of Carbapenem and Aminoglycoside Resistance Genes in Carbapenem-Resistant *Pseudomonas aeruginosa* Clinical Strains: A Challenge for Tertiary Care Hospitals. Antibiotics (Basel). 2024 Feb 16;13(2):191. PMID: 38391577.

González-Vázquez MC, Rocha-Gracia RDC, Carabarín-Lima A, Bello-López E, Huerta-Romano F, Martínez-Laguna Y, Lozano-Zarain P. Location of OprD porin in *Pseudomonas aeruginosa* clinical isolates. APMIS. 2021 Apr;129(4):213-224. PMID: 33471435.

Gottschalk KE, Soskine M, Schuldiner S, Kessler H. A structural model of EmrE, a multi-drug transporter from *Escherichia coli*. Biophys J. 2004 Jun;86(6):3335-48. PMID: 15189838.

Gupta K, Marques CN, Petrova OE, Sauer K. Antimicrobial tolerance of *Pseudomonas aeruginosa* biofilms is activated during an early developmental stage and requires the two-component hybrid SagS. J Bacteriol. 2013 Nov;195(21):4975-87. PMID: 23995639.

Gutiérrez O, Juan C, Cercenado E, Navarro F, Bouza E, Coll P, Pérez JL, Oliver A. Molecular epidemiology and mechanisms of carbapenem resistance in *Pseudomonas aeruginosa* isolates from Spanish hospitals. Antimicrob Agents Chemother. 2007 Dec;51(12):4329-35. PMID: 17938181.

Hall CW, Zhang L, Mah TF. PA3225 Is a Transcriptional Repressor of Antibiotic Resistance Mechanisms in *Pseudomonas aeruginosa*. Antimicrob Agents Chemother. 2017 Jul 25;61(8):e02114-16. PMID: 28584154.

Hancock RE, Brinkman FS. Function of pseudomonas porins in uptake and efflux. Annu Rev Microbiol. 2002;56:17-38. PMID: 12142471.

Hancock RE, Decad GM, Nikaido H. Identification of the protein producing transmembrane diffusion pores in the outer membrane of *Pseudomonas aeruginosa* PA01. Biochim Biophys Acta. 1979 Jul 5;554(2):323-31. PMID: 114220.

Hancock RE, Egli C, Benz R, Siehnel RJ. Overexpression in *Escherichia coli* and functional analysis of a novel PPi-selective porin, oprO, from *Pseudomonas aeruginosa*. J Bacteriol. 1992 Jan;174(2):471-6. PMID: 1370289.

Hancock RE, Speert DP. Antibiotic resistance in *Pseudomonas aeruginosa*: mechanisms and impact on treatment. Drug Resist Updat. 2000 Aug;3(4):247-255. PMID: 11498392.

Hancock, RE., Carey AM. Protein D1 - A glucose inducible, pore-forming protein from the outer membrane of *Pseudomonas aeruginosa*. FEMS Microbiology Letters, Volume 8, Issue 2, 1980 pp:105–109.

Hannauer M, Braud A, Hoegy F, Ronot P, Boos A, Schalk IJ. The PvdRT-OpmQ efflux pump controls the metal selectivity of the iron uptake pathway mediated by the siderophore pyoverdine in *Pseudomonas aeruginosa*. Environ Microbiol. 2012 Jul;14(7):1696-708. PMID: 22187978.

Harino T, Kayama S, Kuwahara R, Kashiyama S, Shigemoto N, Onodera M, Yokozaki M, Ohge H, Sugai M. Meropenem resistance in imipenem-susceptible meropenem-resistant *Klebsiella pneumoniae* isolates not detected by rapid automated testing systems. J Clin Microbiol. 2013 Aug;51(8):2735-8. PMID: 23720796.

Hashimoto M, Komori T, Kamiya T. Nocardicin A, a new monocyclic beta-lactam antibiotic II. Structure determination of nocardicins A and B. J Antibiot (Tokyo). 1976 Sep;29(9):890-901. PMID: 993130.

Hassan KA, Jackson SM, Penesyan A, Patching SG, Tetu SG, Eijkelkamp BA, Brown MH, Henderson PJ, Paulsen IT. Transcriptomic and biochemical analyses identify a family of chlorhexidine efflux proteins. Proc Natl Acad Sci U S A. 2013 Dec 10;110(50):20254-9. PMID: 24277845.

Hassan KA, Liu Q, Elbourne LDH, Ahmad I, Sharples D, Naidu V, Chan CL, Li L, Harborne SPD, Pokhrel A, Postis VLG, Goldman A, Henderson PJF, Paulsen IT. Pacing across the membrane: the novel PACE family of efflux pumps is widespread in Gram-negative pathogens. Res Microbiol. 2018 Sep-Oct;169(7-8):450-454. PMID: 29409983.

Hassan KA, Naidu V, Edgerton JR, Mettrick KA, Liu Q, Fahmy L, Li L, Jackson SM, Ahmad I, Sharples D, Henderson PJF, Paulsen IT. Short-chain diamines are the physiological substrates of

PACE family efflux pumps. Proc Natl Acad Sci U S A. 2019 Sep 3;116(36):18015-18020. PMID: 31416917.

Hassan R, El-Naggar W, Abd El-Aziz AM, Shaaban M, Kenawy HI, Ali YM. Immunization with outer membrane proteins (OprF and OprI) and flagellin B protects mice from pulmonary infection with mucoid and nonmucoid *Pseudomonas aeruginosa*. J Microbiol Immunol Infect. 2018 Jun;51(3):312-320. PMID: 28291719.

He GX, Kuroda T, Mima T, Morita Y, Mizushima T, Tsuchiya T. An H(+)-coupled multidrug efflux pump, PmpM, a member of the MATE family of transporters, from *Pseudomonas aeruginosa*. J Bacteriol. 2004 Jan;186(1):262-5. PMID: 14679249.

Heacock-Kang Y, Sun Z, Zarzycki-Siek J, Poonsuk K, McMillan IA, Chuanchuen R, Hoang TT. Two Regulators, PA3898 and PA2100, Modulate the *Pseudomonas aeruginosa* Multidrug Resistance MexAB-OprM and EmrAB Efflux Pumps and Biofilm Formation. Antimicrob Agents Chemother. 2018 Nov 26;62(12):e01459-18. PMID: 30297364.

Hearn EM, Patel DR, Lepore BW, Indic M, van den Berg B. Transmembrane passage of hydrophobic compounds through a protein channel wall. Nature. 2009 Mar 19;458(7236):367-70. PMID: 19182779.

Hellemans J, Mortier G, De Paepe A, Speleman F, Vandesompele J. qBase relative quantification framework and software for management and automated analysis of real-time quantitative PCR data. Genome Biol. 2007;8(2):R19. PMID: 17291332.

Henderson JC, Zimmerman SM, Crofts AA, Boll JM, Kuhns LG, Herrera CM, Trent MS. The Power of Asymmetry: Architecture and Assembly of the Gram-Negative Outer Membrane Lipid Bilayer. Annu Rev Microbiol. 2016 Sep 8;70:255-78. PMID: 27359214.

Hentzer M, Teitzel GM, Balzer GJ, Heydorn A, Molin S, Givskov M, Parsek MR. Alginate overproduction affects *Pseudomonas aeruginosa* biofilm structure and function. J Bacteriol. 2001 Sep;183(18):5395-401. PMID: 11514525.

Heo YJ, Chung IY, Cho WJ, Lee BY, Kim JH, Choi KH, Lee JW, Hassett DJ, Cho YH. The major catalase gene (katA) of *Pseudomonas aeruginosa* PA14 is under both positive and negative control of the global transactivator OxyR in response to hydrogen peroxide. J Bacteriol. 2010 Jan;192(2):381-90. PMID: 19933365.

Heung LJ, Luberto C, Del Poeta M. Role of sphingolipids in microbial pathogenesis. Infect Immun. 2006 Jan;74(1):28-39. PMID: 16368954.

Higgins CF. ABC transporters: physiology, structure and mechanism--an overview. Res Microbiol. 2001 Apr-May;152(3-4):205-10. PMID: 11421269.

Hoang HH, Nickerson NN, Lee VT, Kazimirova A, Chami M, Pugsley AP, Lory S. Outer membrane targeting of *Pseudomonas aeruginosa* proteins shows variable dependence on the components of Bam and Lol machineries. mBio. 2011 Dec 6;2(6):e00246-11. PMID: 22147293.

Hombach M, Bloemberg GV, Böttger EC. Effects of clinical breakpoint changes in CLSI guidelines 2010/2011 and EUCAST guidelines 2011 on antibiotic susceptibility test reporting of Gram-negative bacilli. J Antimicrob Chemother. 2012 Mar;67(3):622-32. PMID: 22167240.

Hong DJ, Bae IK, Jang IH, Jeong SH, Kang HK, Lee K. Epidemiology and Characteristics of Metallo-β-Lactamase-Producing *Pseudomonas aeruginosa*. Infect Chemother. 2015 Jun;47(2):81-97. PMID: 26157586.

Hua C, Huang J, Wang T, Sun Y, Liu J, Huang L, Deng X. Bacterial Transcription Factors Bind to Coding Regions and Regulate Internal Cryptic Promoters. mBio. 2022 Oct 26;13(5):e0164322. PMID: 36200779.

Huang H, Hancock RE. Genetic definition of the substrate selectivity of outer membrane porin protein OprD of *Pseudomonas aeruginosa*. J Bacteriol. 1993 Dec;175(24):7793-800. PMID: 8253668.

Huang H, Jeanteur D, Pattus F, Hancock RE. Membrane topology and site-specific mutagenesis of *Pseudomonas aeruginosa* porin OprD. Mol Microbiol. 1995 Jun;16(5):931-41. PMID: 7476190.

Huang Q, Yang J, Li C, Song Y, Zhu Y, Zhao N, Mou X, Tang X, Luo G, Tong A, Sun B, Tang H, Li H, Bai L, Bao R. Structural characterization of PaFkbA: A periplasmic chaperone from *Pseudomonas aeruginosa*. Comput Struct Biotechnol J. 2021 Apr 25;19:2460-2467. PMID: 34025936.

Huang W, Hamouche JE, Wang G, Smith M, Yin C, Dhand A, Dimitrova N, Fallon JT. Integrated Genome-Wide Analysis of an Isogenic Pair of *Pseudomonas aeruginosa* Clinical Isolates with Differential Antimicrobial Resistance to Ceftolozane/Tazobactam, Ceftazidime/Avibactam, and Piperacillin/Tazobactam. Int J Mol Sci. 2020 Feb 4;21(3):1026. PMID: 32033143.

Huszczynski SM, Lam JS, Khursigara CM. The Role of *Pseudomonas aeruginosa* Lipopolysaccharide in Bacterial Pathogenesis and Physiology. Pathogens. 2019 Dec 19;9(1):6. PMID: 31861540.

Hwang S, Kim CY, Ji SG, Go J, Kim H, Yang S, Kim HJ, Cho A, Yoon SS, Lee I. Network-assisted investigation of virulence and antibiotic-resistance systems in *Pseudomonas aeruginosa*. Sci Rep. 2016 May 19;6:26223. PMID: 27194047.

Imperi F, Ciccosanti F, Perdomo AB, Tiburzi F, Mancone C, Alonzi T, Ascenzi P, Piacentini M, Visca P, Fimia GM. Analysis of the periplasmic proteome of *Pseudomonas aeruginosa*, a metabolically versatile opportunistic pathogen. Proteomics. 2009 Apr;9(7):1901-15. PMID: 19333994.

Isabella VM, Campbell AJ, Manchester J, Sylvester M, Nayar AS, Ferguson KE, Tommasi R, Miller AA. Toward the rational design of carbapenem uptake in *Pseudomonas aeruginosa*. Chem Biol. 2015 Apr 23;22(4):535-547. PMID: 25910245.

Iyer R, Sylvester MA, Velez-Vega C, Tommasi R, Durand-Reville TF, Miller AA. Whole-Cell-Based Assay To Evaluate Structure Permeation Relationships for Carbapenem Passage through the *Pseudomonas aeruginosa* Porin OprD. ACS Infect Dis. 2017 Apr 14;3(4):310-319. PMID: 28157293.

Iyobe S, Watanabe M, Mitsuhashi S, Inoue M. Estimation of outer membrane permeability of carbapenem antibiotics to *Pseudomonas aeruginosa*. J Infect Chemother. 1999 Sep;5(3):168-170. PMID: 11810510.

Jacoby GA. AmpC beta-lactamases. Clin Microbiol Rev. 2009 Jan;22(1):161-82, Table of Contents. PMID: 19136439.

Jansen KB, Baker SL, Sousa MC. Crystal structure of BamB from *Pseudomonas aeruginosa* and functional evaluation of its conserved structural features. PLoS One. 2012;7(11):e49749. PMID: 23189157.

Jeannot K, Elsen S, Köhler T, Attree I, van Delden C, Plésiat P. Resistance and virulence of *Pseudomonas aeruginosa* clinical strains overproducing the MexCD-OprJ efflux pump. Antimicrob Agents Chemother. 2008 Jul;52(7):2455-62. PMID: 18474583.

Jevons MP. “Celbenin” - resistant Staphylococci. Br Med J. 1961 Jan 14;1(5219):124–5.

Jo JT, Brinkman FS, Hancock RE. Aminoglycoside efflux in *Pseudomonas aeruginosa*: involvement of novel outer membrane proteins. Antimicrob Agents Chemother. 2003 Mar;47(3):1101-11. PMID: 12604548.

Joris B, Ledent P, Kobayashi T, Lampen JO, Ghuysen JM. Expression in *Escherichia coli* of the carboxy terminal domain of the BLAR sensory-transducer protein of *Bacillus licheniformis* as a water-soluble Mr 26,000 penicillin-binding protein. FEMS Microbiol Lett. 1990 Jun 15;58(1):107-13. PMID: 2204571.

Juan C, Maciá MD, Gutiérrez O, Vidal C, Pérez JL, Oliver A. Molecular mechanisms of beta-lactam resistance mediated by AmpC hyperproduction in *Pseudomonas aeruginosa* clinical strains. Antimicrob Agents Chemother. 2005 Nov;49(11):4733-8. PMID: 16251318.

Jurado-Martín I, Sainz-Mejías M, McClean S. *Pseudomonas aeruginosa*: An Audacious Pathogen with an Adaptable Arsenal of Virulence Factors. Int J Mol Sci. 2021 Mar 18;22(6):3128. PMID: 33803907.

Kahan FM, Kahan JS, Cassidy PJ, Kropp H. The mechanism of action of fosfomycin (phosphonomycin). Ann N Y Acad Sci. 1974 May 10;235(0):364-86. PMID: 4605290.

Kahan JS, Kahan FM, Goegelman R, Currie SA, Jackson M, Stapley EO, Miller TW, Miller AK, Hendlin D, Mochales S, Hernandez S, Woodruff HB, Birnbaum J. Thienamycin, a new beta-lactam antibiotic. I. Discovery, taxonomy, isolation and physical properties. J Antibiot (Tokyo). 1979 Jan;32(1):1-12. PMID: 761989.

Karaiskos I, Galani I, Daikos GL, Giamarellou H. Breaking Through Resistance: A Comparative Review of New Beta-Lactamase Inhibitors (Avibactam, Vaborbactam, Relebactam) Against Multidrug-Resistant Superbugs. Antibiotics (Basel). 2025 May 21;14(5):528. PMID: 40426594.

Kearse M, Moir R, Wilson A, Stones-Havas S, Cheung M, Sturrock S, Buxton S, Cooper A, Markowitz S, Duran C, Thierer T, Ashton B, Meintjes P, Drummond A. Geneious Basic: an integrated and extendable desktop software platform for the organization and analysis of sequence data. Bioinformatics. 2012 Jun 15;28(12):1647-9. PMID: 22543367.

Kessler RE. Cefepime microbiologic profile and update. Pediatr Infect Dis J. 2001 Mar;20(3):331-6. PMID: 11303846.

Khedr A, Mathew BM, Mushtaq H, Nelson CA, Poehler JL, Jama AB, Borge JM, von Lehe JL, Gomez Urena EO, Khan SA. *Pseudomonas* infection reduction in the ICU: a successful multidisciplinary quality improvement project. Infez Med. 2022 Dec 1;30(4):577-586. PMID: 36482956.

Kiely PD, O'Callaghan J, Abbas A, O'Gara F. Genetic analysis of genes involved in dipeptide metabolism and cytotoxicity in *Pseudomonas aeruginosa* PAO1. Microbiology (Reading). 2008 Aug;154(Pt 8):2209-2218. PMID: 18667554.

Kim JS, Jeong H, Song S, Kim HY, Lee K, Hyun J, Ha NC. Structure of the tripartite multidrug efflux pump AcrAB-TolC suggests an alternative assembly mode. Mol Cells. 2015;38(2):180-6. PMID: 26013259.

Klebba PE, Hofnung M, Charbit A. A model of maltodextrin transport through the sugar-specific porin, LamB, based on deletion analysis. EMBO J. 1994 Oct 3;13(19):4670-5. PMID: 7925308.

Klein K, Sonnabend MS, Frank L, Leibiger K, Franz-Wachtel M, Macek B, Trunk T, Leo JC, Autenrieth IB, Schütz M, Bohn E. Deprivation of the Periplasmic Chaperone SurA Reduces Virulence and Restores Antibiotic Susceptibility of Multidrug-Resistant *Pseudomonas aeruginosa*. Front Microbiol. 2019 Feb 21;10:100. PMID: 30846971.

Klockgether J, Munder A, Neugebauer J, Davenport CF, Stanke F, Larbig KD, Heeb S, Schöck U, Pohl TM, Wiehlmann L, Tümmler B. Genome diversity of *Pseudomonas aeruginosa* PAO1 laboratory strains. J Bacteriol. 2010 Feb;192(4):1113-21. PMID: 20023018.

Knak T, Abdullaziz MA, Höfmann S, Alves Avelar LA, Klein S, Martin M, Fischer M, Tanaka N, Kurz T. Over 40 Years of Fosmidomycin Drug Research: A Comprehensive Review and Future Opportunities. Pharmaceuticals (Basel). 2022 Dec 14;15(12):1553. PMID: 36559004.

Knirel YA, Bystrova OV, Kocharova NA, Zähringer U, Pier GB. Conserved and variable structural features in the lipopolysaccharide of *Pseudomonas aeruginosa*. J Endotoxin Res. 2006;12(6):324-36. Erratum in: J Endotoxin Res. 2010 Aug;16(4):274. PMID: 17254386.

Kocíncová D, Lam JS. Structural diversity of the core oligosaccharide domain of *Pseudomonas aeruginosa* lipopolysaccharide. Biochemistry (Mosc). 2011 Jul;76(7):755-60. PMID: 21999536.

Köhler J, Dorso KL, Young K, Hammond GG, Rosen H, Kropp H, Silver LL. In vitro activities of the potent, broad-spectrum carbapenem MK-0826 (L-749,345) against broad-spectrum beta-lactamase-and extended-spectrum beta-lactamase-producing *Klebsiella pneumoniae* and *Escherichia coli* clinical isolates. Antimicrob Agents Chemother. 1999 May;43(5):1170-6. PMID: 10223931.

Köhler T, Epp SF, Curty LK, Pechère JC. Characterization of MexT, the regulator of the MexE-MexF-OprN multidrug efflux system of *Pseudomonas aeruginosa*. J Bacteriol. 1999**b** Oct;181(20):6300-5. PMID: 10515918.

Köhler T, Michea-Hamzehpour M, Epp SF, Pechere JC. Carbapenem activities against *Pseudomonas aeruginosa*: respective contributions of OprD and efflux systems. Antimicrob Agents Chemother. 1999**a** Feb;43(2):424-7. PMID: 9925552.

Köhler T, Michéa-Hamzehpour M, Henze U, Gotoh N, Curty LK, Pechère JC. Characterization of MexE-MexF-OprN, a positively regulated multidrug efflux system of *Pseudomonas aeruginosa*. Mol Microbiol. 1997 Jan;23(2):345-54. PMID: 9044268.

Kojo H, Shigi Y, Nishida M. Enterobacter cloacae outer membrane permeability to ceftizoxime (FK 749) and five other new cephalosporin derivatives. J Antibiot (Tokyo). 1980 Mar;33(3):317-21. PMID: 6247313.

Kolayli F, Karadenizli A, Savli H, Ergen K, Hatirnaz O, Balikci E, Budak F, Vahaboglu H. Effect of carbapenems on the transcriptional expression of the oprD, oprM and oprN genes in *Pseudomonas aeruginosa*. J Med Microbiol. 2004 Sep;53(Pt 9):915-920. PMID: 15314200.

Kondakova T, D'Heygère F, Feuilloley MJ, Orange N, Heipieper HJ, Duclairoir Poc C. Glycerophospholipid synthesis and functions in *Pseudomonas*. Chem Phys Lipids. 2015 Sep;190:27-42. PMID: 26148574.

Kothari A, Kumar SK, Singh V, Kumar P, Kaushal K, Pandey A, Jain N, Omar BJ. Association of multidrug resistance behavior of clinical *Pseudomonas aeruginosa* to pigment coloration. Eur J Med Res. 2022 Jul 16;27(1):120. PMID: 35842687.

Kovach ME, Elzer PH, Hill DS, Robertson GT, Farris MA, Roop RM 2nd, Peterson KM. Four new derivatives of the broad-host-range cloning vector pBBR1MCS, carrying different antibiotic-resistance cassettes. Gene. 1995 Dec 1;166(1):175-6. PMID: 8529885.

Kucharska I, Seelheim P, Edrington T, Liang B, Tamm LK. OprG Harnesses the Dynamics of its Extracellular Loops to Transport Small Amino Acids across the Outer Membrane of *Pseudomonas aeruginosa*. Structure. 2015 Dec 1;23(12):2234-2245. PMID: 26655471.

Kuck NA, Jacobus NV, Petersen PJ, Weiss WJ, Testa RT. Comparative in vitro and in vivo activities of piperacillin combined with the beta-lactamase inhibitors tazobactam, clavulanic acid, and sulbactam. Antimicrob Agents Chemother. 1989 Nov;33(11):1964-9. PMID: 2558615.

Kulp A, Kuehn MJ. Biological functions and biogenesis of secreted bacterial outer membrane vesicles. Annu Rev Microbiol. 2010;64:163-84. PMID: 20825345.

LaBauve AE, Wargo MJ. Growth and laboratory maintenance of *Pseudomonas aeruginosa*. Curr Protoc Microbiol. 2012 May;Chapter 6:Unit 6E.1. PMID: 22549165.

Laddomada F, Miyachiro MM, Jessop M, Patin D, Job V, Mengin-Lecreulx D, Le Roy A, Ebel C, Breyton C, Gutsche I, Dessen A. The MurG glycosyltransferase provides an oligomeric scaffold for the cytoplasmic steps of peptidoglycan biosynthesis in the human pathogen *Bordetella pertussis*. Sci Rep. 2019 Mar 15;9(1):4656. PMID: 30874582.

Laemmli UK. Cleavage of structural proteins during the assembly of the head of bacteriophage T4. Nature. 1970 Aug 15;227(5259):680-5. PMID: 5432063.

Lakaye B, Dubus A, Joris B, Frère JM. Method for estimation of low outer membrane permeability to beta-lactam antibiotics. Antimicrob Agents Chemother. 2002 Sep;46(9):2901-7. PMID: 12183245.

Lamas Ferreiro JL, Álvarez Otero J, González González L, Novoa Lamazares L, Arca Blanco A, Bermúdez Sanjurjo JR, Rodríguez Conde I, Fernández Soneira M, de la Fuente Aguado J. *Pseudomonas aeruginosa* urinary tract infections in hospitalized patients: Mortality and prognostic factors. PLoS One. 2017 May 26;12(5):e0178178. PMID: 28552972.

Lambert PA. Cellular impermeability and uptake of biocides and antibiotics in Gram-positive bacteria and mycobacteria. Symp Ser Soc Appl Microbiol. 2002;(31):46S-54S. PMID: 12481828.

Lamers RP, Cavallari JF, Burrows LL. The efflux inhibitor phenylalanine-arginine beta-naphthylamide (PAβN) permeabilizes the outer membrane of Gram-negative bacteria. PLoS One. 2013;8(3):e60666. PMID: 23544160.

Lamont IL, Beare PA, Ochsner U, Vasil AI, Vasil ML. Siderophore-mediated signaling regulates virulence factor production in *Pseudomonas aeruginosa*. Proc Natl Acad Sci U S A. 2002 May 14;99(10):7072-7. PMID: 11997446.

Lassaux P, Traoré DA, Loisel E, Favier A, Docquier JD, Sohier JS, Laurent C, Bebrone C, Frère JM, Ferrer JL, Galleni M. Biochemical and structural characterization of the subclass B1 metallo-β-lactamase VIM-4. Antimicrob Agents Chemother. 2011 Mar;55(3):1248-55. PMID: 21149620.

Lauretti L, Riccio ML, Mazzariol A, Cornaglia G, Amicosante G, Fontana R, Rossolini GM. Cloning and characterization of blaVIM, a new integron-borne metallo-beta-lactamase gene from a *Pseudomonas aeruginosa* clinical isolate. Antimicrob Agents Chemother. 1999 Jul;43(7):1584-90. PMID: 10390207.

Lee J, Pothula KR, Kleinekathöfer U, Im W. Simulation Study of Occk5 Functional Properties in *Pseudomonas aeruginosa* Outer Membranes. J Phys Chem B. 2018 Aug 30;122(34):8185-8192. PMID: 30075620.

Lee M, Abbey T, Biagi M, Wenzler E. Activity of aztreonam in combination with ceftazidime-avibactam against serine- and metallo-β-lactamase-producing *Pseudomonas aeruginosa*. Diagn Microbiol Infect Dis. 2021 Jan;99(1):115227. PMID: 33086177.

Lee Y, Song S, Sheng L, Zhu L, Kim JS, Wood TK. Substrate Binding Protein DppA1 of ABC Transporter DppBCDF Increases Biofilm Formation in *Pseudomonas aeruginosa* by Inhibiting Pf5 Prophage Lysis. Front Microbiol. 2018 Jan 24;9:30. PMID: 29416528.

Levy SB, McMurry L. Plasmid-determined tetracycline resistance involves new transport systems for tetracycline. Nature. 1978 Nov 2;276(5683):90-2. PMID: 368642.

Li A, Schertzer JW, Yong X. Molecular dynamics modeling of *Pseudomonas aeruginosa* outer membranes. Phys Chem Chem Phys. 2018 Sep 19;20(36):23635-23648. PMID: 30191217.

Li H, Luo YF, Williams BJ, Blackwell TS, Xie CM. Structure and function of OprD protein in *Pseudomonas aeruginosa*: from antibiotic resistance to novel therapies. Int J Med Microbiol. 2012 Mar;302(2):63-8. PMID: 22226846.

Li S, Wang Y, Li X, Lee BS, Jung S, Lee MS. Enhancing the Thermo-Stability and Anti-Biofilm Activity of Alginate Lyase by Immobilization on Low Molecular Weight Chitosan Nanoparticles. Int J Mol Sci. 2019 Sep 14;20(18):4565. PMID: 31540110.

Li XZ, Barré N, Poole K. Influence of the MexA-MexB-oprM multidrug efflux system on expression of the MexC-MexD-oprJ and MexE-MexF-oprN multidrug efflux systems in *Pseudomonas aeruginosa*. J Antimicrob Chemother. 2000 Dec;46(6):885-93. PMID: 11102405.

Li XZ, Nikaido H, Poole K. Role of mexA-mexB-oprM in antibiotic efflux in *Pseudomonas aeruginosa*. Antimicrob Agents Chemother. 1995 Sep;39(9):1948-53. PMID: 8540696.

Li Y, Mima T, Komori Y, Morita Y, Kuroda T, Mizushima T, Tsuchiya T. A new member of the tripartite multidrug efflux pumps, MexVW-OprM, in *Pseudomonas aeruginosa*. J Antimicrob Chemother. 2003 Oct;52(4):572-5. PMID: 12951344.

Liao J, Schurr MJ, Sauer K. The MerR-like regulator BrlR confers biofilm tolerance by activating multidrug efflux pumps in *Pseudomonas aeruginosa* biofilms. J Bacteriol. 2013 Aug;195(15):3352-63. PMID: 23687276.

Liu H, Yang L, Chen Q, Song H, Bo X, Guo J, Li P, Ni M. Time Series Genomics of *Pseudomonas aeruginosa* Reveals the Emergence of a Hypermutator Phenotype and Within-Host Evolution in Clinical Inpatients. Microbiol Spectr. 2022 Aug 31;10(4):e0005722. PMID: 35861512.

Liu J, Eren E, Vijayaraghavan J, Cheneke BR, Indic M, van den Berg B, Movileanu L. OccK channels from *Pseudomonas aeruginosa* exhibit diverse single-channel electrical signatures but conserved anion selectivity. Biochemistry. 2012**b** Mar 20;51(11):2319-30. PMID: 22369314.

Liu J, Wolfe AJ, Eren E, Vijayaraghavan J, Indic M, van den Berg B, Movileanu L. Cation selectivity is a conserved feature in the OccD subfamily of *Pseudomonas aeruginosa*. Biochim Biophys Acta. 2012**a** Nov;1818(11):2908-16. PMID: 22824298.

Livermore DM, Davy KW. Invalidity for *Pseudomonas aeruginosa* of an accepted model of bacterial permeability to beta-lactam antibiotics. Antimicrob Agents Chemother. 1991 May;35(5):916-21. PMID: 1906695.

Livermore DM, Sefton AM, Scott GM. Properties and potential of ertapenem. J Antimicrob Chemother. 2003 Sep;52(3):331-44. PMID: 12917243.

Livermore DM, Tulkens PM. Temocillin revived. J Antimicrob Chemother. 2009 Feb;63(2):243-5. PMID: 19095679.

Livermore DM. beta-Lactamases in laboratory and clinical resistance. Clin Microbiol Rev. 1995 Oct;8(4):557-84. PMID: 8665470.

Locher KP. Review. Structure and mechanism of ATP-binding cassette transporters. Philos Trans R Soc Lond B Biol Sci. 2009 Jan 27;364(1514):239-45. PMID: 18957379.

Lomovskaya O, Warren MS, Lee A, Galazzo J, Fronko R, Lee M, Blais J, Cho D, Chamberland S, Renau T, Leger R, Hecker S, Watkins W, Hoshino K, Ishida H, Lee VJ. Identification and characterization of inhibitors of multidrug resistance efflux pumps in *Pseudomonas aeruginosa*: novel agents for combination therapy. Antimicrob Agents Chemother. 2001 Jan;45(1):105-16. PMID: 11120952.

López-Argüello S, Montaner M, Oliver A, Moya B. Molecular Basis of AmpC β-Lactamase Induction by Avibactam in *Pseudomonas aeruginosa*: PBP Occupancy, Live Cell Binding

Dynamics and Impact on Resistant Clinical Isolates Harboring PDC-X Variants. Int J Mol Sci. 2021 Mar 17;22(6):3051. PMID: 33802668.

Lorusso AB, Carrara JA, Barroso CDN, Tuon FF, Faoro H. Role of Efflux Pumps on Antimicrobial Resistance in *Pseudomonas aeruginosa*. Int J Mol Sci. 2022 Dec 13;23(24):15779. PMID: 36555423.

Luscher A, Moynié L, Auguste PS, Bumann D, Mazza L, Pletzer D, Naismith JH, Köhler T. TonB-Dependent Receptor Repertoire of *Pseudomonas aeruginosa* for Uptake of Siderophore-Drug Conjugates. Antimicrob Agents Chemother. 2018 May 25;62(6):e00097-18. PMID: 29555629.

Macfarlane EL, Kwasnicka A, Ochs MM, Hancock RE. PhoP-PhoQ homologues in *Pseudomonas aeruginosa* regulate expression of the outer-membrane protein OprH and polymyxin B resistance. Mol Microbiol. 1999 Oct;34(2):305-16. PMID: 10564474.

MacLeod DL, Velayudhan J, Kenney TF, Therrien JH, Sutherland JL, Barker LM, Baker WR. Fosfomycin enhances the active transport of tobramycin in *Pseudomonas aeruginosa*. Antimicrob Agents Chemother. 2012 Mar;56(3):1529-38. PMID: 22232284.

Magiorakos AP, Srinivasan A, Carey RB, Carmeli Y, Falagas ME, Giske CG, Harbarth S, Hindler JF, Kahlmeter G, Olsson-Liljequist B, Paterson DL, Rice LB, Stelling J, Struelens MJ, Vatopoulos A, Weber JT, Monnet DL. Multidrug-resistant, extensively drug-resistant and pandrug-resistant bacteria: an international expert proposal for interim standard definitions for acquired resistance. Clin Microbiol Infect. 2012 Mar;18(3):268-81. PMID: 21793988.

Mann EE, Wozniak DJ. Pseudomonas biofilm matrix composition and niche biology. FEMS Microbiol Rev. 2012 Jul;36(4):893-916. PMID: 22212072.

Manzoor S, Ahmed A, Moin ST. Iron coordination to pyochelin siderophore influences dynamics of FptA receptor from *Pseudomonas aeruginosa*: a molecular dynamics simulation study. Biometals. 2021 Oct;34(5):1099-1119. PMID: 34357504.

Martínez E, Estupiñán M, Pastor FI, Busquets M, Díaz P, Manresa A. Functional characterization of ExFadLO, an outer membrane protein required for exporting oxygenated long-chain fatty acids in *Pseudomonas aeruginosa*. Biochimie. 2013 Feb;95(2):290-8. PMID: 23069386.

Martins D, McKay GA, English AM, Nguyen D. Sublethal Paraquat Confers Multidrug Tolerance in *Pseudomonas aeruginosa* by Inducing Superoxide Dismutase Activity and Lowering Envelope Permeability. Front Microbiol. 2020 Sep 25;11:576708. PMID: 33101252.

Maseda H, Saito K, Nakajima A, Nakae T. Variation of the mexT gene, a regulator of the MexEF-oprN efflux pump expression in wild-type strains of *Pseudomonas aeruginosa*. FEMS Microbiol Lett. 2000 Nov 1;192(1):107-12. PMID: 11040437.

Maseda H, Sawada I, Saito K, Uchiyama H, Nakae T, Nomura N. Enhancement of the mexAB-oprM efflux pump expression by a quorum-sensing autoinducer and its cancellation by a regulator, MexT, of the mexEF-oprN efflux pump operon in *Pseudomonas aeruginosa*. Antimicrob Agents Chemother. 2004 Apr;48(4):1320-8. PMID: 15047536.

Maseda H, Uwate M, Nakae T. Transcriptional regulation of the mexEF-oprN multidrug efflux pump operon by MexT and an unidentified repressor in nfxC-type mutant of *Pseudomonas aeruginosa*. FEMS Microbiol Lett. 2010 Oct;311(1):36-43. PMID: 20727012.

Masuda N, Sakagawa E, Ohya S, Gotoh N, Tsujimoto H, Nishino T. Substrate specificities of MexAB-OprM, MexCD-OprJ, and MexXY-oprM efflux pumps in *Pseudomonas aeruginosa*. Antimicrob Agents Chemother. 2000 Dec;44(12):3322-7. PMID: 11083635.

Mathee K, Ciofu O, Sternberg C, Lindum PW, Campbell JIA, Jensen P, Johnsen AH, Givskov M, Ohman DE, Søren M, Høiby N, Kharazmi A. Mucoid conversion of *Pseudomonas aeruginosa* by

hydrogen peroxide: a mechanism for virulence activation in the cystic fibrosis lung. Microbiology (Reading). 1999 Jun;145 (Pt 6):1349-1357. PMID: 10411261.

Matlock W, Shaw LP, Stoesser N. Global genomic epidemiology of *bla*$_{GES-5}$ carbapenemase-associated integrons. Microb Genom. 2024 Dec;10(12):001312. PMID: 39630499.

Matsumura N, Minami S, Watanabe Y, Iyobe S, Mitsuhashi S. Role of permeability in the activities of beta-lactams against Gram-negative bacteria which produce a group 3 beta-lactamase. Antimicrob Agents Chemother. 1999 Aug;43(8):2084-6. PMID: 10428944.

McLean K, Lee D, Holmes EA, Penewit K, Waalkes A, Ren M, Lee SA, Gasper J, Manoil C, Salipante SJ. Genomic Analysis Identifies Novel *Pseudomonas aeruginosa* Resistance Genes under Selection during Inhaled Aztreonam Therapy In Vivo. Antimicrob Agents Chemother. 2019 Aug 23;63(9):e00866-19. PMID: 31285231.

McPhee JB, Tamber S, Bains M, Maier E, Gellatly S, Lo A, Benz R, Hancock RE. The major outer membrane protein OprG of *Pseudomonas aeruginosa* contributes to cytotoxicity and forms an anaerobically regulated, cation-selective channel. FEMS Microbiol Lett. 2009 Jun;296(2):241-7. PMID: 19486157.

Miao L, Liu W, Qiao Q, Li X, Xu Z. Fluorescent antibiotics for real-time tracking of pathogenic bacteria. J Pharm Anal. 2020 Oct;10(5):444-451. PMID: 33133728.

Migula W. Über ein neues System der Bakterien. Arb Bakteriol Inst Karlsruhe 1894; 1:235-238.

Miller AK, Brannon MK, Stevens L, Johansen HK, Selgrade SE, Miller SI, Høiby N, Moskowitz SM. PhoQ mutations promote lipid A modification and polymyxin resistance of *Pseudomonas aeruginosa* found in colistin-treated cystic fibrosis patients. Antimicrob Agents Chemother. 2011 Dec;55(12):5761-9. PMID: 21968359.

Mima T, Joshi S, Gomez-Escalada M, Schweizer HP. Identification and characterization of TriABC-OpmH, a triclosan efflux pump of *Pseudomonas aeruginosa* requiring two membrane fusion proteins. J Bacteriol. 2007 Nov;189(21):7600-9. PMID: 17720796.

Mima T, Kohira N, Li Y, Sekiya H, Ogawa W, Kuroda T, Tsuchiya T. Gene cloning and characteristics of the RND-type multidrug efflux pump MuxABC-OpmB possessing two RND components in *Pseudomonas aeruginosa*. Microbiology (Reading). 2009 Nov;155(Pt 11):3509-3517. PMID: 19713238.

Mima T, Sekiya H, Mizushima T, Kuroda T, Tsuchiya T. Gene cloning and properties of the RND-type multidrug efflux pumps MexPQ-OpmE and MexMN-OprM from *Pseudomonas aeruginosa*. Microbiol Immunol. 2005;49(11):999-1002. PMID: 16301811.

Mishra M, Byrd MS, Sergeant S, Azad AK, Parsek MR, McPhail L, Schlesinger LS, Wozniak DJ. *Pseudomonas aeruginosa* Psl polysaccharide reduces neutrophil phagocytosis and the oxidative response by limiting complement-mediated opsonization. Cell Microbiol. 2012 Jan;14(1):95-106. PMID: 21951860.

Mitchell P. A general theory of membrane transport from studies of bacteria. Nature. 1957 Jul 20;180(4577):134-6. PMID: 13451664.

Miyadera T, Sugimura Y, Hashimoto T, Tanaka T, Iino K, Shibata T, Sugawara S. Synthesis and in vitro activity of a new carbapenem, RS-533. J Antibiot (Tokyo). 1983 Aug;36(8):1034-9. PMID: 6630055.

Montaner M, Lopez-Argüello S, Oliver A, Moya B. PBP Target Profiling by β-Lactam and β-Lactamase Inhibitors in Intact *Pseudomonas aeruginosa*: Effects of the Intrinsic and Acquired Resistance Determinants on the Periplasmic Drug Availability. Microbiol Spectr. 2023 Feb 14;11(1):e0303822. PMID: 36475840.

Moradali, M.F., Rehm, B.H.A. (2019). The Role of Alginate in Bacterial Biofilm Formation. In: Cohen, E., Merzendorfer, H. (eds) Extracellular Sugar-Based Biopolymers Matrices. Biologically-Inspired Systems, vol 12. Springer, Cham. https://doi.org/10.1007/978-3-030-12919-4_13

Morita Y, Cao L, Gould VC, Avison MB, Poole K. nalD encodes a second repressor of the mexAB-oprM multidrug efflux operon of *Pseudomonas aeruginosa*. J Bacteriol. 2006 Dec;188(24):8649-54. PMID: 17028276.

Morita Y, Komori Y, Mima T, Kuroda T, Mizushima T, Tsuchiya T. Construction of a series of mutants lacking all of the four major mex operons for multidrug efflux pumps or possessing each one of the operons from *Pseudomonas aeruginosa* PAO1: MexCD-OprJ is an inducible pump. FEMS Microbiol Lett. 2001 Aug 7;202(1):139-43. PMID: 11506922.

Morita Y, Murata T, Mima T, Shiota S, Kuroda T, Mizushima T, Gotoh N, Nishino T, Tsuchiya T. Induction of mexCD-oprJ operon for a multidrug efflux pump by disinfectants in wild-type *Pseudomonas aeruginosa* PAO1. J Antimicrob Chemother. 2003 Apr;51(4):991-4. PMID: 12654738.

Morita Y, Tomida J, Kawamura Y. MexXY multidrug efflux system of *Pseudomonas aeruginosa*. Front Microbiol. 2012 Nov 28;3:408. PMID: 23233851.

Moyá B, Beceiro A, Cabot G, Juan C, Zamorano L, Alberti S, Oliver A. Pan-β-lactam resistance development in *Pseudomonas aeruginosa* clinical strains: molecular mechanisms, penicillin-binding protein profiles, and binding affinities. Antimicrob Agents Chemother. 2012 Sep;56(9):4771-8. PMID: 22733064.

Moya B, Dötsch A, Juan C, Blázquez J, Zamorano L, Haussler S, Oliver A. Beta-lactam resistance response triggered by inactivation of a nonessential penicillin-binding protein. PLoS Pathog. 2009 Mar;5(3):e1000353. PMID: 19325877.

Mulani MS, Kamble EE, Kumkar SN, Tawre MS, Pardesi KR. Emerging Strategies to Combat ESKAPE Pathogens in the Era of Antimicrobial Resistance: A Review. Front Microbiol. 2019 Apr 1;10:539. PMID: 30988669.

Muller C, Plésiat P, Jeannot K. A two-component regulatory system interconnects resistance to polymyxins, aminoglycosides, fluoroquinolones, and β-lactams in *Pseudomonas aeruginosa*. Antimicrob Agents Chemother. 2011 Mar;55(3):1211-21. PMID: 21149619.

Murakami S, Nakashima R, Yamashita E, Matsumoto T, Yamaguchi A. Crystal structures of a multidrug transporter reveal a functionally rotating mechanism. Nature. 2006 Sep 14;443(7108):173-9. PMID: 16915237.

Murakami S, Nakashima R, Yamashita E, Yamaguchi A. Crystal structure of bacterial multidrug efflux transporter AcrB. Nature. 2002 Oct 10;419(6907):587-93. PMID: 12374972.

Muramatsu H, Horii T, Morita M, Hashimoto H, Kanno T, Maekawa M. Effect of basic amino acids on susceptibility to carbapenems in clinical *Pseudomonas aeruginosa* isolates. Int J Med Microbiol. 2003 Jun;293(2-3):191-7. PMID: 12868655.

Naas T, Oueslati S, Bonnin RA, Dabos ML, Zavala A, Dortet L, Retailleau P, Iorga BI. Beta-lactamase database (BLDB) - structure and function. J Enzyme Inhib Med Chem. 2017 Dec;32(1):917-919. PMID: 28719998.

Nagakubo S, Nishino K, Hirata T, Yamaguchi A. The putative response regulator BaeR stimulates multidrug resistance of *Escherichia coli* via a novel multidrug exporter system, MdtABC. J Bacteriol. 2002 Aug;184(15):4161-7. PMID: 12107133.

Nakae T. Identification of the outer membrane protein of *E. coli* that produces transmembrane channels in reconstituted vesicle membranes. Biochem Biophys Res Commun. 1976 Aug 9;71(3):877-84. PMID: 786294.

Nascimento AP, Ortiz MF, Martins WM, Morais GL, Fehlberg LC, Almeida LG, Ciapina LP, Gales AC, Vasconcelos AT. Intraclonal Genome Stability of the Metallo-β-lactamase SPM-1-producing *Pseudomonas aeruginosa* ST277, an Endemic Clone Disseminated in Brazilian Hospitals. Front Microbiol. 2016 Dec 5;7:1946. PMID: 27994579.

Navare AT, Chavez JD, Zheng C, Weisbrod CR, Eng JK, Siehnel R, Singh PK, Manoil C, Bruce JE. Probing the protein interaction network of *Pseudomonas aeruginosa* cells by chemical cross-linking mass spectrometry. Structure. 2015 Apr 7;23(4):762-73. PMID: 25800553.

Nestorovich EM, Danelon C, Winterhalter M, Bezrukov SM. Designed to penetrate: time-resolved interaction of single antibiotic molecules with bacterial pores. Proc Natl Acad Sci U S A. 2002 Jul 23;99(15):9789-94. PMID: 12119404.

Nestorovich EM, Sugawara E, Nikaido H, Bezrukov SM. *Pseudomonas aeruginosa* porin OprF: properties of the channel. J Biol Chem. 2006 Jun 16;281(24):16230-7. PMID: 16617058.

Nicas TI, Hancock RE. *Pseudomonas aeruginosa* outer membrane permeability: isolation of a porin protein F-deficient mutant. J Bacteriol. 1983 Jan;153(1):281-5. PMID: 6294050.

Nikaido H, Hancock REW. Outer membrane permeability in *Pseudomonas aeruginosa.* In: Sokatch J, ed. The bacteria. Vol 10. Orlando, Florida: Academic Press, 1986:145–93.

Nikaido H, Rosenberg EY, Foulds J. Porin channels in *Escherichia coli*: studies with beta-lactams in intact cells. J Bacteriol. 1983 Jan;153(1):232-40. PMID: 6294048.

Nikaido H. RND transporters in the living world. Res Microbiol. 2018 Sep-Oct;169(7-8):363-371. PMID: 29577985.

Noinaj N, Guillier M, Barnard TJ, Buchanan SK. TonB-dependent transporters: regulation, structure, and function. Annu Rev Microbiol. 2010;64:43-60. PMID: 20420522.

Nordmann P, Dortet L, Poirel L. Carbapenem resistance in *Enterobacteriaceae*: here is the storm! Trends Mol Med. 2012 May;18(5):263-72. PMID: 22480775.

Norrby SR. Imipenem/cilastatin: rationale for a fixed combination. Rev Infect Dis. 1985 Jul-Aug;7 Suppl 3:S447-51. PMID: 3863220.

Nouwens AS, Willcox MD, Walsh BJ, Cordwell SJ. Proteomic comparison of membrane and extracellular proteins from invasive (PAO1) and cytotoxic (6206) strains of *Pseudomonas aeruginosa*. Proteomics. 2002 Sep;2(9):1325-46. PMID: 12362351.

Novelli A, Del Giacomo P, Rossolini GM, Tumbarello M. Meropenem/vaborbactam: a next generation β-lactam β-lactamase inhibitor combination. Expert Rev Anti Infect Ther. 2020 Jul;18(7):643-655. PMID: 32297801.

O'Donnell JN, Lodise TP. New Perspectives on Antimicrobial Agents: Imipenem-Relebactam. Antimicrob Agents Chemother. 2022 Jul 19;66(7):e0025622. PMID: 35727059.

O'Toole GA. To build a biofilm. J Bacteriol. 2003 May;185(9):2687-9. PMID: 12700246.

Oakley BR, Kirsch DR, Morris NR. A simplified ultrasensitive silver stain for detecting proteins in polyacrylamide gels. Anal Biochem. 1980 Jul 1;105(2):361-3. PMID: 6161559.

Ocampo-Sosa AA, Cabot G, Rodríguez C, Roman E, Tubau F, Macia MD, Moya B, Zamorano L, Suárez C, Peña C, Domínguez MA, Moncalián G, Oliver A, Martínez-Martínez L; Spanish Network for Research in Infectious Diseases (REIPI). Alterations of OprD in carbapenem-intermediate and -susceptible strains of *Pseudomonas aeruginosa* isolated from patients with bacteremia in a Spanish multicenter study. Antimicrob Agents Chemother. 2012 Apr;56(4):1703-13. PMID: 22290967.

Ochs MM, Bains M, Hancock RE. Role of putative loops 2 and 3 in imipenem passage through the specific porin OprD of *Pseudomonas aeruginosa*. Antimicrob Agents Chemother. 2000 Jul;44(7):1983-5. PMID: 10858367.

Ochs MM, Lu CD, Hancock RE, Abdelal AT. Amino acid-mediated induction of the basic amino acid-specific outer membrane porin OprD from *Pseudomonas aeruginosa*. J Bacteriol. 1999**b** Sep;181(17):5426-32. PMID: 10464217.

Ochs MM, McCusker MP, Bains M, Hancock RE. Negative regulation of the *Pseudomonas aeruginosa* outer membrane porin OprD selective for imipenem and basic amino acids. Antimicrob Agents Chemother. 1999**a** May;43(5):1085-90. PMID: 10223918.

Ørskov, I., and Ørskov F. 1984. Serotyping of Klebsiella. Methods Microbiol. 14:143-164.

Oura H, Tashiro Y, Toyofuku M, Ueda K, Kiyokawa T, Ito S, Takahashi Y, Lee S, Nojiri H, Nakajima-Kambe T, Uchiyama H, Futamata H, Nomura N. Inhibition of *Pseudomonas aeruginosa* swarming motility by 1-naphthol and other bicyclic compounds bearing hydroxyl groups. Appl Environ Microbiol. 2015 Apr;81(8):2808-18. PMID: 25681177.

Öztürk H, Ozkirimli E, Özgür A. Classification of Beta-lactamases and penicillin binding proteins using ligand-centric network models. PLoS One. 2015 Feb 17;10(2):e0117874. PMID: 25689853.

Papadopoulos A, Busch M, Reiners J, Hachani E, Baeumers M, Berger J, Schmitt L, Jaeger KE, Kovacic F, Smits SHJ, Kedrov A. The periplasmic chaperone Skp prevents misfolding of the secretory lipase A from *Pseudomonas aeruginosa*. Front Mol Biosci. 2022 Oct 24;9:1026724. PMID: 36353734.

Parkin J, Khalid S. Atomistic molecular-dynamics simulations enable prediction of the arginine permeation pathway through OccD1/OprD from *Pseudomonas aeruginosa*. Biophys J. 2014 Oct 21;107(8):1853-1861. PMID: 25418166.

Paton R, Miles RS, Hood J, Amyes SG, Miles RS, Amyes SG. ARI 1: beta-lactamase-mediated imipenem resistance in *Acinetobacter baumannii*. Int J Antimicrob Agents. 1993 Feb;2(2):81-7. PMID: 18611526.

Paulsson M, Su YC, Ringwood T, Uddén F, Riesbeck K. *Pseudomonas aeruginosa* uses multiple receptors for adherence to laminin during infection of the respiratory tract and skin wounds. Sci Rep. 2019 Dec 3;9(1):18168. PMID: 31796854.

Peng X, Xu C, Ren H, Lin X, Wu L, Wang S. Proteomic analysis of the sarcosine-insoluble outer membrane fraction of *Pseudomonas aeruginosa* responding to ampicilin, kanamycin, and tetracycline resistance. J Proteome Res. 2005 Nov-Dec;4(6):2257-65. PMID: 16335974.

Pérez FJ, Gimeno C, Navarro D, García-de-Lomas J. Meropenem permeation through the outer membrane of *Pseudomonas aeruginosa* can involve pathways other than the OprD porin channel. Chemotherapy. 1996 May-Jun;42(3):210-14. PMID: 8983889.

Perron K, Caille O, Rossier C, Van Delden C, Dumas JL, Köhler T. CzcR-CzcS, a two-component system involved in heavy metal and carbapenem resistance in *Pseudomonas aeruginosa*. J Biol Chem. 2004 Mar 5;279(10):8761-8. PMID: 14679195.

Perry CM, Brogden RN. Cefuroxime axetil. A review of its antibacterial activity, pharmacokinetic properties and therapeutic efficacy. Drugs. 1996 Jul;52(1):125-58. PMID: 8799689.

Phan G, Benabdelhak H, Lascombe MB, Benas P, Rety S, Picard M, Ducruix A, Etchebest C, Broutin I. Structural and dynamical insights into the opening mechanism of *P. aeruginosa* OprM channel. Structure. 2010 Mar 14;18(4):507-17. PMID: 20399187.

Piddock LJ. Clinically relevant chromosomally encoded multidrug resistance efflux pumps in bacteria. Clin Microbiol Rev. 2006 Apr;19(2):382-402. PMID: 16614254.

Pier GB, Coleman F, Grout M, Franklin M, Ohman DE. Role of alginate O acetylation in resistance of mucoid *Pseudomonas aeruginosa* to opsonic phagocytosis. Infect Immun. 2001 Mar;69(3):1895-901. PMID: 11179370.

Pirnay JP, De Vos D, Mossialos D, Vanderkelen A, Cornelis P, Zizi M. Analysis of the *Pseudomonas aeruginosa* oprD gene from clinical and environmental isolates. Environ Microbiol. 2002 Dec;4(12):872-82. PMID: 12534469.

Piselli C, Benz R. Fosmidomycin transport through the phosphate-specific porins OprO and OprP of *Pseudomonas aeruginosa*. Mol Microbiol. 2021 Jul;116(1):97-108. PMID: 33561903.

Pletzer D, Braun Y, Dubiley S, Lafon C, Köhler T, Page MGP, Mourez M, Severinov K, Weingart H. The *Pseudomonas aeruginosa* PA14 ABC Transporter NppA1A2BCD Is Required for Uptake of Peptidyl Nucleoside Antibiotics. J Bacteriol. 2015 Jul;197(13):2217-2228. PMID: 25917903.

Pletzer D, Braun Y, Weingart H. Swarming motility is modulated by expression of the putative xenosiderophore transporter SppR-SppABCD in *Pseudomonas aeruginosa* PA14. Antonie Van Leeuwenhoek. 2016 Jun;109(6):737-53. PMID: 26995781.

Pletzer D, Lafon C, Braun Y, Köhler T, Page MG, Mourez M, Weingart H. High-throughput screening of dipeptide utilization mediated by the ABC transporter DppBCDF and its substrate-binding proteins DppA1-A5 in *Pseudomonas aeruginosa*. PLoS One. 2014 Oct 22;9(10):e111311. PMID: 25338022.

Poole K, Gotoh N, Tsujimoto H, Zhao Q, Wada A, Yamasaki T, Neshat S, Yamagishi J, Li XZ, Nishino T. Overexpression of the *mexC-mexD-oprJ* efflux operon in *nfxB*-type multidrug-resistant strains of *Pseudomonas aeruginosa*. Mol Microbiol. 1996 Aug;21(4):713-24. PMID: 8878035.

Poole K. *Pseudomonas aeruginosa*: resistance to the max. Front Microbiol. 2011 Apr 5;2:65. PMID: 21747788.

Pothula KR, Kleinekathöfer U. Theoretical analysis of ion conductance and gating transitions in the OpdK (OccK1) channel. Analyst. 2015 Jul 21;140(14):4855-64. PMID: 25781224.

Poudyal B, Sauer K. The ABC of Biofilm Drug Tolerance: the MerR-Like Regulator BrlR Is an Activator of ABC Transport Systems, with PA1874-77 Contributing to the Tolerance of *Pseudomonas aeruginosa* Biofilms to Tobramycin. Antimicrob Agents Chemother. 2018 Jan 25;62(2):e01981-17. PMID: 29180529.

Prachayasittikul V, Isarankura-Na-Ayudhya C, Tantimongcolwat T, Nantasenamat C, Galla HJ. EDTA-induced membrane fluidization and destabilization: biophysical studies on artificial lipid membranes. Acta Biochim Biophys Sin (Shanghai). 2007 Nov;39(11):901-13. PMID: 17989882.

Purssell A, Fruci M, Mikalauskas A, Gilmour C, Poole K. EsrC, an envelope stress-regulated repressor of the mexCD-oprJ multidrug efflux operon in *Pseudomonas aeruginosa*. Environ Microbiol. 2015 Jan;17(1):186-98. PMID: 25143244.

Queenan AM, Bush K. Carbapenemases: the versatile beta-lactamases. Clin Microbiol Rev. 2007 Jul;20(3):440-58, table of contents. PMID: 17630334.

Quistgaard EM, Löw C, Guettou F, Nordlund P. Understanding transport by the major facilitator superfamily (MFS): structures pave the way. Nat Rev Mol Cell Biol. 2016 Feb;17(2):123-32. PMID: 26758938.

Raneri M, Pinatel E, Peano C, Rampioni G, Leoni L, Bianconi I, Jousson O, Dalmasio C, Ferrante P, Briani F. *Pseudomonas aeruginosa* mutants defective in glucose uptake have pleiotropic phenotype

and altered virulence in non-mammal infection models. Sci Rep. 2018 Nov 15;8(1):16912. PMID: 30442901.

Ranjitkar S, Jones AK, Mostafavi M, Zwirko Z, Iartchouk O, Barnes SW, Walker JR, Willis TW, Lee PS, Dean CR. Target (MexB)- and Efflux-Based Mechanisms Decreasing the Effectiveness of the Efflux Pump Inhibitor D13-9001 in *Pseudomonas aeruginosa* PAO1: Uncovering a New Role for MexMN-OprM in Efflux of β-Lactams and a Novel Regulatory Circuit (MmnRS) Controlling MexMN Expression. Antimicrob Agents Chemother. 2019 Jan 29;63(2):e01718-18. PMID: 30420483.

Rayner B, Verderosa AD, Ferro V, Blaskovich MAT. Siderophore conjugates to combat antibiotic-resistant bacteria. RSC Med Chem. 2023 Mar 1;14(5):800-822. PMID: 37252105.

Reading C, Cole M. Clavulanic acid: a beta-lactamase-inhiting beta-lactam from *Streptomyces clavuligerus*. Antimicrob Agents Chemother. 1977 May;11(5):852-7. PMID: 879738.

Rehm BH, Hancock RE. Membrane topology of the outer membrane protein OprH from *Pseudomonas aeruginosa*: PCR-mediated site-directed insertion and deletion mutagenesis. J Bacteriol. 1996 Jun;178(11):3346-9. PMID: 8655519.

Ribeiro ÁCDS, Crozatti MTL, Silva AAD, Macedo RS, Machado AMO, Silva ATA. *Pseudomonas aeruginosa* in the ICU: prevalence, resistance profile, and antimicrobial consumption. Rev Soc Bras Med Trop. 2019 Dec 20;53:e20180498. PMID: 31859938.

Richmond MH, Clark DC, Wotton S. Indirect method for assessing the penetration of beta-lactamase-nonsusceptible penicillins and cephalosporins in *Escherichia coli* strains. Antimicrob Agents Chemother. 1976 Aug;10(2):215-8. PMID: 791092.

Richter R, Kamal MAM, Koch M, Niebuur BJ, Huber AL, Goes A, Volz C, Vergalli J, Kraus T, Müller R, Schneider-Daum N, Fuhrmann G, Pagès JM, Lehr CM. An Outer Membrane Vesicle-Based Permeation Assay (OMPA) for Assessing Bacterial Bioavailability. Adv Healthc Mater. 2022 Mar;11(5):e2101180. PMID: 34614289.

Ringel MT, Brüser T. The biosynthesis of pyoverdines. Microb Cell. 2018 Aug 28;5(10):424-437. PMID: 30386787.

Roberts IS. The biochemistry and genetics of capsular polysaccharide production in bacteria. Annu Rev Microbiol. 1996;50:285-315. PMID: 8905082.

Rojo F. Carbon catabolite repression in Pseudomonas: optimizing metabolic versatility and interactions with the environment. FEMS Microbiol Rev. 2010 Sep;34(5):658-84. PMID: 20412307.

Rojo-Bezares B, Estepa V, Cebollada R, de Toro M, Somalo S, Seral C, Castillo FJ, Torres C, Sáenz Y. Carbapenem-resistant *Pseudomonas aeruginosa* strains from a Spanish hospital: characterization of metallo-beta-lactamases, porin OprD and integrons. Int J Med Microbiol. 2014 May;304(3-4):405-14. PMID: 24594145.

Ruedas-López A, Alonso-García I, Lasarte-Monterrubio C, Guijarro-Sánchez P, Gato E, Vázquez-Ucha JC, Vallejo JA, Fraile-Ribot PA, Fernández-Pérez B, Velasco D, Gutiérrez-Urbón JM, Oviaño M, Beceiro A, González-Bello C, Oliver A, Arca-Suárez J, Bou G. Selection of AmpC β-Lactamase Variants and Metallo-β-Lactamases Leading to Ceftolozane/Tazobactam and Ceftazidime/Avibactam Resistance during Treatment of MDR/XDR *Pseudomonas aeruginosa* Infections. Antimicrob Agents Chemother. 2022 Feb 15;66(2):e0206721. PMID: 34930034.

Ruijter JM, Ramakers C, Hoogaars WM, Karlen Y, Bakker O, van den Hoff MJ, Moorman AF. Amplification efficiency: linking baseline and bias in the analysis of quantitative PCR data. Nucleic Acids Res. 2009 Apr;37(6):e45. PMID: 19237396.

Ruiz N, Kahne D, Silhavy TJ. Transport of lipopolysaccharide across the cell envelope: the long road of discovery. Nat Rev Microbiol. 2009 Sep;7(9):677-83. PMID: 19633680.

Ryder C, Byrd M, Wozniak DJ. Role of polysaccharides in *Pseudomonas aeruginosa* biofilm development. Curr Opin Microbiol. 2007 Dec;10(6):644-8. PMID: 17981495.

Sadek M, Le Guern R, Kipnis E, Gosset P, Poirel L, Dessein R, Nordmann P. Progressive in vivo development of resistance to cefiderocol in *Pseudomonas aeruginosa*. Eur J Clin Microbiol Infect Dis. 2023 Jan;42(1):61-66. PMID: 36376766.

Sader HS, Castanheira M, Duncan LR, Mendes RE. Antimicrobial activities of ceftazidime/avibactam, ceftolozane/tazobactam, imipenem/relebactam, meropenem/vaborbactam, and comparators against *Pseudomonas aeruginosa* from patients with skin and soft tissue infections. Int J Infect Dis. 2021 Dec;113:279-281. doi: 10.1016/j.ijid.2021.10.022. Epub 2021 Oct 17. PMID: 34670144.

Saint N, Lou KL, Widmer C, Luckey M, Schirmer T, Rosenbusch JP. Structural and functional characterization of OmpF porin mutants selected for larger pore size. II. Functional characterization. J Biol Chem. 1996 Aug 23;271(34):20676-80. PMID: 8702817.

Saito K, Yoneyama H, Nakae T. nalB-type mutations causing the overexpression of the MexAB-OprM efflux pump are located in the mexR gene of the *Pseudomonas aeruginosa* chromosome. FEMS Microbiol Lett. 1999 Oct 1;179(1):67-72. PMID: 10481088.

Sakhtah H, Koyama L, Zhang Y, Morales DK, Fields BL, Price-Whelan A, Hogan DA, Shepard K, Dietrich LE. The *Pseudomonas aeruginosa* efflux pump MexGHI-OpmD transports a natural phenazine that controls gene expression and biofilm development. Proc Natl Acad Sci U S A. 2016 Jun 21;113(25):E3538-47. PMID: 27274079.

Sakyo S, Tomita H, Tanimoto K, Fujimoto S, Ike Y. Potency of carbapenems for the prevention of carbapenem-resistant mutants of *Pseudomonas aeruginosa*: the high potency of a new carbapenem doripenem. J Antibiot (Tokyo). 2006 Apr;59(4):220-8. PMID: 16830889.

Salvà-Serra F, Jaén-Luchoro D, Marathe NP, Adlerberth I, Moore ERB, Karlsson R. Responses of carbapenemase-producing and non-producing carbapenem-resistant *Pseudomonas aeruginosa* strains to meropenem revealed by quantitative tandem mass spectrometry proteomics. Front Microbiol. 2023 Feb 9;13:1089140. PMID: 36845973.

Samanta S, Bodrenko I, Acosta-Gutiérrez S, D'Agostino T, Pathania M, Ghai I, Schleberger C, Bumann D, Wagner R, Winterhalter M, van den Berg B, Ceccarelli M. Getting Drugs through Small Pores: Exploiting the Porins Pathway in *Pseudomonas aeruginosa*. ACS Infect Dis. 2018 Oct 12;4(10):1519-1528. PMID: 30039960.

Sambrook J, Russell DW. Molecular cloning: a laboratory manual 3rd edition. 2001. Coldspring.

Sanganna Gari RR, Seelheim P, Marsh B, Kiessling V, Creutz CE, Tamm LK. Quaternary structure of the small amino acid transporter OprG from *Pseudomonas aeruginosa*. J Biol Chem. 2018 Nov 2;293(44):17267-17277. PMID: 30237175.

Sanger F, Nicklen S, Coulson AR. DNA sequencing with chain-terminating inhibitors. Proc Natl Acad Sci U S A. 1977 Dec;74(12):5463-7. PMID: 271968.

Satake S, Yoneyama H, Nakae T. Role of OmpD2 and chromosomal beta-lactamase in carbapenem resistance in clinical isolates of *Pseudomonas aeruginosa*. J Antimicrob Chemother. 1991 Aug;28(2):199-207. PMID: 1778851.

Sato T, Yamawaki K. Cefiderocol: Discovery, Chemistry, and In Vivo Profiles of a Novel Siderophore Cephalosporin. Clin Infect Dis. 2019 Nov 13;69(Suppl 7):S538-S543. PMID: 31724047.

Savinova TA, Samchenko AA, Bocharova YA, Mayansky NA, Chebotar IV. Computer Program for Detection and Analyzing the Porin-Mediated Antibiotic Resistance of Bacteria. Sovrem Tekhnologii Med. 2021;13(6):15-22. PMID: 35265355.

Schalk IJ, Guillon L. Pyoverdine biosynthesis and secretion in *Pseudomonas aeruginosa*: implications for metal homeostasis. Environ Microbiol. 2013 Jun;15(6):1661-73. PMID: 23126435.

Schroeter, J. "Uber einige durch Bacterien gebildete Pigmente. (1872)". In: F. Cohn (ed.), Beitrage zur Biologie der Pflanzen. J.U. Kern's Verlag, Breslau, 1875, pp. 109-126.

Schulz S, Eckweiler D, Bielecka A, Nicolai T, Franke R, Dötsch A, Hornischer K, Bruchmann S, Düvel J, Häussler S. Elucidation of sigma factor-associated networks in *Pseudomonas aeruginosa* reveals a modular architecture with limited and function-specific crosstalk. PLoS Pathog. 2015 Mar 17;11(3):e1004744. PMID: 25780925.

Sekiya H, Mima T, Morita Y, Kuroda T, Mizushima T, Tsuchiya T. Functional cloning and characterization of a multidrug efflux pump, mexHI-opmD, from a *Pseudomonas aeruginosa* mutant. Antimicrob Agents Chemother. 2003 Sep;47(9):2990-2. PMID: 12937010.

Sennhauser G, Bukowska MA, Briand C, Grütter MG. Crystal structure of the multidrug exporter MexB from *Pseudomonas aeruginosa*. J Mol Biol. 2009 May 29;389(1):134-45. PMID: 19361527.

Sevillano E, Gallego L, García-Lobo JM. First detection of the OXA-40 carbapenemase in *P. aeruginosa* isolates, located on a plasmid also found in *A. baumannii*. Pathol Biol (Paris). 2009 Sep;57(6):493-5. PMID: 18585868.

Sherrard LJ, Wee BA, Duplancic C, Ramsay KA, Dave KA, Ballard E, Wainwright CE, Grimwood K, Sidjabat HE, Whiley DM, Beatson SA, Kidd TJ, Bell SC. Emergence and impact of oprD mutations in *Pseudomonas aeruginosa* strains in cystic fibrosis. J Cyst Fibros. 2022 Jan;21(1):e35-e43. PMID: 33775602.

Siehnel RJ, Egli C, Hancock RE. Polyphosphate-selective porin OprO of *Pseudomonas aeruginosa*: expression, purification and sequence. Mol Microbiol. 1992 Aug;6(16):2319-26. PMID: 1406271.

Sihotang TSU, Widodo ADW, Endraswari PD. Effect of Ciprofloxacin, Levofloxacin, and Ofloxacin on *Pseudomonas aeruginosa*: A case control study with time kill curve analysis. Ann Med Surg (Lond). 2022 Sep 16;82:104674. PMID: 36268299.

Silveira MC, Albano RM, Asensi MD, Carvalho-Assef AP. Description of genomic islands associated to the multidrug-resistant *Pseudomonas aeruginosa* clone ST277. Infect Genet Evol. 2016 Aug;42:60-5. PMID: 27108807.

Simonet V, Malléa M, Pagès JM. Substitutions in the eyelet region disrupt cefepime diffusion through the *Escherichia coli* OmpF channel. Antimicrob Agents Chemother. 2000 Feb;44(2):311-5. PMID: 10639355.

Simpson JA, Smith SE, Dean RT. Alginate may accumulate in cystic fibrosis lung because the enzymatic and free radical capacities of phagocytic cells are inadequate for its degradation. Biochem Mol Biol Int. 1993 Aug;30(6):1021-34. PMID: 8220249.

Singh M, Sykes EME, Li Y, Kumar A. MexXY RND pump of *Pseudomonas aeruginosa* PA7 effluxes bi-anionic β-lactams carbenicillin and sulbenicillin when it partners with the outer membrane factor OprA but not with OprM. Microbiology (Reading). 2020 Nov;166(11):1095-1106. PMID: 32909933.

Sivaneson M, Mikkelsen H, Ventre I, Bordi C, Filloux A. Two-component regulatory systems in *Pseudomonas aeruginosa*: an intricate network mediating fimbrial and efflux pump gene expression. Mol Microbiol. 2011 Mar;79(5):1353-66. PMID: 21205015.

Six DA, Krucker T, Leeds JA. Advances and challenges in bacterial compound accumulation assays for drug discovery. Curr Opin Chem Biol. 2018 Jun;44:9-15. PMID: 29803973.

Slack FJ, Serror P, Joyce E, Sonenshein AL. A gene required for nutritional repression of the *Bacillus subtilis* dipeptide permease operon. Mol Microbiol. 1995 Feb;15(4):689-702. PMID: 7783641.

Smalley NE, Schaefer AL, Asfahl KL, Perez C, Greenberg EP, Dandekar AA. Evolution of the Quorum Sensing Regulon in Cooperating Populations of *Pseudomonas aeruginosa*. mBio. 2022 Feb 22;13(1):e0016122. PMID: 35294222.

Smith JD, Kumarasiri M, Zhang W, Hesek D, Lee M, Toth M, Vakulenko S, Fisher JF, Mobashery S, Chen Y. Structural analysis of the role of *Pseudomonas aeruginosa* penicillin-binding protein 5 in β-lactam resistance. Antimicrob Agents Chemother. 2013 Jul;57(7):3137-46. PMID: 23629710.

Sobel ML, Hocquet D, Cao L, Plesiat P, Poole K. Mutations in PA3574 (nalD) lead to increased MexAB-OprM expression and multidrug resistance in laboratory and clinical isolates of *Pseudomonas aeruginosa*. Antimicrob Agents Chemother. 2005**b** May;49(5):1782-6. PMID: 15855496.

Sobel ML, Neshat S, Poole K. Mutations in PA2491 (mexS) promote MexT-dependent mexEF-oprN expression and multidrug resistance in a clinical strain of *Pseudomonas aeruginosa*. J Bacteriol. 2005**a** Feb;187(4):1246-53. PMID: 15687188.

Solov'eva TF, Novikova OD, Portnyagina OY. Biogenesis of β-barrel integral proteins of bacterial outer membrane. Biochemistry (Mosc). 2012 Nov;77(11):1221-36. PMID: 23240560.

Sonnleitner E, Valentini M, Wenner N, Haichar FZ, Haas D, Lapouge K. Novel targets of the CbrAB/Crc carbon catabolite control system revealed by transcript abundance in *Pseudomonas aeruginosa*. PLoS One. 2012;7(10):e44637. PMID: 23115619.

Soundararajan G, Bhamidimarri SP, Winterhalter M. Understanding Carbapenem Translocation through OccD3 (OpdP) of *Pseudomonas aeruginosa*. ACS Chem Biol. 2017 Jun 16;12(6):1656-1664. PMID: 28440622.

Srikumar R, Paul CJ, Poole K. Influence of mutations in the mexR repressor gene on expression of the MexA-MexB-oprM multidrug efflux system of *Pseudomonas aeruginosa*. J Bacteriol. 2000 Mar;182(5):1410-4. PMID: 10671465.

Staudinger BJ, Muller JF, Halldórsson S, Boles B, Angermeyer A, Nguyen D, Rosen H, Baldursson O, Gottfreðsson M, Guðmundsson GH, Singh PK. Conditions associated with the cystic fibrosis defect promote chronic *Pseudomonas aeruginosa* infection. Am J Respir Crit Care Med. 2014 Apr 1;189(7):812-24. PMID: 24467627.

Stover CK, Pham XQ, Erwin AL, Mizoguchi SD, Warrener P, Hickey MJ, Brinkman FS, Hufnagle WO, Kowalik DJ, Lagrou M, Garber RL, Goltry L, Tolentino E, Westbrock-Wadman S, Yuan Y, Brody LL, Coulter SN, Folger KR, Kas A, Larbig K, Lim R, Smith K, Spencer D, Wong GK, Wu Z, Paulsen IT, Reizer J, Saier MH, Hancock RE, Lory S, Olson MV. Complete genome sequence of *Pseudomonas aeruginosa* PAO1, an opportunistic pathogen. Nature. 2000 Aug 31;406(6799):959-64. PMID: 10984043.

Sugawara E, Nestorovich EM, Bezrukov SM, Nikaido H. *Pseudomonas aeruginosa* porin OprF exists in two different conformations. J Biol Chem. 2006 Jun 16;281(24):16220-9. PMID: 16595653.

Swain J, El Khoury M, Kempf J, Briée F, Van Der Smissen P, Décout JL, Mingeot-Leclercq MP. Effect of cardiolipin on the antimicrobial activity of a new amphiphilic aminoglycoside derivative on *Pseudomonas aeruginosa*. PLoS One. 2018 Aug 20;13(8):e0201752. PMID: 30125281.

Sykes RB, Cimarusti CM, Bonner DP, Bush K, Floyd DM, Georgopapadakou NH, Koster WM, Liu WC, Parker WL, Principe PA, Rathnum ML, Slusarchyk WA, Trejo WH, Wells JS. Monocyclic beta-lactam antibiotics produced by bacteria. Nature. 1981 Jun 11;291(5815):489-91. PMID: 7015152.

Tamber S, Hancock RE. Involvement of two related porins, OprD and OpdP, in the uptake of arginine by *Pseudomonas aeruginosa*. FEMS Microbiol Lett. 2006 Jul;260(1):23-9. PMID: 16790014.

Tamber S, Maier E, Benz R, Hancock RE. Characterization of OpdH, a *Pseudomonas aeruginosa* porin involved in the uptake of tricarboxylates. J Bacteriol. 2007 Feb;189(3):929-39 PMID: 17114261.

Tamber S, Ochs MM, Hancock RE. Role of the novel OprD family of porins in nutrient uptake in *Pseudomonas aeruginosa*. J Bacteriol. 2006 Jan;188(1):45-54. PMID: 16352820.

Tan X, Cheng X, Hu M, Zhang Y, Jia A, Zhou J, Zhu G. Transcriptional analysis and target genes discovery of *Pseudomonas aeruginosa* biofilm developed ex vivo chronic wound model. AMB Express. 2021 Nov 27;11(1):157. PMID: 34837552.

Tang XK, Su YB, Ye HQ, Dai ZY, Yi H, Yang KX, Zhang TT, Chen ZG. Glucose-Potentiated Amikacin Killing of Cefoperazone/Sulbactam Resistant *Pseudomonas aeruginosa*. Front Microbiol. 2022 Mar 3;12:800442. PMID: 35310395.

Tausk F, Evans ME, Patterson LS, Federspiel CF, Stratton CW. Imipenem-induced resistance to antipseudomonal beta-lactams in *Pseudomonas aeruginosa*. Antimicrob Agents Chemother. 1985 Jul;28(1):41-5. PMID: 3929679.

Taylor PK, Zhang L, Mah TF. Loss of the Two-Component System TctD-TctE in *Pseudomonas aeruginosa* Affects Biofilm Formation and Aminoglycoside Susceptibility in Response to Citric Acid. mSphere. 2019 Mar 6;4(2):e00102-19. PMID: 30842268.

Teitzel GM, Geddie A, De Long SK, Kirisits MJ, Whiteley M, Parsek MR. Survival and growth in the presence of elevated copper: transcriptional profiling of copper-stressed *Pseudomonas aeruginosa*. J Bacteriol. 2006 Oct;188(20):7242-56. PMID: 17015663.

Tian ZX, Yi XX, Cho A, O'Gara F, Wang YP. CpxR Activates MexAB-OprM Efflux Pump Expression and Enhances Antibiotic Resistance in Both Laboratory and Clinical nalB-Type Isolates of *Pseudomonas aeruginosa*. PLoS Pathog. 2016 Oct 13;12(10):e1005932. PMID: 27736975.

Tielen P, Rosin N, Meyer AK, Dohnt K, Haddad I, Jänsch L, Klein J, Narten M, Pommerenke C, Scheer M, Schobert M, Schomburg D, Thielen B, Jahn D. Regulatory and metabolic networks for the adaptation of *Pseudomonas aeruginosa* biofilms to urinary tract-like conditions. PLoS One. 2013 Aug 13;8(8):e71845. PMID: 23967252.

Tipper DJ, Strominger JL. Mechanism of action of penicillins: a proposal based on their structural similarity to acyl-D-alanyl-D-alanine. Proc Natl Acad Sci U S A. 1965 Oct;54(4):1133-41. PMID: 5219821.

Tognon M, Köhler T, Luscher A, van Delden C. Transcriptional profiling of *Pseudomonas aeruginosa* and *Staphylococcus aureus* during in vitro co-culture. BMC Genomics. 2019 Jan 10;20(1):30. PMID: 30630428.

Toleman MA, Simm AM, Murphy TA, Gales AC, Biedenbach DJ, Jones RN, Walsh TR. Molecular characterization of SPM-1, a novel metallo-beta-lactamase isolated in Latin America: report from the SENTRY antimicrobial surveillance programme. J Antimicrob Chemother. 2002 Nov;50(5):673-9. PMID: 12407123.

Touw DS, Patel DR, van den Berg B. The crystal structure of OprG from *Pseudomonas aeruginosa*, a potential channel for transport of hydrophobic molecules across the outer membrane. PLoS One. 2010 Nov 29;5(11):e15016. PMID: 21124774.

Trias J, Nikaido H. Outer membrane protein D2 catalyzes facilitated diffusion of carbapenems and penems through the outer membrane of *Pseudomonas aeruginosa*. Antimicrob Agents Chemother. 1990**b** Jan;34(1):52-7. PMID: 2109575.

Trias J, Nikaido H. Protein D2 channel of the *Pseudomonas aeruginosa* outer membrane has a binding site for basic amino acids and peptides. J Biol Chem. 1990**a** Sep 15;265(26):15680-4. PMID: 2118530.

Ude J, Tripathi V, Buyck JM, Söderholm S, Cunrath O, Fanous J, Claudi B, Egli A, Schleberger C, Hiller S, Bumann D. Outer membrane permeability: Antimicrobials and diverse nutrients bypass porins in *Pseudomonas aeruginosa*. Proc Natl Acad Sci U S A. 2021 Aug 3;118(31):e2107644118. PMID: 34326266.

Ulrey RK, Barksdale SM, Zhou W, van Hoek ML. Cranberry proanthocyanidins have anti-biofilm properties against *Pseudomonas aeruginosa*. BMC Complement Altern Med. 2014 Dec 16;14:499. PMID: 25511463.

Underhill SAM, Cabeen MT. Redundancy in Citrate and cis-Aconitate Transport in *Pseudomonas aeruginosa*. J Bacteriol. 2022 Dec 20;204(12):e0028422. PMID: 36321838.

Uwate M, Ichise YK, Shirai A, Omasa T, Nakae T, Maseda H. Two routes of MexS-MexT-mediated regulation of MexEF-OprN and MexAB-OprM efflux pump expression in *Pseudomonas aeruginosa*. Microbiol Immunol. 2013 Apr;57(4):263-72. PMID: 23586630.

van Delden C, Page MG, Köhler T. Involvement of Fe uptake systems and AmpC β-lactamase in susceptibility to the siderophore monosulfactam BAL30072 in *Pseudomonas aeruginosa*. Antimicrob Agents Chemother. 2013 May;57(5):2095-102. PMID: 23422914.

van den Berg B, Bhamidimarri SP, Winterhalter M. Crystal structure of a COG4313 outer membrane channel. Sci Rep. 2015 Jul 7;5:11927. PMID: 26149193.

van den Berg B. Bacterial cleanup: lateral diffusion of hydrophobic molecules through protein channel walls. Biomol Concepts. 2010 Oct 1;1(3-4):263-70. PMID: 25962002.

van den Berg B. Structural basis for outer membrane sugar uptake in pseudomonads. J Biol Chem. 2012 Nov 30;287(49):41044-52. PMID: 23066028.

van Duin D, Bonomo RA. Ceftazidime/Avibactam and Ceftolozane/Tazobactam: Second-generation β-Lactam/β-Lactamase Inhibitor Combinations. Clin Infect Dis. 2016 Jul 15;63(2):234-41. PMID: 27098166.

Vandesompele J, De Preter K, Pattyn F, Poppe B, Van Roy N, De Paepe A, Speleman F. Accurate normalization of real-time quantitative RT-PCR data by geometric averaging of multiple internal control genes. Genome Biol. 2002 Jun 18;3(7):RESEARCH0034. PMID: 12184808.

Vatansever C, Menekse S, Dogan O, Gucer LS, Ozer B, Ergonul O, Can F. Co-existence of OXA-48 and NDM-1 in colistin resistant *Pseudomonas aeruginosa* ST235. Emerg Microbes Infect. 2020 Jan 21;9(1):152-154. PMID: 31964275.

Vergalli J, Dumont E, Pajović J, Cinquin B, Maigre L, Masi M, Réfrégiers M, Pagés JM. Spectrofluorimetric quantification of antibiotic drug concentration in bacterial cells for the characterization of translocation across bacterial membranes. Nat Protoc. 2018 Jun;13(6):1348-1361. PMID: 29773906.

Vollmer W, Blanot D, de Pedro MA. Peptidoglycan structure and architecture. FEMS Microbiol Rev. 2008 Mar;32(2):149-67. PMID: 18194336.

Vora A, Tiwaskar M. Biapenem. J Assoc Physicians India. 2022 Jan;70(1):11-12. PMID: 35062817.

Walsh CT, Zhang W. Chemical logic and enzymatic machinery for biological assembly of peptidyl nucleoside antibiotics. ACS Chem Biol. 2011 Oct 21;6(10):1000-7. PMID: 21851099.

Wang D, Seeve C, Pierson LS 3rd, Pierson EA. Transcriptome profiling reveals links between ParS/ParR, MexEF-OprN, and quorum sensing in the regulation of adaptation and virulence in *Pseudomonas aeruginosa*. BMC Genomics. 2013 Sep 13;14:618. PMID: 24034668.

Wang L, Zhu J, Chen L, Du H. Cefiderocol: Clinical application and emergence of resistance. Drug Resist Updat. 2024 Jan;72:101034. PMID: 38134561.

Wang Y, Zhao X, Sun B, Yu H, Huang X. Molecular dynamics simulation study of the vanillate transport channel of Opdk. Arch Biochem Biophys. 2012 Aug 15;524(2):132-9. PMID: 22633976.

Wargo MJ. Homeostasis and catabolism of choline and glycine betaine: lessons from *Pseudomonas aeruginosa*. Appl Environ Microbiol. 2013 Apr;79(7):2112-20. PMID: 23354714.

Watanabe M, Iyobe S, Inoue M, Mitsuhashi S. Transferable imipenem resistance in *Pseudomonas aeruginosa*. Antimicrob Agents Chemother. 1991 Jan;35(1):147-51. PMID: 1901695.

Weber DJ, Rutala WA, Sickbert-Bennett EE, Samsa GP, Brown V, Niederman MS. Microbiology of ventilator-associated pneumonia compared with that of hospital-acquired pneumonia. Infect Control Hosp Epidemiol. 2007 Jul;28(7):825-31. PMID: 17564985.

Wei Q, Tarighi S, Dötsch A, Häussler S, Müsken M, Wright VJ, Cámara M, Williams P, Haenen S, Boerjan B, Bogaerts A, Vierstraete E, Verleyen P, Schoofs L, Willaert R, De Groote VN, Michiels J, Vercammen K, Crabbé A, Cornelis P. Phenotypic and genome-wide analysis of an antibiotic-resistant small colony variant (SCV) of *Pseudomonas aeruginosa*. PLoS One. 2011;6(12):e29276. PMID: 22195037.

Weiner-Lastinger LM, Abner S, Edwards JR, Kallen AJ, Karlsson M, Magill SS, Pollock D, See I, Soe MM, Walters MS, Dudeck MA. Antimicrobial-resistant pathogens associated with adult healthcare-associated infections: Summary of data reported to the National Healthcare Safety Network, 2015-2017. Infect Control Hosp Epidemiol. 2020 Jan;41(1):1-18. PMID: 31767041.

Wendel AF, Kolbe-Busch S, Ressina S, Schulze-Röbbecke R, Kindgen-Milles D, Lorenz C, Pfeffer K, MacKenzie CR. Detection and termination of an extended low-frequency hospital outbreak of GIM-1-producing *Pseudomonas aeruginosa* ST111 in Germany. Am J Infect Control. 2015 Jun;43(6):635-9. PMID: 25868648.

Werner JP, Mitchell JM, Taracila MA, Bonomo RA, Powers RA. Exploring the potential of boronic acids as inhibitors of OXA-24/40 β-lactamase. Protein Sci. 2017 Mar;26(3):515-526. PMID: 27997706.

Wessel AK, Liew J, Kwon T, Marcotte EM, Whiteley M. Role of *Pseudomonas aeruginosa* peptidoglycan-associated outer membrane proteins in vesicle formation. J Bacteriol. 2013 Jan;195(2):213-9. PMID: 23123904.

Whitney JC, Colvin KM, Marmont LS, Robinson H, Parsek MR, Howell PL. Structure of the cytoplasmic region of PelD, a degenerate diguanylate cyclase receptor that regulates exopolysaccharide production in *Pseudomonas aeruginosa*. J Biol Chem. 2012 Jul 6;287(28):23582-93. PMID: 22605337.

WHO Bacterial Priority Pathogens List, 2024: bacterial pathogens of public health importance to guide research, development and strategies to prevent and control antimicrobial resistance. Geneva: World Health Organization; 2024.

Widya M, Pasutti WD, Sachdeva M, Simmons RL, Tamrakar P, Krucker T, Six DA. Development and Optimization of a Higher-Throughput Bacterial Compound Accumulation Assay. ACS Infect Dis. 2019 Mar 8;5(3):394-405. PMID: 30624052.

Wilkens S. Structure and mechanism of ABC transporters. F1000Prime Rep. 2015 Feb 3;7:14. PMID: 25750732.

Williams, Tomas JM. The pathogenicity of *Klebsiella pneumoniae*. Rev Med Microbiol. 1990;1: 196-204.

Willsey GG, Wargo MJ. Sarcosine Catabolism in *Pseudomonas aeruginosa* Is Transcriptionally Regulated by SouR. J Bacteriol. 2015 Oct 26;198(2):301-10. PMID: 26503852.

Winterhalter M, Ceccarelli M. Physical methods to quantify small antibiotic molecules uptake into Gram-negative bacteria. Eur J Pharm Biopharm. 2015 Sep;95(Pt A):63-7. PMID: 26036449.

Wozniak DJ, Wyckoff TJ, Starkey M, Keyser R, Azadi P, O'Toole GA, Parsek MR. Alginate is not a significant component of the extracellular polysaccharide matrix of PA14 and PAO1 *Pseudomonas aeruginosa* biofilms. Proc Natl Acad Sci U S A. 2003 Jun 24;100(13):7907-12. PMID: 12810959.

Wright BW, Kamath KS, Krisp C, Molloy MP. Proteome profiling of *Pseudomonas aeruginosa* PAO1 identifies novel responders to copper stress. BMC Microbiol. 2019 Apr 1;19(1):69. PMID: 30935370.

Wu M, Guina T, Brittnacher M, Nguyen H, Eng J, Miller SI. The *Pseudomonas aeruginosa* proteome during anaerobic growth. J Bacteriol. 2005 Dec;187(23):8185-90. PMID: 16291692.

Wylie JL, Worobec EA. The OprB porin plays a central role in carbohydrate uptake in *Pseudomonas aeruginosa*. J Bacteriol. 1995 Jun;177(11):3021-6. PMID: 7768797.

Yamamoto M, Ueda A, Kudo M, Matsuo Y, Fukushima J, Nakae T, Kaneko T, Ishigatsubo Y. Role of MexZ and PA5471 in transcriptional regulation of mexXY in *Pseudomonas aeruginosa*. Microbiology (Reading). 2009 Oct;155(Pt 10):3312-3321. PMID: 19589837.

Yamano Y, Nishikawa T, Komatsu Y. Cloning and nucleotide sequence of anaerobically induced porin protein E1 (OprE) of *Pseudomonas aeruginosa* PAO1. Mol Microbiol. 1993 May;8(5):993-1004. PMID: 8394980.

Yamano Y, Nishikawa T, Komatsu Y. Involvement of the RpoN protein in the transcription of the oprE gene in *Pseudomonas aeruginosa*. FEMS Microbiol Lett. 1998 May 1;162(1):31-7. PMID: 9595661.

Ye J, van den Berg B. Crystal structure of the bacterial nucleoside transporter Tsx. EMBO J. 2004 Aug 18;23(16):3187-95. PMID: 15272310.

Yero D, Díaz-Lobo M, Costenaro L, Conchillo-Solé O, Mayo A, Ferrer-Navarro M, Vilaseca M, Gibert I, Daura X. The *Pseudomonas aeruginosa* substrate-binding protein Ttg2D functions as a general glycerophospholipid transporter across the periplasm. Commun Biol. 2021 Apr 9;4(1):448. PMID: 33837253.

Yeterian E, Martin LW, Guillon L, Journet L, Lamont IL, Schalk IJ. Synthesis of the siderophore pyoverdine in *Pseudomonas aeruginosa* involves a periplasmic maturation. Amino Acids. 2010 May;38(5):1447-59. PMID: 19787431.

Yin Y, Withers TR, Wang X, Yu HD. Evidence for sigma factor competition in the regulation of alginate production by *Pseudomonas aeruginosa*. PLoS One. 2013 Aug 22;8(8):e72329. PMID: 23991093.

Yonehara R, Yamashita E, Nakagawa A. Crystal structures of OprN and OprJ, outer membrane factors of multidrug tripartite efflux pumps of *Pseudomonas aeruginosa*. Proteins. 2016 Jun;84(6):759-69. PMID: 26914226.

Yoneyama H, Ocaktan A, Gotoh N, Nishino T, Nakae T. Subunit swapping in the Mex-extrusion pumps in *Pseudomonas aeruginosa*. Biochem Biophys Res Commun. 1998 Mar 27;244(3):898-902. PMID: 9535764.

Yoneyama H, Yamano Y, Nakae T. Role of porins in the antibiotic susceptibility of *Pseudomonas aeruginosa*: construction of mutants with deletions in the multiple porin genes. Biochem Biophys Res Commun. 1995 Aug 4;213(1):88-95. PMID: 7639767.

Yoshihara E, Nakae T. Identification of porins in the outer membrane of *Pseudomonas aeruginosa* that form small diffusion pores. J Biol Chem. 1989 Apr 15;264(11):6297-301. PMID: 2539376.

Yoshimura F, Nikaido H. Permeability of *Pseudomonas aeruginosa* outer membrane to hydrophilic solutes. J Bacteriol. 1982 Nov;152(2):636-42. PMID: 6813310.

Yoshimura F, Zalman LS, Nikaido H. Purification and properties of *Pseudomonas aeruginosa* porin. J Biol Chem. 1983 Feb 25;258(4):2308-14. PMID: 6296139.

Young ML, Bains M, Bell A, Hancock RE. Role of *Pseudomonas aeruginosa* outer membrane protein OprH in polymyxin and gentamicin resistance: isolation of an OprH-deficient mutant by gene replacement techniques. Antimicrob Agents Chemother. 1992 Nov;36(11):2566-8. PMID: 1336952.

Zakharian E. Recording of ion channel activity in planar lipid bilayer experiments. Methods Mol Biol. 2013. 998:109-18. PMID: 23529424.

Zapun A, Contreras-Martel C, Vernet T. Penicillin-binding proteins and beta-lactam resistance. FEMS Microbiol Rev. 2008 Mar;32(2):361-85. PMID: 18248419.

Zarei O, Shokoohizadeh L, Hossainpour H, Alikhani MY. Molecular analysis of *Pseudomonas aeruginosa* isolated from clinical, environmental and cockroach sources by ERIC-PCR. BMC Res Notes. 2018 Sep 15;11(1):668. PMID: 30219108.

Zhanel GG, Lawrence CK, Adam H, Schweizer F, Zelenitsky S, Zhanel M, Lagacé-Wiens PRS, Walkty A, Denisuik A, Golden A, Gin AS, Hoban DJ, Lynch JP 3rd, Karlowsky JA. Imipenem-Relebactam and Meropenem-Vaborbactam: Two Novel Carbapenem-β-Lactamase Inhibitor Combinations. Drugs. 2018 Jan;78(1):65-98. PMID: 29230684.

Zhang L, Fritsch M, Hammond L, Landreville R, Slatculescu C, Colavita A, Mah TF. Identification of genes involved in *Pseudomonas aeruginosa* biofilm-specific resistance to antibiotics. PLoS One. 2013 Apr 24;8(4):e61625. PMID: 23637868.

Zhao J, Hellwig N, Djahanschiri B, Khera R, Morgner N, Ebersberger I, Wang J, Michel H. Assembly and Functional Role of PACE Transporter PA2880 from *Pseudomonas aeruginosa*. Microbiol Spectr. 2022 Apr 27;10(2):e0145321. PMID: 35377188.

Zhou Y, Joubran C, Miller-Vedam L, Isabella V, Nayar A, Tentarelli S, Miller A. Thinking outside the "bug": a unique assay to measure intracellular drug penetration in Gram-negative bacteria. Anal Chem. 2015 Apr 7;87(7):3579-84. PMID: 25753586.

Zhu YF, Curran IH, Joris B, Ghuysen JM, Lampen JO. Identification of BlaR, the signal transducer for beta-lactamase production in *Bacillus licheniformis*, as a penicillin-binding protein with strong homology to the OXA-2 beta-lactamase (class D) of *Salmonella typhimurium*. J Bacteriol. 1990 Feb;172(2):1137-41. PMID: 2404938.

Zimmermann W, Rosselet A. Function of the outer membrane of *Escherichia coli* as a permeability barrier to beta-lactam antibiotics. Antimicrob Agents Chemother. 1977 Sep;12(3):368-72. PMID: 334063.

Zimmermann W. Penetration of beta-lactam antibiotics into their target enzymes in *Pseudomonas aeruginosa*: comparison of a highly sensitive mutant with its parent strain. Antimicrob Agents Chemother. 1980 Jul;18(1):94-100. PMID: 6774666.

Zincke D, Balasubramanian D, Silver LL, Mathee K. Characterization of a Carbapenem-Hydrolyzing Enzyme, PoxB, in *Pseudomonas aeruginosa* PAO1. Antimicrob Agents Chemother. 2015 Nov 30;60(2):936-45. PMID: 26621621.

8 Annex

Name	Sequence	Lenght
blaR-fw	CCATGCAAAAAGAAACACGC	20
blaR-seq-rev	ACAGGACAAAGCCCCCTGAGGCTG	24
blaR-rev	TTCTTGCCTCCAAGTTCCGT	20
omp1-rev	TGACACCACGATGCCTGCAG	20
pkt-fw-1	CAGCTGAAACGGGAAGCTCA	20
pkt-rev-1	TGAGCTTCCCGTTTCAGCTG	20
pkt-fw-2	ATGCTCTTCTGCTCCTGCAG	20
pkt-rev-2	CTGCAGGAGCAGAAGAGCAT	20
309-fw	CTATGAACATGAATGATGCGCAAA	24
tet-fw	GCTCCGAGAACGGGTGCGCAT	21
tet-rev	ACCATCAGGGACAGCTTCAA	20
309-inf-fw	GTATGCTCTTCTGCTCCTGCAGGCATCGTGGTGTCACGC	39
309-inf-rev	TGAGCTTCCCGTTTCAGCTGGTTAACGGCGGGATATAACATGAG	44
tet-rev-seq	TATTCTCAGAATGACTTGGTTGAGT	25
240-ori-rev	TCGGTCTGCCGCCACGCCAG	20
laci-fw	CGGTGTCTCTTATCAGACCG	20
tet-fw-seq	CCAGGGTGACGGTGCCGAGG	20
neg1-fw	AATAGGCGTATCACGAGGCCCTTTGCGTTCAGGCTGCTAAAGATG	45
neg1-rev	TCATGGTCTATTGCCTCCCG	20
neg2-fw	CGGGAGGCAATAGACCATGA	20
neg2-rev	CAAAGGGCCTCGTGATACGC	20
gmr-eco-fw	CGCCGGAATTCCGGGTTACGCCGTGGGTCGATGT	34
gmr-eco-rev	CGCCGGAATTCCGGAATTTACCGAACAACTCCGC	34
oprD-fw	ATGAAAGTGATGAAGTGGAGCG	22
oprD-rev	TTACAGGATCGACAGCGGATAG	22
opdB-fw	ATGATCCGCGTTCGACCGGTCG	22
opdB-rev	TCAGAGCGAGCCTTTGAGTGGG	22
opdC-fw	ATGAGGAATCTGTTCGCCTTGA	22
opdC-rev	TCAGAACACGTCGATGGGATAG	22
opdP-fw	GTGATGAGAAACCAACGTGTGA	22
opdP-rev	TTACAGCAGGTTGAAGGGGAAG	22
opdT-fw	ATGCAAGGGGATGGAAAGAAAC	22
opdT-rev	TCAGAGGACTTGCAGCGGGTAT	22
oprD-flankF	CGGCTGAGGGGAAAGTCGCC	20
oprD-flankR	TACGCGGTCATTCTCGGGCG	20
oprD-rev-seq1	CGCTCCACTTCATCACTTTCAT	22
oprD-rev-seq2	CAGAGTGTAGGCTGCCGCCAGG	22
oprD-rev-seq3	CTGCTTCAAGGGTTGGTTGC	20
oprD-rev-seq4	GATCGCTGACGAATGCGTCG	20
oprD-rev-seq5	GCCCTCGGTGAAGTGGCCTG	20
oprD-fw-seq1	GTCCGGCCAAGGACCTGTCG	20
mexR-fw	CGCCATGGCCCATATTCAG	19
mexR-rev	GGCATTCGCCAGTAAGCGG	19
rpoS-fw	ATGGCACTCAAAAAAGAAGG	20
rpoS-rev	TCACTGGAACAGCGCGTCAC	20
rpsL-fw	ATGGCAACTATCAACCAGCT	20
rpsL-rev	TTACTTCGGACGCTTGGCGC	20
nalD-ext-fw	GATTCGACTACCCAGCACAG	20
nalD-ext-rev	CCCAGGTACTCGAGGCGATC	20
PA2480-fw	ATGAGCCTGCGCCTGCGCCT	20
PA2480-rev	TCACTCGCGCAGCGGCATTT	20
PA2480-rev-seq	GTCGAACGACAGGCTGCCTT	20
PA4500-int-fw	CTACGGCTGCGACTCGATCA	20
PA4500-ext-rev	CCTTTATTGTTGTCGTTGGC	20
PA4501-ext-rev	GTACTGGACGATATCGAAGC	20
PA4500-fw	ATGCGTAAGATCCTTCCCCT	20
PA4500-rev	TCAGGGCTGGTTGGCTACGC	20
mexT-fw	ATGCCTGTCAGTGATCCTAT	20
mexT-rev	TCAGAGACTGTCCGGATCGC	20
lasR-fw	ATGGCCTTGGTTGACGGTTT	20
lasR-rev	TCAGAGAGTAATAAGACCCAAA	22
opdP-gib-fw2	CTTTAAGAAGGAGATATACCATGGCTAGAAACCAACGTGTGACCAG	46
opdP-gib-fw3	CTTTAAGAAGGAGATATACCATGGCTGCCGACGAGCAGGAAAACCC	46

Table S1: list of primers used for PCR amplification and/or Sanger sequencing.

Name	Sequence	Lenght	Reference
oprD-rt-fw	ATCTACCGCACAAACGATGAAGG	23	Caille *et al*., 2007
oprD-rt-rev	GCCGAAGCCGATATAATCAAACG	23	Caille *et al*., 2007
opdB-rt-fw	GCTCAACCGCAACTACTTCC	21	
opdB-rt-rev	GCGTCGGAATACTCGCTGGC	20	
opdC-rt-fw	GCTGAAGATCCGCGCCTTC	19	
opdC-rt-rev	GCTGAGATGATGGCTGTCGC	20	
opdP-rt-fw	CAACACCGAATTCAAGGCC	19	
opdP-rt-rev	CCGTACTCGGTGGTCATGTC	20	
opdT-rt-fw	GCTTCACCCTGGTCAACGAC	21	
opdT-rt-rev	GAAGCTGGTGCCGGCGTAGT	20	
PA3340-rt-fw	GCTTGCAGTTCCTCAACGAG	21	Costaglioli *et al*., 2014
PA3340-rt-rev	CACCAGGAAATTCAGGTAGGG	22	Costaglioli *et al*., 2014
gyrA-rt-fw	TGTGCTTTATGCCATGAGCGA	21	Bragonzi *et al*., 2005
gyrA-rt-rev	TCCACCGAACCGAAGTTGC	20	Bragonzi *et al*., 2005
cysG-rt-fw	GCAGCAGCGCCGGGTGTTC	19	
cysG-rt-rev	ACGTCGGCCTGCTGCATC	18	
rpsL-rt-fw	GCAAGCGCATGGTCGACAAGA	21	Dumas *et al*., 2006
rpsL-rt-rev	CGCTGTGCTCTTGCAGGTTGTGA	23	Dumas *et al*., 2006
proC-rt-fw	CAGGCCGGGCAGTTGCTGTC	21	Savli *et al*., 2003
proC-rt-rev	GGTCAGGCGCGAGGCTGTCT	21	Savli *et al*., 2003
gapA-rt-fw	CAACGACCAGAACCTCTCCG	20	
gapA-rt-rev	ACCTGCACGGTGAGATCGAC	20	
mreB-rt-fw	CTGTCGATCGACCTGGG	17	Gupta *et al*., 2013
mreB-rt-rev	GATCACGCCGTCTTTCATCG	20	
rho-rt-fw	GCAACGGCTCCACCGAAGAC	20	
rho-rt-rev	GTCACTTCCTCAGGGCGCTC	20	
recA-rt-fw	GAATCCTCGGGCAAGACCAC	20	
recA-rt-rev	CACGTCGACCGCGTTGGAGC	20	
mutL-rt-fw	CAAGTTCCTGCGTGCCGAGA	20	
mutL-rt-rev	CAGCGCCTGCTCGAGGAATG	20	
PA2875-rt-fw	AGTTTCCAGCGCATCCAGTT	21	Costaglioli *et al*., 2014
PA2875-rt-rev	CGGGATGGAAGACGAATTG	20	Costaglioli *et al*., 2014
rpoS-rt-fw	CTCCCCGGGCAACTCCAAAAG	21	Savli *et al*., 2003
rpoS-rt-rev	CGATCATCCGCTTCCGACCAG	21	Savli *et al*., 2003

Table S2: list of primers used for qRT-PCR.

Antibiotics	Absorbance (nm)	Molar extinction coefficient ε (M^{-1} cm^{-1})
Ampicillin	235	1860
Benzylpenicillin	235	1200-1300
Piperacillin	235	1800
Cephaloridin	260	12000-12500
Cefoxitin	260	8250
Cefuroxime	260	15700
Cefotaxime	260	16000
Ceftazidime	260	22000
Cefepime	260	19000
Imipenem	297	9000
Meropenem	297	6900
Ertapenem	298	9000
Doripenem	296	7540
Biapenem	296	7540
Nitrocefin	482	15000

Table S3: Molar extinction coefficients for antibiotics tested for permeability coefficient determination.

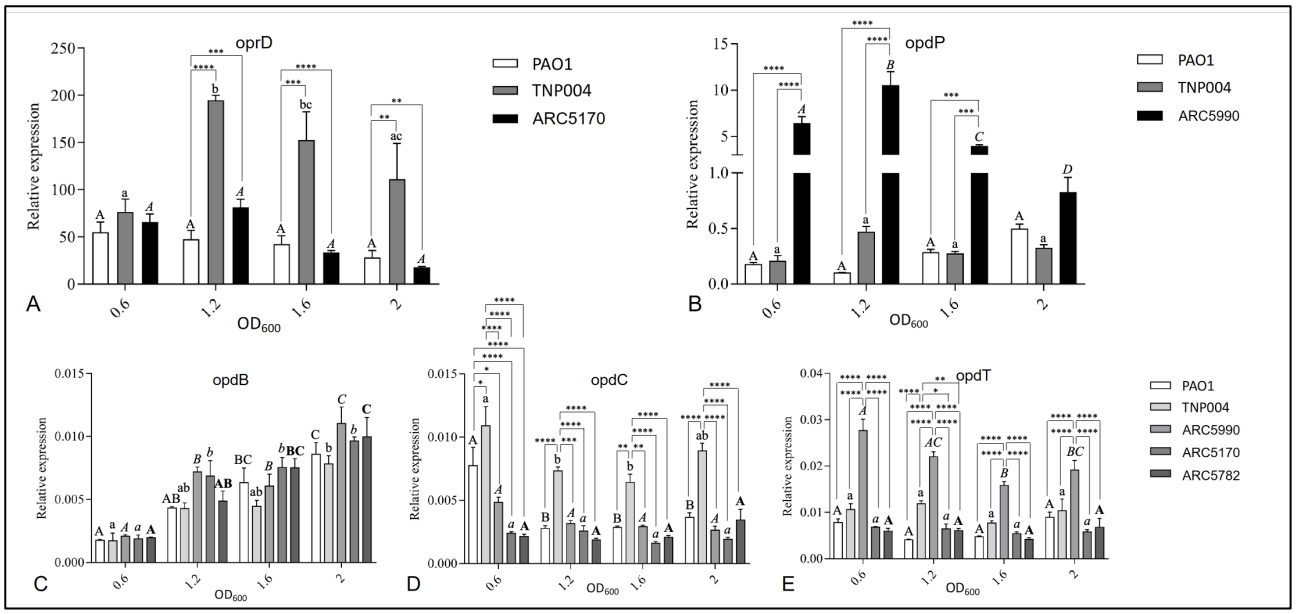

Figure S1: Relative expressions of (A) *oprD*, (B) *opdP*, (C) *opdB*, (D) *opdC*, and (E) *opdT* mRNAs in *P. aeruginosa* PAOI and four porin(s) mutant strains at 4 different points of cellular growth (OD_{600} = 0.6, 1.2, 1.6 and 2). Data were analyzed by two-way analysis of variance (ANOVA), followed by Bonferroni multiple comparison *post-test*. Statistically significant differences between means between strains are indicated by stars (* P<0.05, ** P<0.01, *** P<0.001, **** P<0.0001; the absence of an asterisk implies the lack of a statistical difference between different strains) or between different OD_{600} within strains by different letters (P<0.05).

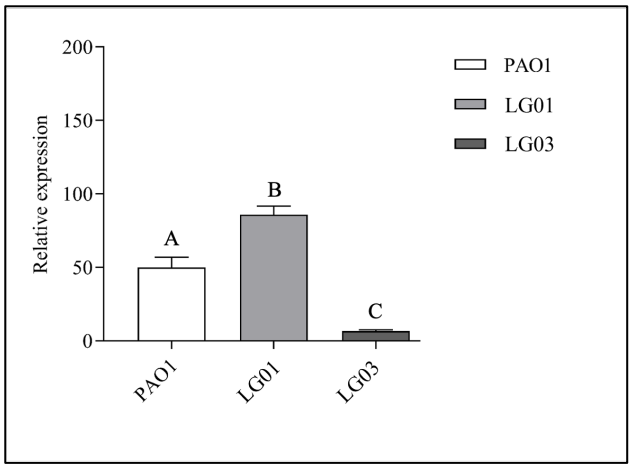

Figure S2: Relative expression of *oprD* mRNA in *P. aeruginosa* PAOI, LG01, and LG03 at OD_{600} = 1.6. Data were analyzed by two-way analysis of variance (ANOVA), followed by Bonferroni multiple comparison *post-test*. Statistically significant differences between means between strains are indicated by different letters (P<0.05).

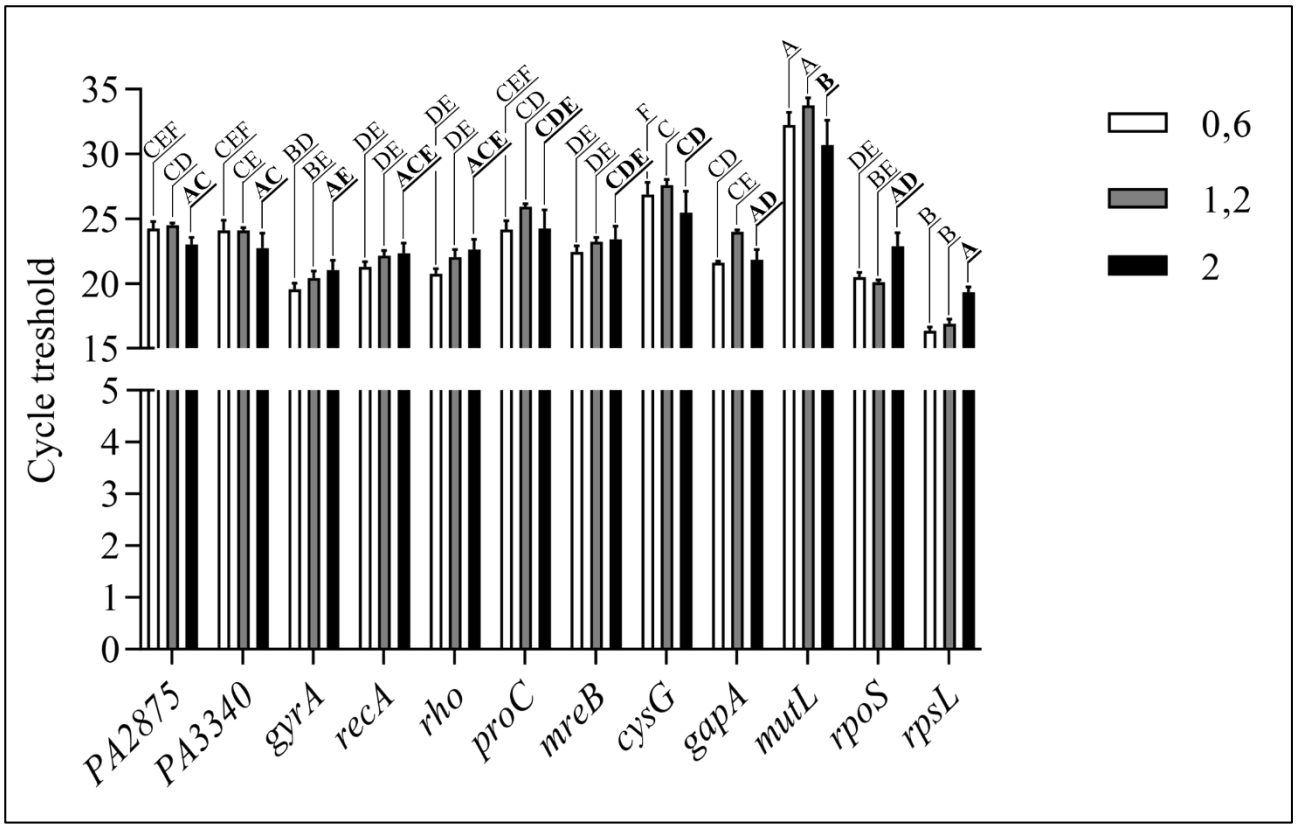

Figure S3: Relative expression of *PA2875*, *PA3340*, *gyrA*, *recA*, *rho*, *proC*, *mreB, cysG*, *gapA* and *mutL* in *P. aeruginosa* PAO1 at OD_{600} = 0.6, 1.2 and 2; the relative expression reported on the y axis is the expression of the target gene relative to the mean expression level of two genes used as reference (*rpoS* and *rpsL*). Data were analyzed by two-way analysis of variance (ANOVA) followed by Bonferroni multiple comparison post-test. Statistically significant differences between means between genes are indicated by different letters (P<0.05).

8.1 References (annex)

Bragonzi A, Worlitzsch D, Pier GB, Timpert P, Ulrich M, Hentzer M, Andersen JB, Givskov M, Conese M, Doring G. Nonmucoid *Pseudomonas aeruginosa* expresses alginate in the lungs of patients with cystic fibrosis and in a mouse model. J Infect Dis. 2005 Aug 1;192(3):410-9. PMID: 15995954.

Caille O, Rossier C, Perron K. A copper-activated two-component system interacts with zinc and imipenem resistance in *Pseudomonas aeruginosa*. J Bacteriol. 2007 Jul;189(13):4561-8. PMID: 17449606.

Costaglioli P, Barthe C, Fayon M, Christoflour N, Bui S, Derlich L, Domblides P, Crouzet M, Vilain S, Garbay B. Selection of *Pseudomonas aeruginosa* reference genes for RT-qPCR analysis from sputum of cystic fibrosis patients. Mol Cell Probes. 2014 Feb;28(1):10-2. PMID: 24075879.

Dumas JL, van Delden C, Perron K, Köhler T. Analysis of antibiotic resistance gene expression in *Pseudomonas aeruginosa* by quantitative real-time-PCR. FEMS Microbiol Lett. 2006 Jan;254(2):217-25. PMID: 16445748.

Savli H, Karadenizli A, Kolayli F, Gundes S, Ozbek U, Vahaboglu H. Expression stability of six housekeeping genes: A proposal for resistance gene quantification studies of *Pseudomonas aeruginosa* by real-time quantitative RT-PCR. J Med Microbiol. 2003 May;52(Pt 5):403-408. PMID: 12721316.